Transcriptional Regulation of and by NFATc1 in Lymphocytes

This thesis submitted in partial fulfillment of the requirements for the award of the degree Doctor rerum naturalium of the Julius-Maximilians-University Würzburg

Submitted by

Ronald Rudolf

from

Stuttgart, Baden-Württemberg

Würzburg

2013

Eingereicht am: ....

Mitglieder der Promotionskommission:

Vorsitzender: Prof. Dr. W. Rössler..

1. Gutachter: Prof. Dr. E. Serfling…..

2. Gutachter: Prof. Dr. T. Müller...

Tag des Promotionskolloquiums: ....

Doktorurkunde ausgehändigt am: ....

Affidavit

I hearby confirm that my thesis entitled "Transcriptional Regulation of and by NFATc1 in Lymphocytes" is the result of my own work. I did not receive any help or support from commercial consultants. All sources and/or materials applied are listed and specified in the thesis.

Furthermore, I confirm that this thesis has not yet been submitted as part of another examination process neither in identical nor in similar form.

Place, Date..

Signature..

Eidesstattliche Erklärung

Hiermit erkläre ich an Eides statt, die Dissertation „Transcriptional Regulation of an by NFATc1 in Lymphocytes" eigenständig, d.h. insbesondere selbstständig und ohne Hilfe eines kommerziellen Promotionsberaters, angefertigt und keine anderen als die von mir angegebenen Quellen und Hilfsmittel verwendet zu haben.

Ich erkläre außerdem, dass die Dissertation weder in gleicher noch in ähnlicher Form bereits in einem anderen Prüfungsverfahren vorgelegen hat.

Ort, Datum..

Unterschrift..

CONTENT

CONTENT

I. INTRODUCTION

1.1 The adaptive immune system

Any ecological environment challenges higher organisms to develop a versatile set of mechanisms to ensure their existence. The fundamental basis of any immune system are cells that are capable of distinguishing tissues and organs which are a legitimate part of their host from foreign invaders. Beyond that, these cells must be equipped to eliminate so called "non-self" invaders which are prevalently pathogenic viruses or bacteria. Additionally, the immune system is also able to recognize alterations in the integrity of its own cells, e.g. by injury or cancer, and clear these structures [1]. Major components of the innate immune system are physical and chemical barriers, such as epithelia and anti-microbial chemicals produced at epithelial surfaces. Phagocytic mononuclear cells, such as neutrophils and macrophages (MOs), dendritic cells (DCs), and natural killer (NKs) cells, play a substantial role in host defence. Furthermore, blood born proteins, including members of the complement system and mediators of inflammation, as well as cytokines orchestrate many of the activities of the cells of innate immunity [2].

It is estimated that more than 500 million years ago two different types of recombinatorial adaptive immune systems appeared in vertebrates (Figure 1.1). Whereas innate immunity is based on a type of receptors which recognize highly conserved pathogen-associated molecular patterns (PAMPs), in *Gnathostomata*, i.e. in vertebrates with jaws, an additional system based on lymphocytes emerged [3]. The adaptive immune system is defined by lymphocytes, antigen receptors [B- and T- cell receptor (BCR, TCR)], Major-Histocompatibility-Complex (MHC) I and II, genes involved in rearrangement [e.g. Recombination Activating Gene (RAG)], somatic hypermutation, gene conversion and specialized primary and secondary lymphoid tissues [4]. In this system, T-lymphocytes mediate cellular immunity whereas B-lymphocytes are responsible for humoral immunity. Along with NK-cells, these specialized lymphocytes arise from committed progenitors in hematopoietic tissues, which undergo unique V(D)J rearrangements of their antigen receptors to become clonally diverse [3]. This ability to rearrange immunoglobulin (Ig) V, D and J gene segments is the basic element of the adaptive immune system, thereby generating a lymphocyte receptor repertoire of sufficient diversity to recognize the antigen component of any potential pathogen or toxin [4].

I. INTRODUCTION
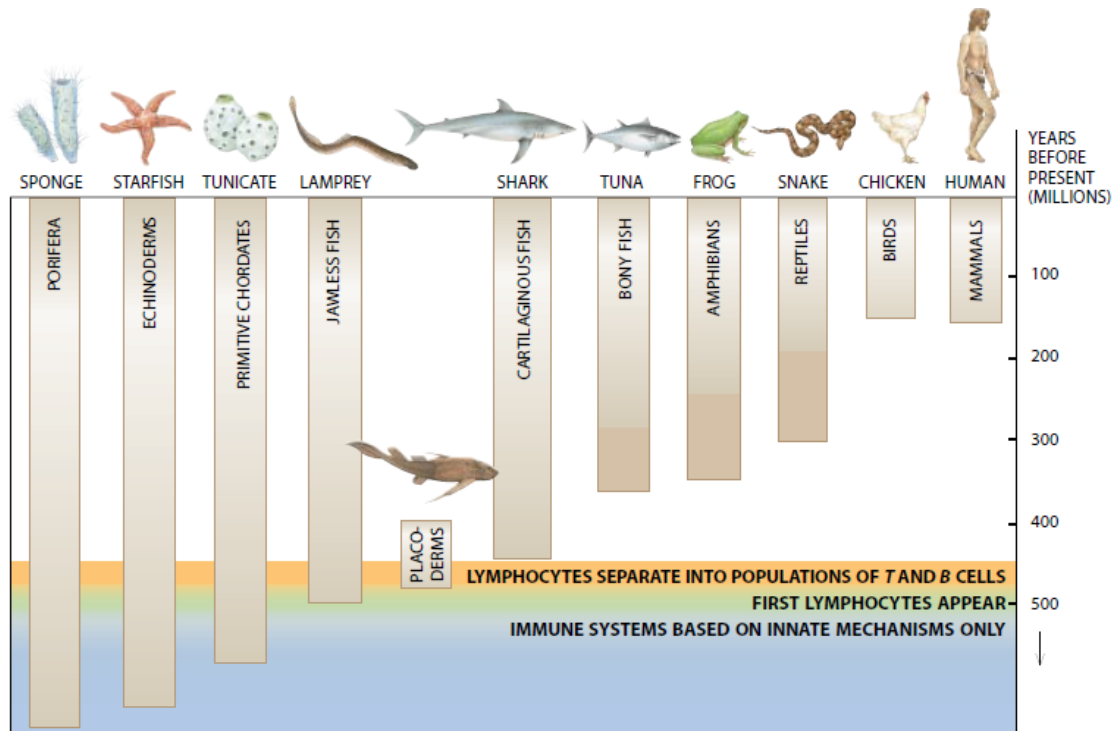
Figure 1.1 | Immunological Milestones

Lymphocytes appeared 500 million years ago. At the same time the first creatures with backbones (vertebrates) occurred, e.g. lamprey. Later on, lymphocytes separated into two main distinct populations, T- and B- cells. Invertebrates have a family of cells that resemble vertebrate immune cells in some respect [3].

Antibodies, proteins produced and secreted by B-lymphocytes, are specifically directed against microbial antigens. These proteins recognize and neutralize the infectivity of the microbes, and target extracellular pathogens and toxins for elimination by various effector mechanisms. Cell-mediated immunity, to a large extent mediated through T-cells, is directed against intracellular microbes, such as viruses and bacteria that are able to survive and proliferate within phagocytes and other host cells [2].

Lymphocytes usually only produce a single receptor out of billions possible. Many experiments have established that if this receptor is self-reactive, a variety of strategies are employed to handle this threat, e.g. death by clonal deletion (Burnet), VDJ SHM editing, biochemical or genetic alterations leading to clonal anergy and more [5]. But still, defects in a single checkpoint (e.g. the expression or function of AIRE (Autoimmune regulator)) can lead to severe autoimmune diseases [5]. Autoimmune diseases, which are often chronic, are significant causes for morbidity and mortality. They develop when self-reactive lymphocytes escape from tolerance and become activated. The mechanisms of self-tolerance can be divided into central tolerance and peripheral tolerance. In central tolerance, immature lymphocytes which recognize

self-antigens in generative lymphoid organs (the bone marrow for B-cells and thymus for T-cells) die by apoptosis; in peripheral tolerance, mature self-reactive lymphocytes encounter self-antigens in peripheral tissues and are killed or shut down. The principal mechanisms of peripheral tolerance are anergy (functional unresponsiveness), deletion (apoptotic cell death), and suppression by regulatory T-cells [6, 7]. In general, autoimmunity is a combination of genetic variants, possible acquired environmental triggers like infections, and stochastic events [6].

1.2 Development and function of T-lymphocytes

1.2.1 T-cell development

Cellular immunity is mediated by T-cells. T-cell progenitors arise in the bone marrow, migrate to the thymus and mature. There are two major subsets of T-cells, distinguished by function and surface molecules, CD4$^+$ or helper T-cells, and CD8$^+$ or cytotoxic T-cells (CTLs). Both subsets express an antigen receptor called the $\alpha\beta$-receptor (a smaller subpopulation of T-cells expresses a different antigen receptor, termed $\gamma\delta$). Thymic development of T-lymphocytes is characterized by several distinct stages which require relocation of developing lymphocytes into, within and out of several compartments of the thymus (Figure 1.2) [8]. At the beginning, T-lymphocyte progenitor cells arise from common lymphoid progenitor (CLP) cells in the bone marrow migrate through blood vessels to the thymus, where they become CD4$^+$ CD8$^+$ double positive (DP) thymocytes at the outer cortex. Chemokine signaling through chemokine receptors (CXC, transmembrane receptors with two N-terminal cysteines separated by one random amino acid) mediate migration of thymocytes within the thymus (Figure 1.2). Inside the cortex, the positive and negative selection of DP thymocytes takes place. Subsequently, positively selected cells interact with medullary thymic epithelial cells (mTECs) to ensure central tolerance and complete the development [9-11].

At this stage, antigen-receptor rearrangement takes place which involves the opening of the TCR locus and the joining of DNA segments to generate a functional antigen receptor gene. Nucleotides are randomly added or removed between the gene segments being joined together, thus maximizing variability among receptors. Positive selection facilitates the survival of potentially useful lymphocytes, and this developmental event is linked to lineage commitment, the process by which lymphocyte subsets are generated.
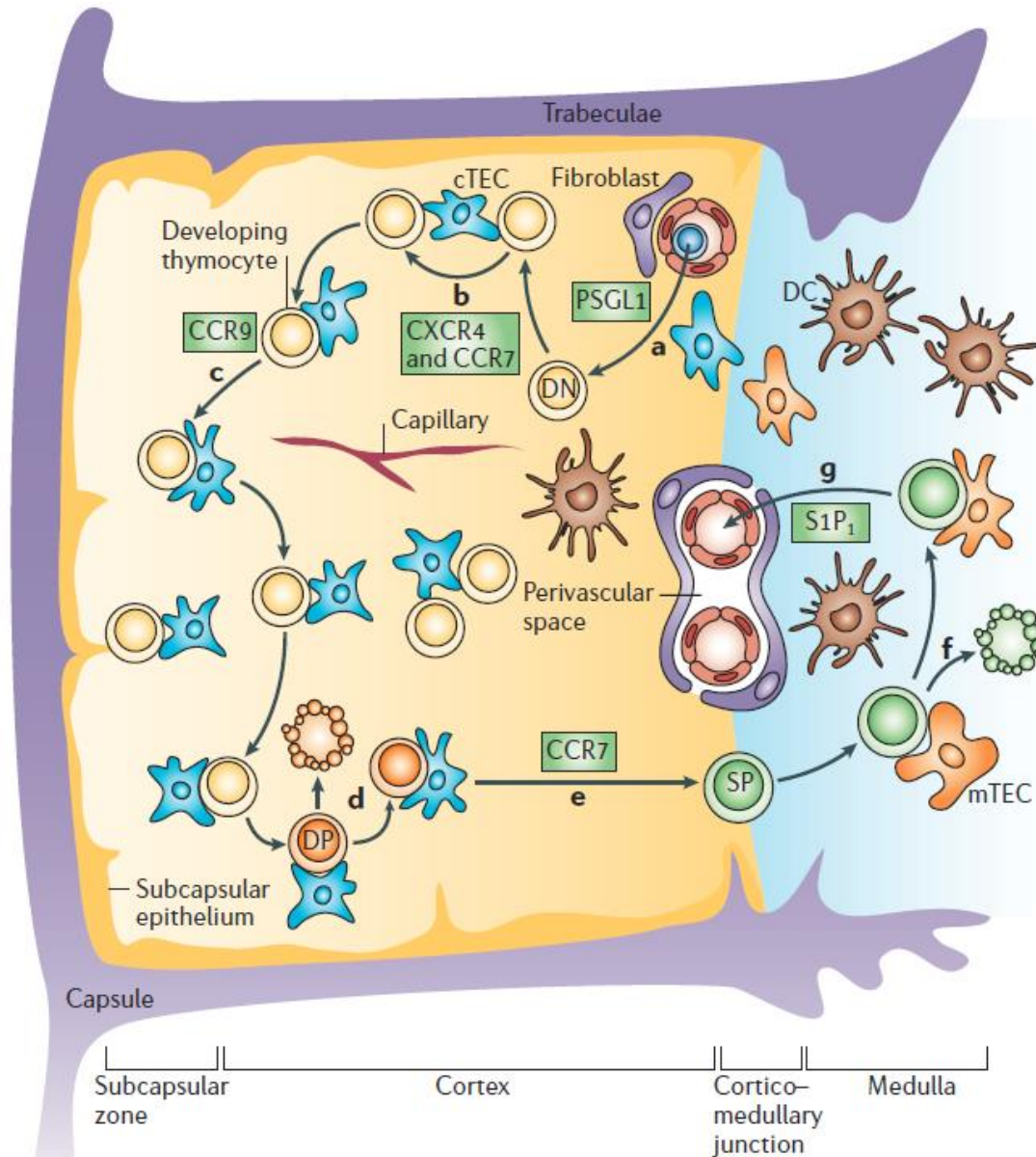
Figure 1.2 | Traffic of thymocytes for T-cell development and selection in the thymus [8]

a) T-lymphoid progenitor cells migrate into the thymic parenchyma through the vasculatures that are enriched around the cortico–medullary junction. b) Outward migration of CD4⁻CD8⁻ double-negative (DN) thymocytes mediated by chemokine signals through CXC chemokine receptor 4 (CXCR4) and CC-chemokine receptor 7 (CCR7). c) Outward migration of the DN thymocytes to the subcapsular region directed by CCR9 signals. d) CD4$^+$CD8$^+$ double-positive (DP) thymocytes generated in the outer cortex are motile, interacting with stromal cells that are localized in the cortex for positive and negative selection. e) Positively selected DP thymocytes that gain the capability to survive and differentiate into CD4 or CD8 single positive (SP) thymocytes show an increase in the surface expression of CCR7. f) In the medulla, further selection of SP thymocytes includes the deletion of tissue-specific-antigen-reactive T-cells and the generation of regulatory T cells. g) Mature SP thymocytes express sphingosine-1-phosphate receptor 1 (S1P1). cTEC, cortical thymic epithelial cell; DC, dendritic cell; mTEC, medullary thymic epithelial cell; PSGL1, platelet-selectin glycoprotein ligand 1.

9

Maturation of T-cells whose receptors weakly recognize self MHC molecules is required. Additionally, expression of the appropriate co-receptor in a T-cell (CD8 or CD4) is matched to the recognition of the appropriate type of MHC (MHC class I or MHC class II). Negative selection eliminates or alters developing lymphocytes whose antigen receptors bind strongly to self-antigens present in the generative lymphoid organs. T-cells with a high affinity for self-antigens are eliminated by apoptosis, a process designated as clonal deletion [2].

1.2.1.1 Molecular mechanisms controlling T-cell development

Transition from a CLP to a developing $\alpha\beta$- (or $\gamma\delta$ -) T-cell requires the accessibility of the T-cell receptor β locus. Transcription factors of the Notch family, represented by four homologs in mammals (Notch-1-Notch-4), play an important role in early T-cell development [2]. These proteins interact with a number of surface-bound or secreted ligands (Delta-like 1, Delta-like 3, Delta-like 4, Jagged 1 and Jagged 2) [12, 13], mediated and modulated by proteins of the Fringe family (Lunatic, Manic and Radical Fringe). Once its surface component gets engaged with one of its ligands on neighboring cells, members of the ADAM protease (A Disintegrin And Metalloproteinase) family proteolytically cleave the transmembrane protein. The intracellular part of the protein is released from the cell membrane into the cytoplasm and translocated to the nucleus, where it acts on its target genes [13]. In lymphoid progenitor cells, Notch-1 is activated and collaborates with GATA-3 to commit developing lymphocytes to the T-lineage. Target genes include components of the pre-TCR machinery. One of the more important target genes of Notch-1 belongs to a family of bHLH (basic Helix-Loop-Helix) proteins known as HES (Hairy-Enhancer of Split)[14]. Interference of the *Hes-1* genes has critical consequences including defects in thymic development [15]. Another important target in T-cell development appears to be NF-κB2 (p100/p52). By converting CBF-1 (C-promoter Binding Factor 1) from a transcriptional repressor to a transcriptional activator, Notch-1 increases the expression of NF-κB2 [16]. NF-κB activity has been associated with protection from apoptosis in lymphoid tissue it is likely that its expression has significant effects on cell death of lymphoid cells [15]. Notch-1 deletion in the bone marrow and thymus of mice leads to severe deficiencies in thymic growth at the $CD44^{+}CD25^{-}CD3^{-}$ DN1 stage [17]. Remarkably, $B220^{+}$ -cells start developing in the thymus of these mice suggesting that in the absence of Notch-signaling early lymphoid precursors choose a B-cell fate in a bone marrow independent manner [15].

I. INTRODUCTION

Early T-cell development is further characterized by the proliferation of committed progenitors induced by cytokine-derived signals consequently creating a large pool of individual progenitor cells. This provides a highly diverse repertoire of mature, antigen-specific lymphocytes [2]. Interleukin-7 (IL-7) was shown to play a pivotal role in this process by promoting survival and differentiation of progenitor cells [18]. After binding to its heterodimeric receptor consisting of the IL-7 receptor α-chain (*Il-7 Rα*) and the common γ-chain (γc), IL-7 activates the tyrosine kinases JAK1 (Janus Kinase 1) and JAK3, which ends in the activation of STAT5 and, as shown by *Amiya K. Patra* in our laboratory, in NFATc1 activation (s. Fig. 1.3) [19-21].
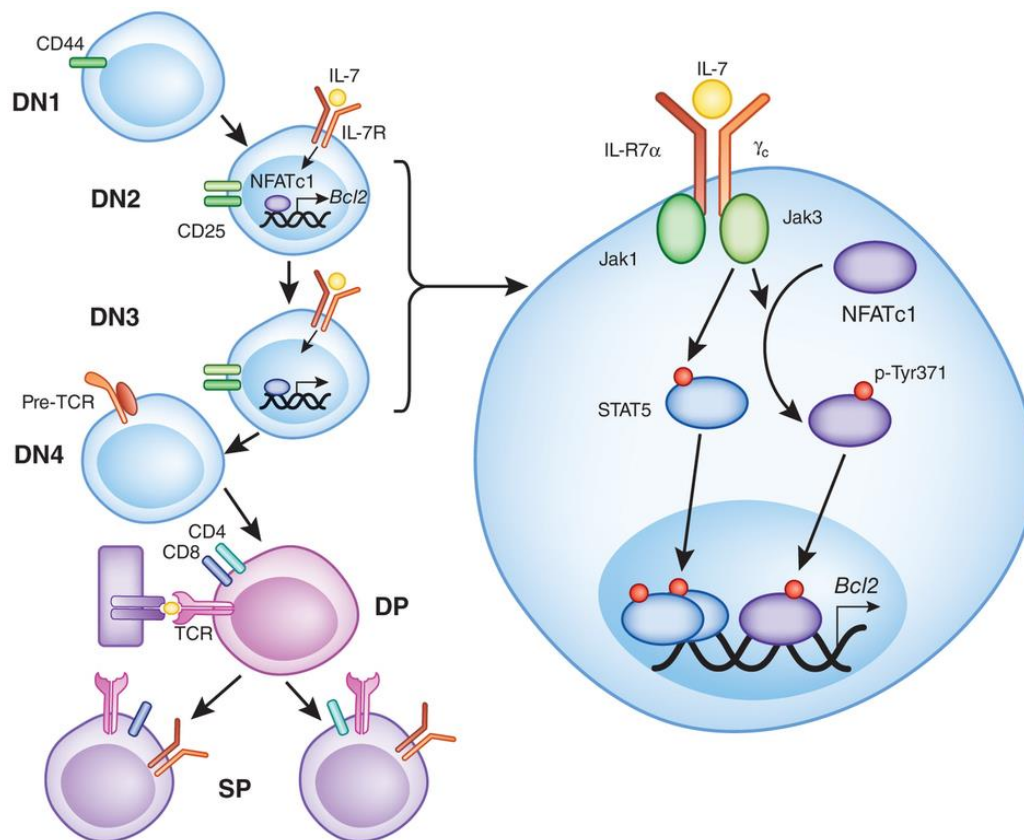
Figure 1.3 | Thymocytes receive survival signals provided by the engagement of different receptors at different stages of development [19, 22]
In DN2 and DN3 thymocytes, *Bcl2* expression is induced as a consequence of non-canonical activation of NFATc1. Engagement of IL-7R recruits JAK3 to the common γ-chain (γc), which then phosphorylates NFATc1 at Tyr371 (p-Tyr371). This modification induces translocation of NFATc1 to the nucleus and binding of this transcription factor to the *Bcl2* promoter, where it acts together with STAT5 to induce the transcription of *Bcl2* to maintain thymocyte viability. CD44, hyaluronic acid receptor; CD25, IL-2 receptor α-chain [22].

Due to a block in the differentiation of DN1 cells into DN2 cells, it has been demonstrated that mice deficient in IL-7 (*Il-7 -/-*) or IL-7 Rα (*Il-7r -/-*) have a very small thymus and a much smaller peripheral T-cell population [19, 23, 24]. These effects can be rescued by the transgenic

expression of *Bcl-2* suggesting BCL-2 as a critical downstream molecule of IL-7 signaling (Figure 1.3) [25-27]. Moreover, IL-7 dependent activation of JAK3 leads to tyrosine phosphorylation of NFATc1, which results in its activation and translocation to the nucleus. This alternative NFAT-activation pathway is calcineurin independent and critical for the survival and differentiation of early DN thymocytes before β-selection [19]. *Bcl-2* expression in DN thymocytes seems to be an NFATc1 dependent event because neither NFATc2 nor NFATc3 - both of which are also expressed in DN thymocytes - can compensate for the absence of NFATc1 after its knockdown in DN cells [19, 22]. Hence, NFATc1 and STAT5 are likely to act together to induce the transcription of *Bcl2*, as suggested by the finding that NFATc1-deficient DN thymocytes still express *Bcl2*, but to a much lesser extend [19, 22].

1.2.2 T-cell activation

TCRs are able to recognize only a few activating, non-self peptide-MHC (pMHC) complexes within a much larger pool of self-pMHC expressed and presented by antigen presenting cells (AP-Cs). *In vivo*, this recognition appears very rapidly while presenting and recognizing cells pass each other. TCRs are exclusive and clonal, generated by random swapping and editing of DNA segments prior to any exposures with associated pMHC [28]. Apparently, the receptor recognition system is highly capable of identifying rare pathogen-associated ligands while learning to ignore self and benign foreign antigens. Since the effects of errors are sincere, a failure to recognize or mount an appropriate response to pathogen-associated antigens can lead to autoimmunity from inappropriate recognition of self to chronic infection or death. This communication of T-cells with AP-Cs has been divided into three distinct stages [28, 29]. The first stage includes initial transient T-cell – AP-C interactions characterized by continued rapid T-cell migration which might last, depending on the pMHC density, 30 minutes to 8 hours. The second step is a period of ongoing interactions between the T-cell and the AP-C counterpart that may last for up to 12 hours. During this period of time cytokines, such as IL-2, are produced. Phase 3 displays a return to the transient T-cell – AP-C interaction and rapid T-cell movement throughout the T-cell divides multiple times and subsequently exits the lymphoid tissue [28]. An exact interpretation of these stop and go signals is vital for the origination of effector and memory T-cells [28, 30].

By means of fixed-cell imaging studies, the formation of a so-called bull´s eye pattern with a central cluster of TCR-pMHC was revealed that is defined as the cSMAC (central

I. INTRODUCTION

Supramolecular Activation Complex), which is surrounded by a ring of the cognate integrin LFA-1 (Lymphocyte Function-Associated antigen 1) and its immunoglobulin superfamily ligand ICAM-1 (Intercellular Adhesion Molecule 1), designated as the pSMAC (peripheral SMAC). The area around the pSMAC, defined by the high expression of CD45, is referred to as dSMAC (distal SMAC). Importantly, it was shown that the formation of an Immunological Synapse (IS) through a nascent intermediate in which activating TCR clusters form first in the dSMAC and then move to the cSMAC region, in an F-Actin-dependent manner, occurs within a few minutes [28, 31]. Establishment of the IS correlates with full T-cell activation over a timescale of several hours. Signaling events sustained by the TCR are constantly engaged within the dSMAC and progress towards the cSMAC in many cases. This progression of cluster formation and migration ends in TCR signal termination [28, 32].

The exact mechanism of initial TCR triggering is still unknown and remains to be elucidated. Signaling proteins of the immune receptor family are often found closely to non-receptor tyrosine kinases of the Src-family (cellular homologue of the transforming protein of the Rous sarcoma virus, called c-SRC, a prototype for a family of non-receptor tyrosine kinases) [2]. Tyrosine residues, located within the cytoplasmic part of immune receptor molecules as a part of signaling proteins, commonly belong to one of two tyrosine based motifs. ITAMs (Immunoreceptor Tyrosine-based Activation Motifs) are involved in activation processes, whereas ITIMs (Immunoreceptor Tyrosine-based Inhibitory Motifs) are part of the inhibition of cellular events [2]. Phosphorylation occurs on two possible tyrosine residues present on the cytoplasmic part of ITAMs by SRC-family kinases (e.g. *Lck*) during immune receptor activation. SYK/ZAP-70, a distinct tyrosine kinase harboring tandem SH2 domains, that each binds to one of the two phosphorylated YxxL/I motifs, is recruited towards phosphorylated ITAMs (Figure 1.4).
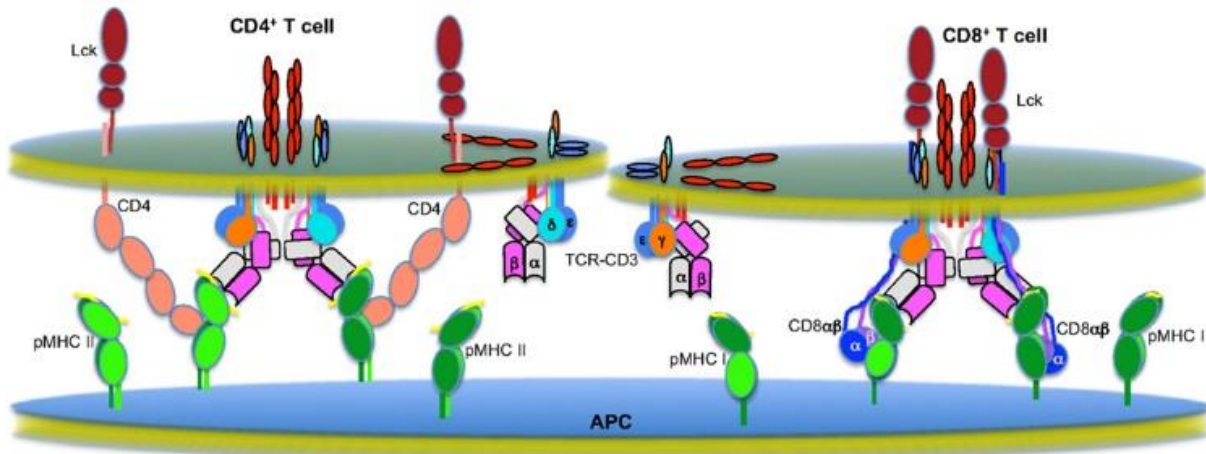
Figure 1.4 |The T-cell signaling machinery [33]
The multi-molecular higher-order assemblies that mediate sustained TCR signaling on CD4$^+$ (left) and CD8$^+$ (right) T cells.

This particular binding of SYK (or ZAP-70) to a phosphorylated ITAM results in a conformational change within this kinase and therefore its activation [2]. *In vivo*, TCR engagement also involves co-ligation of either the CD4 or CD8 co-receptor, respectively. In consequence, LCK is released from CSK inhibition (Figure 1.5). This leads to LAT (Linker for Activation of T-cells) activation, phosphorylated by ZAP-70, it ligates phospholipase Cc1 (PLCc1), GRB2/SOS/RAS and GADS/SLP-76 (SH2-domain-containing leucocyte protein of 76 kDa)/VAV and activates the respective downstream signaling pathways of Ca^{2+}/InsP3 (IP3), RAS/RAF/ERK and RHOA which leading to gene regulation, proliferation and actin-reorganization. This gene regulation, in turn, leads to the activation of the tyrosine kinases of the Src family, such as *Lck* and *Fyn,* as well as the release from inhibition by the tyrosine kinase CSK [34]. Co-activation by B7 interaction with CD28 involves the TEC family of PTKs (*Itk*), whereas activation via the Toll-like receptor pathway (TLR-4) or cellular stress triggers the nuclear factor κB (NFκB) pathway involving Ser/Thr kinases (e.g. IκB kinases) [34]. Activation of PLCγ1 leads to the cleavage of plasma membrane-bound PIP2, generating diacylglycerol (DAG), which activates members of the protein kinase C (PKC) family and also RAS-dependent pathways, and 1,4,5-inositol trisphosphate (IP3). These events initiate the entry of Ca^{2+} to the cytosol from the endoplasmatic reticulum (ER) and, subsequently, from the extracellular space. Calcium influx is maintained for approximately 2 hours keeping NFAT in the nucleus [35] and thereby keeping it transcriptionally active (Figure 1.5) [36].
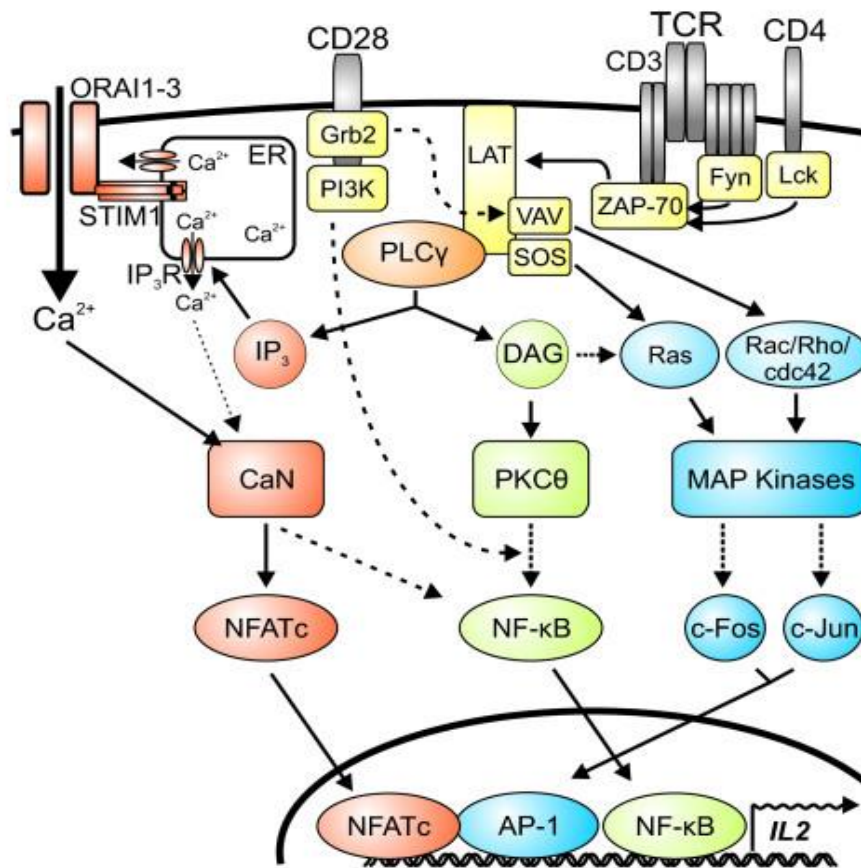
Figure 1.5 | Intracellular signaling pathways and kinases in T-cell activation [37]
The engagement of TCRs and costimulatory CD28 receptors promote signalling cascades of kinases and adaptor proteins (yellow). They trigger pathways resulting in the activation of the transcription factors NFATc (red), NF-κB (green) and AP-1 (blue). Ca^{2+} depletion is sensed by STIM1, which is directly coupled to the ORAI CRAC channels. Influx of extracellular Ca^{2+} into the cytosol activates calcineurin (CN), leading to the dephosphorylation and nuclear translocation of NFATc.

1.3 Development and function of B-lymphocytes

1.3.1 B-cell development

B (*bursal* or bone marrow derived) -cells represent a subset of lymphocytes that express clonally diverse cell surface Ig receptors which are capable of recognizing specific antigenic epitopes. The development of B-cells is subdivided in several distinct stages that begin in primary lymphoid tissue (fetal liver and fetal/adult bone marrow), followed by sequential functional maturation in secondary lymphoid organs (lymph nodes and spleen). The

physiological end-point of B-cell development is the generation of antibody producing and terminally differentiated plasma cells [38].

Firstly, a functional division of labor between cells in the chicken bursa of Fabricius responsible for antibody production and cells that required an intact thymus for manifestation of delayed-type hypersensitivity was described by Max Cooper and Robert Good [39, 40]. Antibody production was connected to B-cells by studies which used surface Ig expression as markers to characterize normal and abnormal (e.g. leukemic) B-cells [41, 42]. A hallmark of B-cells is the functional rearrangement of the Ig loci. This event occurs in an error-prone manner involving the combinatorial rearrangement of the V, D, and J gene segments in the Ig heavy (H) chain locus and the V and J gene segments in the light (L) chain loci. Ordered Ig H and L chain loci rearrangement is a characteristic of early stage B-cell development, and Ig proteins are actively regulating this process [43]. Early stage pre-B-cells originate from progenitor (pro-B) cells which express neither a pre-B cell receptor (BCR) nor surface Igs [44]. The expression of the BCR is mandatory for B cell development and survival in the periphery [45]. Activation and differentiation of B-cells, driven by antigen induction, are mediated by dynamic changes in gene expression which, in the end, lead to the germinal center (GC) reaction (Figure 1.6). This process is discriminated by clonal expansion, class switch recombination (CSR) at the IgH locus, somatic hypermutaion (SHM) of V_H genes, and selection for increased affinity of a BCR for its unique antigenic epitope through affinity maturation. CSR, also known as isotype switching, and SHM are mediated by an enzyme designated as activation-induced cytidine deaminase (AID). Expression of AID is induced during GC formation where CSR and SHM occur [46].

1.3.1.1 Molecular mechanisms controlling B-cell development

A variety of transcription factors regulate the early stages of B-cell development. Among them are E2A, EBF and PAX5 (Paired Box 5) that are particularly important in promoting B lineage commitment and differentiation [47]. For example, PAX5-deficient mice have an arrest in B-cell development at the transition from DJ to VDJ rearrangement. Pro-B cells lacking PAX5 have the capacity to adapt non-B-lineage fates and can develop into other hematopoietic lineages [48].
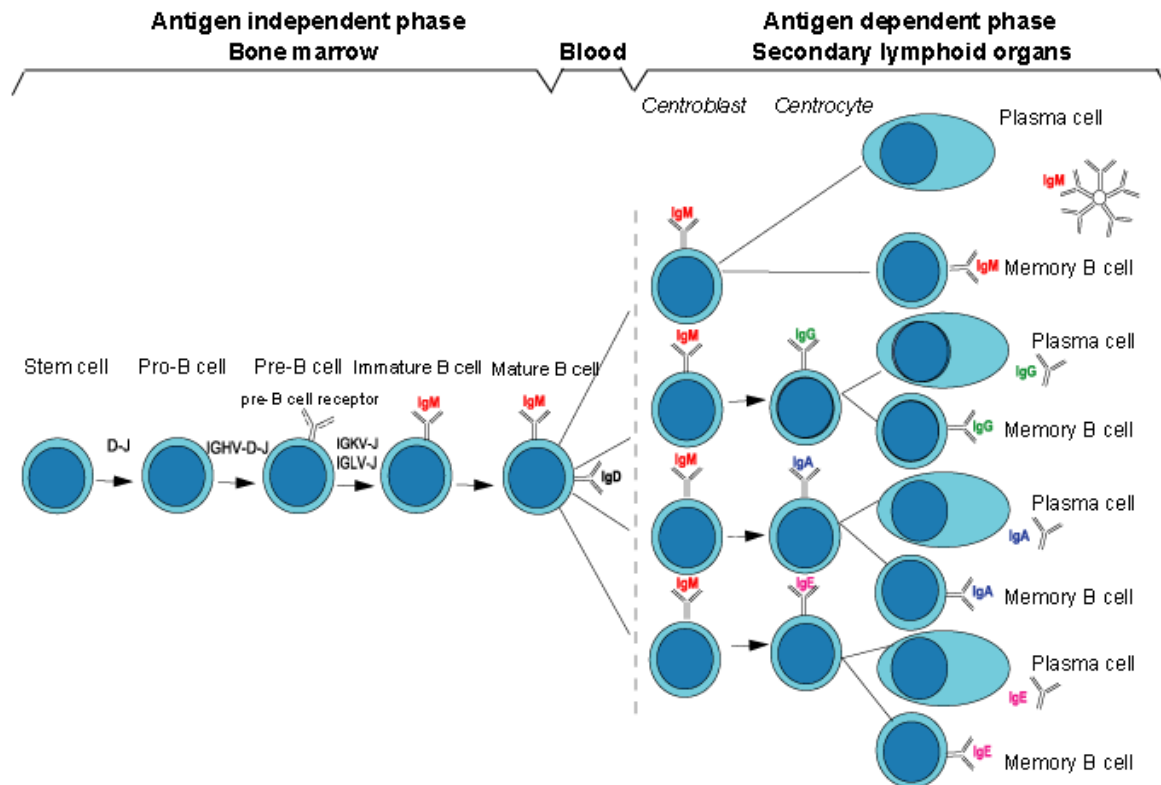
Figure 1.6 | Stages of B cell development
B-cell differentiation from hematopoietic stem cells to mature B-cells in the bone-marrow is antigen-independent. The final differentiation stages, from the mature B-cell to the plasma cell and memory B-cell, in the germinal centers of the secondary lymphoid organs is antigen dependent. It requires cooperation between B- and T-cells [49].

Conditional PAX5 deletion in mature murine B-cells can lead to de-differentiation to an uncommitted hematopoietic progenitor and furthermore to subsequent differentiation into T-lineage cells [50]. Additionally, dysregulation of PAX5 frequently leads to the development of high-grade lymphomas [50].

The majority of mature B-cells belongs to the subset of follicular B-cells which, in addition to IgM, produces IgD. These cells co-express μ and δ heavy chains using the same VDJ exon to generate the V domain, and in association with the same κ or λ light chain, produce two membrane receptors with the same antigen specificity. Co-expression of IgM and IgD is complemented by the ability to recirculate and the acquisition of functional competence [2]. Different types of B-cells, such as marginal zone (MZ) B-cells or B-1 cells with a broad spectrum of specialized functions have been described. B-1 cells, for instance, show unique characteristics concerning phenotypical function, localization and natural antibody production, when compared to conventional B (or B-2) cells [51]. Peritoneal B-1 cells can be subdivided in CD5$^+$ (B-1a) and CD5$^-$ (B-1b) but so far it has not been clarified whether or not these cells

17

derive from the same progenitors as B-2 [52]. Both B-1, MZ and GC B-cells contribute to the circulating natural antibody pool. Furthermore, these cells generate the thymic-independent IgM antibody responses by terminal differentiation into plasma cells, the effector cells of humoral immunity [53, 54]. Two transcription factors, BLIMP-1 (B-Lymphocyte-Induced Maturation Protein-1) and BCL-6, are prominent regulators of plasma cell development [55]. Antigen-specific antibodies, derived from so-called long-lived plasma cells, are systemically present over decades. Primary and secondary immune responses generate pools of long-lived plasma cells in the spleen, which migrate to the bone marrow where they occupy essential survival niches and can persist throughout a life time without the need for self-replenishment or turnover [56].

1.3.2 B-cell activation and function

B-cell activation begins with the binding of antigen to the BCR, followed by signaling events which lead to proliferation and differentiation of memory or plasma B-cells. The BCR consists of an antigen binding membrane immunoglobulin (mIgM) component in complex with an Igα/Igβ sheath containing immunoreceptor tyrosine activation motifs (ITAMs), which enable the transmission of intracellular signaling. Receptor clustering, also termed receptor cross-linking, and subsequent ITAM phosphorylation by the Src-family kinase LYN (Lck/Yes related novel tyrosine kinase) succeed antigen encounter on the surface of a B-cell. A multiprotein-complex of intracellular signaling molecules, such as SYK, PLCγ2 (Phospholipase-Cγ2), PI3K (Phosphoinositide 3-kinase), BTK (Bruton´s tyrosine kinase), VAV and several adaptor molecules, such as B-cell linker (BLNK) assembles within the cell [57-60]. This so-called signalosome orchestrates the coordinated regulation of succeeding downstream cellular events, including signaling through second messengers, like calcium, and, finally, gene induction. Antigen processed in the endosomes is loaded onto major histocompatibility complexes (MHCs) and presented on the cell surface [61]. It was suggested that BCRs may interact within the resting membranes, forming an oligomeric structure prior to antigen stimulation [62]. But FRET (Fluorescence Resonance Energy Transfer) studies revealed no direct interactions between Igα-molecules, suggesting that the BCR exists in a monomeric form on resting cells [63]. Still, the exact mechanism remains elusive by which extracellular antigen engagement is communicated across the membrane to trigger B-cell activation.
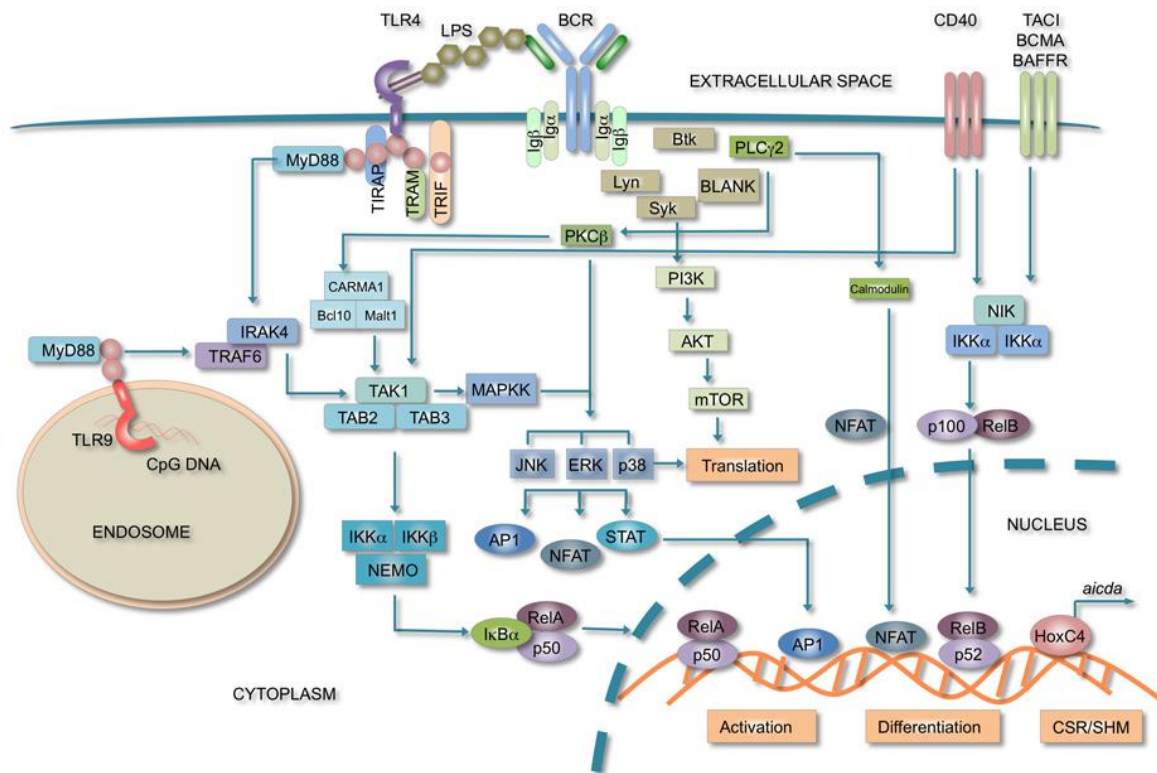
Figure 1.7| Signaltransduction during B cell activation[64]
BCR engagement triggers Src-family of TKs (Fyn and Blk) which leads to tyrosine phosphorylation at the cytoplasmic tails of Igα− and Igβ-docking sites for SYK. SYK activates PLCγ2 by tyrosine phosphorylation. PLCγ2 hydrolyses PIP$_2$, which produces DAG and IP3 activates PKC that in turn activates CREB. The RAS-pathway initiates a MAP kinase cascade, and subsequent nuclear translocation of ERK. Transcription factors, such as AP-1, NFAT and NFκB are activated. By involvement of TLR4, triggered by LPS, the proteins MyD88 and IRAK4 are activated, and in turn activate the RELA/p50 complex. Endosomal TLR9 may also activate MyD88 upon activation which triggers TRAFs, MAPKK and NF-κB. CD40 activation leads to NIK, IKKα and in turn p100/RELB activation. BAFFR engagement triggers TRAF3, degrading TRAF2 and thereby releasing NIK which also activates p100/RELB. (TK: tyrosine kinase; PLCγ2: phospholipase C γ2; PKC: protein kinase C; LPS: Lipopolysaccharide; TLR: Toll-like receptor; NIK: NF-κB inducing kinase; TRAF: TNF receptor associated factor).

Nevertheless, it is assumed that B-cell activation is a result of multimerization of monomeric receptor units. This assumption is supported by imaging studies that show cross-linked BCRs located in a cap structure right after stimulation with soluble multimeric antigen [58, 65, 66]. This structure creates proximity between ITAM motifs of numerous Igα/Igβ sheaths within the membrane entailing phosphorylation and terminally the assembly of the signalosome. Alternatively, a higher order structure of the BCR within the cell membrane was suggested. In this scenario, activation of the BCRs may be triggered by antigen binding and disruption of an

existing oligomeric structure [67]. BCR microclusters were observed to form promptly in the B-cell membrane following contact with antigen, in concert with the initiation of calcium signaling [58]. These microclusters are thought to contain 50 to 500 molecules of BCRs, and in primary B cells, they may consist of IgM alone, IgD alone, or a mixture of both isotypes [58]. Microcluster formation apparently does not depend on BCR signaling since it was observed in membranes of *Lyn*-deficient B cells. It was also shown that the formation is abrogated if cells were treated with actin polymerization inhibitors [58, 68, 69]. Microcluster formation, post antigen engagement, triggers rapid phosphorylation of several downstream molecules, such as PLC-γ2, BTK and others, by the tyrosine protein kinases LYN and SYK. Phosphorylated B-cell receptor adaptor proteins, such as SLP-65/BLNK [70], assemble to supramolecular complexes that transmit BCR signals to downstream serine/threonine protein kinases and subsequently activate transcription factors. PLC-γ2 affects the release of Ca^{2+} from intracellular stores and consequently the influx of extracellular Ca^{2+} [70]. Elevated intracellular calcium levels activate the Ca^{2+}/calmodulin dependent Ser/Thr-specific phosphatase CN, which in turn leads to de-phosphorylation, translocation and activation of NFAT proteins [71]. Mice deficient for NFATc1 in B cells revealed impaired responses to BCR activation in terms of proliferation and higher susceptibility to activated-induced cell death (AICD). Furthermore, B-cells from these mice showed a strong decrease in Ig class-switch to IgG3 upon immunization with T-cell-independent type II antigens and IgG3$^+$ plasmablast formation [70]. Besides antibody production, B-cells are necessary for the initiation of T-cell immune responses [72]. Following antigen internalization and processing, B-cells present peptide fragments to T-cells in an MHC-restricted manner [73]. T-cell proliferation as well as secretion of IL-2 and Interferon-γ (IFN$-\gamma$) upon stimulation by B-cells was shown to be markedly reduced in B-cells deficient for NFATc1 (*Nfatc1$^{-/-}$*). The increase in number of CD1d^{high}CD5$^+$ IL-10 producing B-cells may also contribute to a mild clinical course of experimental autoimmune encephalomyelitis (EAE) observed in these mice [70].

1.4 B-cell lymphomas

1.4.1 B-cell lymphoma classification

According to the National Cancer Institute´s (U.S.) working formulation of non-Hodgkin´s lymphomas (NHL) for clinical usage, NHLs are grouped in several subclasses. Overall, there is an agreement of determining lymphomas by clinical, pathological, and experimental

characteristics into low-, intermediate- and high-grade malignant lymphomas [74]. Low-grade malignant lymphomas are characteristically not curable by chemotherapy although patients have relatively long survival rates. Lymphomas of this type show an indolent clinical course with a non-destructive growth pattern and are responsive to regulatory influences. High-grade malignant lymphomas, on the other hand, show an aggressive clinical course and a short survival rate without clinical treatment. These lymphomas display a destructive and autonomous growth pattern [74]. Low-grade lymphomas can be further subdivided into i) small lymphocytic, ii) follicular, predominantly small cleaved cells, and iii) follicular, mixed small cleaved and large cells. Intermediate-grade lymphomas may be i) follicular, predominantly large, ii) diffuse with small cleaved, mixed or large cleaved cells. High-grade malignant lymphomas can be divided in i) large cells and immunoblastic or, ii) lymphoblastic, or iii) small, non-cleaved cells [75].

The largest group of the low-grade malignant B-cell lymphoma are follicular lymphoma, accounting to approximately 45% of all cases. As an adult stage disease, it occurs equally often in males and females. Defined by neoplastic growth, cells form follicular aggregates that have a tendency to mimic normal lymphoid follicles. Cytologically, these cells strongly resemble cells within the normal germinal center formation [75]. The larger part of non-Hodgkin´s lymphomas diagnosed in the U.S. and Europe are of B-cell origin and fall into the midstage of B-cell differentiation. Commonly, cells at this stage express monoclonal surface Ig, mostly IgM, with or without IgD, and usually express pan-B-cell antigens, such as CD19, CD20 and CD22 [76].

WEHI-231 cells were described to resemble the characteristics of human mantle cell lymphoma (MCL) in great detail, which are a particularly difficult type to treat [77]. MCL is a malignant NHL of the B-cell lineage and its normal cell counterpart is thought to be IgM^+, IgD^+ (naïve) B-cell in the mantle zone of lymphoid follicle [78]. Like chronic lymphocyte leukemia (CLL), MCL cells do also express CD5 on their surface. Furthermore they express the pan-B-cell markers CD19, CD20 and CD24. But in contrary to CLL, they do not express CD23 which, therefore, is used as a clinical marker to distinguish CLL from MCL. Similarly to the MCL phenotype, all WEHI-231 lines are also positive for surface IgM, CD5, CD19 and CD22. Additionally, like MCL, WEHI-231 cells do express CD79b and are also $CD23^-$ negative [75, 79]. Furthermore, BCL-6 that is mainly present in normal germinal center B-cells and related to follicle center and marginal zone lymphomas, is not expressed in MCL and also not in WEHI-

231 cells [79]. Unlike follicular lymphomas, which show selective involvement of germinal centers, in MCL residual normal germinal centers are predominantly uninvolved by the neoplastic process. This particular mantle zone growth pattern becomes obvious in the small intestine, in the bone marrow and other extranodal sites and, thereby, provides verification for a mantle zone derivation of the malignant cells. Mantle cell lymphomas appear to be unique since a greater proportion of these cases express monoclonal λ-light chains instead of monoclonal κ. Most of the NHL demonstrate a predominance of κ, and there is a preponderance of normal κ-bearing cells in peripheral blood. Unlike all other intermediate-grade malignant lymphomas, the survival curve of MCL patients does not show a plateau or evidence of a cured population, and in this respect they resemble low grade lymphomas [75, 80]. However, the median survival rate is only 5 years, i.e. somewhat less than other low-grade malignant lymphomas.

1.4.2 WEHI-231 B-lymphoma cells

The murine B-cell lymphoma WEHI-231 has been commonly used to study immature B-lymphocytes because it can readily undergo apoptosis in response to antigen engagement [81-83]. Contrary to the classical IgM^+ / IgD^- phenotype of immature B-lymphocytes, WEHI-231 cells are both IgM^+ and IgD^+ [82, 84]. Nonetheless, cross-linking of surface IgM with anti-Ig antibody reagents causes WEHI-231 cells to arrest in the G_0/G_1 phase of the cell cycle, and they die 24-48 hours later. Programmed cell death (PCD) can be avoided in these cells by co-culturing them in the presence of bacterial Lipopolysaccharide (LPS) [85] or Th2 cell clones plus antigen [86]. LPS has been shown to react with LPS-binding protein present in the serum which in turn provides a stimulatory signal by binding to CD14 on the surface of B-lymphocytes. The capacity of Th2 clones to circumvent anti-IgM-induced apoptosis in WEHI-231 cells is partially due to the interaction of CD40 on the B-cell surface with its ligand GP39 on the T-cell [86]. Biochemical inducers of apoptosis, such as Cyclosporine A (CsA) and Forskolin (FK-506), but not Rapamycin, are known to block activation-induced apoptosis in T-cell hybridomas and thymocytes [87, 88]. These three naturally occurring anti-fungal agents have been shown to be powerful immunosuppressants. CsA and FK-506 inhibit antigen dependent signaling events required for IL-2 gene transcription [89]. Both inhibitors interfere with the transcription of a wide array of early phase T-cell activation genes, such as IL-2, IL-3, IL-4, IFNγ, GM-CSF, and TNFα genes [90, 91]. It was originally shown that CsA and FK-506 target the induction of NFAT factors and disturb the generation and ability to interact with

regulatory elements of target genes [92]. In contrast, Rapamycin blocks biochemical events necessary for IL-2 dependent progression from G_1 to S phase in the cell cycle [89]. CsA and FK-506 are capable of inducing growth arrest and PCD in WEHI-231 cells, displaying one characteristic of apoptosis, i. e. the internucleosomal DNA fragmentation after treatment [93].

1.5 Cell death

1.5.1 Apoptosis and Activation Induced Cell Death

Cell death is an important physiological process coordinating the development of tissue and organs in multicellular organisms. During the development of the nervous system, for example, neurons that fail to make the correct connections are prone to die. Cell death occurs during the development of the gut, the remodeling of limb buds, cartilage and bones [94]. Both inhibition of cell death and inappropriate cell death are deleterious and often lead to cancerogenesis. Degenerative neurological diseases, such as Alzheimer disease and Parkinson disease, are associated with the premature death of particular subsets of neurons. In contrast, inhibition of PCD may contribute to diseases of the immune system by allowing the persistence of self-reactive B- and T-cells, thereby promoting autoimmunity [94, 95]. Likewise, cells evading failsafe mechanisms may undergo further transformation and become cancerogenic [94, 96].

As a member of the tumor necrosis receptor family, CD40 is expressed on B-lymphocytes. Its interaction with the CD40L (CD154), expressed on activated T-lymphocytes, is critical for B-cell survival. The expression of the *Bcl-2* gene was shown to inhibit apoptosis in terms of programmed cell death triggered by events like growth factor withdrawal [97] and apoptotic events mediated by the expression of *c-Myc* [98], but not cytotoxic T-cell killing. When expressed in transgenic mice, *Bcl-2* prolongs B-cell survival [99].

Activation Induced Cell Death (AICD) is mediated by the so-called death receptors, such as FAS (CD95/APO-1), a member of the TNF receptor family. Oligomerization of FAS receptors directs the recruitment of the FAS-adaptor protein, FADD, through several death domains (DDs) [100, 101]. FADD harbors two death effector domains (DEDs) through which it recruits caspase-8 or its enzymatically inactive homologue and FAS inhibitor FLIP [102] (Figure 1.8).
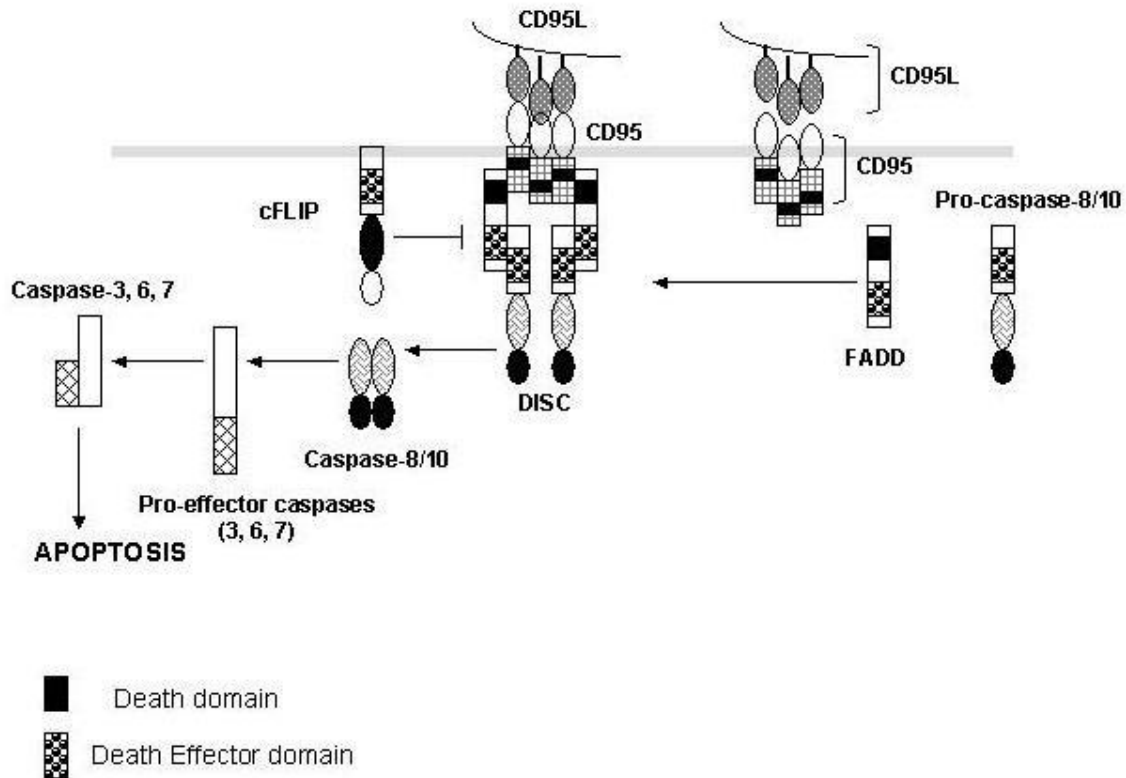
Figure 1.8 | Apoptosis by CD95 ligation
Upon ligation with the CD95-ligand, CD95 undergoes trimerization resulting in the recruitment of FAS-associated Death Domain (FADD) and Procaspase-8 to form Death-Inducing Signaling Complexes (DISC). Procaspase-8 is autolytically activated by homodimerization and released from the DISC into the cytosol, where it cleaves and activates effector caspases to induce apoptosis [103].

Synthesized as pro-enzymes, caspases contain the p20 and p10 domains which are cleaved upon activation to form the active enzyme as a tetramer of two p20-p10 heterodimers. Activated caspase-8 stimulates cleavage of several downstream caspases, like caspase-3, caspase-6 and caspase-7. These effector caspases lack the amino-terminal homo-affinity domains such as DDs, DEDs or CARDS (Caspase Activation and Recruitment Domains) [100, 104], but degrade numerous cellular components, as nuclear lamins, cytoskeletal proteins, like fodrin and gelsolin [105], and the Inhibitor of Caspase-Activated DNAse (ICAD), permitting DNA degradation [106, 107]. Caspase-8 may also cut the BCL-2 homologue BID to produce an active truncated BID (tBID) fragment which interacts and inactivates BCL-2 in the outer mitochondrial membrane, thereby initiating the so called mitochondrial death sequence [100, 108].

In the absence of growth factors, such as IL-2 for activated T-cells, or of a tonic TCR signal for naïve T-cells [109], peripheral T-cells die following strong TCR signaling [110]. During activation, T-cells transiently express FASL and TNFα. Death of mature T-cells induced by

FASL or TNFα may be a homicide by adjacent cells, or suicide [100, 111]. For T-cells, numerous co-stimulatory signals have been described to prevent cells from AICD. CD28 [112], for example, activated by CD80 and CD86 which are expressed on antigen presenting cells, enhances cytokine production and up-regulation of *Bcl$_{XL}$* and *Flip* while it down-regulates *Fasl*. However, CD28 was also shown to augment apoptosis, especially in developing thymocytes [100, 113].

In mature B-cells low levels of the protein c-MYC are expressed. Crosslinkung of membrane-bound IgM (mIgM) on mature resting B-cells induces temporary *c-Myc* up-regulation, and cells enter the cell cycle [114, 115]. Strong activation of mIgM or mIgD may also lead to apoptosis of mature B-cells, unless T-cell help is provided, either by the cytokine IL-4 or by CD40L signaling [116]. For B-lymphoma cell lines (such as WEHI-231, CH31 and ECH408 cells), resembling an immature B-cell state, the situation is different. mIgM crosslinking leads to a transient increase in *c-Myc* mRNA and protein within two hours and a decrease to far below the threshold level at four to eight hours [114, 117-119]. Upon mIgM stimulation this phenomenon was also observed in human Burkitt´s lymphoma cells [120]. Support for the idea that MYC is necessary for anti-IgM induced apoptosis comes from studies in which MYC was overexpressed in WEHI-231 cells, protecting these cells from apoptosis [121, 122]. In WEHI-231 cells *Myc* transcription seems to be regulated by NF-κB [123]. One NF-κB binding-site is located upstream of and one inside the *Myc* promoter [124]. CD40L prevents anti-IgM-induced *Myc* down-regulation via maintaining NF-κB activity in this B-lymphoma cell line [125]. Furthermore, BCL$_{XL}$, an antiapoptotic factor, is also induced upon CD40 ligation [126]. Immunosuppressants, such as rapamycin, FK506 and CsA were shown to initiate growth arrest and apoptosis in immature B-lymphoma whereas BCL$_{XL}$ protects WEHI-231 cells from this apoptosis [93].

Taken together, AICD is an essential part of lymphocyte development and homeostasis and plays an important role in the stability of the immune repertoire, as well as in the regulation of the immune response.

1.6 NFATc proteins

Approximately 500 million years ago the family of genuine Nuclear Factor of Activated T-cell (NFATc) proteins appeared at the same time as the adaptive immune system emerged in

vertebrates [3]. NFATc proteins are present in an inactive, phosphorylated state in cytoplasm of resting cells and translocate to the nucleus after de-phosphorylation. In the nucleus, NFATs bind to specific target sequences, such as promoters or enhancers within regulatory elements of their target genes. CN binds NFAT at specific motifs within the regulatory domain to perform de-phosphorylation [2]. The consensus sequence of this sites was found to be Pro-x-Ile-x-Ile-Thr, in which x can be any amino acid [127, 128]. A peptide of the sequence motif Pro-Val-Ile-Val-Ile-Thr binds CN with high affinity and, therefore, effectively competes with NFAT for CN binding and blocks a de-phosphorylation. This peptide was designated VIVIT and can be used to inhibit NFAT activation [127]. Known NFAT target genes are the cytokine genes encoding IL-2 or IL-4, which contain several strong and weak NFAT binding sites in their regulatory DNA regions [129, 130].

1.6.1 NFAT activation

NFAT is triggered by cell-surface receptor engagement often leading to "store operated" Ca^{2+} influx through PLCγ resulting in elevated intracellular free Ca^{2+} levels. Hydrolysis of PIP2 by PLCγ leads to the generation of IP3 which activates membrane-bound IP3 receptors within the membrane of the Endoplasmatic Reticulum (ER). Due to the depletion of Ca^{2+} stores in the ER this event leads to a massive increase in cytoplasmic Ca^{2+} concentrations. STIM (stromal interaction molecule) proteins act as calcium sensors within the ER and interact with ORAI proteins, components of plasma membrane-bound Ca^{2+} release activated Ca^{2+} (CRAC) channels, to replenish Ca^{2+} levels after ER depletion [131]. The strong increase of free Ca^{2+} leads to the activation of several Calmodulin (CAM)-dependent enzymes, such as the phosphatase CN. CN de-phosphorylates multiple phosphoserines in the regulatory region of NFATc proteins which leads to their nuclear translocation and activation [132]. CN is a heterodimer of a catalytic A subunit (CN A) of approximately 60 kDa in size and a regulatory B subunit (CN B) of approximately 19 kDa. CN A harbors an N-terminal catalytic domain, a helical CN B binding segment, a calmodulin binding segment and an auto-inhibitory peptide [128]. The participation of two distinct EF-hand motifs leads to the activation of CN, including CN B and calmodulin. The regulatory component (CN B) is directly connected to CN A, while calmodulin binding to CN A is Ca^{2+} dependent [128]. The immunosuppressive drugs CsA and FK506, commonly used in transplant medicine, directly target CN. CsA and FK506 form complexes with the immunophilins cyclophilin A and FKBP12 (FK506 binding protein), respectively, and inhibit the phosphatase activity of CN against peptide and protein substrates

[128, 133, 134]. It was shown that the immunosuppressive activity of these compounds is a result of the inhibition of de-phosphorylation of NFAT family member in T-cells and other immune cells [135]. The activation of MAP kinases results in the synthesis of the AP-1 members FOS and JUN which were shown to bind co-operatively with NFAT to composite NF-κB/AP1-sites within the regulatory regions of many target genes [136] (Figure 1.9).

Most NFAT genes are already expressed in naïve T- and B-cells and were also shown to be activated as early as in DN thymocytes. Apparently, unlike numerous lymphokine genes, which are strongly induced by activation of lymphoid progenitor cells or naïve peripheral lymphocytes, in most lymphocytes the *Nfatc1* gene locus is kept in an open chromatin conformation [137]. After a secondary stimulation of T-cells which were skewed into Th1 effector cells, a 5- to 10-fold increase in *Nfatc1* mRNA levels was detected. This finding fits to the appearance of H3K4me3 histone modification marks in Th1 and Th2 cells. In Th17 and regulatory T-cells the *Nfatc1* gene is only weakly expressed [138]. *Nfatc1* is also highly expressed in follicular T-helper cell (T$_{fh}$) and Germinal Center (GC) B-cells [137]. Prodigious differences between *Nfatc1* mRNA and protein levels suggest the existence of posttranscriptional and posttranslational regulatory mechanisms. Remarkably, NFATc1/αA induction upon prolonged incubation of splenic B-cells, stimulated at first by anti-IgM and subsequently by anti-CD40, or LPS, or CpG suggests a close association between NF-κB factors and NFATc1/αA expression in the survival and differentiation of peripheral B-cells [137].
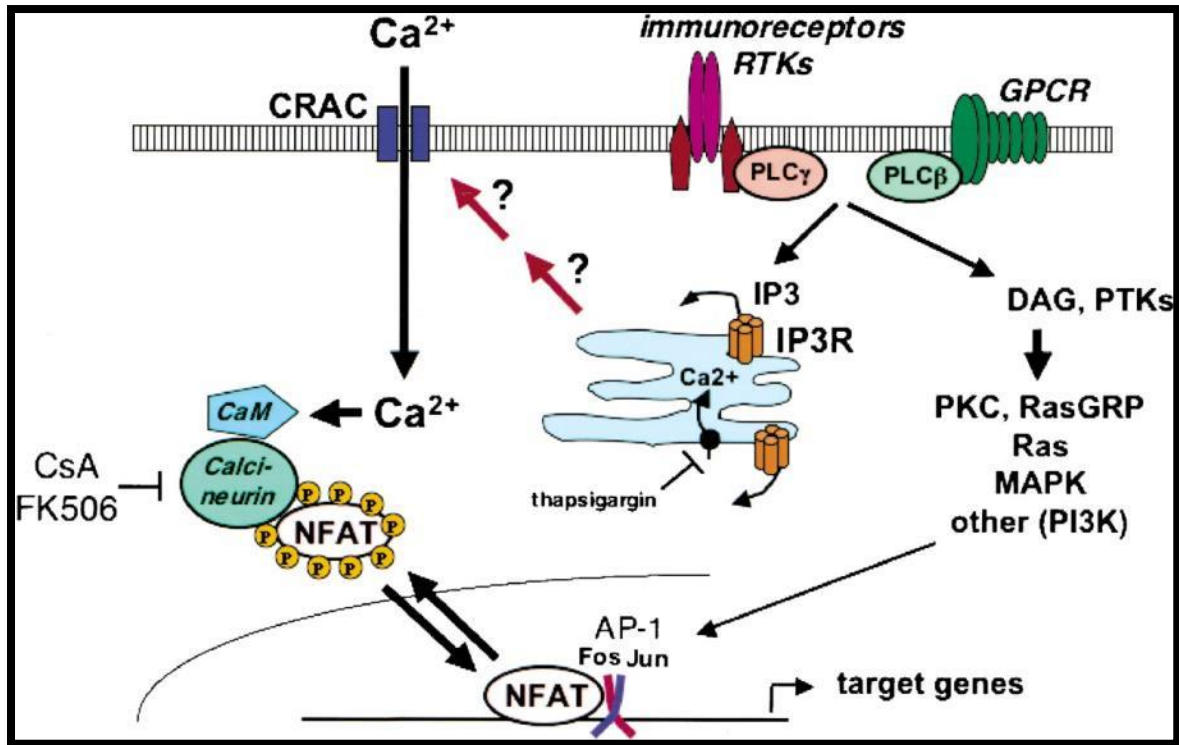
Figure 1.9 | Schematic view of NFAT activation [132]
NFAT is activated by cell-surface receptors coupled to Ca^{2+} mobilization. Immunoreceptors and receptor tyrosine kinases (RTKs) activate phosphatidylinositol-specific PLC-γ, while G-protein-coupled receptors (GPCR) activate PLCβ. PLCγ2 activation raises intracellular free Ca^{2+} levels in several sequential steps which leads to subsequent calcineurin activation. Activated NFAT factors interact with members of the AP-1 factor family and regulate the expression of target genes.

NFAT proteins get inactivated in the nucleus by the coordinated action of a multitude of NFAT kinases. After re-phosphorylation, NFAT is shuttled out of the nucleus back into the cytoplasm [139, 140]. Phosphorylation sites were found within multiple serine-rich motifs in NFAT`s regulatory domain, in particular in the SRR1- and Ser-Pro-x-x repeat motifs SP1, SP2 and SP2 [71]. NFAT kinases which act in the cytoplasm to keep NFAT in a fully phosphorylated state are referred to as "maintenance kinases". These proteins prevent NFAT translocation and activation under resting conditions. Glycogen synthase kinase 3 (GSK3), on the other hand, is an "export kinase" that phosphorylates SP2 and SP3 motifs, but only after the action of "priming kinases", like Protein Kinase A (PKA) or the Dual-specificity tyrosine-Y-phosphorylation Regulated Kinase (DYRK) that have already phosphorylated one of these sites [139, 140]. The kinases DYRK1A and DYRK2 are capable of directly phosphorylating the conserved SP3 motif harbored in the NFAT regulatory domain and, thus, prime for succeeding phosphorylation of

the SP2 and SRR motifs by GSK3 and CK1, respectively [71]. CK1 was shown to act as both a maintenance and export kinase [141].
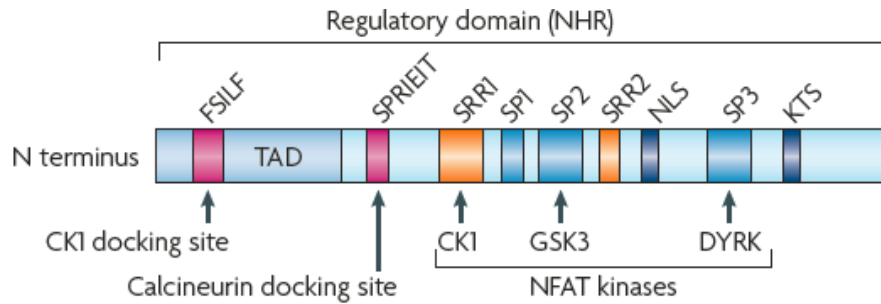
Figure 1.10 | Scheme of the regulatory domain of NFAT Proteins
This scheme shows the amino terminal regulatory domain of NFAT proteins, starting at the N-terminus with a CK1 docking site, the FSILF motif. Followed by the SPRIEIT motif, a site of calcineurin binding, and several phosphorylation sites. These are the serine-rich motifs SRR1, SP1, SP2, SRR2, SP3 and KTS. The corresponding kinases CK1, GSK3 and DYRK are depicted. In between a Nuclear localization site (NLS) is shown [71].

1.6.2 The NFAT family

The NFAT family of transcription factors has five known members named NFATc1-c4 (also known as NFAT1-NFAT4) and NFAT5 / TonEBP. The latter is evolutionarily related to the members of REL/NF-κB family (Figure 1.10) [132]. Due to the conformational analogy to the REL/NF-κB DNA binding domain, these proteins share a common DNA binding domain of approximately 300 amino acid (aa) residues which is named RSD [142]. Within their RSD, NFATc1-NFATc4 show 70% sequence homology whereas NFAT5 shares only about 40% similarity. Furthermore, NFAT5 is the only NFAT member which is not translocated into the nucleus upon calcium dependent de-phosphorylation by CN, and therefore, lacks the regulatory domain of four NFATc proteins [143].

NFATc1 and NFATc2 (also designated as NFAT1 or NFATp) are highly expressed in peripheral T-cells and control their effector functions [142]. NFATc3 (also designated as NFAT4 or NFATx) is also expressed in lymphocytes but at lower level, and its role is less well understood. Inactivation of individual *Nfatc* genes in mice demonstrated a common and specific function for these three proteins [144]. Inactivation of the *Nfatc1* gene resulted in prenatal death of the developing mouse embryos at days 14 and 15 upon gestation [145, 146].
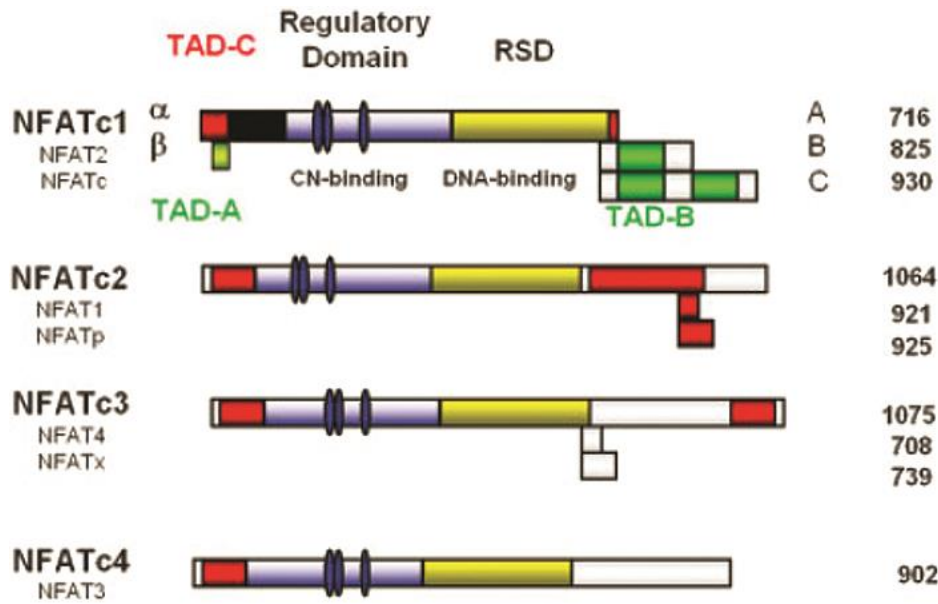
Figure 1.11 | Structure of NFAT family members NFATc1-NFATc4
The DNA binding domains (also designated as RSD) are drawn in yellow, the transactivation domains (TAD) in red (and green) and the regulatory domains in blue. The presence of multiple phosphorylation sites within the regulatory domains is indicated schematically. These are targets of CN [144].

In contrast, *Nfatc2*-deficient mice are born at normal mendelian ratios and appear to be normal within the first weeks after birth [144, 147]. However, starting around 12 weeks and more after birth, $Nfatc2^{-/-}$ mice develop a hyper-proliferative syndrome with significantly elevated primary and secondary immune responses. Due to a decelerated rate of apoptosis, these mice show an at least twofold increase of peripheral lymphocytes, indicating a suppressive role for NFATc2 during the generation of effector lymphocytes [144, 148, 149]. Several properties were found to be markedly enhanced in mice which were deficient for both NFATc2 and NFATc3 [144, 150]. For example, *c2/c3*-double deficiency resulted in hyper-proliferation of peripheral T- and B-cells which, consequently, led to splenomegaly. These animals also show an inclination towards the generation of Th2 cells and a massive production of Th2 cytokines [144, 151]. It was also reported that *c2/c3*-double deficient lymphocytes lack *Fasl* expression and, therefore, show signs of resistance towards apoptosis [144, 150, 152]. $Nfatc3^{-/-}$ mice, in contrast, display 50% less peripheral T-cells, which might also be due to impaired rates of apoptosis in these animals. While they do not show any defects in lymphokine (IL-2, IL-4 and IFNγ) production, they show a mild drop in single positive (SP) CD4$^+$ and CD8$^+$ thymocytes [144, 153]. By generating embryonic stem (ES) cell lines with a homozygous mutation in the *Nfatc1* gene it was shown that $Nfatc1^{-/-}$ effector T-cells produce significantly less IL-4, and to some extent

also less IL-6 after αCD3 TCR stimulation [154, 155]. Upon αIgM stimulation, *Nfatc1*^{-/-} splenic B-cells showed a markedly decreased BCR-initiated proliferation [70]. *Nfatc1*^{fl/fl} x *mb1cre* or *Nfatc1*^{fl/fl} x CD23cre mice exhibited regular splenic B-cell development, but in line with earlier findings these showed a severe (5-10 fold) reduction of peritoneal B1a-cells [70, 144]. In addition to the low proliferation rates upon BCR stimulation, *Nfatc1*^{-/-} splenic B-cells exhibited a decreased competence in stimulating T-cells and an increase in AICD and IL-10 production [70, 144]. The clinical course of EAE induced in *Nfatc1*^{fl/fl} x *mb1cre* mice was found to be reduced. Several of these defects appear to be due to the diminished Ca^{2+} flux which controls proliferation through activating the Ca^{2+}/CN axis [144]. Very recently it has been shown that NFATc1 plays already a critical role in the survival and differentiation of pre-TCR-negative thymocytes. It became apparent that in this context *Nfatc1* induction is dependent on interleukin-7 signaling and tyrosine-phosphorylation by JAK3 [19].

1.6.3 NFATc1 isoforms
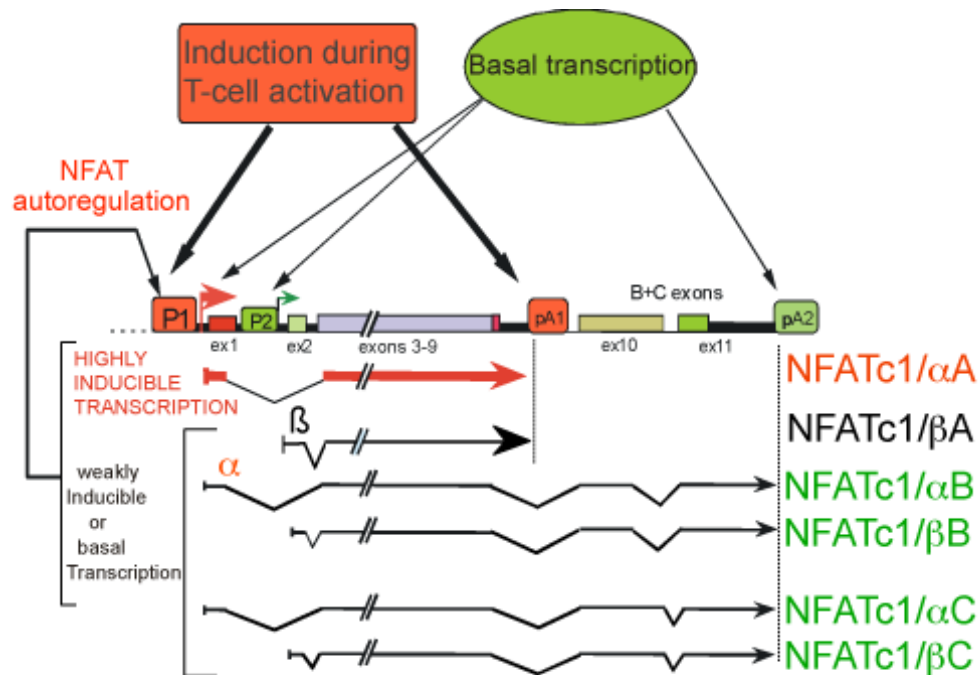
Figure 1.12 | Scheme of transcription of murine *Nfatc1* gene [156]
The transcription of *Nfatc1* is controlled by two promoters, P1 and P2, and two poly A sites, pA1 and pA2. The highly inducible transcription of the short isoform NFATc1/αA in effector T-cells is controlled by the strong promoter P1 and the weak poly A site pA1. The synthesis of the longer isoforms NFATc1/B and C is controlled by either P1 or P2 and by the strong poly A site pA2. The autoregulation of P1 promoter by NFAT factors results in an increase of NFATc1/αA but not NFATc1/B or C synthesis.

I. INTRODUCTION

The *Nfatc1* (or *Nfat2*) gene has two promoters, designated as P1 and P2 (Figures 1.12 and 1.13). The inducible promoter P1 is located upstream of exon 1, whereas the constitutive promoter P2 is located upstream of exon 2. Due to the activity of promoter P2, in resting or naïve effector T-cells three NFATc/β isoforms, especially isoforms βB and βC, are constitutively synthesized [156]. A switch of promoter usage from P2 to P1 was described after antigen receptor engagement in combination with other co-stimulatory signals, such as CD28 or ICOS (Inducible costimulator) in T-cells. This change in promoter usage leads to a predominant synthesis of NFATc1/αA and, to lesser extent, to NFATc1/αB and NFATc1α/C [157]. The activity of P1 is enhanced by an autoreactive feedback loop leading to a constantly elevated level of NFATc1/αA over a longer period of time compared to non-activated cells [156]. NFATc1/αA differs markedly from the longer proteins by its short C-terminal peptide, which lacks a second transactivation/repressor domain typical for the longer NFATc1 isoforms C (spanning 925 aa in [NFATc1/βC] and 939 aa in [NFATc1/αC], respectively) and NFATc2 (Figures 1.11 and 1.12) [144].
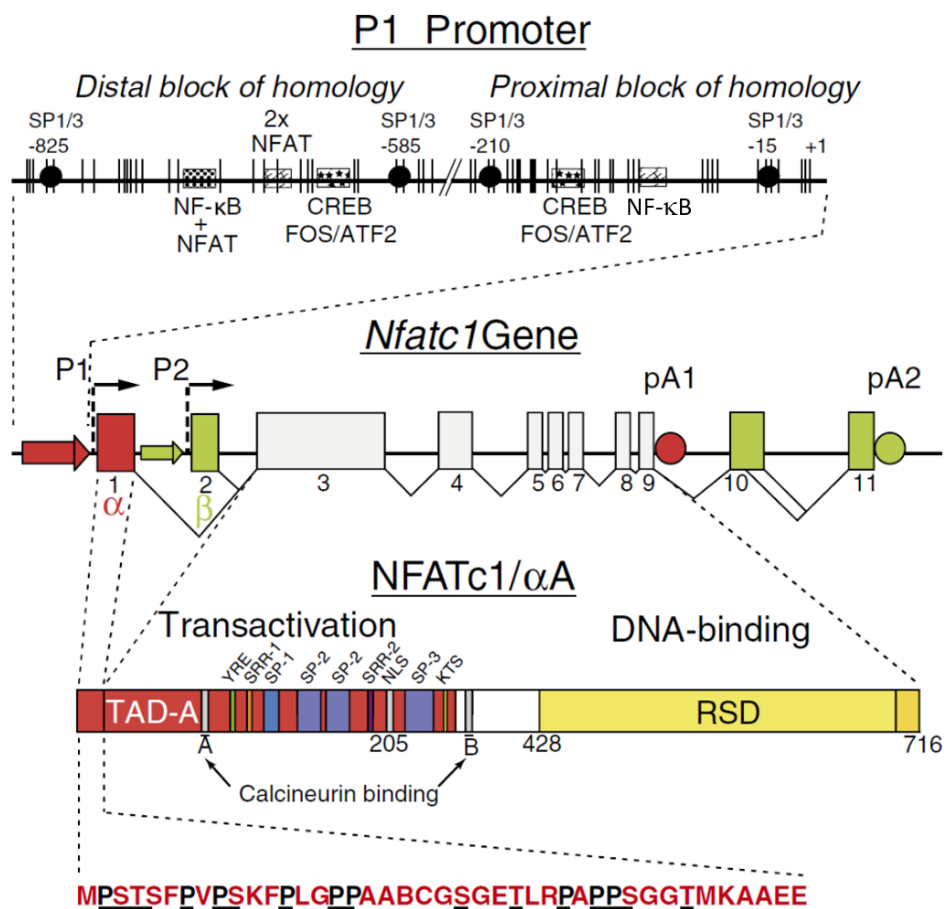
Figure 1.13| Scheme of the murine *Nfatc1*-gene, its inducible promoter P1 and the short isoform NFATc1/αA [144]
Binding sites for transcription factors are shown as filled circles (for Sp1/Sp3 binding) or as boxes for the binding of various other factors. The murine *Nfatc1* gene spans approximately 110 kb DNA and is divided into 11 exons. Its expression is directed by two promoters, P1 and P2, and two poly A addition sites, pA1 and pA2. For the generation of NFATc1/αA RNA, the induction of P1 promoter results in the transcription of exon1, splicing to exon 3 and poly A addition at the poly A site pA1. For NFATc1/αA, the Rel Similarity Domain, RSD, and transactivation domain, TAD-A, are indicated. The two binding sites A and B of calcineurin, a nuclear localization signal, NLS, and several Ser-rich motifs are indicated. Below NFATc1/αA, the aa sequence of the N-terminal α-peptide is shown. All Pro and Ser/Thr residues in the α-peptide are underlined.

1.7 NFAT in non-lymphoid cells

1.7.1 NFAT in bone development

In bones, processes involving breakdown (resorption) and buildup (formation) are mediated by osteoclasts and osteoblasts, respectively. Bones are a major storage site of Ca^{2+} within its proper homeostatic range. Osteoclast differentiation is supported by mesenchymal cells (bone-marrow stromal cells or osteoblasts) through intercellular contact [158]. Essential molecules are provided by cells responsible for this cell-cell contact, e.g. the macrophage colony stimulating factor (M-CSF) and receptor activator of NF-κB ligand (RANKL) as osteoclastogenesis-inducing factors [158, 159]. NFATc1 was identified as a key transcription factor controlling osteoclastogenisis. RANKL, a cytokine and a member of the TNF superfamily, was originally identified as an activator of dendritic cells which was expressed by activated T-cells [158, 160]. Targeted disruption of RANKL or RANK resulted in the defective formation of lymphnodes, but due to abrogated osteoclastogenesis, also in severe osteopetrosis, indicating a critical role for both the immune and bone system [161, 162]. NF-κB and AP-1 are activated by RANKL in the early phase of osteoclast development. But they are also activated by other cytokines, such as IL-1, which are unable to induce osteoclast differentiation. A genome wide analysis revealed NFATc1 as the major transcription factor induced by RANKL [163]. A continuous Ca^{2+} oscillation is instigated by RANKL in BMMs (Bone Marrow-derived Macrophages) and it was shown that overexpression of NFATc1 in the absence of RANKL within these cells supports differentiation towards an osteoclast-like phenotype [158]. NFATc1 mRNA is selectively and effectively induced by RANKL in osteoclasts, whereas *Nfatc2* mRNA is expressed constitutively cells in small amounts in precursor. Inhibition of NFAT activity by FK506 leads to a defective induction of *Nfatc1* but not *Nfatc2* mRNA. Chromatin Immunoprecipitation (ChIP) demonstrated that after stimulation with RANKL, NFATc1 binds

the *Nfatc1* promoter but not to the promoter of *Nfatc2* [158]. This promoter binding was found to persist throughout the terminal differentiation of osteoclasts. Epigenetic modifications were suggested as the reason for the selective activation of *Nfatc1* promoter [164]. Several genes specific for osteoclast differentiation and regulation were found to be targets of NFATc1, e.g. TRAP, calcitonin receptor, cathepsin K, and β3 integrin. Furthermore, the OSteoClast-Associated Receptor (OSCAR), which is an immunoglobulin-like receptor, is a further NFATc1 target that is exclusively expressed on osteoclasts [165]. The Dendritic cell-Specific TRAnsMembrane Protein (DC-STAMP) [166], which was shown to be essential for cell-cell fusion of osteoclast precursor cells, is also directly targeted by NFATc1 [158].

1.7.3 NFAT in heart-valve development

Formation of the endocardial cushion is highly conserved within vertebrates and starts at embryonic day (E) 3 in chicken, E 9.5 in mouse and between E 31 and E 35 in human [167]. The cushion is made of highly proliferative undifferentiated mesenchymal cells localized between the endothelial endocartium and myocardial cell layers in the outflow tract (OFT) and arterioventricular canal (AVC) [168]. NFATc1 was found to be expressed especially at the early stages of endocardial cushion formation in endocardial endothelial cells of the primitive heart tube [145, 168]. Endothelial expression of NFATc1 rescued the heart defects in *Nfatc1*$^{-/-}$ mice indicating a requirement for endothelial expression of *Nfatc1* during normal valve morphogenesis. Studies of *Nfatc1*$^{-/-}$ mice, but also using avian endocardial cushion cell cultures, demonstrated that NFATc1 is necessary for the proliferation of endocardial cushion endothelial cells and the induction of *CtsK* (cathepsin K) gene expression [169, 170]. VEGF (Vascular Endothelial Growth Factor), in conjunction with MEK1-ERK1/2 (Mitogen activated kinase-kinase / Extracellular signal regulated kinase) expression, were found to induce endocardial endothelial cell proliferation upon *Nfatc1* induction. Furthermore, RANKL treatment promotes NFATc1 nuclear translocation and *CtsK* expression, while repressing cell proliferation in combination with JNK (c-Jun N-terminal kinase) [169]. VEGF, NFATc1, and activated ERK1/2 were found to be associated with proliferating endocardial cushion endothelial cells, while RANKL, activated JNK1/2, and CTSK were expressed in the valve primordia during later remodeling stages [168, 169]. In the differentiating heart valve, additional NFATc1 target genes include its own promoter in an autoregulatory interaction, as well as the CN modulator *Rcan1* [168, 171, 172].

1.8 Goals of the experimental work

The role of the transcription factor NFATc1 has been studied extensively in vertebrates. It was shown that NFATc1 plays a crucial role in cells of the lymphoid and myeloid system, but also functions as a regulator of developmental programs in heart cells, muscles cells, bone, skin and pancreas. NFATc1 is involved in cell differentiation and proliferation and acts on a multitude of downstream target genes responsible for many different events such as cytokine production, cell migration, survival and cell death. Moreover, alterations within *Nfatc1* expression and regulation lead to malignancy and cancer [71, 144].

To identify NFATc1 target genes, in particular of target genes which might specifically be controlled by NFATc1/αA and NFATc1/βC, we sought to establish a model to analyze genome-wide binding and transcriptional regulation in lymphocytes. Recently, several approaches which used the combination of ChIP and Next-Generation-Sequencing were published [173, 174]. The concept of ChIP has been well established for many years but it was shown that there are several limitations, in particular the availability and specificity of specific antibodies. Small peptide sequences (tags) which can be used to modify "bait"- proteins are commonly used as alternatives to antibodies, yielding in higher purity and larger amounts of protein/DNA per precipitation. We decided to use a system based on the interaction between biotin and avidin/streptavidin, involving the prokaryotic ligase BirA, which was shown to be highly specific and very efficient in mammalian cells [175]. To study genome-wide NFATc1 binding events in mice, we decided to generate a transgenic mouse model bearing a Bacterial Artificial Chromsome (BAC). Additionally, this model may be used as NFATc1 protein-reporter and furthermore, to identify NFATc1 protein-protein interactions in any given cell type. Initially, to proof the feasibility of this approach, we established an *in vitro* model based on the B-cell lymphoma WEHI-231. This work focuses to a large extent on the generation of this model, starting with the creation of WEHI-231 cells stably expressing two NFATc1 isoforms, NFATc1/αA and NFATc1/βC, modified with a short avidin-tag, by retroviral transduction. To determine regulated target genes, this *in vitro* overexpression model of the NFATc1/αA and NFATc1/βC isoforms was also used to perform whole transcriptome sequencing, and ChIP-sequencing (performed in collaboration with TRON (Translat. Oncology, Univ. Mainz).

II. MATERIAL AND METHODS

2.1 Material

2.1.1 Mouse strains

C57Bl/6J: C57BL/6J is the most widely used mouse inbred strain. It is commonly used as a general background strain for the generation of congenics carrying both spontaneous and induced mutations. Although this strain is refractory to many tumors, it is a permissive background for maximal expression of most mutations. C57BL/6J mice are used in a wide variety of research areas including cardiovascular biology, developmental biology, diabetes and obesity, genetics, immunology, neurobiology, and sensorineural research. C57BL/6J mice are also commonly used in the production of transgenic mice. Overall, C57BL/6J mice breed well, are long-lived, and have a low susceptibility to tumors (Information obtained from ©The Jackson Laboratory website).

C57Bl/6J *Nfatc1/Egfp*: Transgenic mice expressing a chimeric NFATc1/EGF protein under the control of the murine *Nfatc1* gene [137]. In a BAC (Bacterial Artificial Chromosome) pDLSC52 spanning the *Nfatc1* locus, the *Nfatc1*- Exon 3 is fused to a cDNA encoding eGFP (enhanced Green Fluorescence Protein).

C57Bl/6J *Nfatc1/DE1*: Transgenic mice expressing the NFATc1/EGF protein from a BAC harboring a deletion in intron 10 of a regulatory element designated as E1.

C57Bl/6J *Nfatc1/DE2*: Transgenic mice expressing the NFATc1/EGF protein from a BAC harboring a deletion in a regulatory element designated E2 in intron 10.

C57Bl/6 *Rosa26-BirA*: Transgenic knock-in mice constitutively expressing the prokaryotic ligase BirA under the control of the Rosa26-locus.

Nfatc1$^{flx/flx}$ x CD23 cre x *Rosa26* caNFATc1/αA: Mice bearing a B-cell specific conditional knock-out for *Nfatc1* under the control of CD23 cre, crossed to transgenic knock-in animals, expressing a constitutive active version of *Nfatc1* from the Rosa26-locus (kindly provided by Prof. Dr. Ellenrieder, Marburg).

2.1.2 Cell culture

2.1.2.1 Cell lines

<u>HEK 293T-cells:</u>   A cell line derived from human embryonic kidney cells grown in tissue culture. This particular line was generated by the transformation and culturing of normal HEK cells with sheared adenovirus 5 DNA. The transformation resulted in the incorporation of approximately 4.5 kilobases from the viral genome into human chromosome 19 of the HEK cells [176].

<u>WEHI-231 B-cells:</u>   Expresses surface IgM and IgD but does not secrete Ig. Secretion of IgM can be induced with LPS. WEHI 231 is a B-cell lymphoma cell line of BALB/c x NZB F1 origin induced by mineral oil injection [177].

2.1.2.2 Cell culture media

- RPMI (Roswell Parker Memorial Institute)	Gibco®, Life Technologies™
	Homemade, Institute for Virology and Immunobiology, University of Würzburg, Würzburg
- DMEM (Dulbecco´s Modified Eagle Medium)	Gibco®, Life Technologies™
- X-Vivo™	Serum-free medium, Lonza ltd.
- FCS (Fetal Calf Serum)	Gibco®, Life Technologies™

2.1.3 Bacteria

2.1.3.1 Bacterial strains

- *E. coli* DH5α	Chemically competent bacterial strain; suitable for transformation
- *E. coli* K12 DHα	Chemically competent bacterial strain; suitable for transformation
- Pir1/2	The PIR1 and PIR2 One Shot® Chemically Competent *E. coli* are for use with vectors that contain the R6Kγ origin of replication (i.e. pUni/V5-His-TOPO®). The pir gene

encodes the replication protein π, which is required to replicate and maintain plasmids containing the R6Kγ origin (Invitrogen).

2.1.3.2 Bacterial culture media

- LB-Medium

10 g Bacto-Trypton

5 g Yeast extract

5 g NaCl to 1l ddH$_2$O

- SOC-Medium

2% w/v bacto-tryptone

0.5% w/v Yeast extract

10mM NaCl

2.5mM KCl

20mM MgSO$_4$

20mM glucose

$_{dd}$H$_2$O to 1000 mL

- Agar Plate

LB-Medium

+ 1.5% Agar Agar

- 10x M9 Solution

60 g Na$_2$HPO$_4$

30 g KH$_2$PO4

10 g NH$_4$Cl

5 g NaCl to 1l $_{dd}$H$_2$O

- M9 plates

7.5 g Agar

50 ml 10x M9 Solution

0.5 ml 1M MgSO$_4$

0.05 ml 1M CaCl$_2$

5 ml 20% (w/v) Glucose to 500 ml ddH$_2$O

II. MATERIAL AND METHODS

2.1.4 Retroviral expression vectors

pEGZ: pEGZ is a bicistronic vector with an internal ribosomal entry site and a cDNA encoding enhanced GFP. Enhanced GFP serves as a marker for transfected cells. Additionally, this vector carries a gene that grants Zeocin resistance which is used as a selection marker in eukaryotic cells. This vector contains retroviral elements such as Long-Terminal Repeats (LTRs) and a Simian Viral 40 promoter (SV40).

pEGZ-NFATc1/αA-avi: NFATc1α/A C-terminally fused to a biotinylatable peptide cloned into the multiple cloning site (MCS) of the pEGZ expression vector.

pEGZ-NFATc1/βC-avi: NFATc1/βC C-terminally fused to a biotinylatable peptide cloned into the MCS of the pEGZ expression vector.

pEGZ-NFATc1/βC-aviFl: NFATc1/βC C-terminally fused to a biotinylatable peptide, flanked by loxp sites, cloned into the MCS of the pEGZ expression vector.

pMSCV-F-BirA: The prokaryotic ligase BirA was cloned into the MCS of the retroviral expression vector pMSCV-F.

pEGZ-ATG-NLS: A short nucleotide sequence containing a transcriptional start codon (ATG) and a nuclear translocation sequence cloned into the MCS of the pEGZ vector, created as a control plasmid.

pHIT123:   Retroviral packaging vector expressing the murine leukemia virus (MLV) envelope gene (*env*).

pHIT60:   Retroviral packaging vector expressing the MLV genes for nucleocapsid core proteins (*gag*) and a reverse transcriptase, a protease, an integrase and a ribonuclease (*pol*).

2.1.5 Primers

2.1.5.1 Cloning Primers

Primers	Sequence 5´- 3´
ClaI-aNC1for	TTATCGATATGCCAAGTACCAGCTTTCCA
mNc1-1300_rev	GGGCTGCACCTCGATCCGAA
mNc1-1300_for	TTCGGATCGAGGTGCAGCCC
5`BoxEx9_rev	GTAAAAACCTCCTCTCAGCTC
Ex9bio_fwd	GAGCTGAGAGGAGGTTTTTACCAATTGGGCGGTGGAGGTCTG
HpaI-biorev	AAGTTAACTCACGAGCCTCCGGCGTTTGAG
NC1bC_fwd_claI	TTATCGATATGACGGGGCTGGAGCAG
NC1bc_inter1rev	AATGGCAGAGCTGGTATACTGGGT
NC1bc_inter1fwd	ACCCAGTATACCAGCTCTGCCATT
NC1bc_inter2rev	GACAGCACCATCTTCTTCCCG
NC1bc_inter2fwd	CGGGAAGAAGATGGTGCTGTC
NC1bCEx11_biofwd	TCCAGCACGATCCCCCACTCCCAATTGGGCGGTGGAGGTCTG
HpaI-biorev2	AAGTTAAC TCACGAGCCTCCGGCGTTTG
bNC1CcbioEcoRILVXfwd	CTGAATTCATGACGGGGCTGGAGCAGGAC
bNC1CcbioSwaplEGZrev	TAATTTAAATTCACGAGCCTCCGGCGTTTGA
bNC1CccloxbioSwaplEGZrev	GAATTTAAATGTTCTAACGATAGCGTTAGC

2.1.5.2 ChIP-detection Primers

Primers	Sequence 5´- 3´
Il-2 F	CCTGTGTGCAATTAGCTCA
Il-2 R	CTCTTCTGATGACTCTCTGGA
FasI F	ACTTGCTGAGTTGGACCTCA
FasI R	GTAATTCATGGGCTGCTGCA
Rcan1 F	GCGGCATAGTTCCCACTGGTA
Rcan1 R	GAGTGCTGGGCTTTTCATCCA
Tnfsf14 F	TGTCCGTCTGTCCATCCACCA
Tnfsf14 R	GGTGCAAGATGCTTGCATGGA
Ppp3ca F	TTTTCTTCAGGGTGCCAGTC
Ppp3ca R	CAGTCTGTTCCCATCCACCT
Aicda F	ACTGGGCACCTCCATCCAGC
Aicda R	GGCGATCTACAGGTTTGGGA
Prdm1 F	AAACGTGTGGGTACGACCTT
Prdm1 R	AGCGCTGGTTTCTACTGAGG
β-Actin F	CGGTTCCGATGCCCTGAGGCTCTT
β-Actin R	CGTCACACTTCATGATGGAATTGA

2.1.6 Chemicals

- Acetic acid	Roth
- Acrylamide/Bisacrylamide (19:1)	Roth
- Agar-Agar	Roth
- Agarose Type II and IV	Roth
- Ammonium persulfate	Sigma-Aldrich
- Ampicillin	Hoechst
- β-mercaptoethanol	Roth; Life-technologies™
- BigDye® terminator v. 3.1	Invitrogen
- Bradford solution (dil. 5x)	Bio-Rad
- Bromphenol blue	Merck
- BSA Fraction V (Bovine serum albumin)	Boehringer Ingelheim
- Caesiumchloride	Roth
- Chloramphenicol	Roth
- Coomassie brilliant blue G-250/R-250	Roth
- Cold water fish skin gelatine 45%	Sigma-Aldrich
- Cyclosporine A	Sandoz
- DEAE-Dextran	Sigma-Aldrich
- DMSO (25% solution)	Roth
- Diethylpyrocarbonate (DEPC)	Roth
- Dithiothreitol (DTT)	Sigma-Aldrich
- DNA purification kit	Jena-Analytik
- ECL Western blotting analysis system	Pierce, Thermo Scientific
- Ethidiumbromide	Sigma-Aldrich
- Ethyl acetate	Roth

II. MATERIAL AND METHODS

- Glycin (Ultra-pure)   Roth

- Ionomycin (5M)   Life technologies™

- IPTG (isopropyl-β-D-thiogalactosid)   Boehringer- Ingelheim

- Nonident P-40 / Igepal   Sigma-Aldrich

- Phenol   Roth

- Phenol/Chloroform/Isoamylalcohol   Roth

- Phenylmethylsulfonylfluorid (PMSF)   Serva

- poly (dI/dC)   Boehringer- Ingelheim

- poly (dG/dC)   Boehringer- Ingelheim

- Protein-G coupled agarose beads   Sigma-Aldrich

- Protein-A coupled agarose beads   Sigma-Aldrich

- radioactive nucleotides: DuPont
    [α^{32}P]dATP/[α^{32}P]dCTP : 10 mCi/ml
      [g^{32}P]ATP: 10 mCi/ml

- Salmon sperm DNA   Sigma-Aldrich

- SDS (Sodium dodecyl sulfate; ultra-pure)   Roth

- Silver staining kit   GE-Healthcare

- Streptavidin-coupled agarose beads   Sigma-Aldrich

- Temed   Sigma-Aldrich

- 12-O-Tetradecanoylphorbol-13-acetate (TPA)   Sigma-Aldrich

- Trypanblue   Sigma-Aldrich

- Tween   Roth

- Tris (ultra-pure)   Roth

-TRIzol   Invitrogen

2.1.7 Buffers and solutions

2.1.7.1 Laemmli Buffer

5 x Laemmli Buffer 10 ml

- 0.5M Tris-HCL pH6.8 1.75ml
- Glycerol (Glycrin) 4.5ml
- SDS (0.25g dissolved in 1ml Tris-HCL) 2ml 0.5g total
- 0.25% Bromophenol blue (25mg in 10ml H_2O) 0.5ml
- β-mercaptoethanol 1.25ml

2.1.7.2 Ripa-Buffer

- 50 mM Tris-HCl pH 7.4
- 150 mM NaCl
- 1% Triton x-100
- 1% Sodium deoxycholate
- 0.1% SDS
- 1 mM EDTA
- Protease Inhibitors

2.1.7.3 IP-Lysis Buffer

- 1% NP-40
- 1% Glycerol
- 20 mM Tris pH 8.0
- 135 mM NaCl

2.1.7.4 IP-Wash Buffer

- 1% Glycerol
- 20 mM Tris pH 8.0
- 135 mM NaCl

2.1.7.5 IP-swelling Buffer

- 25 mM Hepes, pH 7.8
- 1.5 mM $MgCl_2$
- 10 mM KCl
- 0.5% NP-40
- 1 mM DTT
- and protease inhibitors

2.1.7.6 Sonication Buffer

- 50 mM Tris-HCl,pH 8.1
- 50mM HEPES, pH 7.9
- 1% SDS
- 1 mM EDTA
- 1% Triton X-100

2.1.7.6 LiCl Buffer

- 0.25 M LiCl
- 0.5% Nonidet P-40 (NP-40)
- 0.5% Sodium deoxycholate

2.1.7.7 High Salt Buffer

- 50 mM HEPES, pH 7.9
- 500 mM NaCl
- 1 mM EDTA
- 0.1% SDS
- 1% Triton X-100
- 0.1% Deoxycholate

2.1.7.8 TEV-cleavage Buffer

- 50 mM Tris-HCl, pH 8.1
- TEV (Enzyme) (10 u/150 μl)

2.1.7.9 SDS-elution Buffer

- 50 mM NaCl
- 50 mM Tris-Cl (pH 7.5)
- 0.1 mM PMSF
- 5 mM EDTA
- 1% SDS (w/v)

2.1.8 Antibodies

- NFATc1 sc-7294 (7A6)	Santa Cruz biotechnology, inc.
- NFATc1 α-specific	Immunoglobe
- NFATc2 (4G6-G5)	Santa Cruz biotchnolohy, inc.
- Anti-IgM	R&D Systems
- Anti-CD3	Prof. Schmitt, E. (Mainz); eBioscience;
- Anti-CD28	Prof. Schmitt, E. (Mainz); eBioscience;
- Anti-mouse HRP	R&D Systems
- Anti-rabbit HRP	R&D Systems
- Fluorophore coupled abs	eBioscience; Becton Dickinson;
- Streptavidin-APC	Becton-Dickinson;

2.1.9 Technical equipment

- Autoclave,	Systec Dx45; Memmert
- Brightfield microscope,	Leitz
- Centrifuge,	Beckman; Heraeus
- Chemical balance,	Hartenstein; Precisa 300MC
- Cuvettes,	Hartenstein
- DNA-sequencer,	ABI
- Electrophoresis chamber,	PeqLab
- Heating block,	Liebisch; Eppendorf
- Incubator shaker,	New Brunswick Scientific
- Incubator (cell culture),	Heraeus
- Incubator (bacteria),	Mytron
- FACS Scan,	Becton Dickinson
- FACS canto II,	Becton Dickinson
- Fusion detection system	Vilber Lourmat
- Glassware,	Schott
- Glasspipettes,	Brandt
- Fluorescence microscope,	Leitz
- Gel-Doc XR,	BioRad
- Microwave oven,	Privileg
- Mini-gel system,	Hoefer
- 3MM-Paper,	Whatman
- NanoDrop 3300,	ThermoScientific
- Nitrocellulose membranes,	Whatman
- Neubauer counting-chamber,	Brand
- Thermocycler,	MWG-Biotech; Bio-rad
- Photometer,	Pharmacia GeneQuant
- Parafilm,	American Comp.
- Power-supply (Gel-chamber),	BioRad
- Power-supply (Transfer-chamber),	BioRad
- pH-meter,	Ingold K455
- Plastic-material,	Falcon; Nunc; Greiner;
- Pipettes,	Eppendorf
- ABI Prism 7000 real-time PCR cycler,	Applied Biosystems
- Sterile bench,	Heraeus; Gelaire
- Tabletop centrifuge,	Eppendorf
- Ultrasonic-disintegrater,	Sonicor
- Vibro-shaker,	Hartenstein
- Vortex,	Hartenstein
- Waterbath,	Hartenstein
- Western-blotting transfer chamber,	Hoefer inc.
- X-ray film,	Kodak

2.2 Methods

2.2.1 DNA purification

2.2.1.1 Phenolextraction

To purify dissolved DNA from resident protein, one equal volume Phenol/Chloroform/Isoamyl alcohol (25:24:1) was mixed to the solution at room temperature (RT). Phase separation was achieved upon 15 min. shaking and subsequent centrifugation at maximum speed for 5 min. at RT. The aqueous phase was substracted and further treated with an equal volume of Chloroform/Isoamyl alcohol (24:1) to detach remaining protein residues.

2.2.1.2 Ethanol-preciptation

2.5 volumes of pure ethanol were mixed to DNA solutions and supplemented with 0.1 vol. of 3M NaOAc. DNA was precipitated (for a minimum of 1 hour) at -70°C followed by centrifugation (for 45 min – 1 hour) at maximum speed at 4°C. The DNA pellet was washed once with 75% ethanol and dried at rt. for 30 min. DNA was either solved in TE buffer or DEPC treated $_{dd}H_2O$.

2.2.2 DNA quantification

2.2.2.1 Spectral photometer

To quantify DNA solutions a spectral photometer was used. Measuring optical density (OD) of a given DNA solution at the absorption of 260 nm was applied to quantify single-(ss) and double-stranded (ds) DNA. One OD at 260 nm equals 50μg/ml of ds and 40μg/ml of ss DNA.

2.2.2.2 Estimation upon fractionation in agarose gels

The concentration of a given DNA fragment might be estimated by utilizing a 1% agarose gel (2.2.3.1). The agarose gel is loaded with known amounts of DNA marker and the DNA to be determined. After running the gel at approximately 120 V for 25 min, the amount of unknown DNA can be estimated by comparing the known marker band intensity with the unknown DNA band intensities of choice.

2.2.3 DNA electrophoresis

2.2.3.1 Agarose gels

Gel electrophoresis separates segments of DNA based on their size. Agarose powder is briefly boiled and dissolved in 1 x TAE buffer. The liquid agarose gel matrix is poured into a suitable frame and a comb of choice is added, creating small pockets within the gel. DNA solution is placed in a pocket of the cooled, solid gel matrix. The matrix is put into a box filled with 1xTAE buffer solution and connected to an electric current. This current causes one side of the gel to hold a positive charge and the other side of the gel to have a negative charge. Due to the phosphate groups that constitute the DNA backbone, DNA is a negatively charged molecule. Placing the DNA at the negative end of the gel matrix, when the current is turned on, the DNA will migrate towards the anode of this system separating DNA fragments by their sizes. Dependent on the type and size of the system, 20-180 Volts may be applied. To the DNA solution one has to add "blue juice", containing glycerol and a blue dye to visualize the location of the DNA on the gel. Ethidiumbromide or a non-toxic dye (Midori Green) were added to the gels and used to visualize the separated DNA by UV-light. Pictures were taken with ccd-cameras for further analysis and quantification of DNA fragments.

2.2.3.2 SDS polyacrylamide gels for protein fractionation

Polyacrylamide gels were prepared for the separation of protein extracts from cell lines or primary mouse cells. Dependent on the size of the charged molecules to be analyzed the desired gel might contain higher or lower amounts of Acrylamide/Bis-acrylamide. In most cases, gels were prepared either containing 8% or 10% of acrylamide.

	8%	10%
Acrylamide/Bis-acrylamide	2.7 ml	3.3 ml
H_2O	4.6 ml	4.0 ml
Tris-HCl 1.5M pH. 8.8	2.5 ml	2.5 ml
SDS 10%	100 µl	100 µl
Ammonium persulfate 10%	100 µl	100 µl
TEMED	6 µl	6 µl

For a single gel, one glas- and one aluminum plate (Hoefer) and two plastic spacers were assembled according to manufacturer`s instructions. Immediately after the addition of ammonium persulfate (APS) and Tetramethylethylenediamine (TEMED), catalyzing the

acrylamide polymerization reaction, the gel was poured between the assembled gel cast. Gels were run in 0.4 TBE buffer at approximately 200-300 Volts.

2.2.4 Isolation of DNA fragments

2.2.4.1 Isolation of DNA fragment from agarose gels

Ultra-pure agarose gels were prepared for qualitative DNA extraction according to the protocol in 2.2.3.1. Gels were run at an average voltage of approximately 80 V. Separation of DNA-fragments was monitored and DNA bands were excised using a UV-light table and a fresh, clean scalpel. The collected pieces of agarose gel containing DNA were further handled according to the instruction protocol of the Jena-Analytik "Gel extraction kit". Pieces of agarose gel were dissolved at 50°C in the presence of "Extraction Buffer" for 15 min. under constant shaking. DNA was bound to purification columns and washed at least twice with the provided "Wash-Buffer" containing 90% of ethanol. Column bound DNA was spun for two min. and eluted with either TE-Buffer or "Elution-Buffer". DNA was quantified by spectral photometry (2.2.2.1).

2.2.5 DNA Cloning

2.2.5.1 RNA extraction

As a primary step for any gene cloned during this work, RNA was extracted from either T- or B-cells or a whole-splenocytes mixture from C57Bl/6J mice. Cells were counted and approximately 1×10^7 cells were solved in Trizol (2.1.7) reagent. According to the manufactures instructions, RNA was separated from DNA and proteins by the means of centrifugation. RNA was used directly after phenol/chloroform extraction or purified using a column based system for RNA purification (Qiagen). RNA was dissolved in ultra-pure RNase free water and stored at -70 °C for long term use. Before further use, RNA concentrations were measured with a spectral photometer (Nanodrop, Thermo scientific).

2.2.5.2 Reverse transcription

Complementary DNA (cDNA) was generated from RNA/mRNA extracts (2.2.5.1) isolated from C57Bl/6J lymphocytes. Reverse transcription is a process that includes mRNA templates and a viral enzyme termed reverse transcriptase, yielding in a pool of complementary DNAs. According to the manufactures instruction (BioRad, iScript cDNA Synthesis kit), $250 - 500$ ng of RNA were used as starting material for any reaction. A 20 µl reaction mix was made up of

4 µl 5x iScript reaction mix, 1 µl iScript reverse transcriptase, RNA and ddH$_2$0 up to 20 µl. The reaction mix was incubated according the following protocol:

5 minutes 25°C

30 minutes 42°C

5 minutes 85°C.

After this reaction, cDNA was either directly used for polymerase chain reactions or further diluted, depending on the downstream protocol.

2.2.5.3 PCR amplification

Accession numbers, and the mRNA and protein sequence for any gene cloned were obtained from the National Center for Biotechnology Information (NCBI) database. Primers were designed to amplify whole or partial gene sequences and/or to introduce restriction enzyme sites. For control purposes, standard Taq-polymerase (Fermentas) was used for short and long amplicons. In general, material determined to be used for further cloning experiments were amplified with high performance polymerases including proof-reading abilities and very low tendencies of introducing false nucleotide pairings (e.g. using NEB Q5 High Fidelity Polymerase or NEB Crimson/Crimson Long Range Polymerases). All polymerase chain reactions (PCRs) were performed in standard cyclers (MWG, BioRad). PCR protocols were adapted according to the manufacturer instructions varying in terms of annealing temperature, number of cycles and elongation times but in general as the following protocol:

Initial denaturation: 95-98 °C, 5-10 minutes

Repetitive cycles of: 95-98 °C, 5-10 minutes

                            55-70 °C, 30 seconds – 1 minute   Annealing

                            68-72 °C, 1-3 minutes   Elongation

Final elongation: 68-72 °C, 5-10 minutes.

PCR products were visualized and controlled by agarose gel separation and UV-light imaging.

2.2.5.2 Restriction enzyme digestion of DNA

Enzymatic digestion of DNA was generally used to generate "sticky- or blunt-ends" proceeding a ligation reaction. Dependent on which type of restriction enzyme was used the corresponding restriction enzyme buffers, containing the correct amount of salts, were chosen. Standard

digestion protocols were applied utilizing one unit of restriction enzyme per microgram of DNA to be digested (One unit is defined as the activity of a given enzyme necessary to digest 1 µg of λ-DNA in 1 hour). The amount of restriction enzyme limited to one individual reaction should not exceed 1/10 of the whole preparation. Glycerin, which is commonly used to dissolve and store restriction enzymes, has a negative effect on the enzymatic reaction if present in high concentrations. If not stated otherwise, all restriction enzyme digestions were performed at 37°C for at least one hour, or overnight. DNA digestion was monitored by running 2-5 µl of a given preparation and an appropriate size marker on an agarose gel.

2.2.5.2 Klenow-polymerase reaction

In some cases, it was necessary to create DNA-fragments with "blunt ends" instead of "sticky ends" that were gained by restriction enzyme digestion (2.5.2.1). The Klenow fragment of DNA-polymerase I, generated by partial digestion of DNA-polymerase I, is capable of filling partial nucleotide overlaps. 1 µg of DNA, solved in a suitable buffer, supplemented with 2 mM dNTPs and 2 units of Klenow fragment, were incubated at room temperature for 10 min. DNA was purified by of phenol extraction or ethanol precipitation (2.2.1.2).

2.2.5.3 Alkaline-phosphatase treatment

The 5´- end of a digested DNA molecule harbors a free phosphate residue which has to be released by phosphatase treatment before liagtion. Removing the phosphate residues prevents further nucleotide binding. 2.5 µg of DNA are incubated with alkaline phosphatase (ALKP) in an alkaline phosphatase buffer for 1 hour at 37°C. Afterwards, the enzyme will be heat-inactivated at 65°C for 10 min. DNA may be used for ligation reactions without further treatment.

2.2.5.4 Ligation

To obtain excellent ligation results, DNA concentrations have to be quantified by gel electrophoresis before a ligation reaction. DNA vector and insert were loaded and run on an 1% agarose gel, to compare with known marker band concentrations. A vector concentration in the range of 0.5 – 100 ng is recommended and should not exceed 1/3 of the total reaction compared to the amount of insert DNA. In some cases, several reactions with different amounts of insert DNA were incubated to gain optimal results. In general, 2 µl of T4 ligation buffer (Fermentas) were used in a 20 µl reaction mix, supplement with 0.1 or 10 units of T4 Ligase and $_{dd}H_2O$.

2.2.5.5 Transformation

Plasmid cloning: Chemically competent bacteria, strain DH5α, were purchased from New England Bio-Labs and stored for long term use at -70°C. For each transformation sample, 50 µl bacterial suspension was slowly thawed on ice. Approximately 5 µl ligation mix (2.2.5.4) were added to a 50 µl freshly thawed DH5α aliquot. The mixture was kept on ice for 30 min. After that, a 90 sec "heat-shock" was performed at 42°C using a preheated water-bath incubator. Transformed bacteria were again incubated for 2 min on ice followed by the addition of 250 µl LB- or SOC-medium. In medium-suspended bacteria were incubated for 1-1 ½ hours at 37°C with constant shaking at 250 rpm. Post incubation, 150-200 µl of any bacterial suspension was dispensed on LB-Agar-Agar petri-dishes prepared with a suitable antibiotic if necessary (e.g. ampicillin, chloramphenicol). Plates were incubated over night at 37°C. The next day, colonies which were able to grow under selective conditions were picked and prepared for further analysis.

pLD53.SC2-shuttle vector cloning : For the establishment of donor-vectors, a plasmid vector (pLD53.SC2 [178]) was used encoding an ampicillin resistance gene and two regions of homology towards the *Nfatc1* gene, flanking the avi-tag sequence. Pir1 (2.1.4) bacteria were obtained from Invitrogen. These cells were stored at -70°C for long term use. Transformation with target DNA was performed as described in 2.2.5.5 for plasmid cloning.

BAC RP23-361H16 + RecA: BAC RP23-361H16 bacteria, carrying the Bacterial Artificial Chromosome (BAC) expressing the whole NFATc1 locus were obtained from Source BioSciences LifeSciences and transformed with the bacterial enzyme RecA (Recombinas A). RecA is a prokaryotic recombinase which catalyzes DNA-repair and maintenance and, in doing so, also site-specific homologous-recombination. Donor plasmid DNA which was generated and transformed into a shuttle vector system (2.2.5.5 Shuttle vector cloning), was isolated and transformed into BAC RP23-361H16 + RecA bacteria. This was done by electroporation using the Gene Pulser II (BioRad). The system was set to generate an electric pulse defined by the following conditions:

1.8 kV, 25µF and a resistance of 250 Ohm.

BAC RP23-361H16 + RecA bacteria were thawed and kept on ice for at least 5 min, 500 ng donor plasmid DNA were pipetted to the suspension and kept on ice for, 1 min. The suspension was transferred to a cuvette suitable for electroporation (BioRad) and placed into the Gene Pulser II apparatus. An electric pulse was applied (automatically) for 4.7 ms. Cells were

resuspended in 1 ml SOC (2.1.5) medium and incubated for 1 h at 30°C with shaking (250 rpm). 50 µl transformed H361 A bacteria were spred on a LB-Agar-Agar plate containing the antibiotics ampicillin (50 µg/ml), tetracyclin (10 µg/ml) and chloramphenicol (12,5 µg/ml). Furthermore, 10 µl of the transformed suspension were resuspended in 5 ml LB-medium, supplemented with ampicillin, tetracyclin and chloramphenicol in the before mentioned concentrations. All plates and liquid suspensions were incubated over night at 30°C. Ampicillin was used as a selection marker within the donor vector carrying the site intended for homologous recombination. Tetracyclin was used as a selection marker for the BAC plasmid itself, whereas chloramphenicol was used to positively select for the episomal RecA.

2.2.6 Retroviral infection of cell-lines and primary B-cells:

Protocol for transient virus production in 293T-cells and viral infections

1. **Precipitate DNA before transfection**
   - Aliquot DNAs, 8 µg/tube/each 60 mm plate of 293T cells:
     - 4 µg pHIT60 (MLV ENV)
     - 4 µg pHIT123 (MLV GAG and POL)
     - 8 µg retroviral construct (i.e. pEGZ-NFATc1/αA-avi)
     - 16 µg total
   - Add 1/10 vol. 10 M AmmOAc (or 3 M NaOAc) and 2.5 vol 100% Etoh.
   - Vortex briefly.
   - Spin down at 14K, 15 min, 4°C.
   - Remove supernatant carefully.
   - Wash once with 100 µl 70% Etoh to remove salts.
   - Spin down at 14K rpm, 5 min, 4°C.
   - Remove supernatant.
   - Dry DNA pellet, 15 min.
   - Resuspend pellets in 50-100 µl dH_2O.
   - Incubate at RT until cleared. (assures DNA fully resuspended)
2. **Transfect 293T cells with $CaCl_2$ and 2xHBS and DNAs**
   - Split 293T cells into 60 mm plates and grow until 50-80% confluent.
   - Add fresh medium to 293T cells, (8 ml/60 mm plate) DMEM HEPES within 1 day before transfection.
   - For each plate to be transfected, prepare DNA-$CaCl_2$ mix:
     - Add 65 µl 2 M $CaCl_2$ to 16 µg DNA mix in ddH_2O to a final volume of 500 µl. Flick to mix.
     - Dropwise addition of 500 µl 2 x HBS (pH 7.05) under constant vortexing. Flick to mix.
     - Incubate for 30 min at RT.
   - Add 1 ml mix to plate of 293T cells in a dropwise fashion. Swirl to mix.
   - Change medium after 24 h. Add DMEM + 10 mM NaButyrat for 6 h, change again to regular DMEM.
3. **Viral harvest**
   - Harvest twice, beginning 24 hours after transfection.
   - For each harvest, carefully remove supernatant in 15 ml conical tubes, using 5 ml syringes and 0.45 µM syringe filters (yellow) to filter supernatant

- Refeed each plate with 8 ml fresh medium, slowly adding media along the side of the plate so that cells do not detach.
- Store virus supernatant at -80°C until all harvests are complete.

4. **Viral infection of (proliferating) target cells**
   - One day prior to infection, count and split target cells, induce proliferation if necessary.
   - Aliquot 5×10^5 target cells, per infection sample, in 15 ml tubes.
   - Thaw frozen virus aliquots in 37°C water bath.
   - Add exactly 4 ml of viral supernatant to a sterile tube (12 ml supernatant = 1 sterile tube).
   - Prepare a master mix of medium and polybrene for infection cocktail.
     - 500 µl medium
     - 5 µl 10 mg/ml polybrene (1:1000 dilution)
   - Add 1 ml of master mix to each tube/viral supernatant and let rest 2 min at RT.
   - Mix master mix and pellet together by pipetting, and combine like-virus together (1 ml media + 5 µl polybrene + 4 ml viral supernatant = 5 ml total volume).
   - Add 5 ml infection cocktail to each 15 ml tube containing target cells.
   - Incubate for 30 min at 37° C.
   - Spin tube for 2-3 h at 32° C at 1400g.
   - Incubate for 30 min at 37° C.
   - Aspirate infection cocktail.
   - Refeed cells with 1 ml complete DME medium.

5. **Expansion of infected cells**
   - Change medium at least every second day in the first week.
   - Add selection antibiotic after 7 days.
   - Analyse cells for positive infection (i.e. eGFP expression)
   - Keep under selection pressure as long as non-postive cells are present within the cell pool.

2.2.7 Chromatin Immunoprecipitation

Chromatin Immunoprecipitation (ChIP) is a method for studying *in vivo* interactions between specific proteins or modified forms of proteins and a genomic DNA region. ChIP can be used to determine whether a transcription factor interacts with a candidate target gene or regulatory region. It can also be used to quantify possible bindings, hence monitor the presence of histones with post-translational modifications at specific genomic locations.

2.2.7.1 NFAT biotinylatable fusion proteins as ChIP-bait

Due to the fact that commercially available NFAT antibodies lack the desired degree of specificity and, therefore, generate a high level of background, a non-antibody based approach was chosen. Great specificity is mandatory in Immunoprecipitation experiments, thus targeted proteins or DNA are exclusively bait-protein bound. NFAT fusion proteins, bearing a peptide-tag at the C-terminus which was used for *in-vitro* biotinylation, were generated. The constructs used in our assays were obtained from the Research Institute of Molecular Pathology (kindly

provided by Prof. M. Busslinger) in Vienna. Originally, this approach was published by de Boer *et al.*[175] who showed that this technique is suitable for mammalian cells. The ChIP assays with biotinylatable fusion proteins give rise to excellent results, due to its very high specificity.
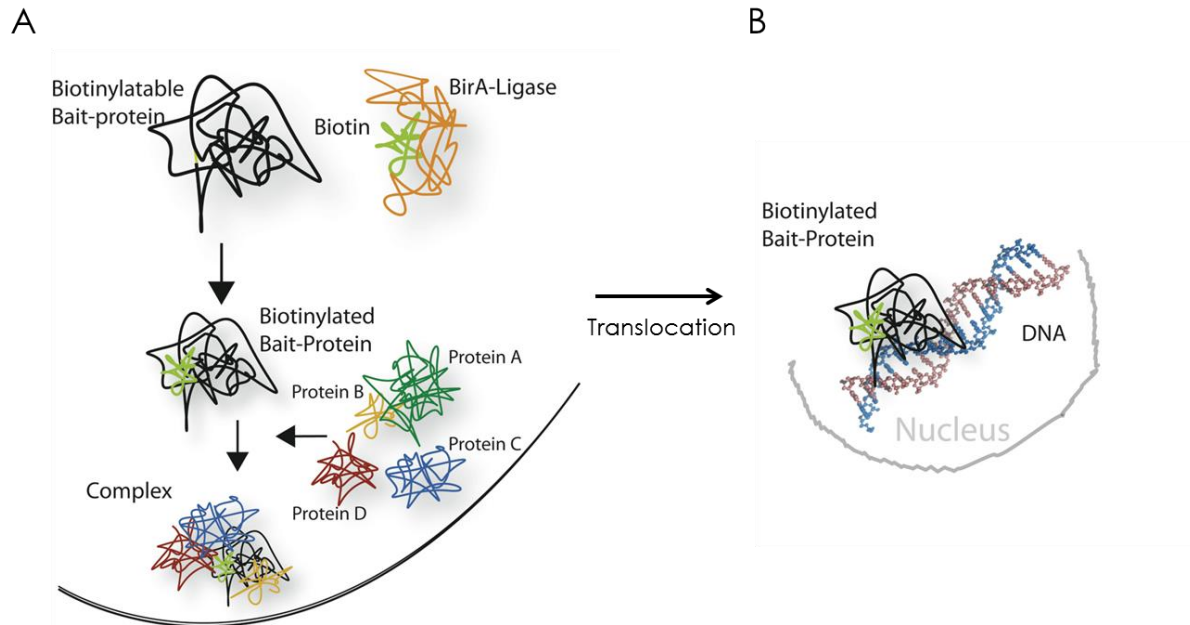
Figure 2.1 | Schematic display of the expression of a biotinylatable fusion protein
(A) Co-expression of a biotinylatable bait-protein and the prokaryotic enzyme BirA. Biotinylation occurs in the presence of the suitable substrate vitamin B7 (Biotin). The bait-protein may interact with natural interaction partners (proteins A-D) either in the cytoplasm or after translocation in the nucleus (B) where it interacts with its target DNA-sequences.

Figure 2.1 shows a modified bait-protein being biotinylated *in vivo* by the *E. coli* derived ligase BirA which has to be expressed in parallel. BirA uses biotin/Vitamin B7 supplemented in the medium as a substrate for this reaction. The very high affinity of biotin to avidin/streptavidin ($K_d = 10^{-15}$ M) allows purification of biotinylated proteins under high stringency conditions, thus reducing background binding often observed with other affinity tags that elute more easily. Furthermore, there are very few naturally occurring biotinylated proteins, thus reducing the chance for crossreaction if using biotinylation in protein purification, as opposed to antibodies that may crossreact with several other, non-related proteins [175].
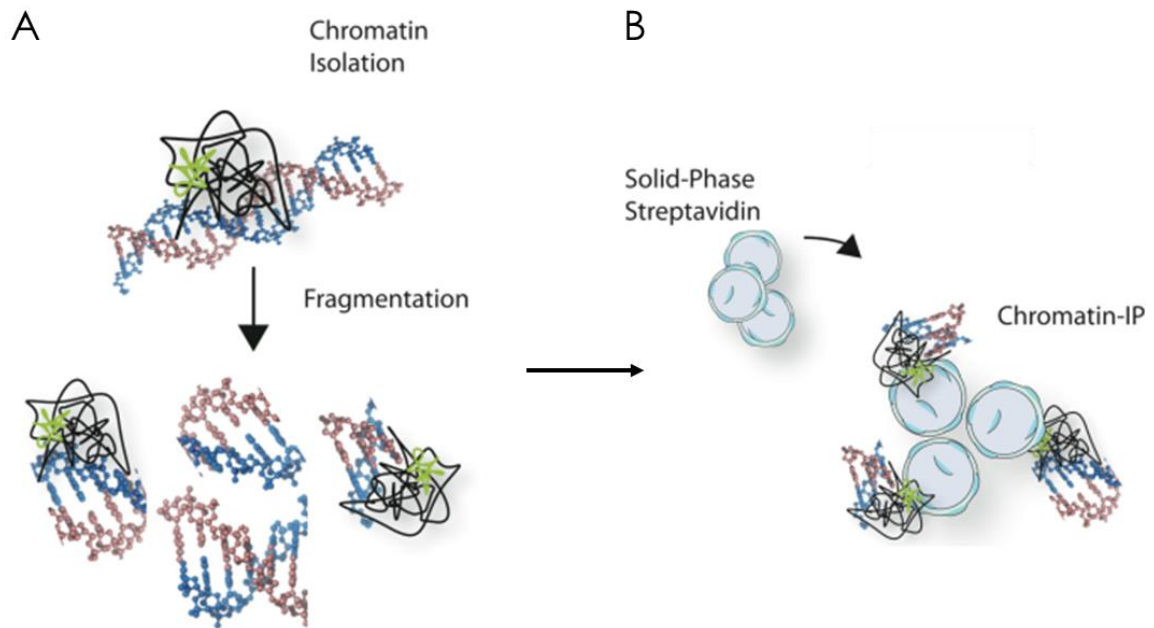
Figure 2.2 | Fragmentation of protein bound chromatin and solid-phase precipitation
Formaldehyde fixation of bait-protein expressing cells and subsequent lysis is followed by (A) fragmentation of chromosomal DNA bound by target proteins. (B)Biotinylated proteins are captured by solid-phase streptavidin beads.

All proteins, including biotinylated bait proteins bound to DNA or to their protein interaction partners, are fixed by formaldehyde. Cells are lysed and nuclei are prepared by standard protocols. The isolated chromatin has to be sheared by sonication or enzymatic digestion (although sonication is preferable, due to a less biased DNA fragmentation). Our protocol uses Streptavidin covered agarose beads (Sigma-Aldrich), but several other solid-phase bound avidin derivatives are also suitable. Bead-bound protein and DNA were washed with washing-buffers, ranging from high to low stringency, and eluted by proteolytic cleavage, utilizing a Tobacco Etch Virus (TEV) cleavage site proximal to the biotinylatable peptide and a corresponding protease. Alternatively, DNA was eluted with SDS-based elution buffers at high temperatures.

2.2.7.2 Chromatin Immunoprecipitation protocol

A minimum of 2 x 10^7 cells were grown at densities of 1-2 x 10^5 /cells/ml in supplemented RPMI medium. Cells were induced for desired time (0.5h -8h) with either PMA/Ionomycin or anti-IgM. Cells were fixed for 10 min. at RT with 1% formaldehyde without previous washing on a wheel. Fixation was quenched with 5 ml 1,372 M glycin for 5 min at RT on a wheel. 2 x 20 ml PBS⁻ were used to wash the cell before the cell pellets were re-suspended in ChIP

II. MATERIAL AND METHODS

Swelling Buffer (s 2.1.7.5). All subsequent steps were performed either on ice in the cold room or on ice alone.

Chromatin extraction: After 30 min. on ice, cells were repeatedly passed through a 23 gauge syringe and supplemented with NP-40 to a final concentration of 0.1%.

Nuclei were centrifuged at 2000 g at 4°C for 5 min, and supernatant was discarded.

Nuclei were re-suspended in 0.75 ml Sonication Buffer (s 2.1.7.6) and sonicated on ice for 10 min. with 30 sec pulses and 15 sec breaks.

Sheared chromatin was de-cross-linked at 65°C ON in the presence of proteinase K. The size of DNA fragments were analyzed on a 1% agarose gel.

Chromatin precipitation: 5-30 µg chromatin per sample were used for one precipitation. Streptavidin-beads and protein-G beads (Sigma-Aldrich) were saturated with 10 µg sonicated salmon sperm DNA, 40 µg BSA and 1% gelatine from cold water fish skin (FGEL) (Sigma-Aldrich).

All lysates were pre-cleared with protein-G beads for 2 h. The samples for antibody immunoprecipitation (IP) were additionally pre-cleared with pre-immune IgG (Cell Signaling) antibody.

30 µl 50 % streptavidin-bead slurry were added to one 0.75 ml or 1 ml sample each and rolled on a wheel for 2 hours at 4°C. In cases of antibody precipitation, the antibody was added to the sample and rolled on a wheel at 4°C ON, followed by protein-G bead capturing for 2 h.

All beads were washed twice with the following buffers for 5 min. on ice: Sonication Buffer, High-Salt Buffer, LiCl Buffer and TEV-Cleavage Buffer or TE-Buffer, respectively.

Streptavidin bound proteins were digested with Tobacco Etch Virus (TEV) protease whereas protein-G bound proteins were eluted with ChIP Elution Buffer.

DNA cross-links were released in the presence of proteinase K and 200mM NaCl at 65°C ON on a wheel.

DNA was solved in nuclease-free water.

2.2.8 Next Generation Sequencing (performed by TRON, Translat. Oncology, Univ. Mainz)

The idea of Next Generation Sequencing (NGS) technology is based on Sanger sequencing methodology [179]. The nucleotides of rather short fragments of DNA are sequentially identified from signals emitted as each fragment is re-synthesized from DNA template strands. In the NGS methodology this process is extended to process millions of reactions in a parallel fashion [180]. This provides rapid sequencing of large stretches of DNA base pairs spanning entire genomes or transcriptomes.

2.2.8.1 Illumina / Solexa Genome Analyzer

A single genomic DNA (gDNA) sample or a pool of complemantary DNA (cDNA) is fragmented into a library of small segments that can be uniformly and accurately sequenced in millions of parallel reactions. Freshly identified strings of bases, named reads, are reassembled using a known reference genome (Re-sequencing), or in the absence of a reference-genome (De-novo sequencing).

Multiplexing:

RNA samples were reverse-transcribed into cDNA and multiplexed. Multiplexing is an approach designed to allow sequencing of large sample numbers simultaneously during a single experiment. For this approach, individual "barcode" sequences are added to each sample making it possible to differentiate this samples during data analysis.

Methodology:

DNA is randomly fragmented and re-ligated with adaptors at both ends. Then the DNA is attached to the internal surface of a flow cell. In this flow cell millions of oligonucleotides forming a dense layer of primer pairs, which are complementary to the DNA adjacent adaptors [181]. The DNA hybridized with the primers in a bridging way initializes solid-phase bridge amplification immediately and the fragments become double-stranded. Further steps including denaturation, re-naturation and synthesis generate a high density of equal DNA fragments in a small area. In the following the actual sequencing takes place. Gradually all four dNTPs carrying a base-specific fluorescent dye are added and incorporated by DNA polymerase. Following each base incorporation step, an image is made by laser excitation for each given cluster. The identity of the first base is recordable. After that, the elimination of the chemically

blocked 3´-OH group and the individually coupled dye follows. Within every new cycle, the DNA chain is elongated and more images are recorded. A base calling algorithm assigns the sequences and evaluates the analysis [179].

DNA and RNA samples were analyzed with the GENOME ANALYZE (Illumina / Solexa), which can be used for conventional DNA sequencing as well as for transcriptome analysis. This was done in collaboration with TRON at the Unviversity Mainz.

2.2.9 Protein (Co-)Immunoprecipitation (Co-IP)

Cells from cell lines either stably or transiently transfected with expression vectors were harvested and washed with PBS. Cells were counted, and up to 10×10^6 cells per sample were lysed with non-stringent lysis buffer (e.g. IP lysis buffer: 20 mM Tris (pH 7.5), 150 mM NaCl, 1 mM EDTA, 1 mM EGTA, 1% Triton X-100, 2.5 mM sodium pyrophosphate, 1 mM β-glycerophosphate, 1 mM Na_3VO_4, 1 µg/ml leupeptin) supplemented with 1x protease inhibitor cocktail (Cell Signaling), 5 mM DTT and 0.1 mM PMSF. Samples were incubated on ice for 30 min and subsequently sonicated 5 times (30 sec pulse, 40% amplitude). Lysates were precleared with protein A or G (Sigma-Aldrich) for 1 hour, rolling at 4°C. In the following, samples were briefly centrifuged at 5000 g, and the supernatants were transferred to new tubes. Precipitation Abs or streptavidin-coupled agarose (Sigma-Aldrich) beads were added and samples were incubated overnight, rolling at 4°C.

Protein A or G (20 µl of 50% bead slurry) beads, blocked with 1% BSA, were added to each sample and kept rolling for one additional hour. Samples were briefly centrifuged, and washed 5 times with IP wash buffer (20 mM Tris (pH 7.5), 650 mM NaCl, 1 mM EDTA, 1% Triton X-100, 2.5 mM sodium pyrophosphate, 1 mM β-glycerophosphate, 1 mM Na_3VO_4, 1 µg/ml leupeptin). Beads were resuspended in 40µl 5x Laemmli buffer and stored at -20°C until western blot analysis was performed.

2.2.10 Flow cytometry

2.2.10.1 Sample preparation:

Cells from cell lines or mouse organs were harvested and washed once with PBS and once with PBS + 0.1% BSA. In general, if not stated otherwise, cells were counted and 1×10^6 cells were used per sample. Cells were either stained with fluorophore-coupled antibodies (abs) or fluorescent dyes (e.g. CFSE). When cells remained unstained these cells expressed a fluorescent marker protein (e.g. eGFP). Samples were prepared and labeled as described in the following.

1 x 10^6 cells/sample were washed with 1 ml cold PBS + 0.1% BSA. Subsequently, all samples were centrifuged at RT, 3000g for 5 min. Supernatants were discarded without disturbing the cell pellets. Washing was repeated twice.

All fluorophore-coupled antibodies and/or dyes were prepared according to manufacturer`s protocols.

Samples were incubated with the appropriate amount of ab-dye dilution and Fc-block (eBioscience) for 30 min at 4°C in the dark. After labeling, all samples were washed with PBS + 0.1 BSA at least twice. If necessary, samples were labeled with secondary abs or additional Abs in the same manner as before. After labeling, all samples were diluted in 350 µl PBS + 0.1% BSA prior analysis.

2.2.10.2 FACS analysis:

Samples were either analysed with a BD FACS Scan or a BD FACS Canto II. Depending on which apparatus was used, CellQuestPro or FACS Diva Software was used to aquire data.

2.2.11 Real-time PCR (qRT-PCR)

Real-time PCR is a quantitative PCR method for the determination of PCR templates, such as DNA or cDNA in a PCR reaction. The method used during this work was intercalator-based. The intercalator-based method, also known as SYBR Green method, requires a double-stranded DNA dye (SYBR Green, Applied Biosystems) in the PCR reaction which binds to newly synthesized double-stranded DNA and emmits fluorescence.

Cells from cell-lines or mouse organs were harvested and lysed with Trizol as described previously. RNA was isolated as described in 2.2.5.1 and cDNA was generated as described in 2.2.5.2.

All primers designed for qRT-PCR were tested in RT-PCR and optimal conditions were determined empirically.

2.2.12 Confocal-microscopy:

2.2.12.1 Cytospins

Cells from cell lines or mouse organs were harvested and washed twice with PBS or used without any washing steps. For cytospins, cells were counted and 2×10^5 cells were used per glass-slide. Cells were spun in a Cytospin II centrifuge (Shandon, Benchmodel) at 350 rpm for 4 min at RT. All samples were dried at 8°C overnight prior fixation. Cells were fixed for 20 min at RT in 4% formaldehyde diluted in PBS.

2.2.12.2 Immunhistochemistry staining

After fixation, cells were washed three times with PBS for 5 min at RT. To permeabilize the cells prior staining, samples were treated with 0.2% Triton X100 in PBS for 5 min at RT. All cells were washed three times. BSA was diluted in PBS to a 1% blocking solution used to prevent unspecific ab binding. Samples were incubated with blocking solution for 20 min at RT. Primary abs were diluted in blocking solution according to established protocols in the laboratory. All samples were incubated for one hour with the primary staining solution and kept in the dark. After primary staining, cells were washed tree times with PBS. Secondary, fluorophore-coupled abs were diluted in 1% blocking solution according to manufacturer`s protocols. Incubation with secondary Abs was performed for 45 min. at RT followed by three times washing. Cells were covered with Fluoroshield (Sigma-Aldrich) with DAPI dye.

2.2.12.3 Microscopy

Images were taken using a confocal microscope (Leica TCS SP2 equipment with an objective-lens [HeX PL APO, 40Å~/1.25–0.75]) and analyzed by Leica LCS software.

III. RESULTS

3.1 *Nfatc1* induction in lymphocytes

NFATc proteins are expressed in many different lymphoid and non-lymphoid cells, regulating their proliferation, differentiation, survival and downstream gene expression. To elucidate differences in the expression pattern of NFATc1 transcription factors in T- and B- lymphocytes, a BAC reporter mouse was generated by Dr. Klein-Hessling [137]. In this model, a sequence encoding enhanced Green Fluorescent Protein (eGFP) was cloned into a BAC construct spanning the entire *Nfact1* locus. In these mice, the induction of the *Nfatc1* gene becomes earsily detectable through the expression of eGFP. The sequence, encoding eGFP, was introduced behind the third nucleotide of the coding sequence of exon 3 of the *Nfatc1* gene. Additionally, a polyadenylation site at the end of the coding sequence of the *Egfp* nt-stretch was inserted which, after transcription and translation, generates a truncated NFATc1-eGFP fusion-protein. In consequence, this transgene displays *Nfatc1* gene induction without producing any additional functional extra-copy of NFATc1 protein.

3.1.1 *Nfatc1* induction in peripheral T-cells

Peripheral T-cells were isolated from transgenic *Nfatc1/Egfp* mice and sorted by MACS according to standard protocols. T-cells were stimulated *ex-vivo* by anti-CD3 [4 µg/ml] and anti-CD28 abs[2 µg/ml], or anti-CD3, anti-CD28 abs and, additionally, either by synthetic CpG or Pam3Cys for 48 h, 72 h and 96 h. Flow cytometry analysis (Figure 3.1) showed the induction of the *Nfatc1* gene locus in T-cells under these conditions.
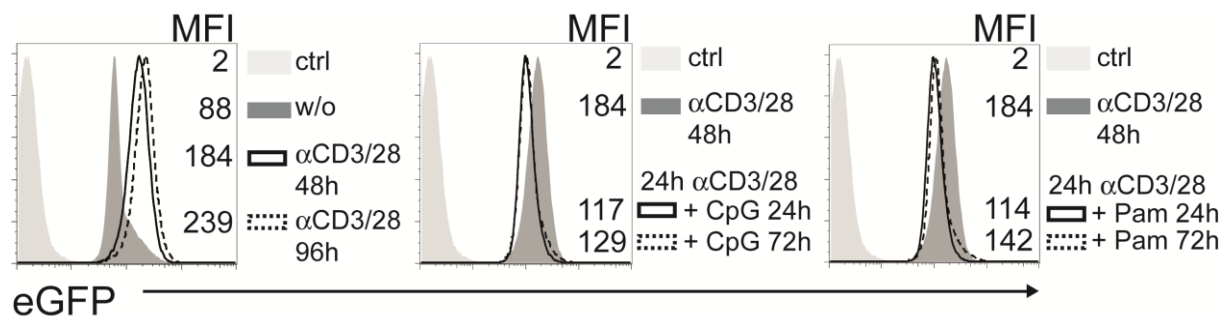
Figure 3.1| *Nfatc1* gene induction in peripheral T-cells from transgenic *Nfatc1/Egfp* mice compared to T-cells from C57BL/6 mice
To analyse the induction of the *Nfatc1*gene locus in T-cells, T-cells from *Nfatc1/Egfp* mice (and wildtype (wt) mice) were isolated and stimulated with anti-TCR ab and co-stmuli. Fluorescence activated cell sorting (FACS) was performed to detect differences in eGFP expression levels in *Nfatc1/Egfp* T-cells compared to non-treated and wt T-cells.

Transcription from the *Nfatc1* gene locus was induced after TCR and co-receptor engagement by anti-CD3 and anti-CD28 stimulation. The detected eGFP emission (MFI) increased from 88 in the resting state to 184 after 48 h and 239 within 96 h of anti-CD3 and anti-CD28 stimulation. Stimulation of Toll-Like Receptor 9 (TLR 9) by synthetic CpG for 24 h or 72 h increased *Nfatc1* induction after an initial 24 h anti-CD3 and anti-CD28 stimulation from MFI 88 to 117 and 129, respectively. TLR 2 engagement by Pam3Cys for 24 h or 72 h increased *Nfatc1* induction after an initial 24 h anti-CD3 and anti-CD28 stimulation from MFI 88 to 114 and 142, respectively.
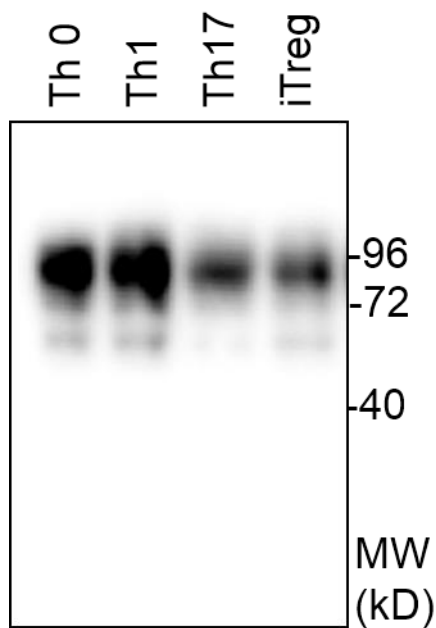
Figure 3.2 | NFATc1 protein expression in primary T-cells
Naïve T-cells from B6 mice were differentiated *in vitro* according to standard protocols for 48 h. Then, the cells were washed and rested for 5 days. Cells were re-stimulated with TPA and ionomycin followed by protein extraction. Western-blotting was performed with whole-cell extracts, and NFATc1 proteins were visualized with a HRP-coupled murine monoclonal ab (7A6) targeting NFATc1 proteins.

Naïve T-cells were isolated from C57BL/6 mice´s spleens and lymphnodes. T-cells were sorted by MACS and cultured in RPMI under Th1, Th17 and iTreg skewing conditions for 48 h. T-cells were washed and kept in medium for three additional days before they were re-stimulated for 5 h with TPA and ionomycin. As shown in Figure 3.2, NFATc1 protein levels were higher after re-stimulation in Th0 and Th1 cells, compared to Th17 and iTreg cells. T-cells cultured in a "Th0" milieu were supplemented with mIL-2 alone, whereas Th1 cells received mIL-2 and IFNγ. TH17 and iTreg cells were differentiated in the presence of mIL-2 and TGFβ.

3.1.2 *Nfatc1* induction in peripheral B-cells

To investigate *Nfatc1* gene expression in B-cells, primary B-cells were isolated from spleen and lymphnodes of *Nfatc1/Egfp* and B6 mice and stimulated *in vitro* for up to four days. B-cells from *Nfatc1/Egfp* mice and wt animals were stimulated with either anti-IgM [10 µg/ml] ab alone or by an initial 24 h anti-IgM stimulation followed by 24 h or 72 h LPS [10 µg/ml] or by 24 h or 72 h anti-CD40 treatment [5 µg/ml].
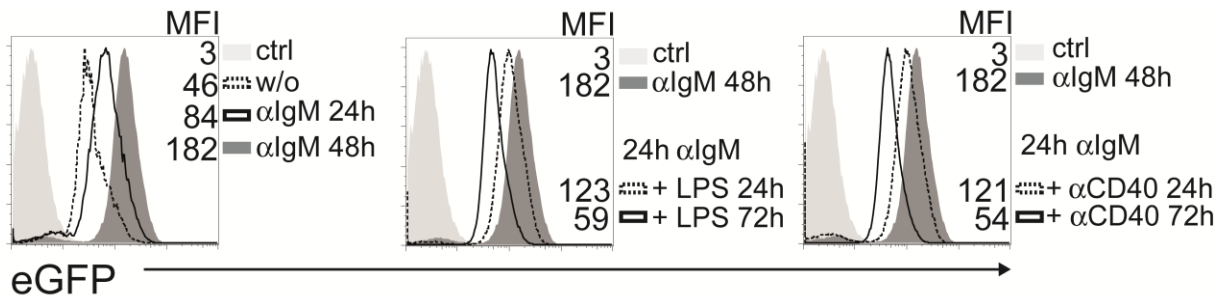
Figure 3.3| *Nfatc1* induction in peripheral B-cells after BCR stimulation
Naïve B-cells were isolated from *Nfatc1/Egfp* and B6-wt control mice, stimulated *in vitro* and analyzed for eGFP expression by FACS.

Nfatc1 induction, detected as eGFP emission intensity, increased from a MFI value of 46 in unstimulated state to 84 after 24 h of anti-IgM stimulation. This induction increased further after 48 h of anti-IgM stimulation reaching its peak at a MFI of 182. Stimulation of B-cells with anti-IgM for more than 48 h led to apoptosis followed by cell-death, unless additional stimuli, e.g. LPS or anti-CD40, were induced. EGFP emission reached a MFI of 124 in B-cells treated with anti-IgM for 24 h followed by an additional stimulation with LPS for 24 h, but dropped to a MFI of 59 as the LPS treatment was extended to 72 h. Engagement of the CD40 receptor on B-cells with anti-CD40 ab for 24 h, after an initial 24 h anti-IgM stimulation, elevated *Nfatc1* induction to a MFI of 121. Prolonged stimulation with anti-CD40 also resulted in a decline of eGFP expression as detected after 72 h (MFI 54).

It was previously reported that B1a-cells, which reside within the peritoneal cavity and display the characteristic expression pattern CD19^{+}, B220^{high} and CD5^{high}, are in very reduced numbers present in *Nfatc1[flx/flx]* x *mb1*-cre mice [70].

The reduction of B1a-cells in mice with a conditional knock-out for *Nfatc1* in early B-cells led to the conclusion that the development of B1a-cells relies on the expression of particular NFATc1-isoforms. To determine the rate of *Nfatc1* induction in B1a-cells, these cells were

isolated from *Nfatc1/Egfp* mice and this rate of *Egfp* induction was compared to B- and T-lymphocytes from the same animals and B- and T-cells from B6 wt animals.
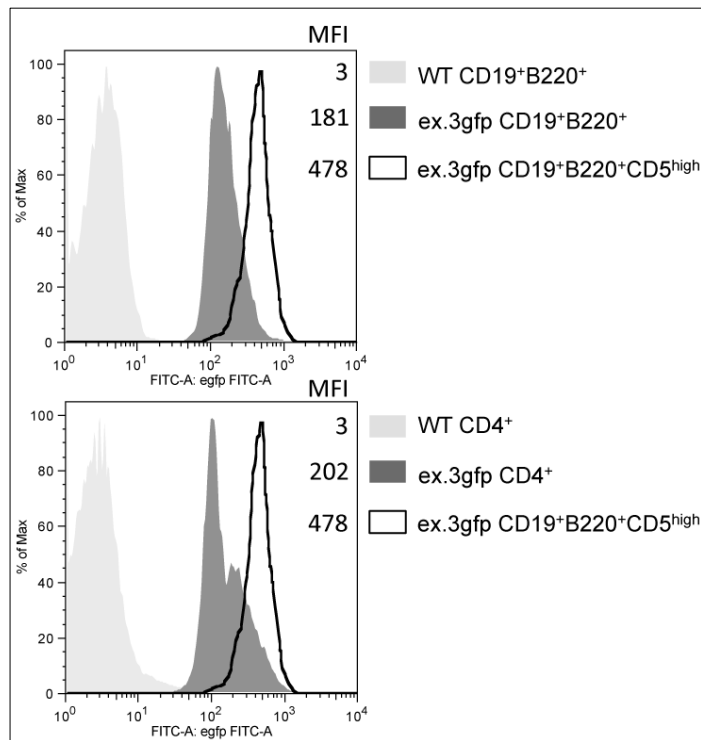
Figure 3.4 | *Nfatc1* induction in B1a-cells analyzed by flow cytometry
Naïve B-, T- and B1a-cells were isolated from B6 wt and *Nfatc1/Egfp* animals and without further treatment analysed by FACS (*Nfatc1/Egfp* cells are revered to as ex.3gfp).

Figure 3.4 shows a FACS analysis comparison between B-, T- and B1a - cells from *Nfatc1/Egfp* mice. Lymphocytes were isolated either from spleen and lymphnodes or, in case of the B1a-cells, from the peritoneal cavity. Wt B-, T- and B1a-cells were also collected from B6 control animals. Without any further treatment, B- and T- cells were stained with abs against specific surface markers and analyzed by flow cytometry. Peripheral B-cells, or B2-cells, expressing CD19 and B220 but no CD5 surface marker, showed an eGFP expression value (MFI) of 181. T-cells (CD4$^+$) isolated from the same organs showed a slightly higher tonic level of *Nfatc1* (MFI 202) expression, compared to conventional B-cells, but B1a-cells, expressing CD19$^+$, B220$^+$ and CD5^{high}, showed the highest *Nfatc1* induction levels with a MFI of 478.

NFATc1/α- and -β-isoforms are transcribed from two separate promoters upstream of exons 1 or 2 designated as P1 and P2 (s. Figure 1.13). The induction of P1 results in the transcription of exon 1 spliced to exon 3, whereas the induction through P2 generates products that are encoded in exon 2 and spliced to exon 3. Induction of P1 generates NFATc1/α-isoforms whereas the products transcribed from P2 are designated as NFATc1/β-isoforms.
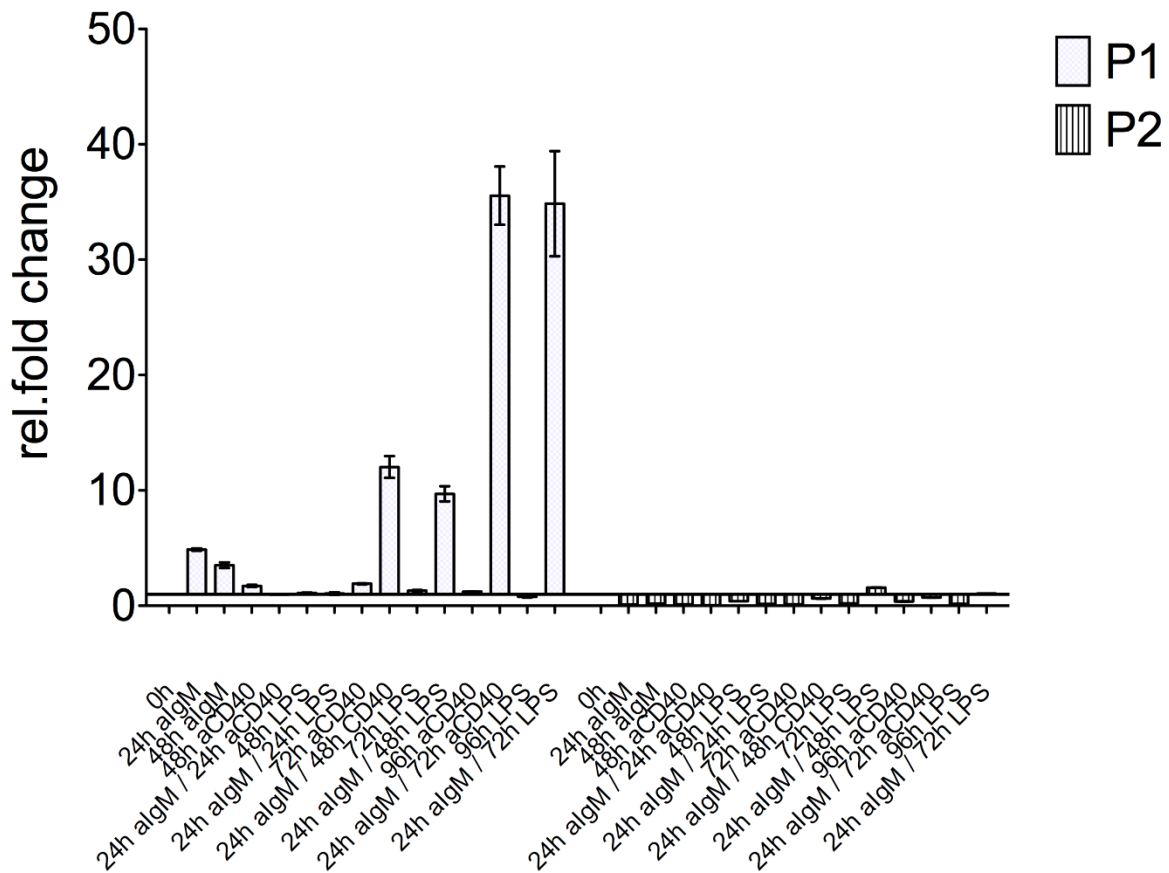
Figure 3.5 | Quantitative Real-Time PCR analysis of *Nfatc1* P1 and P2 induction
RNA was isolated from splenic B-cells stimulated *ex vivo* for up to 96 h. RNA was transcribed into cDNA and quantitative Real-Time PCR for *Nfatc1* mRNA was performed, using two sets of primer pairs. One set of primers were directed against *Nfatc1* exon 1 and exon 3, whereas set two were directed against exon 2 and exon 3, reflecting the usage of promoter P1 or P2, respectively.

Primary B-cells were isolated from spleens and lymphnodes of B6 wt mice and cultured in *ex vivo* medium for further stimulations. As shown in Figure 3.5, there was an increase in P1 transcripts after 24 h and 48 h of anti-IgM stimulation compared to non-stimulated cells, but there was only little, if any *Nfatc1* induction detectable after stimulation with anti-CD40 ab for 48 h alone and none for LPS alone over the same period of time. When the BCR in these cells was triggered by anti-IgM stimulation for 24 h prior a 48 h stimulation with anti-CD40 ab or LPS, a more than 10-fold increase in P1 transcripts was detected. Furthermore, B-cells which were stimulated for 24 h with anti-IgM ab and subsequently cultured in the presence of anti-CD40 or LPS for additional 72 h showed an increase, up to 35 fold, of *Nfatc1* P1 transcripts compared to non-treated cells. There were no significant increase or decrease of P2 transcripts with these stimuli.

3.2 Regulation of *Nfatc1* transcription in lymphocytes

3.2.1 Characterization of two regulatory elements within the *Nfatc1* locus

The *Nfatc1* locus is located on chromosome 18 in mouse and spans eleven exons and ten introns over 106.87 kbs. Induction of *Nfatc1* transcription is controlled by the two promoters P1 and P2. Both promoters were reported to generate DNase-I-hypersensitive chromatin sites and are embedded in CpG islands which are hyper-methylated in non-lymphoid cells and de-methylated in effector T-cells [142] (Figure 3.6). Two elements, designated as E1 and E2 (Enhancer 1 and Enhancer 2), are located in intron 10, situated between exon 10 and exon 11. Both elements show strong DNase-I-hypersensitivity in non-lymphoid cells and E2, but not E1, also correlates with DNase-I-hypersensitivity in CD3$^+$ T-cells. To elucidate the role of E1 and E2 on *Nfatc1* induction *in vivo*, two BAC-transgenic reporter mouse lines bearing specific deletions within the sequences of either E1 or E2 were generated, respectively (unpublished data; Dr. Klein-Hessling).
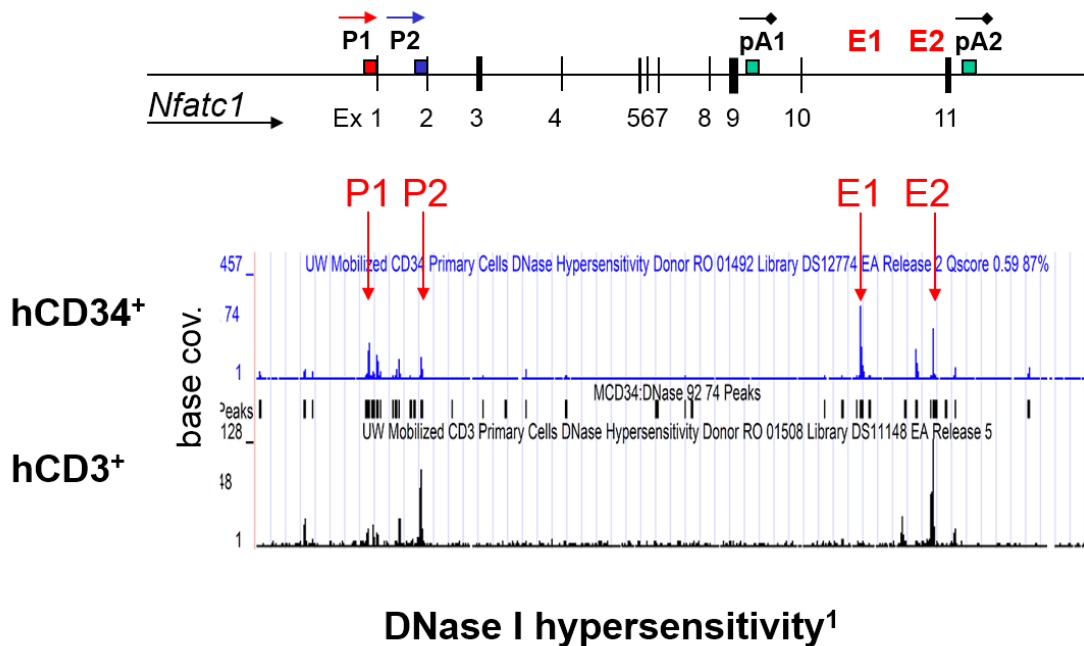
Figure 3.6| DNase I hypersensitivity sites within the *Nfatc1* locus in hCD34$^+$ and hCD3$^+$ cells The *Nfatc1* gene locus includes 11 exons and 10 introns, two promoters (P1 red, P2 blue), two polyadenylation sites, designated pA1 and pA2 (grenn), and two potentially regulatory elements named E1 and E2. The lower two panels show DNase-I-hypersensitivity sites found in human CD34$^+$ and human CD3$^+$ cells (source[1]: The NIH Roadmap Epigenomics Mapping Consrotium; *Bernstein et al.[182]*). The Dnase I hypersensitivity of *Nfatc1*promoters was also described previously.

A

B
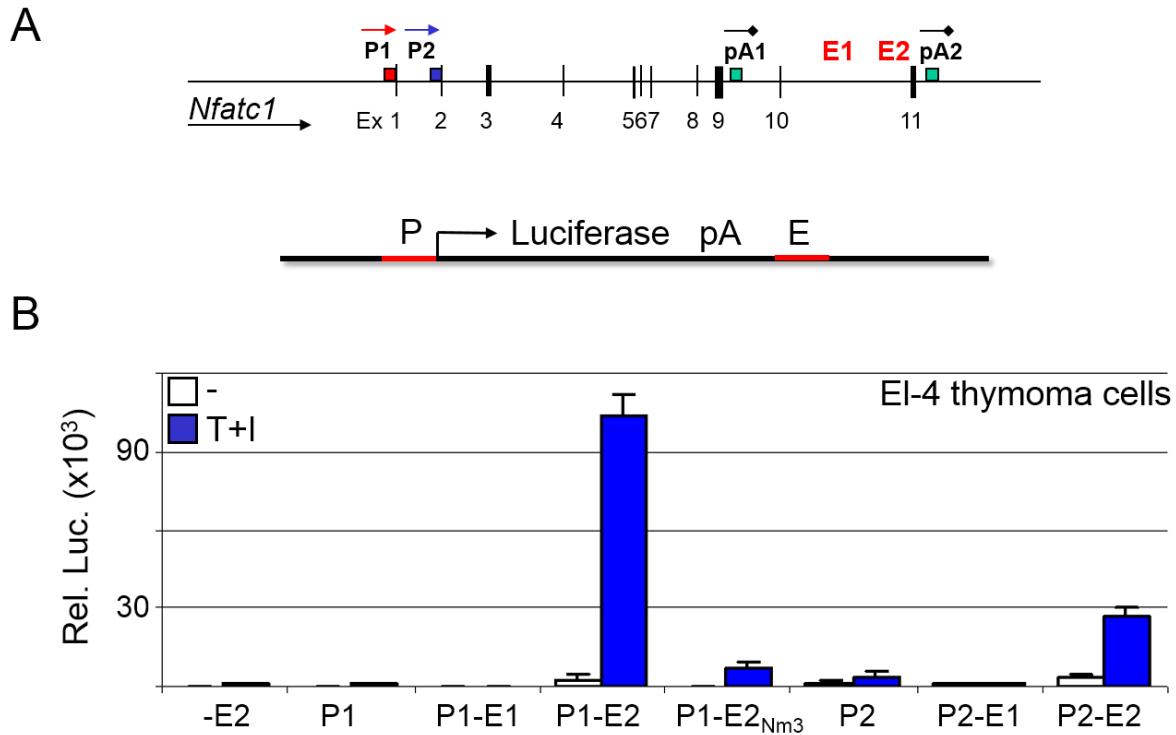
Figure 3.7 | *Nfatc1* **promoter regulation through the regulatory element E2**
A) Schematic drawing of the *Nfatc1* locus. Firefly-luciferase reporter constructs were used containing one of the two promoters, one of the two regulatory elements (E1 or E2) or a combination of both. Furthermore, a luciferase construct was cloned expressing the promoter P1 and a mutated version of E2, $E2_{Nm3}$, bearing three mutated NFAT bining sites. B) Quantification of luciferase reporter assays upon transfection of *Nfatc1* luciferase constructs into El-4 thymoma cells (unpublished data, Dr. Klein-Hessling).

To determine a potential regulatory role for the elements E1 and E2, luciferase reporter constructs were generated and introduced by transfection into El-4 thymoma cells (Figure 3.7). Transfected El-4 cells were stimulated with TPA and ionomycin for 5 h, or left untreated prior luciferase emission analysis. Cells transfected with vectors containing only E2, P1, P2 or a combination of P1 and E1 or P2 and E1 showed no induction. A combination of P1 and element E2 in an expression vector showed the highest induction of luciferase followed by the construct P2-E2. The construct $P1$-$E2_{Nm3}$, expressing a version of E2 with three mutated NFAT sites which abolished NFAT binding, did not induce any significant reporter activity. Luciferase expression was normalized to El-4 cells expressing a luciferase control plasmid (unpublished data from Dr. S. Klein-Hessling).

3.2.2 Regulation of *Nfatc1* expression by the two intronic elements E1 and E2 in primary lymphocytes

Two BAC transgenes, designated as *Nfatc1/DE1* and *Nfatc1/DE2*, were cloned and injected into fertilized mouse oocytes in collaboration with the animal research facility in Mainz (Collab. Dr. K. Reifenberg). For both constructs the previously described BAC-transgene *Nfatc1/Egfp* was modified by introducing nucleotide deletions within the potential regulatory elements E1 and E2. T- and B-cells from *Nfatc1/DE1*, Nfatc1/DE2 and *Nfatc1/Egfp* mice were isolated from spleens and lymphnodes. Cells were stimulated with anti-IgM for 48 h or left untreated and stained for specific T- and B-cell surface markers and subsequently analyzed by flow-cytometry. B6 wt animals were used as negative controls, whereas *Nfatc1/Egfp* mice were used as reference for *Nfatc1* induction.
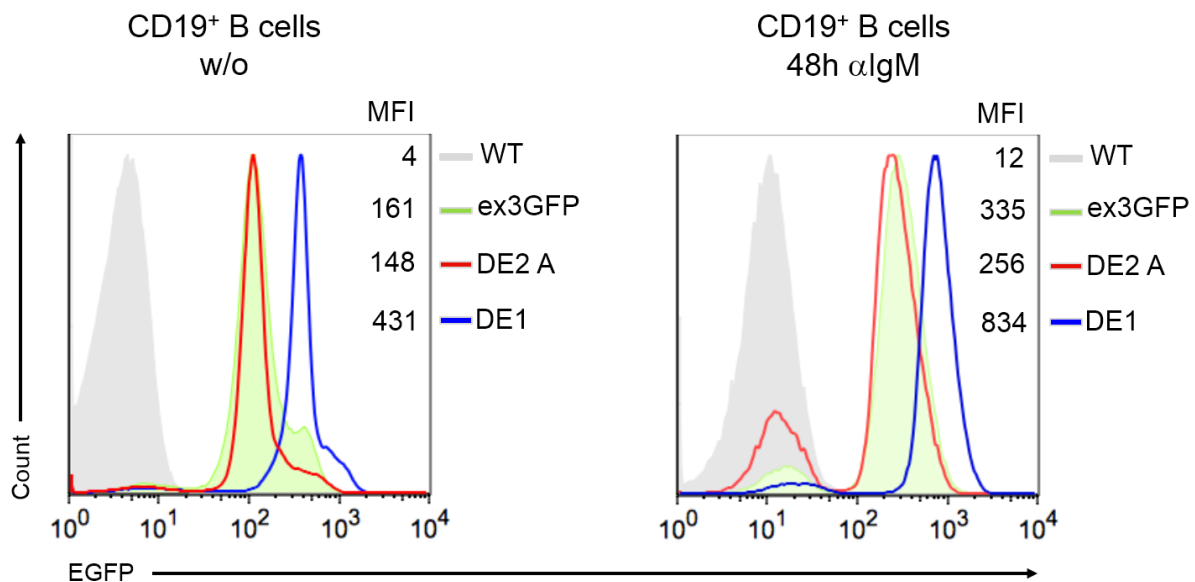
Figure 3.8 | *Nfatc1* induction in B-cells from the BAC-transgenic reporter mouse lines *Nfatc1/DE1* and *Nfatc1/DE2*
Primary B-cells from *Nfatc1/DE1*, *Nfatc1/DE2*, *Nfatc1/Egfp* and B6 wt animals were isolated and stimulated *in vitro* with an ab directed against surface IgM. Individual founder-animals were generated and analysed. WT: C57Bl/6; ex3GFP: *Nfatc1/Egfp*; DE1: *Nfatc1/DE1*; DE2 A: *Nfatc1/DE2* founder A

B-cells from *Nfatc1/DE1* animals, selected by ab-staining against the surface marker CD19, showed the strongest expression of eGFP, reaching a MFI of 431 in an unstimulated state (Figure 3.8). EGFP expression in untreated B-cells from *Nfatc1/Egfp* mice reached a MFI of 161, and a MFI of 148 was detected in CD19⁺ cells from *Nfatc1/DE2* A animals. After 48 h anti-IgM stimulation, eGFP expression doubled to a MFI of 335 in *Nfatc1/Egfp* B-cells and

increased to a MFI of 256 and a MFI of 834 in *Nfatc1/DE2* A and *Nfatc1/DE1* B-cells, respectively.
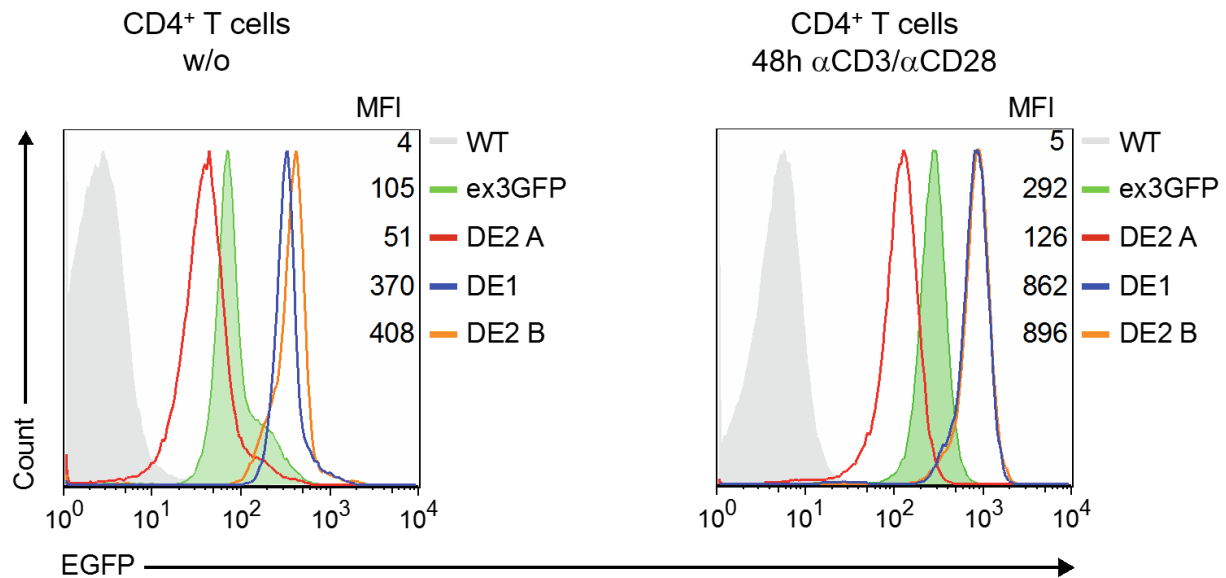

Figure 3.9 | NFATc1 induction in T-cells from the BAC transgenic reporter mouse lines *Nfatc1*/DE1 and *Nfatc1*/DE2
T-cells from *Nfatc1/DE1*, *Nfatc1/DE2*, *Nfatc1/Egfp* and B6 wt animals were isolated and stimulated *in vitro* with abs directed against the TCR and the co-receptor CD28. Individual founder-animals were generated and analyzed. WT: C57Bl/6; ex3GFP: *Nfatc1/Egfp*; DE1: *Nfatc1/DE1*; DE2 A: *Nfatc1/DE2* founder A; DE2 B: *Nfatc1/DE2* founder B.

CD4^{+} T cells were isolated from spleens and lymphnodes of *Nfatc1/Egfp*, *Nfatc1/DE1*, B6 control mice and of two founder lines of *Nfatc1/*DE2. Cells were sorted and either directly analyzed by flow-cytometry or stimulated with abs against CD3 and CD28 for two days. As shown in Figure 3.9, eGFP expression in T-cells from *Nfatc1/DE1* mice displayed an emission of 370 (MFI), a level three times higher than the expression in *Nfatc1/Egfp* T-cells (MFI 105). CD4^{+} T-cells from *Nfatc1/DE2* founder lines showed a low *Egfp* expression level for DE2 A animals (MFI 51) and a strong eGFP fluorescence with an MFI of 408 for cells from DE2 B animals before stimulation. Upon *Nfatc1* induction, eGFP emission, increased to a value of 292 for *Nfatc1/Egfp* CD4^{+} T-cells and was found to be doubled for T-cells from *Nfatc1/DE1*, *Nfatc1/DE2* A and *Nfatc1/DE2* B animals after 48 h of stimulation. The *Egfp* expression increase in *Nfatc1/DE2* A and *Nfatc1/DE2* B T-cells after anti-CD3 and anti-CD28 stimulation was found to be proportional compared to un-stimulated cells, but the difference in the absolute amount of protein expression was determined approximately eight times higher.

The eGFP expression, measured as green light emission by flow-cytometry, reflects *Nfatc1* gene induction. To compare *Nfatc1* gene induction and absolute NFAT protein abundance,

whole-cell protein extracts were prepared from CD3^{+} T-cells. T-cells were isolated from *Nfatc1/Egfp*, *Nfatc1/DE1*, *Nfatc1/DE2* and B6 control mice. They were either freshly lysed and frozen, or stimulated by anti-CD3 and anti-CD28 for two days in RPMI medium and prepared accordingly.
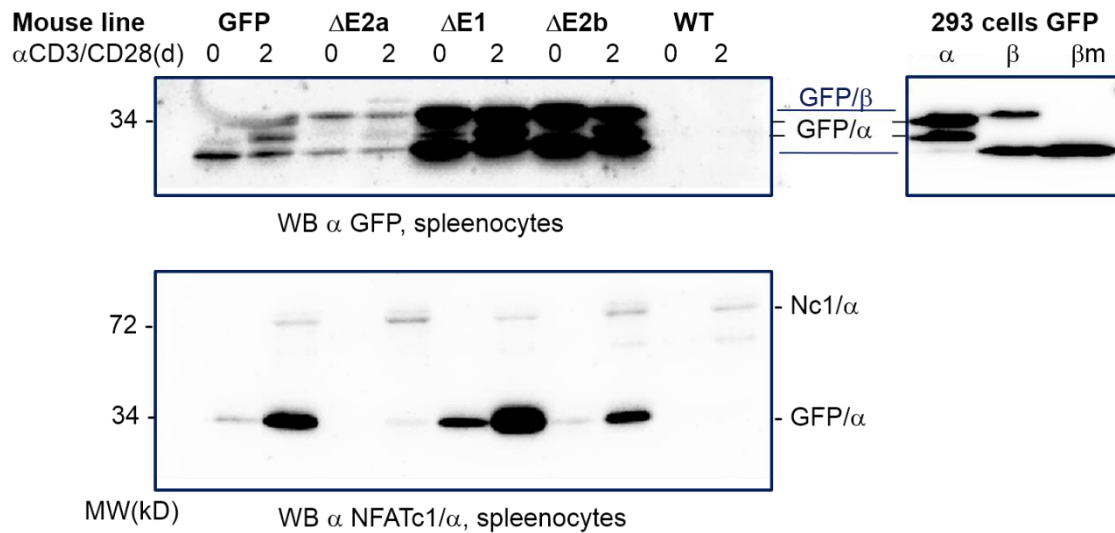
Figure 3.10 | NFATc1 protein expression in T-cells from BAC-transgenic reporter mice
CD3^{+} T-cells were isolated from spleens and lymphnodes of *Nfatc1/Egfp*, *Nfatc1/DE1*, two *Nfatc1/DE2* and B6 wt mice. T-cells were cultured for two days in RPMI medium supplemented with mIL-2 and plate bound anti-CD3 and anti-CD28 abs, or directly lysed and frozen for further preparation. Whole-cell extracts were prepared and equal protein amounts were used to perform SDS-PAGE. Extracts from 293T-cells which were transduced with *Nfatc1/Egfp*-plasmid were used as control samples. GFP: *Nfatc1/Egfp*; ΔE1: N*fatc1/DE1*; ΔE2: *Nfatc1/DE2* (a: founder A; b: founder b); wt: C57Bl/6 mice.

Protein extracts were quantified and used to perform western-blots (Figure 3.10). NFATc1/αA and α-GFP protein expression levels were visualized with HRP-coupled murine ab directed against the NFATc1 α-peptide (Figure 3.10, bottom blot: Nc1/α), the very N-terminus of NFATc1α-isoforms. Additionally, an ab against eGFP was used to display NFATc1-GFP transgene expression abundance. GFP expression levels (Figure 3.10, top blot), presented by anti-GFP ab against all GFP isoforms, mirrored expression levels as shown by FACS analysis in Figure 3.9. All samples revealed an increase in α-GFP expression after TCR and co-receptor stimulation for 48 h. The strong expression of eGFP in *Nfatc1/DE2* B T-cells compared to *Nfatc1/DE2* A cells was also seen in terms of GFP transgene expression, but was not reflected in NFATc1 protein concentrations determined by wb staining using ab against NFATc1 α-peptide, suggesting a difference in copy numbers of transgenes, between the two BAC *Nfatc1*/DE2 lines A and B.

III. RESULTS

3.2 NFATc1-avidin fusion proteins

3.2.1 Cloning of expression plasmid pEGZ-NFATc1/αA-avi

To study the role NFATc1/αA in an overexpression model, the murine *Nfatc1* gene from C57Bl/6 mice was cloned into the retroviral expression vector pEGZ (plasmid Enhanced Green fluorescent protein and Zeocin resistance). The mRNA sequence of the murine *Nfatc1* gene, transcript variant 3 (Figure 3.11), was selected from the sequences provided by the NCBI (National Center for Biotechnology Information) database and used for cloning.

Mus musculus nuclear factor of activated T cells, cytoplasmic, calcineurin dependent 1 (Nfatc1), transcript variant 3, mRNA

>gi|255759918|ref|NM_001164109.1| Mus musculus nuclear factor of activated T cells, cytoplasmic, calcineurin dependent 1 (Nfatc1), transcript variant 3, mRNA
atgccaagtaccagctttccagtcccttccaagtttccactcggccctccggccgcagtctgcgggagcggagaaactttgcggcccgcgccgccctccggcggcaccatgaa
ggcggccgaggaagaacactacagttatgtgtccctagtgtcacctcgaccctgccccttcccacagcacactctgccttgccagcagcatgccacgacctccagacgtcc
accccgggtatctcagctgttccttcagccaatcatcccccccagttacggaggggctgtggacagcgggccttcgggatacttcctgtcctctggcaacaccagacccaacggg
gccccgactctggagagtccgagaatcgagatcacctcctacctgggcctacaccatggcagcggccagttttccacgacgtggaggtggaagacgtacttcctagctgcaa
gcgctcaccgtctacagcaaccctgcacctgcccagcctggaagcctacagagacccctcctgcctgagcccagccagcagtctctcctccagaagctgtaactctgaggcct
cctcctacgagtccaactactcctacccatacgcgtcccccagacctctccgtggcagtcaccctgcgtgtctcccaagaccacggacccggaggagggtttccccgaagcc
tgggtgcctgccacctgctaggatcgcccaggcactccccatccacctctcctcgggcaagcatcacggaggagagctggctcggtgcccgcggctcccggcccacgtcccc
ctgcaacaagcgcaagtacagtctcaatggccggcagccctcctgctcaccccaccactcacccacaccatcccccatggctccctcgggtcagtgtgaccgaagataccт
ggctcggtaacaccacccagtataccagctctgccattgtggcagccatcaacgccctgaccaccgatagcactctggacctgggtgatggggtccctatcaagtctcgaaaga
cagcactggagcatgcgccctctgtggccctcaaagtagagccagctggggaagacctgggcaccactccacccacttctgacttcccacccgaggagtacaccttccagca
ccttcggaagggtgcctttgcgagcagtatctgtcggtgccacaggcctcgtatcagtgggcgaagcccaagtctctttccccgacatcatatatgagcccatccttgcctgccctt
gactggcagctcccgtcacattctggtccatacgagcttcggatcgaggtgcagcccaagtctcaccacagggctcactatgagacggaaggcagccgggggggctgtgaagg
cttcagctggaggacacccccattgtgcagctacacggttacttggagaatgaacctctcacgctacagctgttcattgggacggctgacgaccgcctgctgaggccccacgcctt
ctaccaggtccaccggatcacggggaagactgtctccaccaccagccacgagatcatcctgtccaacaccaaagtcctggagatccccgttgcttccagaaaataacatgcga
gccatcatcgactgtgctgggatcctgaagctcagaaactctgatattgagctgaggaaaggggagacagacatcgggaggaagaacaccagggtgaggctggtcttccggt
tcacatcccacagcccaatggccggacgctgtctctccaggtggcctcgaacccatcgagtgttcccagcggtcagcccaggagctgcccctcgtggagaagcagagcaca
gacagctacccagtcatcggcgggaagaagatggtgctgtctggccataacttctgcaagactccaaagtcattttcgtggagaaggctccagatggccaccacgtctgggag
atggaagcaaagactgaccgggacctgtgcaagccaaATTCCCTGGTGGTTGAGATACCACCTTTCCGCAACCAGAGGATAACCAGCCC
CGTCCAAGTCAGTTTCTATGTCTGCAACGGGAAACGGAAGAGAAGCCAGTACCAGCGTTTCACGTACCTTCCTGCCAAT
GgtaactctgtctttctaAccttaagctctgagagtgagctgagaggaggtttttacCAATTGGGCGGTGGAGGTCTGGAAGTTCTGTTCCAGGGACC
TGACTACAAGGACGATGACGATAAAGGGAAGCCAATCCCTAATCCCCTTCTGGGACTCGACTCTACCGAAAACTTGTAC
TTCCAGGGACCACGGGAAAATCTGTACTTTCAGGGAATGGCATCGAGTCTACGGCAAATCCTCGACTCGCAGAAGATGG
AGTGGCGCTCAAACGCCGGAGGCTCGTGA

Figure 3.11 | Nucleotide sequence and cloning strategy for NFATc1/αA-avi, modified from the mRNA sequence of murine *Nfatc1* mRNA, transcript variant 3
Murine mRNA sequence of *Nfatc1* transcript variant 3.The translational start, indicated in red, starting with atg was used as first amplification site. The sequence-motif indicated in green was used as second amplification site. The blue nucleotide strecht indicates exon 9 of the *Nfatc1* gene, followed by a transition to the avidin-tag sequence in dark-red and dark red, highlighted in yellow, respectively. The sequence motif, highlighted in yellow, was used as third amplification site. The avidin-tag peptide sequence, black underlined letters, was substituted with a TGA stop-codon (red), introduced through modified primer-addition (not displayed).

A plasmid, designated as pMSCV-Bio-iPuro encoding the avidin-tag (bio-tag) nucleotide sequence, a prescission-site, a Flag-tag, V5 tag and two TEV (Tobacco Etch Virus) cleavage sites, was kindly provided by Prof. M. Busslinger (IMP,Vienna). The avidin-tag was amplified,

slightly modified at both ends and used to create the NFATc1/αA-avi and NFATc1/βC-avi fusion-proteins.

As shown in Figure 3.12, NFATc1/αA-avi is a full-length variant of NFATc1/αA including a fully functional N-terminal TAD-A domain (Transactivation Domain A) and the full length DNA binding domain (RSD: Rel-Similarity Domain). C-terminally, the original TGA stop-codon was deleted and replaced by the avi-tag and a new stop-codon was introduced, creating a fully functional protein.
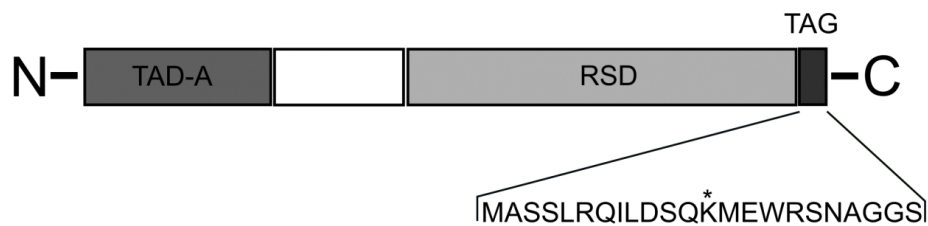
Figure 3.12 | Schematic drawing of the NFATc1/αA-avi protein
Schematic drawing of the C-terminally tagged NFATc1/αA-avi protein. The asterisk (*) indicates the biotinylatable lysine residue within the avidin-tag. TAD-A: Transactivatory domain; RSD: Rel-similarity domain. TAG: avidin-tag

Initially, two individual variants of NFATc1/αA-avi and NFATc1/βC-avi were cloned, but it was shown that the N-terminally tagged variants of NFATc1/αA-avi and NFATc1/βC did not function in *in vitro* assays (data not shown). In Figure 3.12, the avidin-tag amino acid (AA) sequence is displayed. The asteriks indicates the reactive lysin residue which serves as a biotin receptor for the enzyme BirA, a prokaryotic ortholog to the human holocarboxylase synthetase (HCS).

The NFATc1/αA-avi protein is 792 AA long and encoded by 2376 nucleotides. The modified "*Nfatc1/αA* gene" was amplified and cloned in a two-step process. As shown in Figure 3.13, three individual overlapping PCR templates, designated as C-terminal αA-bio, αA1-1300 and αA1300-2100 were amplified by PCR. The avidin-peptide sequence was amplified from the original pMSCV-Bio-iPuro plasmid. To create an overlap, it was extended at the 5´- end with 21 nucleotides of *Nfatc1* exon 9. Fragments αA1-1300 and αA1300-2100 were cloned from C57Bl/6 cDNA, synthesized by reverse transcription from RNA which was isolated from untreated B6 B-cells. A high efficient, long-amp polymerase (Crimson Long-AmP; NEB) was used to amplify the full length sequence of *Nfatc1/αA*, including an N-terminal restriction enzyme site for ClaI and a C-terminal site for HpaI.
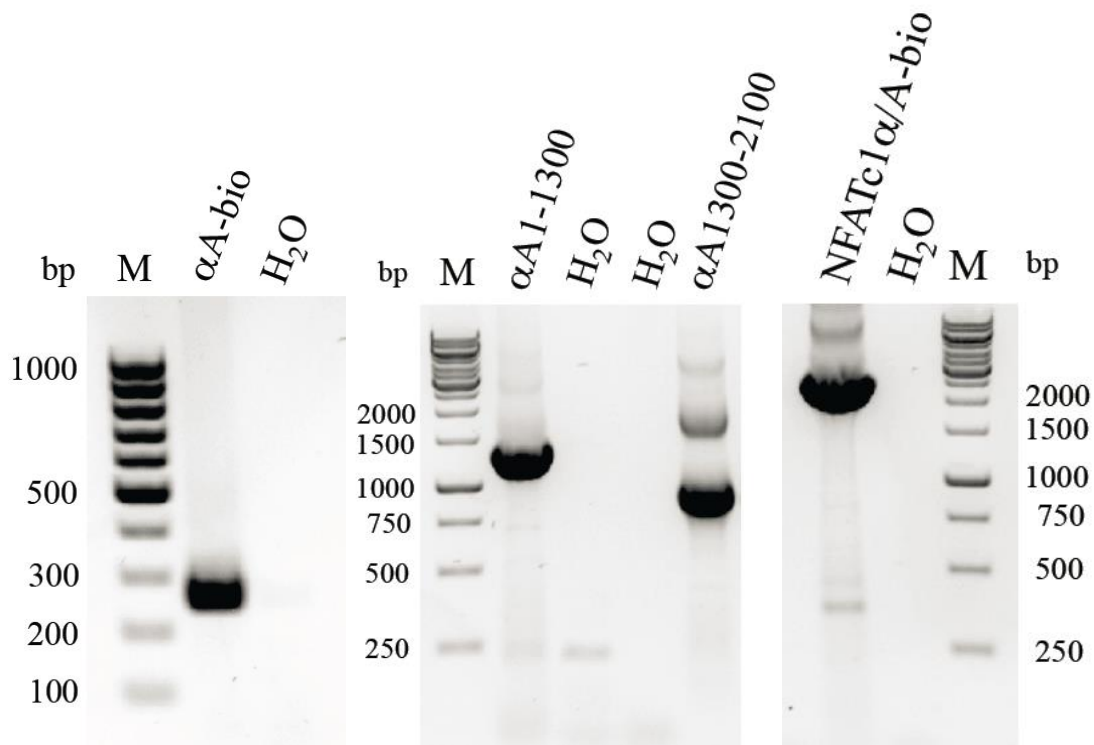
Figure 3.13 | PCR amplicons generated to create a C-terminal tagged NFATc1/αA
1-1.5% agarose gels of PCR amplicons generated as templates to amplify a new, avidin-tagged NFATc1/αA. From left to right: The C-terminal avi-tag sequence was amplified from the pMSCV-bio-iPuro plasmid and extended, gaining a 21 nucleotide overlap (in total 256 nts), partially spanning *Nfatc1* exon 9. Fragment αA1-1300, starting at the initial *Nfatc1* ATG and terminating at nt 1305 of the mRNA sequence, and fragment αA1300-2100 covering the *Nfatc1* mRNA sequence from nts 1286 to 2154. NFATc1α/A-bio: Entire *Nfatc1/αA-avi*, 2376 nts, generated from all three PCR products.

The full-length *Nfatc1/αA-avi* PCR-product (NFATc1α/A-bio; Figure 3.13) was extracted and purified using standard agarose gel extraction protocols. It was enzymatically digested, purified and introduced into the retroviral vector pEGZ (s.2.1.4) by ligation. After transformation of pEGZ-*NFATc1/αA-avi* into DH5α *E.coli*, bacteria were grown in the presence of ampicillin on agar-agar-plates. Individual clones from the construct pEGZ-NFATc1/αA-avi were sequenced and functionally tested by *in vitro* transfection into HEK-cells (Human Embryonic Kidney cells) and FACS analysis.

3.2.2 Cloning of expression plasmids pEGZ-NFATc1/βC-avi and pEGZ-NFATc1/βC-aviFl

As described for NFATc1/αA (3.2.1), a tagged variant of NFATc1/βC, designated NFATc1/βC-avi, was cloned into the pEGZ expression plasmid for *in vitro* analysis. Furthermore, a modified variant of NFATc1/βC-avi, designated NFATc1/βC-aviFl, harboring two loxp sites adjacent to the avi-tag sequence, was cloned into the pEGZ vector. For both

III. RESULTS

constructs, exons 2-11 of the murine *Nfatc1* gene were amplified from RNA, extracted from

C57Bl/6 mice. The mRNA sequence of *mNfatc1*, transcript variant 5 (Figure 3.14), was selected

from the sequences provided by the NCBI database.

Mus musculus nuclear factor of activated T cells, cytoplasmic, calcineurin dependent 1 (Nfatc1), transcript variant 5, mRNA

>gi|255759924:1-140 Mus musculus nuclear factor of activated T cells, cytoplasmic, calcineurin dependent 1 (Nfatc1), transcript variant 5, mRNA

atgacggggctggagcaggacccggagttcgacttcgatttcctcttcgagttcgatcagagcggcgggggcgccgcggccgcagaacactacagttatgtgtcccctagtgtcacctcgaccctgccccttcccacagcacactctgccttgccagcagcatgccacgacctccagacgtccaccccgggtatctcagctgttccttcagccaatcatcccccagttacggaggggctgtggacagcgggccttcgggatacttcctgtcctctggcaacaccagacccaacgggccccgactctggagagtccgagaatcgagatcacctcctacctgggcctacaccatggcagcggccagttttttccacgacgtggaggtggaagacgtacttcctagctgcaagcgctcaccgtctacagcaaccctgcacctgcccagcctggaagctacagagacccctcctgcctgagcccagccagcagtctctcctccagaagctgtaactctgaggcctcctcctacgagtccaactactcctaccatacgcgtgcccccccagacctctccgtggcagtcacccctgcgtgtctcccaagaccacggaccccggaggagggttttccccgaagcctgggtgcctgccacctgctaggatcgcccaggcactccccatccacctctcctcgggcaagcatcacggaggagagctggctcggtgcccgcggctcccggcccacgtcccctgcaacaagcgcaagtacagtctcaatggccggcagccctcctgctcaccccaccactcacccacaccatcccccccatggctccctcgggtcagtgtgaccgaagatacctggctcggtaacaccacccagtataccagctctgccattgtggcagccatcaacgccctgaccaccgatagcactctggacctgggtgatggggtccctatcaagtctcgaaagacagcactggagcatgcgccctctgtggccctcaaagtagagccagctgggggaagacctgggcaccactccacccacttctgacttcccaccccgaggagtacaccttccagcaccttcggaagggtgccttttgcgagcagtatctgtcggtgccacaggcctcgtatcagtgggcgaagcccaagtctctttccccgacatcatatatgagcccatccttgcctgcccttgactggcagctcccgtcacattctggtccatcgagcttcggatcgaggtgcagcccaagtctcaccacagggctcactatgagacggaaggcagccggggggcgtgtgaaggcttcagctggaggacaccccattgtgcagctacacggttacttggagaatgaacctctcacgctacagctgttcattgggacggctgacgaccgcctgctgaggcccccacgccttctaccaggtccaccggatcacggggaagactgtctccaccaccagccacgagatcatcctg**t**caacaccaaagtcctggagatcccgttgcttccagaaaataacatgcgagccatcatcgactgtgctgggatcctgaagctcagaaactctgatattgagctgaggaaaggggagacagacatcgggaggaagaacaccagggtgaggctggtcttccgagttcacatcccacagcccaatggccggacgctgtctctccaggtggcctcgaacccatcgagtgttcccagcggtcagcccaggagctgcccctcgtggagaagcagagcacagacagctacccagtcatcgg**cggggaagaagatggtgctgtc**tggccataacttctgcaagactccaaagtcattttcgtggagaaaggctccagatggccaccacgtctgggagatggaagcaaagactgaccgggacctgtgcaagccaaattccctggtggttgagataccacctttccgcaaccagagggataaccagccccgtccaagtcagtttctatgtctgcaacgggaaacggaagagaagccagtaccagcgtttcacgtaccttcctgccaa**tgttccaattataaagacaga**acccacggacgactttgagccagctctgacctgtggaccaatgagccaggggattagtcctctgccgaggccttactacagccaacagctcaccatgcctcccgacccccggctcctgcctcgtggctggcttcgcccctgctcccagaggaacacgctgatgcccacgcctcccaacgcaagcccgaagctccacgacctttcctctcctgcctacaccaagggcctcaccaacccgggccacagtggtcaccttggacttcagccacccgcttcggaggcccccaccatgcaggaagtgccgagacccatggccatccaacccaactcgcctgagcagcccccatccgccaggctacagccgcaggtgagtccacatctgaacagtagctgtccccttggtcgccgacaagtgctctgtcccaacagcccctcttctccacttccatctgctgcccaagagccagcctgcttacagtcctcagccctccctcctgacatgggccaccggcagccacaaccgcagaaggttcaaagaaatgaatctccagccgtattgccagaggtgtgtgaggacagtggccataacttggcccctattcctgtagtgatcaag**caagagcctgaggaattggaccagttgtacttggatgatgtaaatgagatcatacgtaacgacctc**<mark>tccagcacgatcccccactcc</mark>caattgggcggtggaggctggaagttctgttccagggacctgactacaaggacgatgacgataaagggaagcaatccctaatcccttctgggactcgactctaccgaaaacttgtacttcagggaccacgggaaaatctgtactttcagggaatggcatcgagtctacggcaaatcctcgactcgcagaagatggagtggcgct**caaacgccggaggctcg**tga

Figure 3.14 | Nucleotide sequence and cloning strategy for NFATc1/βC-avi, modified from the mRNA sequence of murine *Nfatc1* mRNA, transcript variant 5
The mRNA sequence of *Nfatc1* transcript variant 5, NFATc1/βC (*mus musculus*).The transcriptional start, indicated in dark red, starting with <u>atg</u>, was used as first amplification site. The sequence motifs indicated in green, purple and light blue were used as second, third and fourth amplification sites. The blue nucleotide stretch indicates a part of exon 11 of the *Nfatc1* gene, followed by a transition to the avidin-tag sequence, highlighted in yellow. This sequence motif was used as reverse binding site for the fourth amplicon. The avidin-tag peptide sequence, in black underlined letters, was substituted with a TGA stop-codon (red).

Figure 3.14 displays the sequence encoding NFATc1/βC-avi. NFATc1/βC-avi, a C-terminaly

avi-tagged version of NFATc1/βC, is similar to the previously described NFATc1/αA-avi and,

additionally, to a modified variant of NFATc1/βC-aviFL. This modified variants expresses a

loxp-flanked version of the avidin-tag, termed NFATc1/βC-aviFl. Both proteins are full-length

variants of NFATc1/βC including the N-terminal TAD-C domain (<u>T</u>ransactivation <u>D</u>omain <u>C</u>)

and the RSD. For NFATc1/βC, the original TGA stop-codon was deleted and replaced by the avi-tag and a new stop-codon, allowing the generation of a functional protein. NFATc1/βC-aviFl was cloned by introducing loxp sites in-front and behind the avidin-tag sequence. Additionally, two stop codons were introduced, one terminating the avidin-tag and one behind the second loxp site.
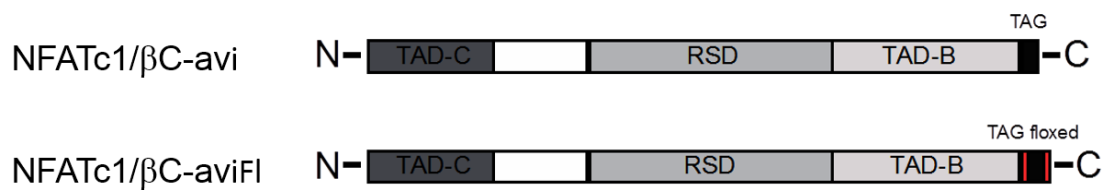
Figure 3.15 | Scheme of NFATc1/βC-avi and NFATc1/βC-aviFl proteins
Schematic drawing of NFATc1/βC-avi and NFATc1/βC-aviFl. The full length NFATc1/βC proteins include an N-terminal TAD-C, a RSD and a C-terminal TAD-B. Both proteins express an avi-tag at the C-terminus. In case of NFATc1/βC-aviFl, the avi-tag was flanked with loxp sites. TAD-C: Transactivation Domain C; RSD: Rel-Simillarity Domain; TAD-B: Transactivation Domain B.

NFATc1/βC-aviFL was designed as a variant of NFATc1/βC-avi, providing the possibility to delete the avi-tag next to exon 11 using cre-recombinase activity. The plasmid pEGZ-NFATc1/βC-aviFL was generated to serve as a control for *in vitro* assays and to proof applicability of cre-deletion for BAC transgenic mouse which we intend to create.

The NFATc1/βC-avi protein is 1001 AA long. It is encoded by 3003 nts. Similar to NFATc1/αA-avi, the modified *Nfatc1/βC* cDNA was amplified and cloned in a two-step process. As shown in Figure 3.16, four overlapping PCR products, designated N-term, inter-1 and inter-2 and Ex11-avi and Ex11-aviFL, respectively, were amplified by PCR for each construct. To create an overlapping region, the avi-tag sequence was generated from the original pMSCV-Bio-iPuro plasmid and extended at the 5´- end for 19 nucleotides of *Nfatc1* exon 11. Fragments N-term, inter-1 and inter-2 were synthesized by reverse transcription from RNA isolated from untreated B6 B-cells and cloned. To create NFATc1/βC-aviFl, an additional PCR template with two loxp sites up- and downstream of the avi-tag was created (individual PCRs are not shown). NFATc1/βC-aviFl spans 3033 nts encoding a protein of 1011 AA.
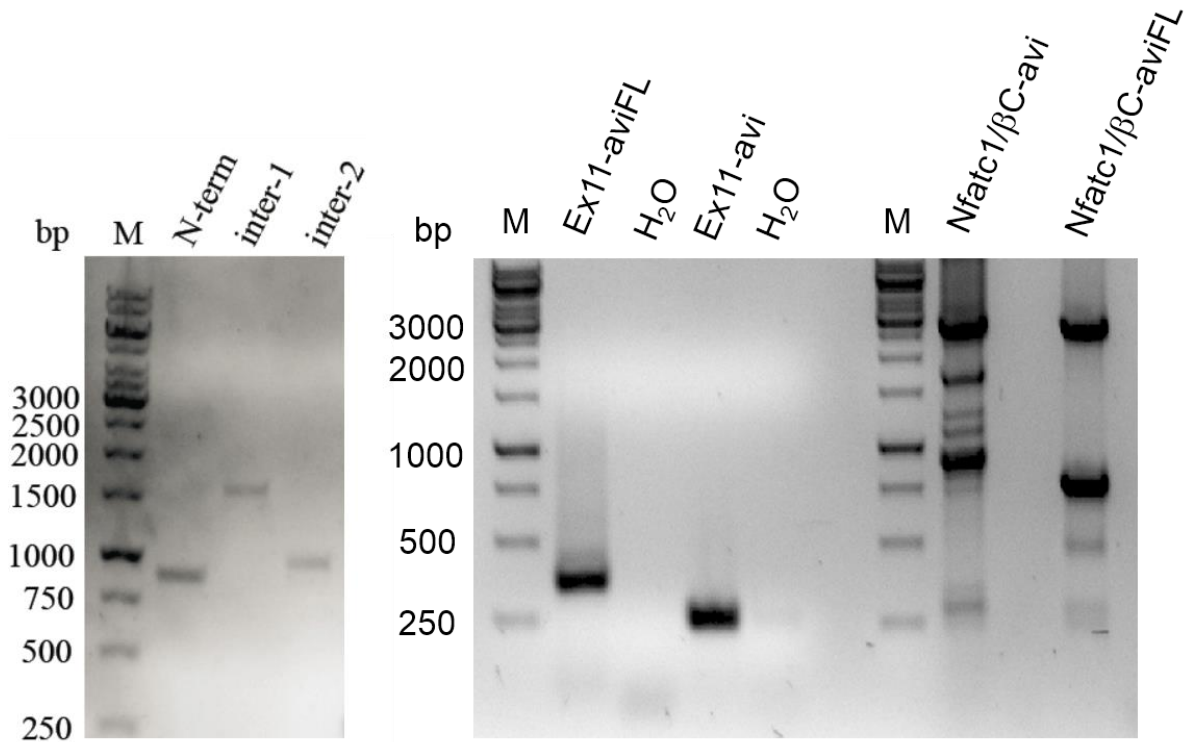
Figure 3.16 | PCR amplicons generated to create two C-terminally tagged NFATc1/βC proteins
1-1.5% agarose gels for the fractionation and isolation of PCR amplicons generated as templates to amplify two avi-tagged "*Nfatc1/βC* cDNAs". From left to right: Fragment N-term is shown, starting at the initial *Nfatc1* (exon2) ATG and terminating at nt 901 of the mRNA sequence. Fragment inter1, covering *Nfatc1* mRNA sequence from nt 569 to 2071 and inter-2 are shown next, spanning all nucleotides from 1791 to 2776. The C-terminal avi-tag sequence was amplified from the pMSCV-bio-iPuro plasmid and extended gaining a 19 nucleotide overlap (in total 254 nts) partially spanning *Nfatc1* exon 11. Additionally, loxp sites were introduced flanking the avi-tag creating the product Ex11-aviFl.The complete NFATc11/βC-avi, amplified through overlapping, long-range PCR products from four template products was established yielding a 3003 nt product, and NFATc1/βC-aviFL, amplified accordingly, spanning 3033 nts.

Long-range PCR amplification was applied for both constructs to create the full-length sequences of NFATc1/βC-avi and NFATc1/βC-aviFl, including an N-terminal restriction enzyme site for ClaI and a C-terminal site for HpaI, respectively. The full length products were extracted after agarose gel separation and purified using a standard agarose gel extraction protocol. DNA was enzymatically digested, purified and introduced into the pEGZ (s. 2.1.4) plasmid. The pEGZ vector-plasmids were transformed into DH5α *E.coli* and grown on ampicillin-supplemented agar-medium. Individual clones from the products pEGZ-NFATc1/βC-avi and pEGZ-NFATc1/βC-aviFl were sequenced and functionally tested by *in vitro* transduction into HEK-cells followed FACS analysis (data not shown).

3.3 Bacterial Artificial Chromosome *Nfatc1 Ex.9-avidin*

Bacterial artificial chromosomes (BACs) are large DNA fragments, in average 100-300 kb in size, and cloned into bacterial vectors which are feasible for stable propagation of large DNA segments in bacteria [183]. In order to analyze *Nfatc1* gene expression, it is possible to modify genes of interest and generate BAC transgenic mouse lines by pronuclear injection of fertilized mouse oocytes with a purified BAC fragment. The BAC methodology is a solid and fast alternative to gene knock-in technology in embryonic stem (ES) cells for the study of gene expression *in vivo*. Due to the large size of BACs they are normally inserted into the mouse genome as unique copy, and the expression of gene(s) cloned in the BAC behaves like the endogenous gene.

3.3.1 Cloning of the shuttle-vector pLD53.SC2 *Nfatc1 Ex.9-avidin*

In order to study the expression of a biotinylatable short NFATc1 isoform in a BAC transgenic reporter line, the avi-tag had to be introduced into a BAC vector spanning ~210-kb DNA of the *Nfatc1* gene (BAC RP23-361H16) by homologous recombination. The avi-tag was amplified by PCR and fused to two 1kb stretches of cDNA which are homologous to the side of insertion in the *Nfatc1* locus.
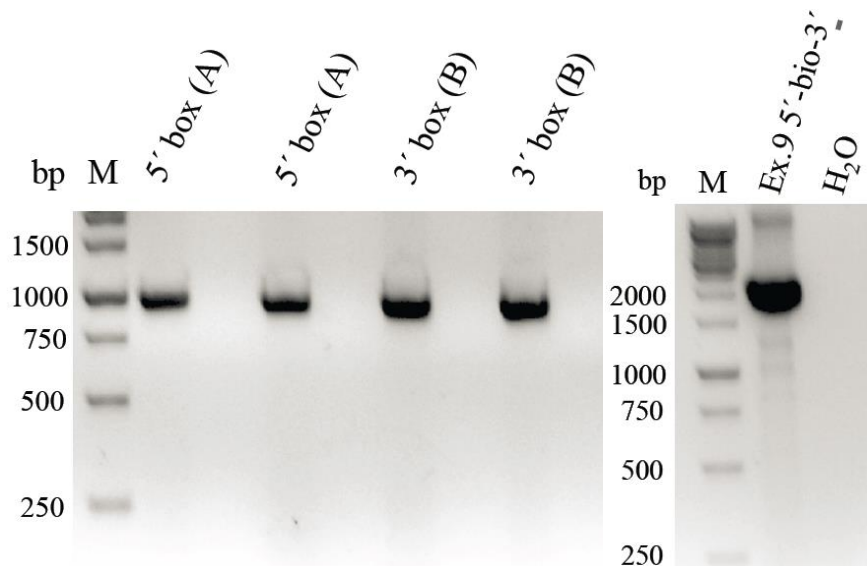
Figure 3.17 | Cloning of *Nfatc1* Ex9 avidin-tag homology region
A 1.5% agarose gel (left) shows the PCR products, amplified with primer pairs flanking a 1kb region (boxA) of homology upstream and a 1kb region (boxB) downstream of the last codon within exon 9 of the *Nfatc1* gene. Right, a 2kb PCR product is shown, generated from three template cDNA fragments, i.e. boxA, boxB and the avi-tag, by long range PCR amplification.

At both ends, the avi-tag was extended with a 1kb stretch of cDNA which is homologous to the intended region of insertion within exon 9 of the *Nfatc1* gene. Therefore, the regions 1kb upstream of the last codon of *Nfatc1* Ex.9 and 1kb downstream of *Nfatc1* Ex.9 were amplified from BAC RP23-361H16 and fused to both sides of the avi-tag sequence by PCR (Figure 3.17). This product was ligated into the shuttle-vector plasmid pLD53.SC2 [178] which also harbors a R6Kγ ori for replication and expresses an ampicillin-resistance gene.
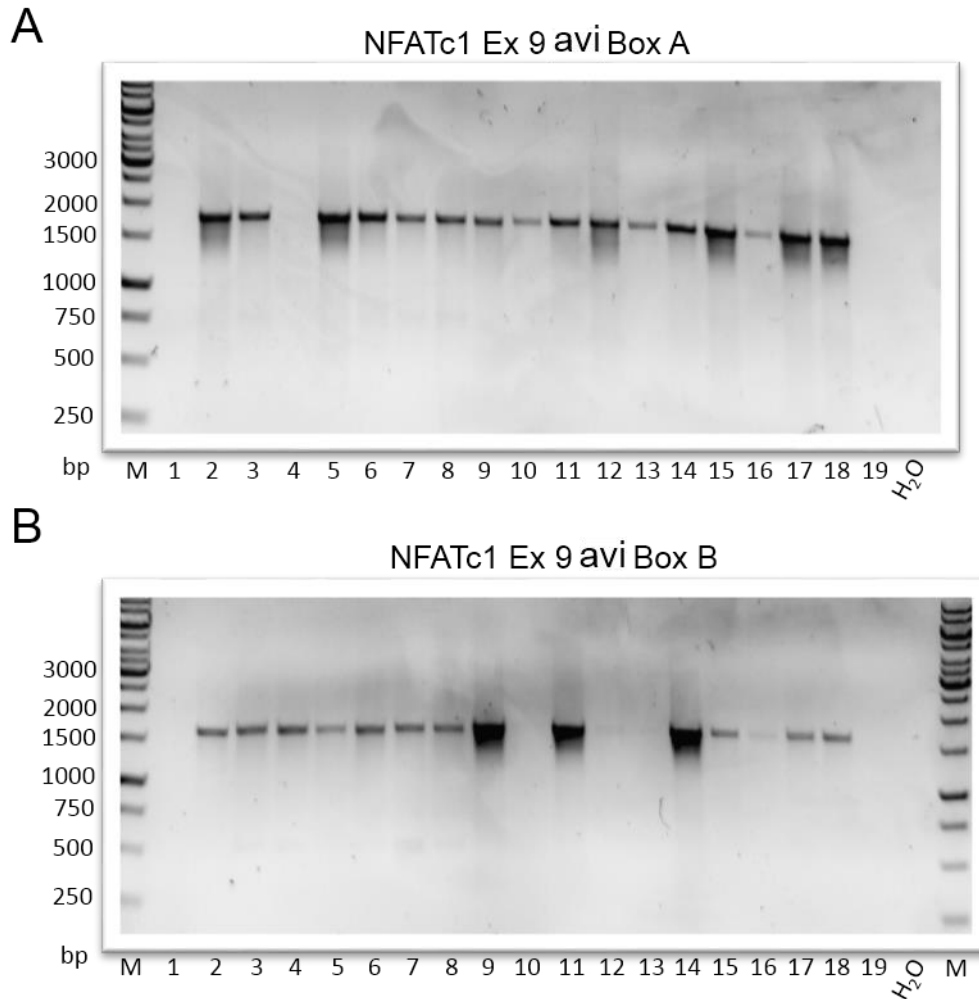
Figure 3.18 | Results of colony screening after the primary recombination of RP23-361H16 and *Nfatc1* Ex. 9-avi
A) PCR-colony screening was performed to identify bacterial clones which were positive for a recombination event between the *Nfatc1* exon 9 region, homologous to BoxA, expressed by RP23-361H16, or B) clones which were positive for recombination events between the *Nfatc1* exon 9 region, homologous to BoxB. Lanes 1-18: miniprep DNA templates from bacterial colonies, lane 19: BAC RP23-361H16 negative control, and line 20: negative water control.

Recombination of the regions which are homolgous between the *Nfatc1* locus within BAC RP23-361H16 and the BoxA and BoxB sequences, flanking the avi-tag within pLD53.SC2, was catalyzed by the enzyme Recombinase A (RECA), which was additionally introduced into the

E.coli strain that expressed BAC RP23-361H16 DNA. The targeted introduction of the avi-tag sequence into exon 9 of the *Nfatc1* locus, expressed by BAC RP23-361H16, and the necessary release of the introduced shuttle-vector pLD53.SC2, delivering the avi-tag, required two steps of recombination (Figures 3.18 and 3.19). A relatively high background was detected when colony screening was performed to identify positive clones for the first recombination event (Figure 3.18). Three clones, positively identified for recombination of homology BoxB (clone #9, clone #11 and clone #14 in Fig. 3.18 B), were chosen for a second round of selection and recombination on M9 minimal medium agar-agar-plates. In case of a positive second recombination, i.e. a recombination event with homology BoxA, the pLD53.SC2 shuttle vector was released from the BAC plasmid. Bacteria without functional pLD53.SC2 gained a growth advantage, as sucrose was the only organic compound in M9 medium present and, due to their sizes, were chosen for further colony screening.
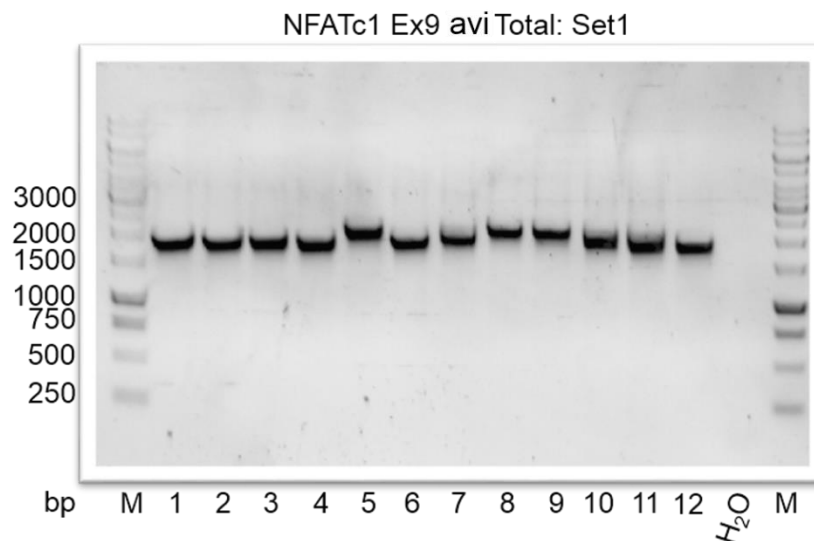
Figure 3.19 | Colony screening for second recombination of BAC RP23-361H16 and pLD53.SC2 *Nfatc1* Ex.9 avidin
PCR-colony screening was performed to identify bacterial clones which were positive for a second recombination event between the *Nfatc1* exon 9 region within pLD53.SC2 *Nfatc1* Ex.9-avi, homologous to BoxA, expressed by RP23-361H16. Lanes 1-11: miniprep DNA templates from bacterial colonies, selected by M9 conditions, lane 12: BAC RP23-361H16 negative control and lane 20: negative water control.

Single-colonies, grown on M9 minimal medium agar-agar plates, were picked, and DNA was prepared for PCR screening. As shown in Figure 3.19, three single-colony clones (clone #5, clone #8 and clone #9, in Fig. 19) were identified for full integration of the avi-tag into the *Nfatc1* locus. Three primer pairs designed to create products of 2000 bp length for the unmodified BAC RP23-361H16 and products of 2228 bp length for BAC RP23-361H16 in case of a successful recombination, were designed and applied in PCRs. All three clones were also

screened for the integration of BoxA and BoxB, with one of the primers binding to the avi-tag. DNA from all clones were used as PCR templates and were found to generate products of the correct sizes (data not shown).

BAC DNA was linearized by Nru I to cut the DNA upstream and downstream of the *Nfatc1* locus within BAC RP23-361H16 *Nfatc1* Ex.9 avi.
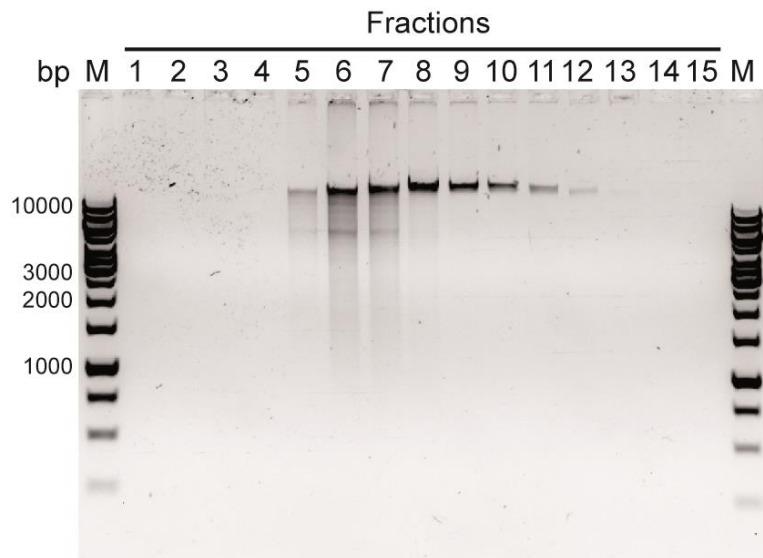
Figure 3.20 | *Nfatc1* Ex.9 avi-tag BAC fractions after enzymatic linearization
BAC RP23-361H16 *Nfatc1* Ex.9-avi was enzymatically digested by the restriction enzyme NruI. The cut DNA was loaded onto a sepharose-column and fractioned by size. Aliquots from 15 fraction samples were loaded onto a 0.8% agarose gel.

Sepharose-columns were used for size fractioning and buffer-exchange to eliminate all unwanted remaining fragments after BAC RP23-361H16 *Nfatc1* Ex.9 avi DNA by NruI. As shown in Figure 3.20, 15 fractions were collected and samples of each fraction were loaded and, thereby, checked on an agarose gel. Fractions 5-8 contained visible shorter BAC RP23-361H16 fragments after the NruI digestion. Therefore, fraction #9 which showed no remaining residues and was chosen for oocyte injection.

Figure 3.21 shows a schematic drawing of the *Nfatc1* locus cloned in the BAC RP23-361H16 *Nfatc1* Ex.9-avidin construct. The *Nfatc1* gene is modified through homologous recombination with the biotinylatable avidin-tag, and several other features that were included.
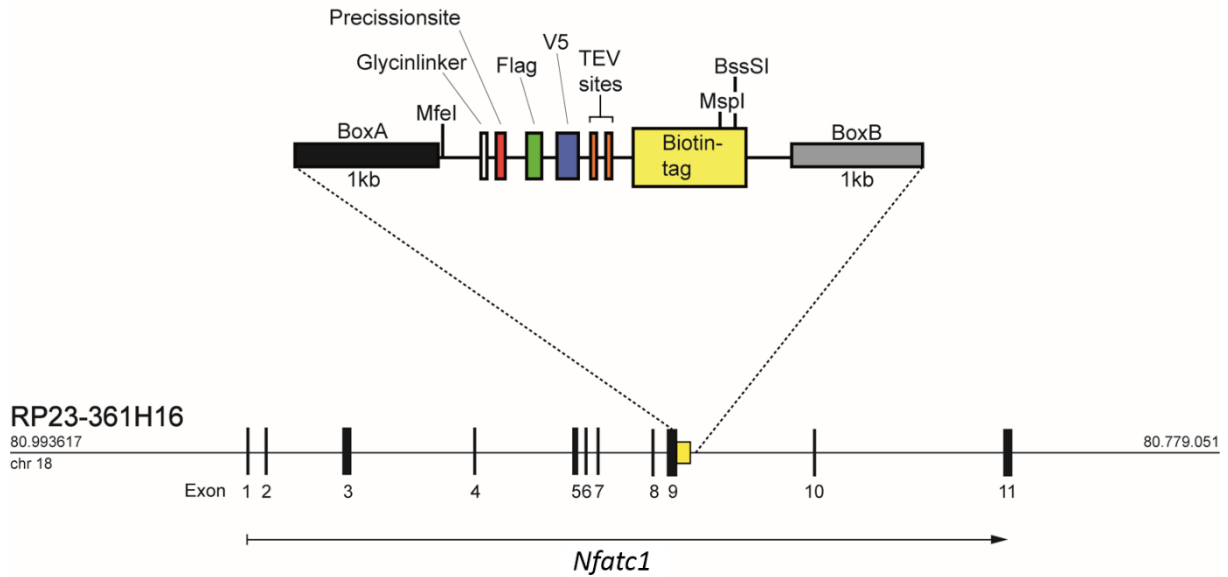
Figure 3.21 | Schematic drawing of the modified *Nfatc1* gene which was cloned in the BAC vector RP23-361H16 Ex.9-avidin
Scheme of the *Nfatc1* locus within in BAC RP23-361H16 *Nfatc1* Ex.9-avidin. The horizontal black line indicates the gene locus, exons 1 to 11 are shown as vertical bars. A biotinylatable avidin-tag (yellow box) as well as a precission site (red bar), a Flag-tag (green bar), a V5-tag (blue bar) and two TEV-clevage sites (orange bars) were introduced by homologues recombination. BoxA (black box) and BoxB (grey box) were used as specific sites of homology.

3.4 Functional analysis of biotinylatable NFATc1 protein isoforms

To determine the expression of NFATc1/αA-avi, NFATc1/βC-avi and NFATc1/βC-aviFl proteins, HEK 293T-cells were transiently transfected with the retroviral expression plasmids pEGZ-NFATc1/αA-avi, NFATc1/βC-avi and NFATc1/βC-aviFL (3.2.1 and 3.2.2).

3.4.1 Transient expression of NFATc1-avi proteins in HEK 293T-cells

HEK 293T-cells were cultured to a density of approximately 60% in DMEM medium prior calcium phosphate transfection with DNAs encoding pEGZ-NFATc1/αA-avi, pEGZ-NFATc1/βC-avi, pEGZ-NFATc1/βC-aviFL or pMSCV-F-BirA.
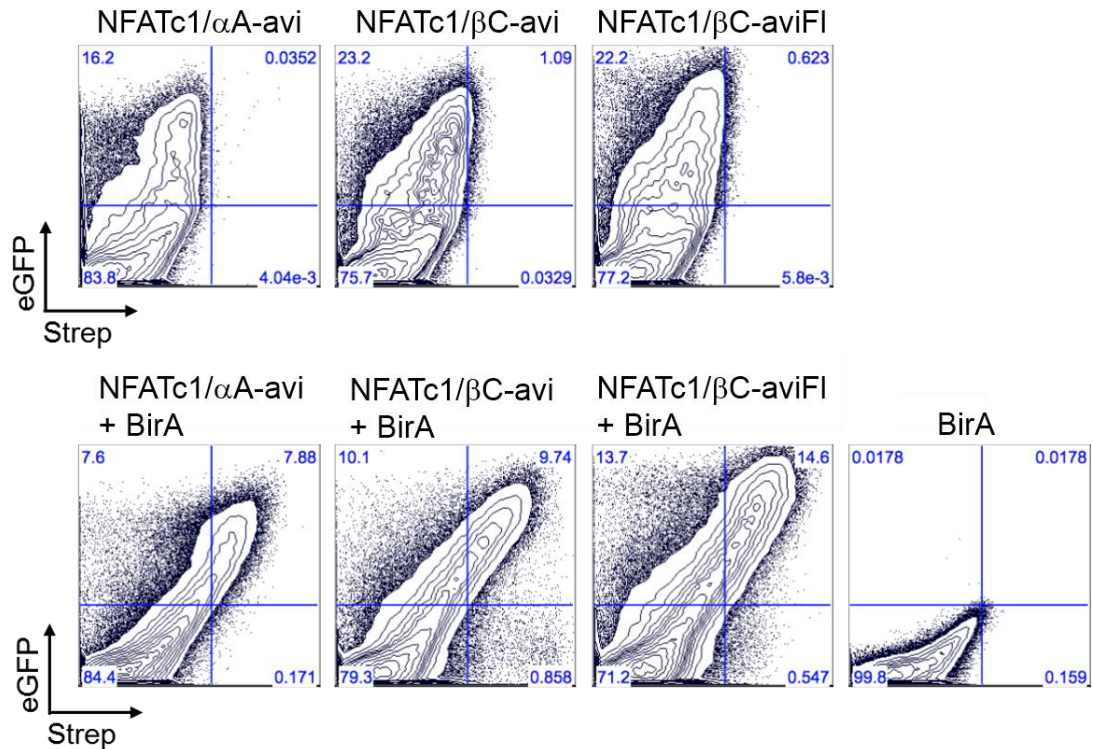
Figure 3.22 | HEK 293T cells transfected with pEGZ-NFATc1-avi constructs
Top row: 293T cells transfected with either pEGZ-NFATc1α/A-bio, pEGZ-NFATc1β/C-bio, pEGZ-NFATc1β/C-bioFl alone, without a BirA construct. Bottom row: 293T cells transfected with pEGZ-NFATc1α/A-bio, pEGZ-NFATc1β/C-bio or NFATc1β/C-bio in combination with pMSCV-F-BirA. In the last panelm pMSCV-F-BirA DNA was transfected alone as control.

The expression plasmids pEGZ-NFATc1/αA-avi, pEGZ-NFATc1/βC-avi and pEGZ-NFATc1/βC-aviFl expressed, under the control of a CMV promoter, an IRES (Internal Ribosome Entry Site)-eGFP which served as expression marker. Following standard calcium phosphate transfection protocols, HEK 293T-cells were transiently transfected with NFATc1 pEGZ-plasmids. The enzymatic biotinylation of avidin by BirA required the addition of biotin [5mM] to the DMEM during the transfection. Transfected cells were cultured for 24 h followed by stimulation with TPA and ionomycin for 5 h. Cells were fixed and permeabilized for intracellular staining with streptavidin-APC. As shown by FACS analysis in Figure 3.22, HEK 293 T-cells were positive for eGFP expression, and therefore successfully transduced with pEGZ expression plasmids. HEK 293T-cells transduced with pMSCV-F-BirA served as negative control since pMSCV-F-BirA did not encode any fluorescent marker protein. HEK 293T-cells expressing NFATc1/αA-avi, NFATc1/βC-avi and NFATc1/βC-aviFl in

combination with BirA (Figure 3.22, bottom) were found to be positive for eGFP expression and APC staining, indicating the successful biotinylation and streptavidin binding.

3.4.2 Retroviral infection of WEHI-231 B-lymphoma cells

HEK293T-cells transiently transduced with the retroviral packaging plasmids pHIT60 (MLV *env* gene) and pHIT123 (*gag* and *pol*) were used to generate retroviral particles containing pEGZ-NFATc1/αA-avi, pEGZ-NFATc1/βC-avi and pMSCV-F-BirA DNAs, respectively, or in combination pEGZ-NFATc1/αA-avi and BirA or pEGZ-NFATc1/βC-avi and pMSCV-F-BirA. These retroviral particles were used to infect WEHI-231 B-lymphoma cells with either pEGZ-NFATc1/αA-avi and pMSCV-F-BirA, pEGZ-NFATc1/βC-avi and pMSCV-F-BirA or pMSCV-F-BirA alone. (WEHI-231 B-lymphoma cells were also infected with pEGZ-NFATc1/αA-avi and NFATc1/βC-avi without pMSCV-F-BirA, respectively. Data not shown). Positively infected WEHI-231 cells were cultured in the presence of the antibiotics zeocin [200µg/ml] and puromycin [1µg/ml] for 2 weeks to select for stable integration of pEGZ-NFATc1-isoforms and pMSCV-F-BirA plasmids.
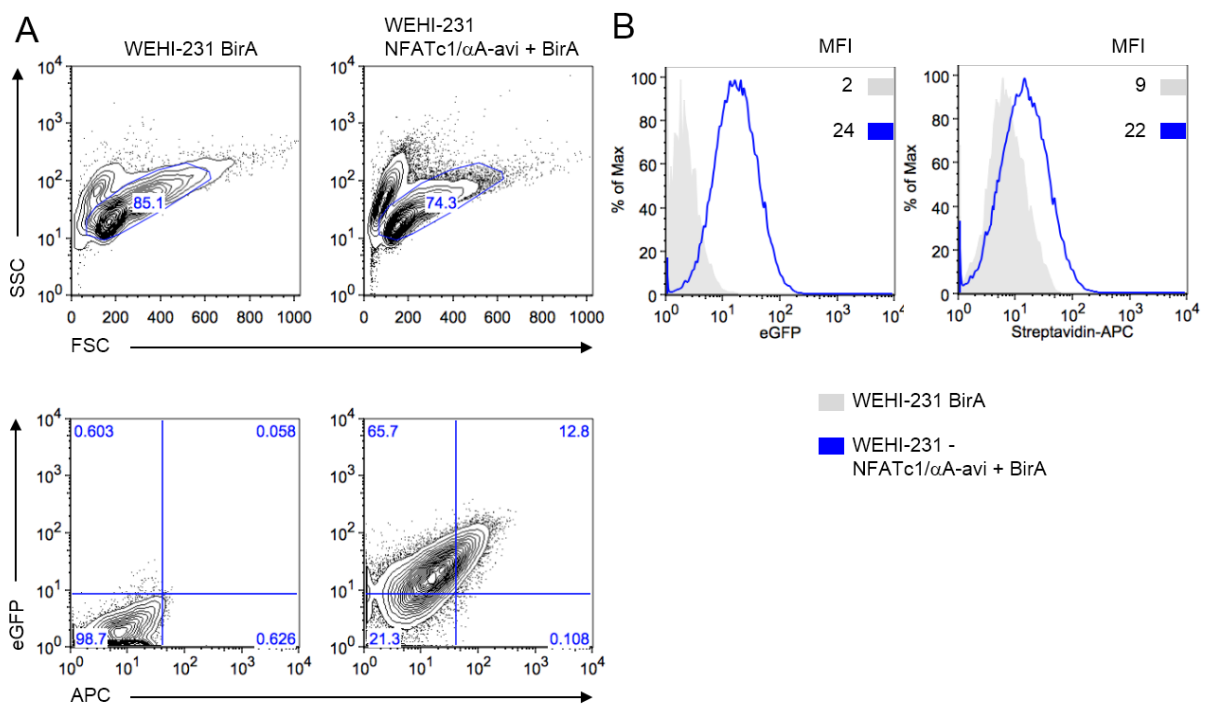
Figure 3.23 | WEHI-231 B-lymphoma cells retrovirally infected express NFATc1/αA-avi
The murine B-cell lymphoma line WEHI-231 was retrovirally infected with pEGZ-NFATc1/αA-avi and pMSCV-F-BirA expression plasmids. A) WEHI-231 BirA and WEHI-231 NFATc1/αA-avi + BirA were intracellularly stained with streptavidin-APC. Living cells were gated in SSC and FSC dot-plots and analyzed for eGFP (Fl-1) and APC expression. B) FACS-histograms of eGFP and APC expression of WEHI-231 BirA and WEHI-231 NFATc1/αA-avi + BirA cells. FSC: Forward scatter; SSC: Sideward scatter; MFI: Mean Fluorescence Intensity.

WEHI-231 cells stably over-expressing NFATc1/αA-avi and BirA, as well as cells stably over-expressing BirA alone, were intracellularly stained with streptavidin coupled to the fluorophore APC and analyzed by flow-cytometry (Figure 3.23). WEHI-231 BirA cells, expressing the prokaryotic ligase BirA only, were negative for eGFP and APC emission. WEHI-231 expressing NFATc1/αA-avi and BirA were found to be positive for eGFP and APC emission. As shown in Figure 3.23 B, a relatively strong background for streptavidin-APC was detected in WEHI-231 expressing BirA alone (MFI 9) compared to WEHI-231 cells expressing NFATc1/αA-avi and BirA (MFI 22). A comparison of streptavidin-APC stained WEHI-231 cells, over-expressing either BirA alone, NFATc1/αA-avi alone, NFATc1/αA-avi and BirA or no expression plasmid at all is shown in Figure 3.24. WEHI-231 and WEHI-231 BirA cells, intracellularly stained with streptavidin-APC, become slightly positive for APC, but were clearly less positive as WEHI-231 cells expressing NFATc1/αA-avi.
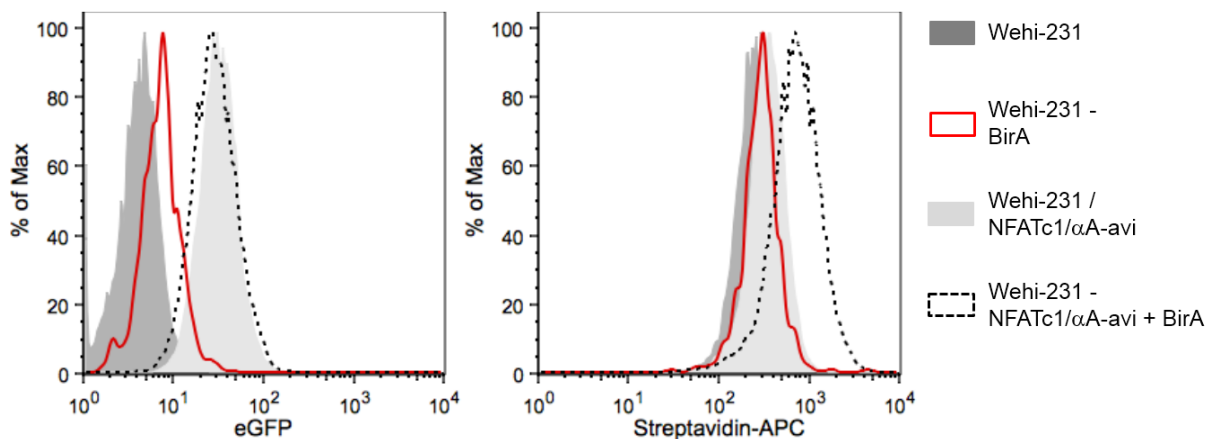
Figure 3.24 | FACS of WEHI-231 B-lymphoma cells and WEHI-231 cells stably expressing BirA, NFATc1/αA-avi, NFATc1/αA-avi and/or BirA
FACS histogram-analysis of WEHI-231 B-lymphoma cells expressing BirA, NFATc1/αA-avi, a combination of both or no (wt) cells, displayed in histograms. Cells were analyzed for eGFP and APC emission.

WEHI-231 cells, infected with pEGZ-NFATc1/βC-avi and/or pMSCV-F-BirA were also fixed and intracellularly stained with streptavidin-APC. In Figure 3.24, the results of flow-cytometry assays are presented.
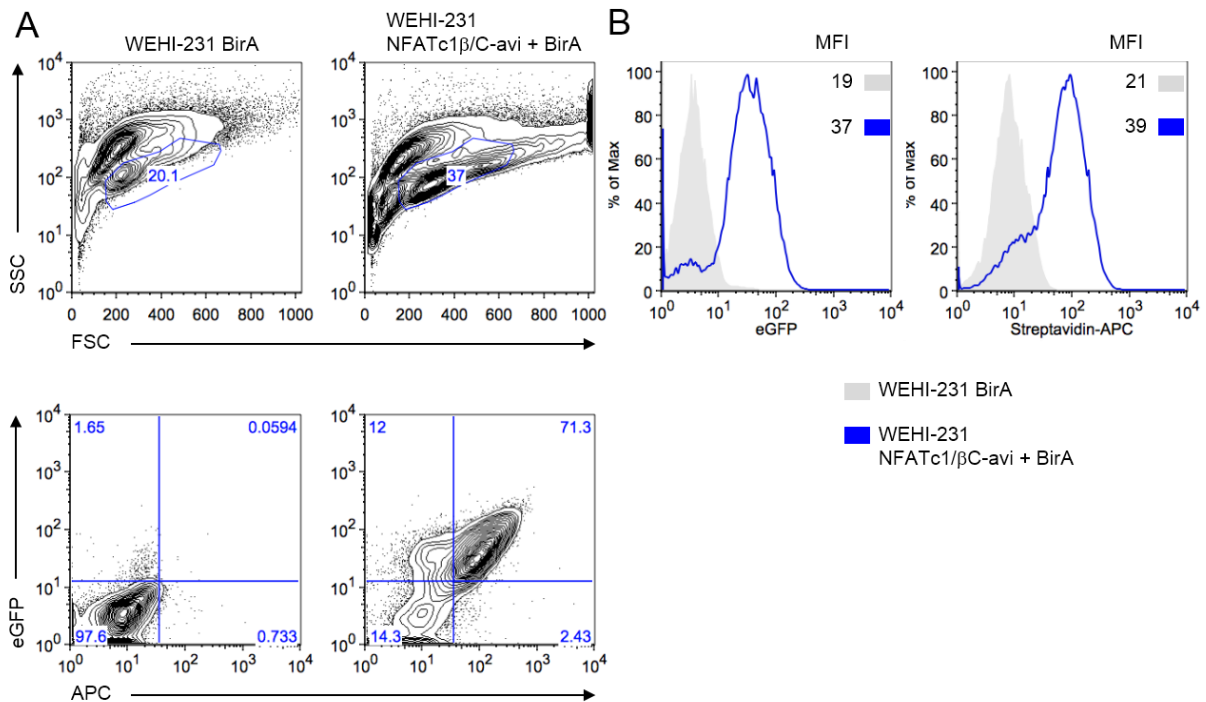
Figure 3.25 |WEHI-231 cells retrovirally infected and stably expressing *Nfatc1/βC*-avi
WEHI-231 cells were retrovirally infected with pEGZ-NFATc1/βC-avi and pMSCV-F-BirA expression plasmids.A) WEHI-231 BirA and WEHI-231 NFATc1/αA-avi + BirA were intracellularly stained with streptavidin APC. Living cells were gated in SSC and FSC dot-plots and analyzed for eGFP (Fl-1) and APC expression. B) FACS-histrograms of eGFP and APC expression of WEHI-231 BirA and WEHI-231 NFATc1/αA-avi + BirA cells. FSC: Forward scatter; SSC: Sideward scatter; MFI: Mean Fluorescence Intensity.

WEHI-231 NFATc1/βC-avi cells, over-expressing NFATc1/βC and the ligase BirA, were found to be positive for eGFP and APC expression, compared to WEHI-231 cells only expressing BirA.

3.4.3 Transcription induction of NFATc1/α- and NFATc1/β-isoforms in WEHI-231 cells

In order to compare *Nfatc1* mRNA expression levels directed by the promoters of *Nfatc1* P1 and P2, between "normal" WEHI-231 cells and WEHI-231 cells stably over-expressing NFATc1/αA-avi, NFATc1/βC-avi and Bir A, cells were stimulated with anti-IgM ab for 24 h. Total RNA was isolated and in PCR assays the activity of *Nfatc1* promoters was measured. cDNA was synthesized by reverse transcription (2.2.5).
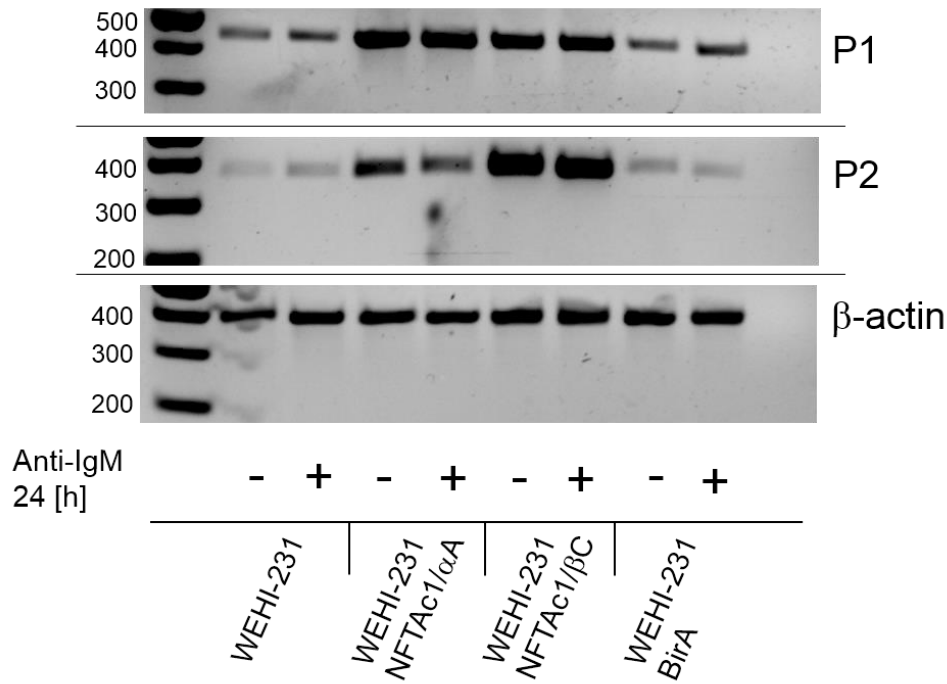
Figure 3.26 | RT-PCR of *Nfatc1* transcripts directed by the promoters P1 and P2 of endogenous *Nfatc1* gene in wt WEHI-231 cells and in WEHI-231 cells overexpressing NFATc1/αA-avi and NFATc1/βC-avi after induction
Transcription analysis using cDNA from WEHI-231, WEHI-231 NFATc1/αA-avi, WEHI-231 NFATc1/βC-avi and WEHI-231 BirA cells. PCRs were done with primers for the detection of *β-actin*, *Nfatc1* P1 and *Nfatc1* P2 transcripts. PCR primers are located within exon 1 and exon 3 for detecting *Nfatc1* P1 and within exon 2 and exon 3 of *Nfatc1* for detecting P2 directed transcripts, respectively.

RT-PCRs for the expression of the housekeeping gene *β-actin* showed equal expression levels for all cDNA samples. *Nfatc1* P1-directed transcripts were identified in all WEHI-231 cells, but the amount of expression was elevated in cells over-expressing NFATc1/αA-avi, compared to wt WEHI-231 cells and WEHI-231 cells over-expressing the prokaryotic ligase BirA. P1-directed transcripts were also elevated in WEHI-231 cells over-expressing NFATc1/βC-avi, but slightly less compared to WEHI-231 NFATc1/αA-avi. No differences in *Nfatc1* P1 and P2 induction were seen in either WEHI-231, WEHI-231 NFATc1/αA-avi, NFATc1/βC-avi or BirA, regarding treatment with anti-IgM compared to non-treated cells. Transcription of P2-directed mRNA was strongest in WEHI-231 cells overexpressing NFATc1/βC-avi, but P2 transcription was found to be slightly higher in WEHI-231 NFATc1/αA-avi cells, compared to wt and BirA expressing cells.

3.4.4 Expression of NFATc1/αA-avi and NFATc1/βC-avi proteins in WEHI-231 cells overexpressing NFATc1/αA-avi or NFATc1/βC-avi

3.4.4.1 Western-blotting and IP with protein extracts from WEHI-231 cell lines

Normal WEHI-231 cells or WEHI-231 cells overexpressing NFATc1/αA, NFATc1/βC-avi and/or BirA were lysed with IP-lysis buffer (2.1.7.3), and whole-protein extracts were isolated. Protein IP was performed using streptavidin-coupled agarose beads, followed by SDS-PAGE separation and immunoblotting using abs directed against NFATc1 and biotin.

As shown in Figure 3.27 A), NFATc1 isoforms were detected with anti-NFATc1 HRP (Horse Radish Peroxidase)-ab in lysates from WEHI-231, WEHI-231 BirA, WEHI-231 NFATc1/αA-avi and WEHI-231 NFATc1/βC-avi cells, with protein sizes between approximately 100 kDa and 130 kDa. NFATc1 was also detected in samples from WEHI-231 cells expressing NFATc1/αA-avi and NFATc1/βC-avi after IP with streptavidin coupled agarose beads. In Figure 3.27 B), the same lysates were used to perform immunoblotting with a polyclonal HRP-ab specifically directed against the N-terminal α-peptide of NFATc1/α-isoforms. NFATc1/α-isoforms were present in all WEHI-231 lysates, but biotinylated NFATc1/α protein was only detected in the WEHI-231 NFATc1/αA-avi IP sample. In Figure 3.27 C), the same lysates and IP samples as used in 3.27 A) and 3.27 B) were analyzed. Streptavidin-coupled to HRP was applied to detect *in vitro* biotinylated proteins. No proteins were detected in lysates from WEHI-231 cells and WEHI-231 cells over-expressing BirA, but biotinylated proteins were present in lysates and IP samples from WEHI-231 cells over-expressing NFATc1/αA-avi and NFATc1/βC-avi. Some background binding of streptavidin-HRP was seen in IP samples from WEHI-231 and WEHI-231 BirA cells, with sizes of approximately 120 kDa.
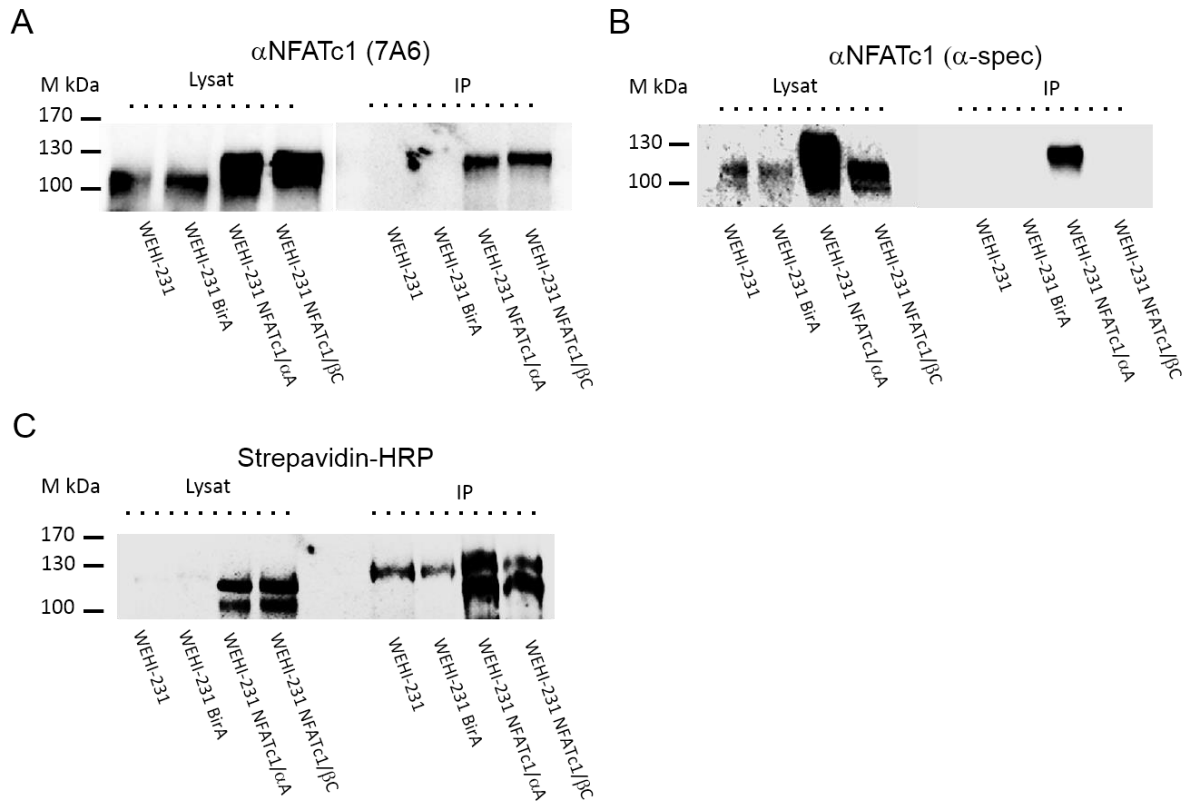
Figure 3.27 | NFATc1/αA-avi and NFATc1/βC-avi protein expression levels in WEHI-231 B-lymphoma cells
A) WB of a 8% PAA-gel loaded with whole cell lysates and protein after IP from WEHI-231 cells or WEHI-231 cells overexpressing BirA, NFATc1/αA-avi and WEHI-231 NFATc1/βC-avi. NFATc1 was detected with a monoclonal anti-NFATc1 ab (7A6). B) WB of a 8% PAA-gel loaded with the same protein extracts as described in A. A polyclonal rabbit ab, specifically targeting the N-terminal α-peptide (α-spec), was used to visualize the NFATc1/α-isoforms. C) WB of a 8% PAA-gel loaded with the same protein extracts as in A and B, treated with streptavidin-HRP to detect biotinylated proteins.

3.4.4.2 Intracellular staining of NFATc1/αA-avi and NFATc1/βC-avi

Normal WEHI-231 or WEHI-231 cells overexpressing NFATc1/αA-avi, WEHI-231 NFATc1/βC-avi and/or WEHI-231 BirA were stimulated for 48 h with anti-IgM ab or left untreated. Therefore, fixed and intracellularly stained with Streptavidin-Alexa Fluor 488 and ab (m7A6) directed against NFATc1 proteins. Additionally, all cells were stained with DAPI (4,6-Diamidino-2-Phenylindole, Dilactate) which labels A-T rich DNA stretches within the cell nucleus.
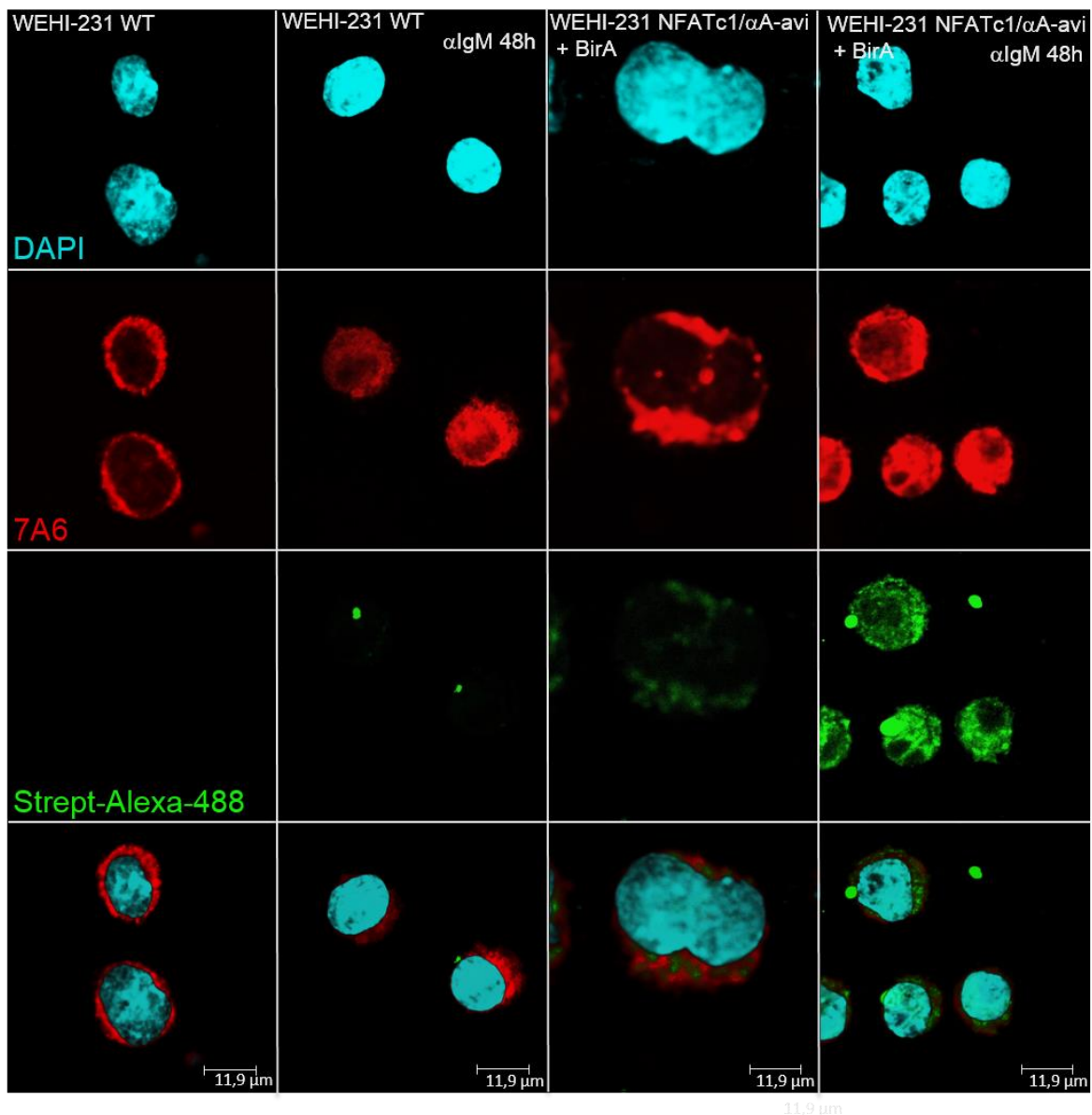
Figure 3.28 | Intracellular staining of NFATc1 and NFATc1/αA-avi in WEHI-231 cells
WEHI-231 wt cells and WEHI-231 cells overexpressing NFATc1/αA-avi were fixed on glass-slides and intracellularly stained with a murine ab against NFATc1 (and a secondary fluorophore–coupled ab) and Streptavidin-Alexa-Fluor 488. Cells were stained with DAPI. 7A6: monoclonal murine NFATc1 ab; Strept-Alexa-488: Streptavidin-Alexa-Fluor 488.

Confocal microscopy revealed that NFATc1 proteins, labeled with NFATc1 ab, were predominatly located in the cytoplasm of untreated WEHI-231 wt and WEHI-231 NFATc1/αA-avi cells, but shifted to the nucleus after 48 h of anti-IgM stimulation (Figure 3.28). Streptavidin coupled to the fluorophore Alexa-Fluor-488 did not stain protein in WEHI-231 wt cells, but stained biotinylated proteins within WEHI-231 cells overexpressing NFATc1/αA-avi. The pattern of NFATc1 ab binding and the binding-pattern of Streptavidin-Alexa-Fluor 488 were found to be very similar for stimulated and unstimulated WEHI-231 NFATc1/αA-avi cells.
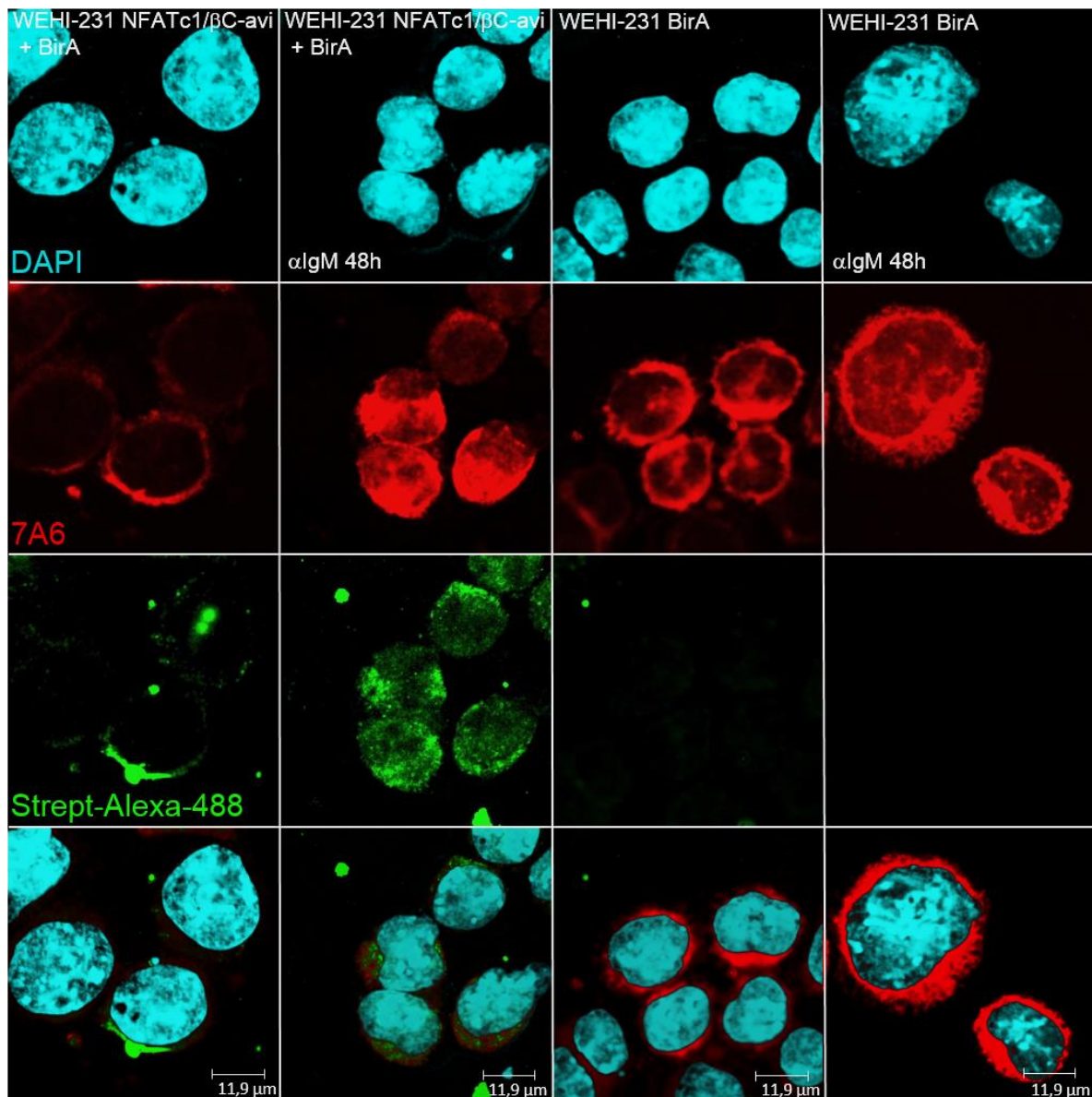
Figure 3.29 | Intracellular staining of NFATc1 and NFATc1/βC-avi in WEHI-231 cells
WEHI-231 wt cells and WEHI-231 cells overexpressing NFATc1/βC-avi, fixed on glass slides and intracellularly stained with a murine ab against NFATc1 (and a secondary fluorophore-coupled anti-mouse ab) and Streptavidin-Alexa-Fluor 488. Cells were stained with DAPI. 7A6: monoclonal murine NFATc1 ab; Strept-Alexa-488: Streptavidin-Alexa-Fluor 488.

In Figure 3.29, pictures of WEHI-231 cells overexpressing BirA and NFATc1/βC-avi taken by confocal microscopy are displayed. Intracellular staining with anti-NFATc1 ab showed staining of NFATc1 in the cytoplasm in untreated WEHI-231 BirA and WEHI-231 NFATc1/βC-avi cells. Cells that were stimulated for 48 h with anti-IgM ab also showed NFATc1 staining within the cell nucleus. In WEHI-231 NFATc1/βC-avi cells Streptavidin-Alexa-Fluor 488 binding was found, mostly in the cytoplasm of unstimulated cells and in cytoplasm as well as nucleus in cells treated for 48 h with anti-IgM ab. WEHI-231 BirA cells showed only very little staining for Alexa-Fluor-488.

3.4.5 Retroviral infections of primary B-cells with pEGZ-NFATc1/αA-avi

In order to test the function of avidin-tagged NFATc1 proteins in primary B-cells *in vivo*, we sought to infect primary B-cells with the retroviral construct pEGZ-NFATc1/αA-avi. Subsequently, these cells were stained with streptavidin-coupled to APC. Therefore, primary B-cells were isolated from spleens and lymphnodes of C57Bl/6 Rosa26-BirA mice, constitutively expressing the prokaryotic enzyme BirA (kindly provided by Dr. M.Schäfer and Prof. M. Busslinger; IMP; Vienna). The cells were cultured in *x-vivo* medium and stimulated with LPS for 24 h thereby inducing proliferation before they could be infected with retroviral particles. Retroviruses, carrying the expression plasmid pEGZ-NFATc1/αA-avi were produced in HEK-293T-cells (2.2.7) and freshly applied to approximately 5×10^5 LPS-stimulated B-cells per sample. Post infection, B-cells were cultured for 5 additional days in the presence of low amounts of LPS, before they were fixed and intracellularly stained with streptavidin-APC.

All cells were equally stimulated and treated in culture-medium by LPS. As shown in Figure 3.30, unstained Rosa26-BirA B-cells were negative for eGFP expression and streptavidin-APC binding, and served as control. Roughly 8% of Rosa26-BirA B-cells transfected with NFATc1/αA-avi showed expression of eGFP, encoded in the pEGZ-NFATc1/αA-avi plasmid. About one third of this population was also found to be positive for Streptavidin-APC binding. Rosa26-BirA B-cells, not infected with pEGZ-NFATc1/αA-avi and stained with streptavidin-APC, showed relatively high APC staining levels, compared to Rosa26-BirA B-cells, which were not treated with Streptavidin-APC. A direct comparison of streptavidin-APC staining for all three samples (bottom panel Fig. 3.30) shows the differences in streptavidin-APC binding,
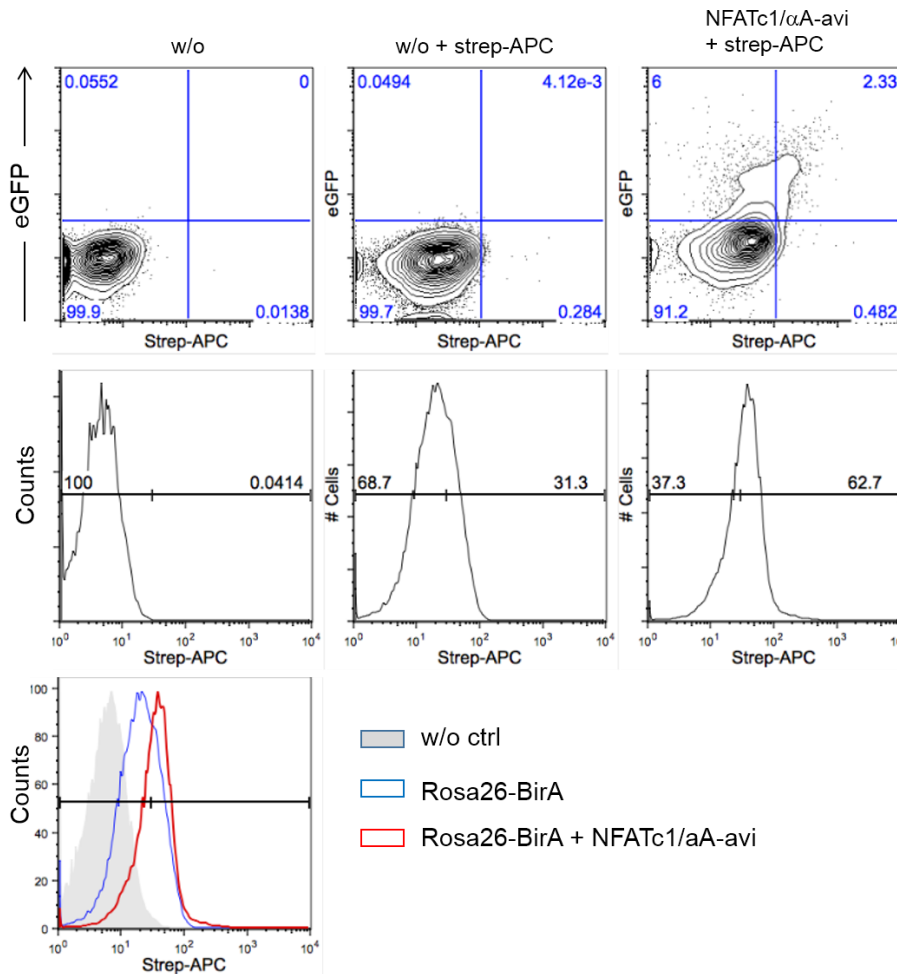
Figure 3.30 | Primary B-cells from Rosa26-BirA mice retrovirally infected with pEGZ-NFATc1/αA-avi

Flow-cytometry analysis of primary B-cells infected with pEGZ-NFATc1/αA-avi and controls. B-cells were fixed and intracellularly stained with streptavidin-APC. First row, B-cells from Rosa26-BirA mice that were not infected and not stained with streptavidin-APC. Middle row, B-cells from Rosa26-BirA animals, not infected, stained with Streptavidin-APC. Third row, B-cells from Rosa26-BirA mice, infected with pEGZ-NFATc1/αA-avi and intracellulary stained with streptavidin-APC.

and illustrated the successful biotinylation of NFATc1/aA upon transduction into primary B-cells.

3.5 Apoptosis and cell-death of WEHI-231 cells overexpressing individual NFATc1 proteins

3.5.1 BCR-triggered induction of apoptosis in WEHI-231 cells

WEHI-231 cells and WEHI-231 cells stably expressing either the short isoform NFATc1/αA or the long isoform NFATc1/βC (both avidin tagged (3.2.1 and 3.2.2), were cultured in RPMI medium. They were kept unstimulated or stimulated up to 4 days with anti-IgM ab or anti-IgM

ab and anti-CD40 ab. The cells were harvested and stained with annexin V, a marker for the induction of cellular apoptosis, and analyzed by FACS.
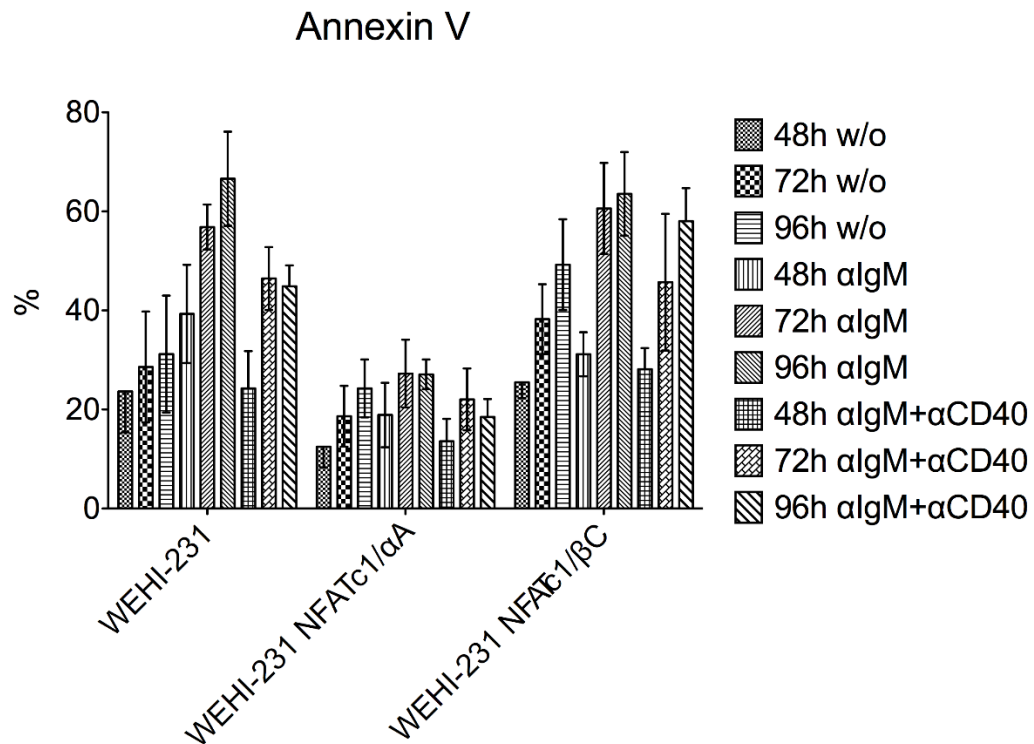
Figure 3.31 | WEHI-231 cell lines stained with annexin V after stimulation *in vitro*
WEHI-231 cells were cultured in RPMI medium and stimulated with anti-IgM ab or anti-IgM ab and anti-CD40 ab. Cells were stained with annexin V and analysed by flow-cytometry. (n=3)

During logarithmic growth in culture, wt WEHI-231 cells showed populations of approximately 20-30 % of annexin V positive cells, whereas WEHI-231 NFATc1/αA-avi cells appeared to be faster growing and less apoptotic, showing 10-15% of annexin V positive cells. Similar to wt cells, WEHI-231 NFATc1/βC-avi cells showed, without stimulation, a proportion of 25-35% annexin V positive cells. Stimulation with anti-IgM ab induced apoptosis in all three cell lines, but was found to be significantly less in WEHI-231 NFATc1/αA-avi cells, as shown in Figure 3.31. Additional stimulation of the CD40 receptor with anti-CD40 ab reduced the number of annexin V positive cells in each WEHI line. This induction was found to be most prominent in WEHI-231 NFATc1/αA-avi cells. The ameliorating effect of anti-CD40 stimulation towards apoptosis induction was weak in WEHI-231 cells overexpressing NFATc1/βC-avi.

3.5.2 Cell-death in WEHI-231 B-lymphoma cells

Upon anti-IgM and anti-IgM + anti-CD40 stimulation, cell death was analyzed by propidium iodide staining of WEHI-231 cell lines by flow-cytometry (Figure 3.32).
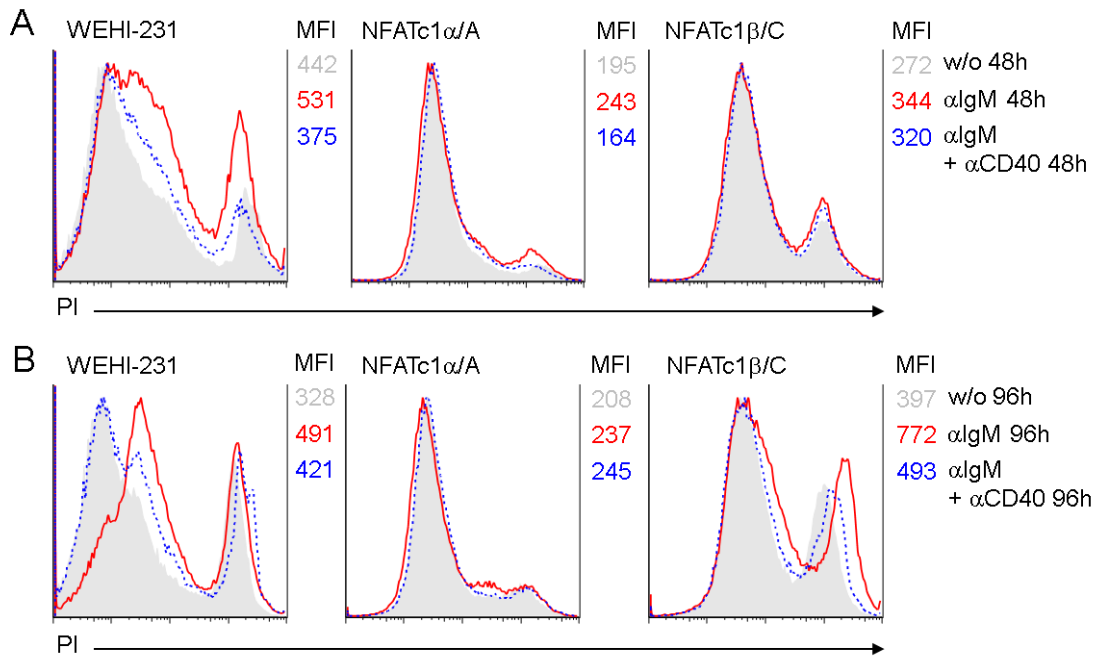
Figure 3.32 | WEHI-231 cell lines stained with propidium iodide after stimulation with anti-IgM and anti-IgM + anti-CD40 for two and four days
A) Histograms of PI-stained WEHI-231, WEHI-231 NFATc1/αA-avi and WEHI-231 NFATc1/βC-avi cells, stimulated for 48 h with anti-IgM or anti-IgM ab in combination with anti-CD40 ab. B) Histograms of PI-stained WEHI-231, WEHI-231 NFATc1/αA-avi and WEHI-231 NFATc1/βC-avi cells, stimulated for 96 h with anti-IgM or anti-IgM ab in combination with anti-CD40 ab.

After 48 h of anti-IgM stimulation, WEHI-231 wt cells became highly apoptotic, and a large proportion of cells died. Parallel stimulation with anti-CD40 ab significantly reduced the amount of dead WEHI-231 wt cells (Figure 3.32 A). Similar effects were seen after 96 h of anti-IgM and anti-IgM together with anti-CD40 stimulation. WEHI-231 cells overexpressing NFATc1/αA-avi had almost no increase in dead cells after 48 h or 96 h of anti-IgM or anti-IgM together with anti-CD40 stimulations. WEHI-231 overexpressing the long NFATc1 isoform NFATc1/βC-avi showed some increase in cell-death after 48 h after BCR engagement, and a strong increase in cell-death after 96 h. After 96 h of culturing, the effect triggered by anti-IgM was significantly reduced in presence of anti-CD40 stimulation.

3.6 Transcriptome sequencing of WEHI 231 cells overexpressing NFATc1/αA-avi and NFATc1/βC-avi

3.6.1 Quantification of NFATc1/α- and NFATc1/β-isoform transcript expression

In order to analyze all *Nfatc1* transcripts in WEHI-231 B-lymphoma cells stably overexpressing NFATc1/αA or NFATc1/βC, WEHI-231 B-lymphoma cell lines (described in chapter 3.5)

were analyzed in RNA-seq assays. While in logarithmic growth, these cells were cultured and stimulated with anti-IgM ab. They were harvested after 6 h, 24 h and 96 h of anti-IgM stimulation. Untreated cells were used as control samples. RNA was isolated, purified, quantified and sent to TRON (Translationale Onkologie an der Universitätsmedizin Mainz GmbH) in Mainz, where barcoded RNA-seq libraries were generated. They were clustered on a cBot using the Truseq PE cluster kit V3, using 10 pM, and 1 x 50 bps were sequenced on the Illumina HiSeq2500 apparatus (50 cycles).
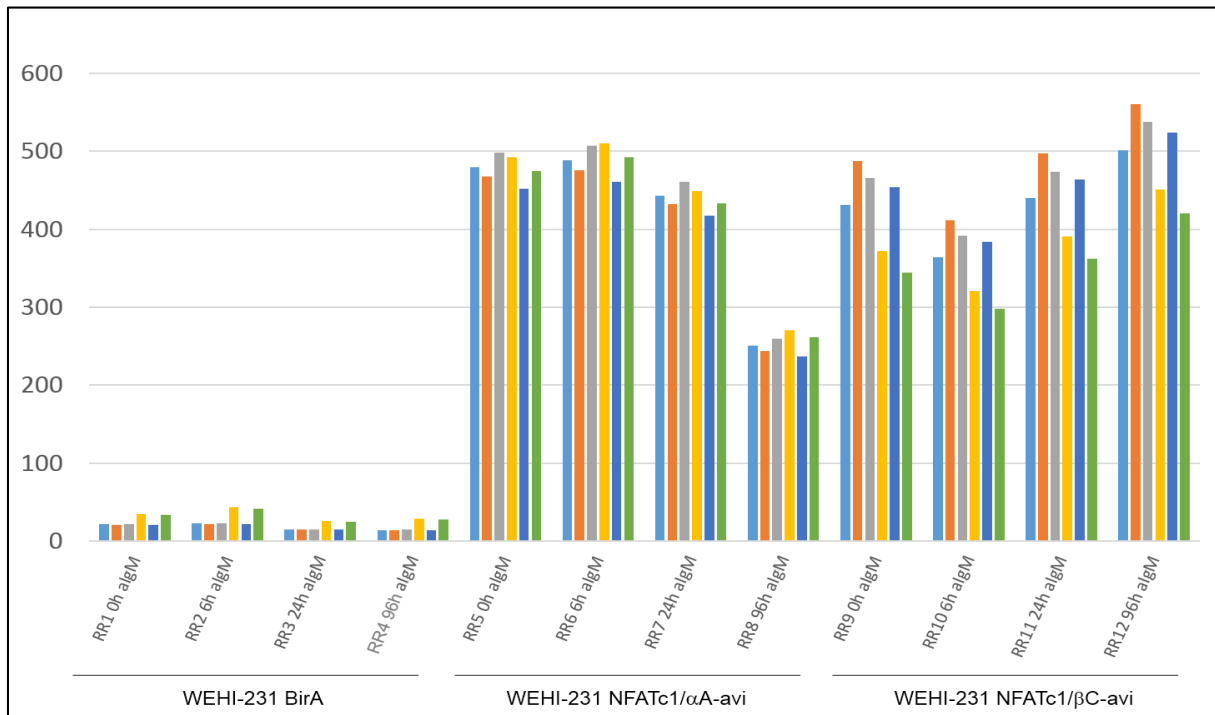
Figure 3.33 | *Nfatc1* **total mRNA expression in WEHI-231 NFATc1/αA-avi, WEHI-231 NFATc1/βC-avi and WEHI-231 BirA cells**
Displayed are the number of reads which were mapped per kilobase of transcripts, per million mapped reads for each transcript of NFATc1 transcripts. RR1-RR4: WEHI-231 BirA cells, αIgM 0-96 h; RR5-RR8: WEHI-231 NFATc1/αA-avi cells, αIgM 0-96h; RR9-RR-12: WEHI-231 NFATc1/βC-avi cells 0-96 h. The colors indicate the six individual NFATc1 isoforms.

As mentioned above, *Nfatc1* is expressed in the 6 isoforms NFATc1/αA, -αB, -αC and NFATc1/βA, -βB and -βC. In Figure 3.33, a summary of all sequences is displayed that were aligned to the *Nfatc1* gene. Individual NFATc1-isoforms vary in exon usage. The α-isoforms are encoded by exon 1 and exons 3-9, 3-10 or 3-11, the NFATc1-β-isoforms are encoded by exon 2 and exons 3-9, 3-10 or 3-11. Due to computational correlation, all sequenced transcripts spanning exons 3-11 were assigned to all six NFATc1-isoforms. *Nfatc1* expression in WEHI-231 BirA cells reflects endogenous *Nfatc1* expression, whereas the high *Nfatc1* transcript

numbers in samples RR5-8 and RR9-12 were the result of NFATc1/αA-avi and NFATc1/βC-avi overexpression.
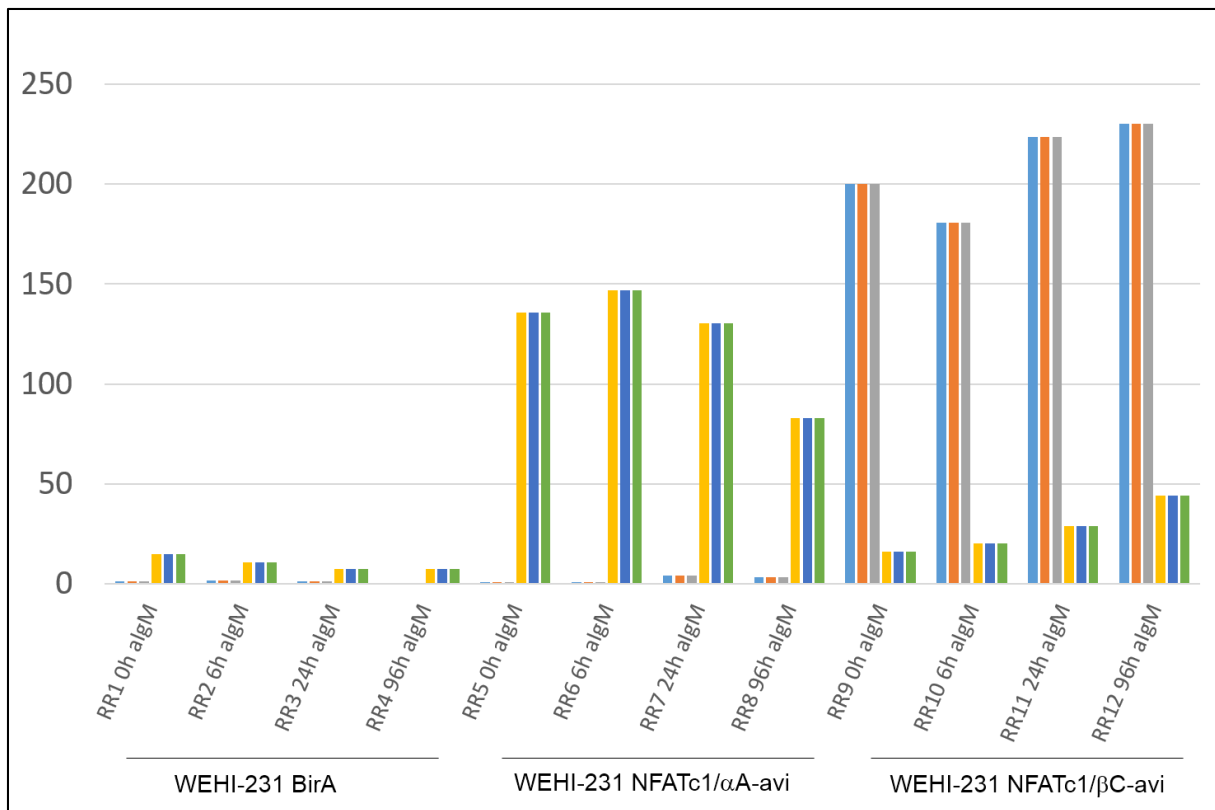
Figure 3.34 | Distribution of *Nfatc1* exon 1 and exon 2 transcripts in WEHI-231 cells overexpressing NFATc1/αA-avi and NFATc1/βC-avi
Number of reads mapped per kilobase of transcripts, per million mapped reads for each transcript of NFATc1 exon 1 and exon 2. RR1-RR4: WEHI-231 BirA, αIgM 0-96 h; RR5-RR8: WEHI-231 NFATc1/αA-avi αIgM 0-96 h; RR9-RR-12: WEHI-231 NFATc1/βC-avi αIgM 0-96 h. Colors yellow, blue and green: NFATc1/α-isoforms; light blue, red and grey: NFATc1/β-isoforms.

In Figure 3.34, all sequenced reads were selected and solely assigned to *Nfatc1* exon 1 and *Nfatc1* exon 2 transcripts. Samples RR1-RR4, WEHI-231 BirA cells, showed slightly more reads for *Nfatc1* exon 1, reflecting moderate NFATc1/α-isoform expression. As expected, cells overexpressing NFATc1/αA-avi (samples RR5-RR8) showed particularly high numbers of sequenced reads for *Nfatc1* exon 1, but almost no reads for exon 2. High numbers of *Nfatc1* exon 2 reads were sequenced in samples RR9-RR12, reflecting the overexpression of NFATc1/βC in these cells. Enhanced exon 1 reads were also found in significant numbers in WEHI-231 NFATc1/βC cells which illustrates the autoregulation of *Nfatc1* expression through the P1 promoter. In contrast, no remarkable increase was detected for P2-directed transcripts in cells overexpressing NFATc1/αA-avi.

3.6.2 Transcriptional regulation by NFATc1/αA and NFATc1/βC in WEHI-231 B-lymphoma cells

Whole transcriptome-sequencing (2.2.8) showed that in WEHI-231 cells 13.607 genes were expressed. Among them, 3452 genes exhibited a 2-fold increase or decrease in expression in WEHI-231 NFATc1/αA-avi cells, and 2573 genes in WEHI-231 cells overexpressing NFATc1/βC-avi. An evaluation of all genes regulated by NFATc1/αA and/or NFATc1/βC cells revealed that the expression of 1267 genes were changed in both cell lines (Figure 3.36 A). The Database for Annotation, Visualization and Integrated Discovery (DAVID v 6.7 [184]) was used to perform functional gene classification on a gene-to-gene similarity matrix based on shared functional annotation. Genes regulated in WEHI-231 cells overexpressing NFATc1/αA-avi and NFATc1/βC-avi were merged, classified and annotated, (Figure 3.35 A), or they were classified and annotated individually (Figure 3.36). To do so, medium stringency conditions were applied to compile balanced statistics to generate gene-ontology clusters. Of all genes significantly regulated, in WEHI-231 cells overexpressing NFATc1/αA and NFATc1/βC, 8 % were clustered into the group of "Apoptosis". 15 % of all reads sequenced were assigned to the cluster "Programmed Cell Death" (PCD), and another 15 % of all genes were classified to participate in the "Regulation of Transcription". Additionally, among the top 10 clusters, the following groups were found: "Cell Cycle" 13 %, "Regulation of Cell Activation" 8 %, "Differentiation" 6 %, "Intracellular Signaling" 6 % and "Hemopoiesis" 4 %. Genes listed within the section "Others", approximately one-fourth of all genes were compiled and distributed into a multitude of lower enrichment score clusters (Fig. 3.35)

Individual clustering of genes regulated by NFATc1/αA or NFATc1/βC showed clear-cut difference in gene-ontology patterns and number of reads (Figure 3.36). In NFATc1/αA-avi overexpressing cells "Regulation of Transcription" was the largest grouped cluster for all genes with an expression change of at least 2-fold. The corresponding cluster was also found for WEHI-231 NFATc1/βC-avi overexpressing cells. However, from 2573 genes only 7 % were found within the cluster "Regulation of Transcription". The largest two groups found to be regulated by NFATc1/βC overexpression were "PCD" with 27 % of all genes, and "Apoptosis" with 14 %. These two clusters represented only 5 % for "PCD" and 4 % of genes controlled by NFATc1/αA-avi or NFATc1/βC-avi overexpression.

A

B
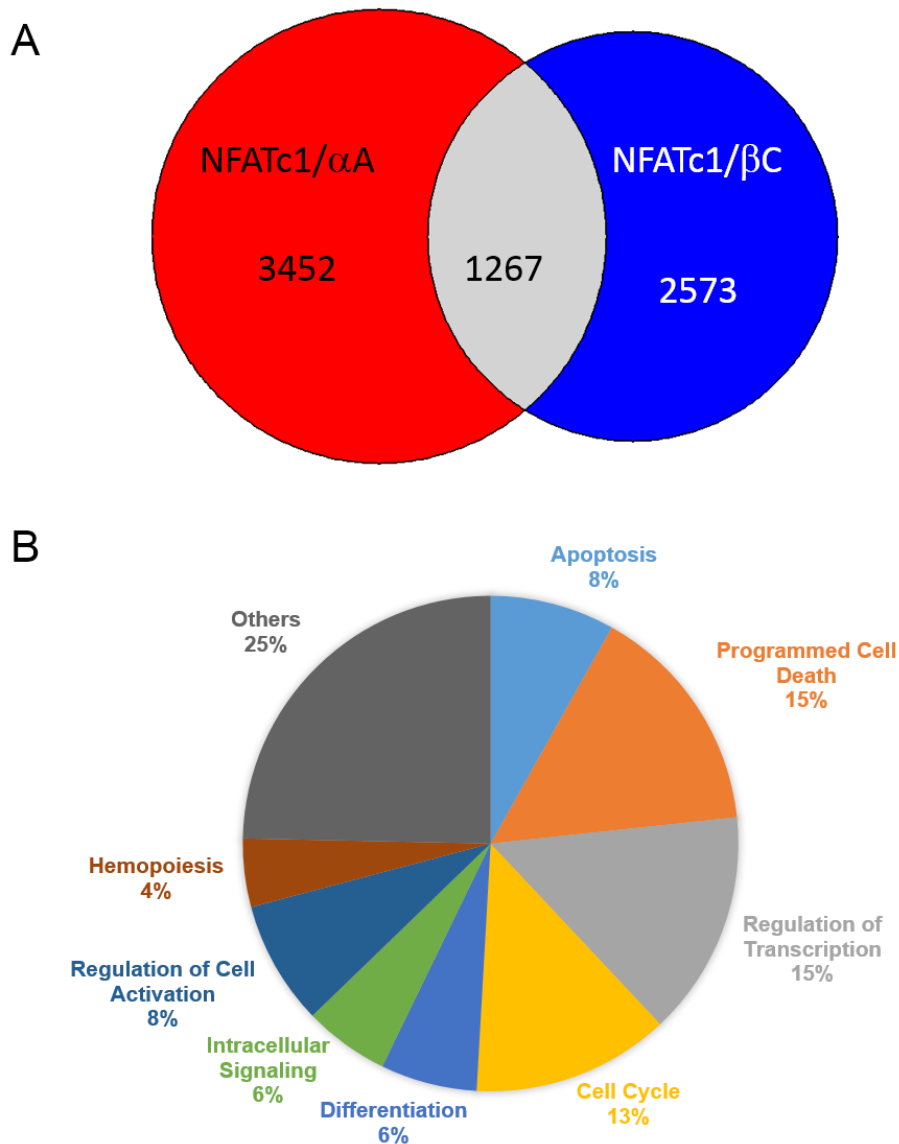
Figure 3.35 | Transcriptional regulation in WEHI-231 cells overexpressing the NFATc1/αA-or NFATc1/βC-isoforms
A) All genes regulated in WEHI-231 cells overexpressing either NFATc1/αA or NFATc1/βC, anti-IgM stimulated for 0-96 h, at least 2-fold changed at any given time-point. B) Gene ontology clustering for all genes changed by WEHI-231 overexpressing NFATc1/αA and NFATc1/βC compared to WEHI-231 BirA cells.

Roughly similar numbers of genes involved in cell activation processes and hemopoiesis were found to be regulated in WEHI-231 cells overexpressing NFATc1/αA-avi or WEHI-231 NFATc1/βC-avi. "Lymphocyte Differentiation" was also grouped for both cell lines: 7 % of all genes regulated in WEHI-231 NFATc1/αA-avi cells and 4 % of all reads represented in WEHI-231 NFATc1/βC-avi cells were assembled in this category. Therefore, "Regulation of Transcription" (28 %), "Intracellular Signaling" (11 %) and the "Regulation of Cell Activation" (10 %) were the three major groups of genes regulated by NFATc1/αA-avi in WEHI-231 cells,
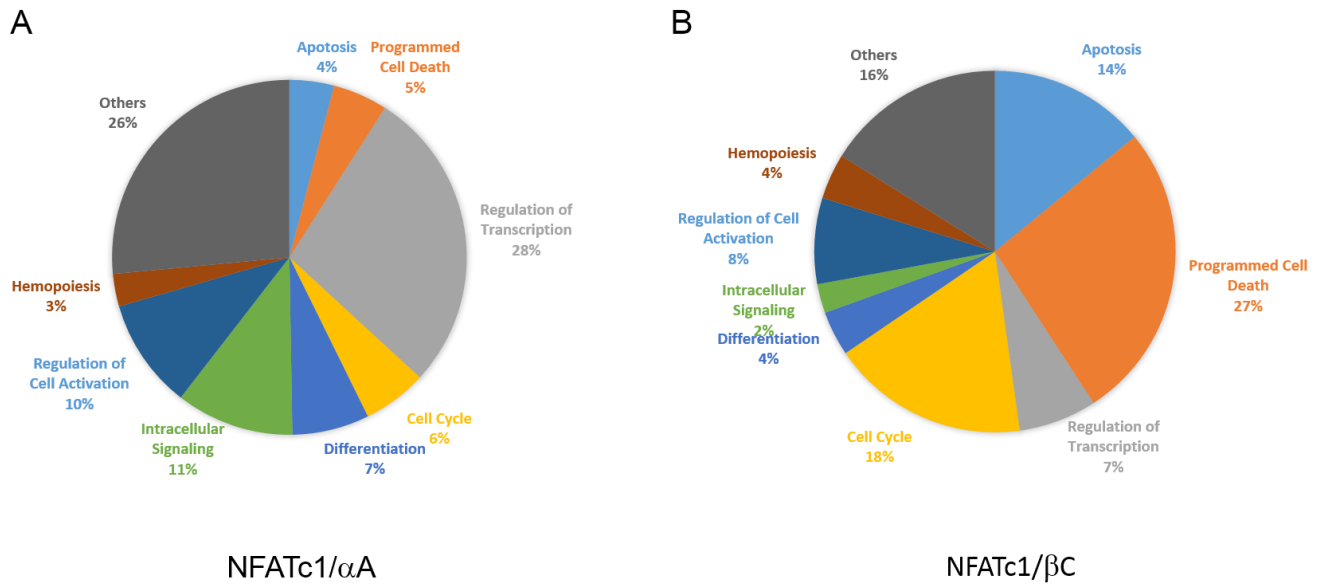
Figure 3.36| Gene-ontology profiles of WEHI-231 cells overexpressing NFATc1/αA-avi or NFATc1/βC-avi
A) Pie-diagram of gene-clusters with highest enrichment scores for all genes, regulated at least 2-fold, in WEHI-231 NFATc1/αA-avi cells, compared to BirA control cells. B) Pie-diagram of gene-clusters with the highest enrichment scores for all genes, regulated at least 2-fold, WEHI-231 NFATc1/βC-avi cells, compared to BirA control cells.

whereas "PCD" (27 %), "Cell Cycle" (18 %) and "Apoptosis" (14 %) were found to be the most significant groups of genes regulated in WEHI-231 NFATc1/βC-avi cells. For many genes which were regulated by both NFATc1/αA and NFATc1/βC, the individual NFATc1 proteins exerted an opposite effect on gene expression.

3.6.3 Gene clustering of transcripts from WEHI-231 cells overexpressing NFATc1/αA-avi or NFATc1/βC-avi

3.6.3.1 Apoptotic genes

As shown in Figure 3.37, 8 % of all sequenced reads in WEHI-231cells overexpressing NFATc1/αA-avi and WEHI-231 NFATc1/βC-avi were mapped to genes related to cellular apoptosis. Members of the Programmed Cell Death (PDCD) family, such as *Pdcd1*, *Pdcd10* and *Pdcd4,* were found to be up- and down-regulated in both cell lines. Expression levels of Tumor necrosis factor (*Tnf*) and members of the TNF superfamily, like Lymphotoxins-α and -β(*Ltα/Ltβ*) and the lymphocyte-specific protein tyrosine kinase (*Lck*), were down-regulated in WEHI-231 cells overexpressing NFATc1/αA, but expression-levels were up-regulated in WEHI-231 cells overexpressing the long isoform NFATc1/βC. *Fas* (Tnf receptor superfamily, member 6) was weakly expressed in wt cells, up-regulated in WEHI-231 cells overexpressing
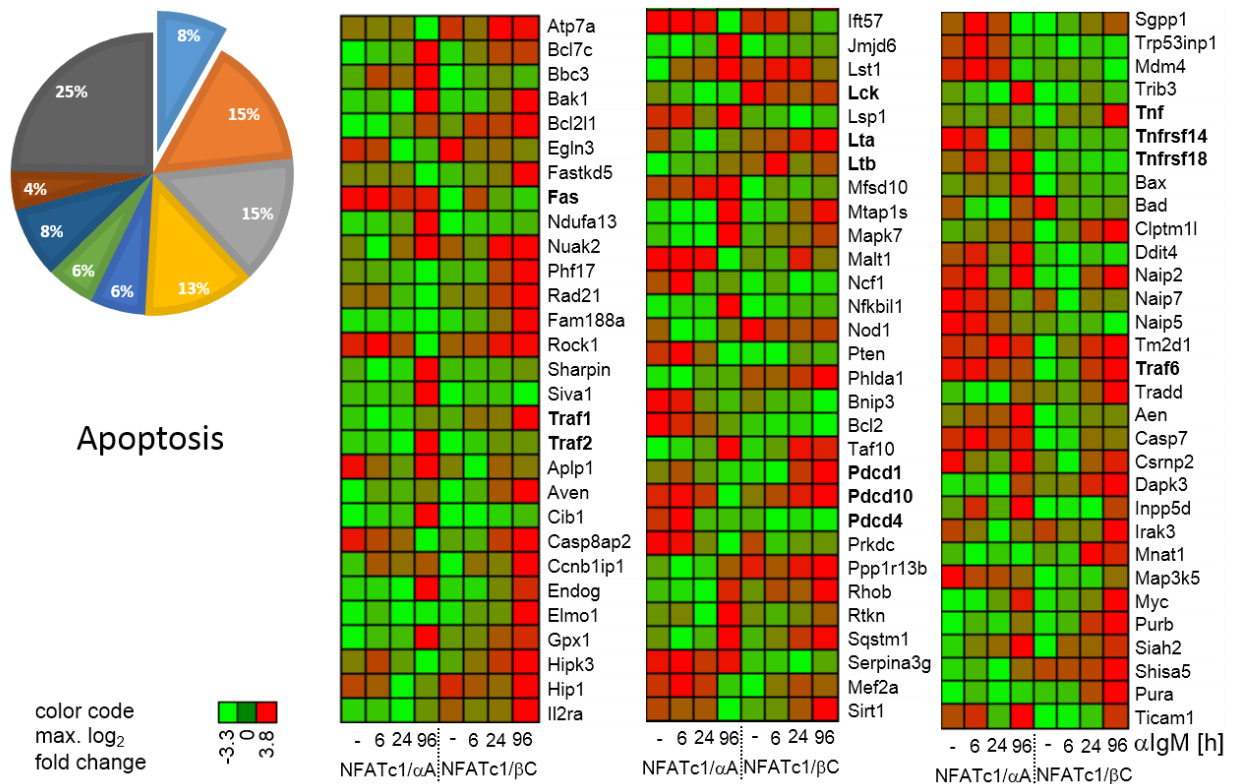
Figure 3.37 | Apoptotic genes regulated in WEHI-231 cells overexpressing NFATc1/αA and NFATc1/βC

A selection of 90 genes regulated in WEHI-231 cells overexpressing NFATc1/αA-avi and WEHI-231 cells overexpressing NFATc1/βC avi attributed to the cluster of apoptosis (DAVID). 8% of all sequenced reads from WEHI-231 NFATc1/αA-avi and NFATc1/βC-avi were represented within the cluster of cellular apoptosis (pie-diagram). Heatmap color-code (log$_2$ scaled) indicates maximum log$_2$ fold changes. Red indicates transcriptional increase; light green indicates transcriptional decrease; dark green indicates no transcriptional change. Data were normalized for each row.

NFATc1/αA-avi and down-regulated in WEHI-231 cell overexpressing NFATc1/βC-avi. Members of the TRAF family (TNF receptor associated factor), such as *Traf1*, *Traf2* and *Traf6*, but also Tumor necrosis factor receptor superfamily members, such as *Tnfrsf 14* and *18*, were regulated in both NFATc1 overexpressing cell lines, under these conditions.

3.6.3.2 Genes controlling Programmed Cell Death (PCD)

Several genes which were either induced or repressed by NFATc1/αA or NFATc1/βC, grouped into the cluster of Apoptosis, were also present in the group "Regulation of Programmed Cell Death". Some of these genes are shown in Figure 3.38. Additionally, transcriptional regulation was shown for many members of the *Bcl2* (B-cell CLL/lymphoma2) -family, such as *Bcl2*, *Bcl2a1a, Bcl2a1b*, *Bcl2a1c* and *Bcl2a1d* and, furthermore, for *Bax* (*Bcl2* associated X protein), *Bcl2l1* (*Bcl2*-like1) and *Bad* (*Bcl2* associated agonist of cell death) and other *Bcl2*-associated genes. Genes, like *Foxo1* (Forkhead box O1), *Vegfa* (Vascular endothelial growth factor α),
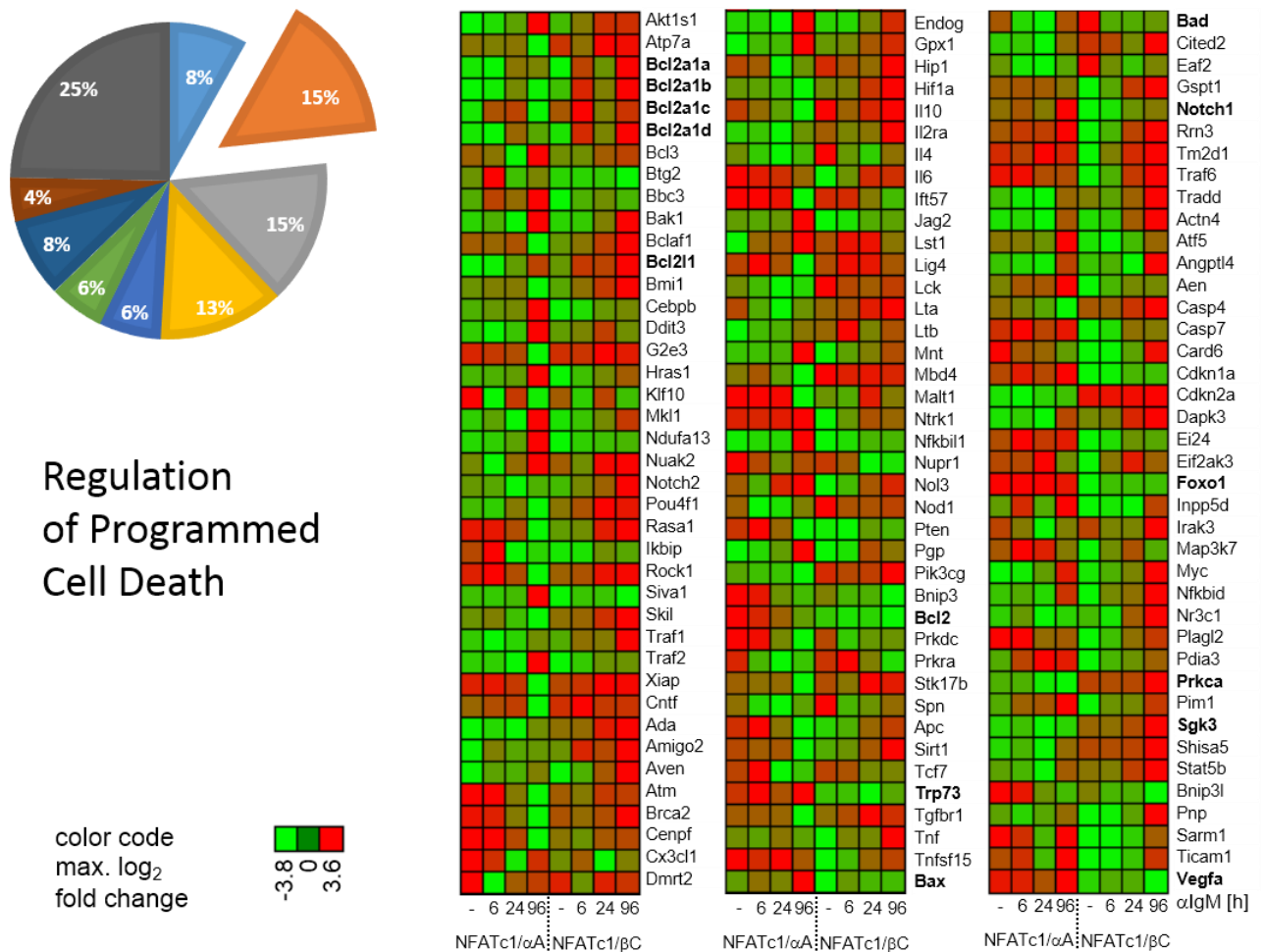
Figure 3.38 | PCD genes regulated in WEHI-231 cells overexpressing NFATc1/αA and NFATc1/βC

A selection of 120 genes regulated in WEHI-231 NFATc1/αA-avi or WEHI-231 NFATc1/βC avi cells were attributed to the cluster of Programmed Cell Death. 15% of all sequenced reads from WEHI-231 NFATc1/αA-avi and NFATc1/βC-avi cells were compiled into the cluster of PCD (pie-diagram).Heatmap color-code (log$_2$ scaled) indicates maximum log$_2$ fold changes. Red indicates transcriptional increase; light green indicates transcriptional decrease; dark green indicates no transcriptional change. Data were normalized for each row.

Prkca (protein kinase c, alpha) and *Trp73* (Tumor protein p73), but also *Notch1* (translocation associated Notch protein) and *Sgk3* (Serum/Glucocorticoid Regulated Kinase 3) were up- or down-regulated in WEHI-231 cells either overexpressing NFATc1/αA-avi or NFATc1/βC-avi.

3.6.3.3 Genes controlling transcription

15% of all genes regulated in WEHI-231 cells, stably transfected with NFATc1/αA or NFATc1/βC, were designated as genes involved in transcriptional regulation (Figure 3.39). Members of the NF-κB family, like *Rela* (Reticuloendotheliosis Viral Oncogene homolog A) and *Relb*, *Rel* (*c-Rel*) and *Nfkb2* (Nuclear Factor of Kappa Light Polypeptide Gene Enhancer in

B-Cells 2) were significantly induced in WEHI-231 cells overexpressing NFATc1/αA-avi and NFATc1/βC-avi, after 96 h of anti-IgM stimulation, compared to BirA controls.
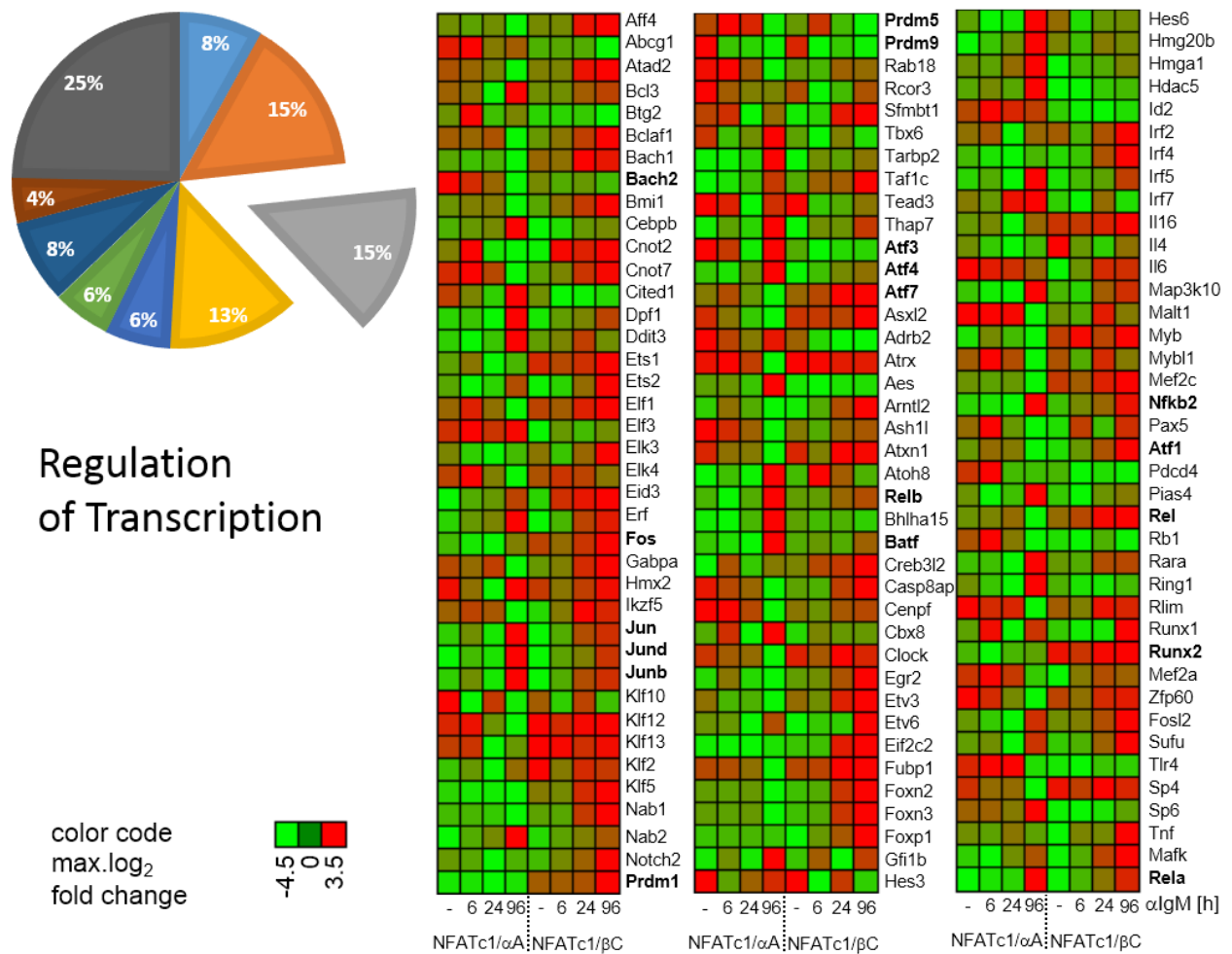
Figure 3.39 | Induction or repression of genes regulating transcription in WEHI-231 cells overexpressing either NFATc1/αA-avi or NFATc1/βC-avi
A selection of 118 genes regulated in WEHI-231 NFATc1/αA-avi cells or WEHI-231 NFATc1/βC avi cells attributed to the cluster of "Regulation of Transcription". 15% of all sequenced reads from WEHI-231 NFATc1/αA-avi and NFATc1/βC-avi cells were compiled into the cluster of Regulation of Transcription (pie-diagram). Heatmap color-code ($\log_2$ scaled) indicates maximum $\log_2$ fold changes. Red indicates transcriptional increase; light green indicates transcriptional decrease; dark green indicates no transcriptional change. Data were normalized for each row.

Prdm1 (PR Domain Containing 1, with ZNF), encoding Blimp-1, was found to be shut down in WEHI-231 cells overexpressing NFATc1/αA, but up-regulated by the overexpression of NFATc1/βC. Other members of the *Prdm* gene-family, *Prdm5* and *Prdm9*, were also expressed and regulated in both cell lines. The c-AMP dependent transcription factor ATF4 (Activating Transcription Factor 4) was highly expressed and regulated in WEHI-231 NFATc1/αA-avi cells, together with *Atf1*, *Atf3* and *Atf7*, to a lesser extent. The *Batf* (B-Cell-Activating Transcription Factor) gene and other genes of the AP-1/ATF family, such as *Jun*, *Junb*, *Jund*

and *Fos,* were also highly expressed in both cell lines and regulated after anti-IgM stimulation. *Runx2* (Runt-related transcription factor 2) transcript levels were highly elevated by NFATc1/βC overexpression and reduced in WEHI-231 NFATc1/αA-avi cells, whereas *Runx1* levels (Runt-related transcription factor 1), related to several types of leukemia, were elevated in both NFATc1-overexpressing cell lines.

3.6.3.4 Regulation of genes involved in cell-cycle control

As shown in Figure 3.40, members of the "Cell Divison Cycle" (*Cdc*) gene family, important for the initiation of DNA replication, like *Cdc6*, *Cdc20*, *Cdc27* and *Cdc73*, were highly expressed and up-regulated, particularly at later stages of anti-IgM stimulation in WEHI-231 cells, overexpressing NFATc1/βC-avi. Cyclin D2 (*Ccnd2*) and Cyclin G1 (*Ccng1*) were up-regulated in NFATc1/αA overexpressing cells, whereas Cyclin G2 (*Ccng2*) was strongly down-regulated in NFATc1/βC overexpressing cells. The cyclin dependent kinase 6 (*Cdk6*) was found to be down-regulated by NFATc1/αA, compared to controls, but expressed at higher levels in NFATc1/βC overexpressing cells. The cyclin dependent kinases *Cdkn1a* (Cyclin-Dependent Kinase Inhibitor 1A; p21), *Cdkn2a* and *Cdkn2b*, were highly expressed in all WEHI-231 cells, and appeared to be counter regulated in WEHI-231 cells overexpressing NFATc1/αA-avi and WEH-231 NFATc1/βC-avi. *Cdkn1a* was up-regulated by NFATc1/αA, but down-regulated by NFATc1/βC, whereas *Cdkn2a* and *Cdkn2b* were regulated in the opposite way.
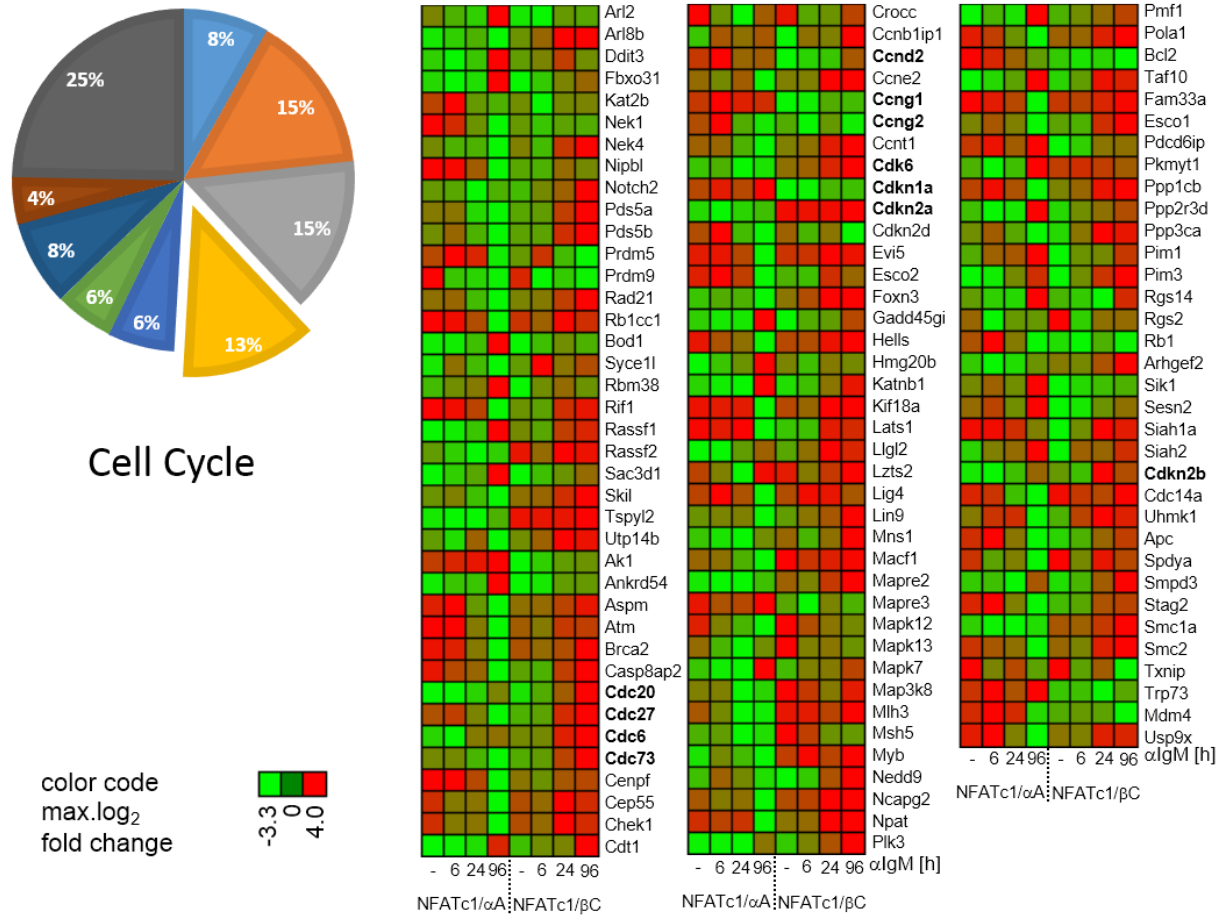
Figure 3.40 | Transcriptional regulation of genes involved in cell-cycle control
A selection of 112 genes regulated in WEHI-231 cells overexpressing NFATc1/αA-avi or WEHI-231 NFATc1/βC-avi which are attributed to the cluster of "Cell Cycle" Control-genes. 13% of all sequenced reads from WEHI-231 NFATc1/αA-avi and NFATc1/βC-avi were compiled into the cluster of genes controlling cell cycle processes (pie-diagram). Heatmap color-code (log$_2$ scaled) indicates maximum log$_2$ fold changes. Red: indicates transcriptional increase; light green indicates transcriptional decrease; dark green indicates no transcriptional change. Data were normalized for each row.

3.6.4 Stimulation-independent gene-induction and repression in WEHI-231 cells overexpressing NFATc1/αA or NFATc1/βC

All data gained from sequencing of RNA from WEHI-231 cells overexpressing NFATc1/αA-avi or NFATc1/βC-avi were systematically analyzed for expression levels and patterns. Data were sorted according to expression, change in transcription and functional gene-ontology (s. 3.6.3). As shown in Table 3.1, from 3452 genes, altered in their expression levels at least 2-fold at one of four given time-points of anti-IgM stimulation in WEHI-231 cells overexpressing NFATc1/αA-avi (compared to WEHI-231 BirA cells Figure 3.36), 92 genes were either induced or repressed at least 2-fold by NFATc1/αA for all four reading points of anti-IgM stimulation.

III. RESULTS

Table 3.1| Regulation of gene expression by NFATc1/αA overexpression, minimum 2-fold change independent from stimulation

All genes depicted in red were at least 2-fold induced by overexpression of NFATc1/αA in WEHI-231 cells at any given time-point of anti-IgM stimulation. All genes in green were repressed by NFATc1/αA overexpression, compared to WEHI-231 BirA controls, for all four time-points.

Gene Symbols

Alkbh7	Trp73	Cd36	Tec	Mfge8	Itga6
Irf7	Fam125b	Ggta1	Vsnl1	Sytl1	Specc1
Ifi27l2a	Ahnak	Cdk6	Mmp10	Hyal1	St8sia6
Itln1	Serpina3g	Celf2	Cr2	Ak1	Slc44a1
Ntrk1	Pgbd5	Il15ra	Rasgrp3	Pdcd1	Alcam
Ckmt1	Nfatc1	St8sia4	Pik3cg	Cpne2	Prl8a8
Lmo4	Pacsin1	Crim1	Lta	Serpina3f	Xcr1
Id2	Sh2b2	Cpd	Tmem176b	Ell3	
Dnm1	Isg20	Foxp1	Tmem176a	Aldoc	
Mxra8	Matn1	Ero1lb	Ptk2b	Pde3b	
Prr19	Pvrl4	Mef2c	Prdm1	Dmd	
Gm14492	Spatc1	Ablim1	Mfsd6l	AV249152	
Cd70	Lrp1	Entpd1	Runx2	Amigo2	
Snn	Avpr1b	Cdkl2	Gpr171	Ptpn12	
Gm4902	Abcg1	Snx9	Rab20	Eif2c2	
C8g	Ankrd44	Cd44	Creb3l4	Elmo1	
Mfge8	Dusp4	Lpxn	Rasgrp1	Uprt	

Cd70 (tumor necrosis factor (ligand) superfamily, member 7), *Lmo4* (LIM Domain Only 4), a gene encoding a protein that was shown to act as a transcriptional regulator and as oncogene, and *Isg20* (Interferon Stimulated Exonuclease Gene 20 kDa), an exonuclease with high specificity for RNA, are examples for genes that were moderately expressed but highly induced in WEHI-231 cells overexpressing NFATc1/αA. Among all genes repressed at least 2-fold by NFATc1/αA are *Cd36* (Thrombospondin Receptor), *Cd44* (GP90 Lymphocyte Homing/Adhesion Receptor), *Foxp1* (Forkhead box p1), *Dusp4* and other prominent members.

In table 3.2, 156 genes are shown which were affected by overexpressing NFATc1/βC-avi at all four time points 70 of which were induced by NFATc1/βC in WEHI-231 cells. They are labeled in red and, 86 of all genes, which were repressed by NFATc1/βC in WEHI-231 cells, are also listed.

III. RESULTS

Table 3.2| Regulation of gene expression by NFATc1/βC overexpression, minimum 2-fold change independent from stimulation
All genes depicted in red were induced 2-fold and more by NFATc1/βC overexpression in WEHI-231 cells at any given time-point of anti-IgM stimulation. All genes in green were repressed by NFATc1/βC overexpression, compared to WEHI-231 BirA controls, for all four time-points.

Gene Symbols

Mpzl2	Spn	Prl8a8	Herc3	Piga	Cp
Pappa2	Mcoln3	Mllt3	Sirpa	Serpinb6b	Wscd2
Gadd45g	Tigit	Faim3	Lipg	Cyp2c55	Adam19
Nos2	Sema7a	Egln3	Rpl22l1	Acot10	Lrrc32
Acoxl	Samd9l	Mir147	Rab9	P2ry2	Tnfsf8
Tnip3	Arhgef40	Ptk2b	Fstl1	Txlng	Cd36
Klrg2	Csn3	Prkca	Fancb	Prps2	Abtb2
Pigr	Creb3l4	Cdkn2a	Bhlha15	Gramd3	Cdkn1a
Fcamr	Xcr1	Acadm	Atg9b	Yy2	Mreg
Usp18	Mfsd10	Vsig10	Ank3	Acot9	Ak1
Tnfrsf8	Ccr10	Pdcd1	Ms4a1	Enc1	Rab20
Gnaq	Tcf7	Ribc1	Ptpdc1	Akr1c13	Nudt7
Upk1a	Megf9	Klf2	Tmem176b	Rnf169	Tnfsf15
Isg20	Grb7	Tspyl2	Sms	Aicda	Ncoa7
Prkra	Lbh	Sbk1	Eif1ax	Ccl22	Kif26a
Prr19	Klhl14	Hsd17b10	Bfsp2	Mbtps2	Ly6e
Ctla4	Enpp5	Gimap7	Sat1	Trp53inp1	Rgs10
Serpinf1	Fxyd5	Tnfrsf19	Zmat3	Klhl6	Ccng1
Il13	Rgl1	Cacna1h	Timd2	Tmem176a	Ckmt1
Mucl1	Alcam	Foxo1	Sema3f	Bcl11a	Lgals3bp
Ptms	Fcgr4	Cybb	Cd80	Spag9	Ephx1
Vmn2r29	Immp2l	Iffo1	Ctso	Serpine2	Ncs1
Mt3	Tmsb10	Ptp4a3	Ccr7	Plac8	Mllt4
Lck	Ptpn22	Dsg2	Sipa1l2	Gdpd5	Nfix
Mfsd6l	Mid1	Lmo2	Fam78a	Slc19a2	Lmcd1
Sgtb	Dhdh	Plekha1	Ephb2	Vsnl1	Il1rn

Examples for genes, moderately expressed but highly induced by NFATc1/βC, are *Lck*, *Tnfrsf8* (Cd30R), *Creb3l4* (cAMP Responsive Element Binding Protein 3-Like 4), *Pdcd1* (Programmed Cell Death 1) and *Ctla4* (Cytotoxic T-Lymphocyte-Associated Protein 4) genes. Genes which were expressed in WEHI-231 BirA control cells and repressed by NFATc1/βC are the *Il1rn* (Interleukin 1 Receptor Antagonist), *Foxo1* (Forkhead box O1), *Ccr7* (Chemokine (C-C Motif) Receptor 7), *Ccl22* (Chemokine (C-C Motif) Ligand 22) and *Tnfsf8* (Tumor Necrosis Factor (Ligand) Superfamily, Member 8, CD30L) genes.
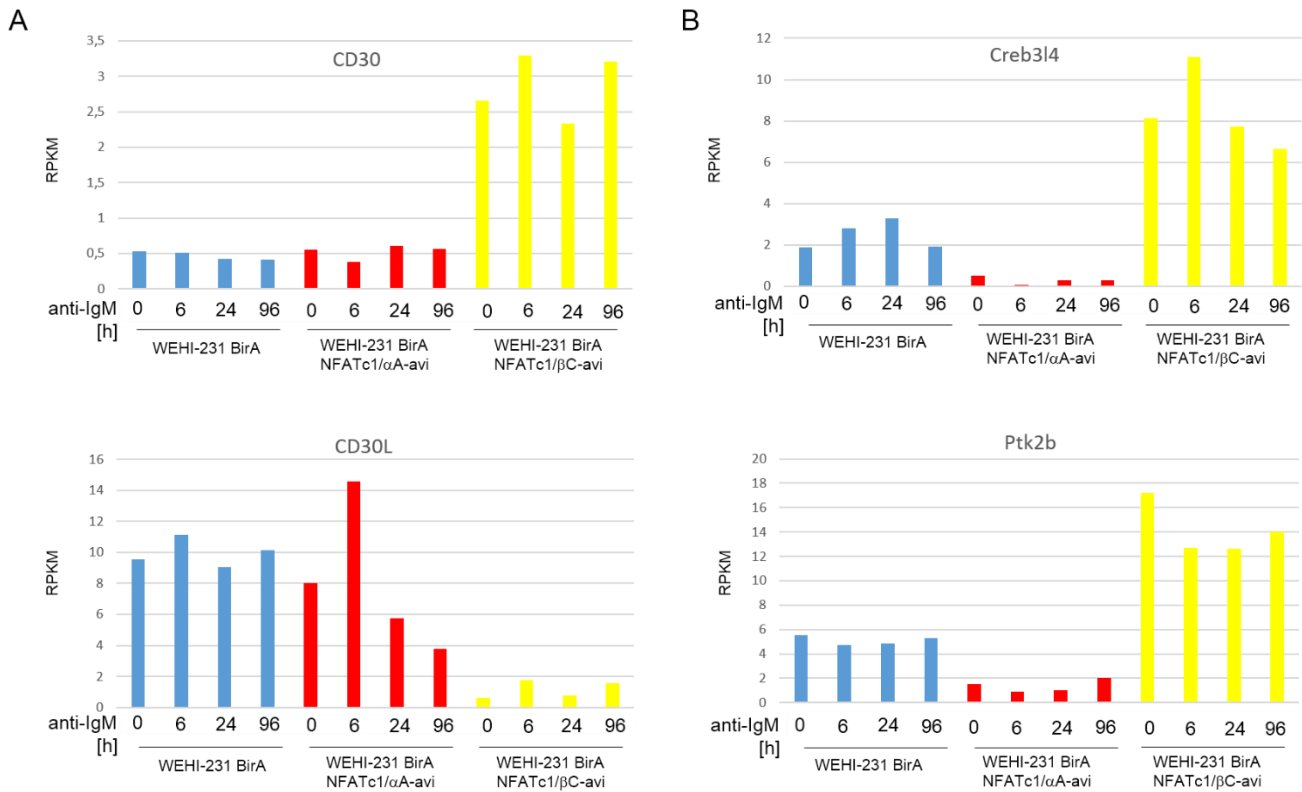
Figure 3.41 | Dichotomy in gene regulation by NFATc/αA and NFATc1/βC in WEHI-231 cells
A) *Tnfrsf 8* (CD30 receptor) and its ligand *Tnfsf8* (CD30L) induced and repressed by NFATc1/βC overexpression, respectively. B) *Creb3l4* and *Ptk2b*, induced by NFATc1/αA ovexpression and repressed by NFATc1/βC overexpression in WEHI-231 cells. RPKM: Reads per kilobase per million reads.

Some of the genes regulated by NFATc1/αA and NFATc1/βC, respectively, e.g. *Cd30* and *Cd30l*, were found to be regulated in an opposite way. Figure 3.41 shows that the expression of the CD30 receptor (*Tnfrsf 8*) was up-regulated by NFATc1/βC, whereas transcription of its ligand (*Tnfsf 8*) was down-regulated by NFATc1/βC overexpressed in WEHI-231 cells. This phenomenon was also found to be true for the expression of *Tnfrsf4* (Tumor Necrosis Factor Receptor Superfamily, Member 4) and, *Traf5*. Genes like *Creb3l4*, a gene encoding for a transcriptional regulator, and *Ptk2b* (Protein Tyrosine kinase 2b), were repressed by NFATc1/αA, but strongly induced by NFATc1/βC in WEHI-231 cells. There are several other genes which are regulated in a similar way by both NFATc1 proteins, such as *Prdm1*.
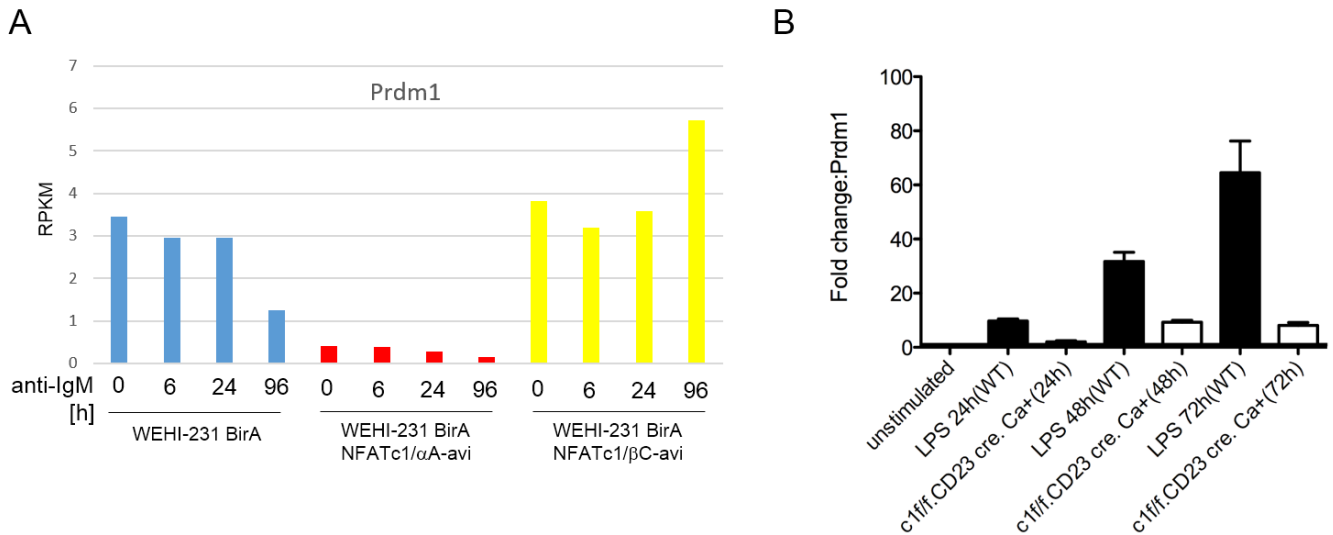
Figure 3.42 | Regulation of Prdm1 (Blimp-1) expression in WEHI-231 and primary B-cells
A) *Prdm1* transcript levels in WEHI-231 BirA, NFATc1/αA-avi and NFATc1/βC-avi overexpressing cells, respectively. B) Induction of *Prdm1* in primary C57Bl/6 cells and in B-cells from *Nfatc1^flx/flx* x CD23cre x Rosa26 caNFATc1/αA mice stimulated by LPS for 24 h to 72 h (Data in Figure 3.43 B were kindly provided by Dr. M. Khalid). RPKM: Reads per kilobase per million reads.

The gene encoding Blimp-1 protein, *Prdm1*, was found to be repressed by the overexpression of NFATc1/αA, but induced by the NFATc1/βC in WEHI-231 cells (Figure 3.42 A). *Prdm1* transcription was repressed at any given point of anti-IgM stimulation, whereas the induction by NFATc1/βC was strongest after 96 h of anti-IgM stimulation. Quantitative Real-Time PCR for *Prdm1* mRNA in primary B-cells from B6 wt and *Nfatc1^flx/flx* x CD23 cre x Rosa26-caNFATc1/αA animals (data kindly provided by Dr. M. Khalid, 3.43 B), stimulated by LPS for 48 h and 72 h, showed similar results. LPS, triggering TLR4, induced *Prdm1* induction, increasing from 24 h to 72 h, whereas *Prdm1* was hardly induced in B-cells constitutively expressing NFATc1/αA.

In this context it should be noted that the expression of the *Aicda* gene which controls germinal center (GC) formation was strongly induced by NFATc1/αA-avi in WEHI-231 cells, whereas its expression was suppressed by NFATc1/βC-avi. Thus, both NFATc1 proteins seem to exert an opposite effect on GC and plasma cell formation. Whereas NFATc1/αA appears to contribute to GC formation and to inhibit plasma cell formation, NFATc1/βC seems to act in an opposite way as it suppresses GC formation and facilitates plasma cell formation. Further experiments are in progress to substantiate this conclusion.

3.7 ChIP assays using WEHI-231 cells overxpressing NFATc1/αA-avi or NFATc1/βC-avi

3.7.1 ChIP assays using WEHI-231 cells overexpressing NFATc1/αA-avi, NFATc1/βC-avi and/or BirA

As described in 2.2.7, WEHI-231 cells expressing NFATc1/αA-avi, NFATc1/βC-avi and/or BirA were cultured to a density of 2-4 x 10^7 cells/sample and stimulated by TPA and ionomycin for 5-6 h. Cells were fixed before chromatin isolation, followed by chromatin shearing through sonication. DNA sizes were checked, and 30 µg DNA was used per ChIP sample. Precipitations were analyzed by PCR and Real-Time PCR for known NFATc1-target genes.
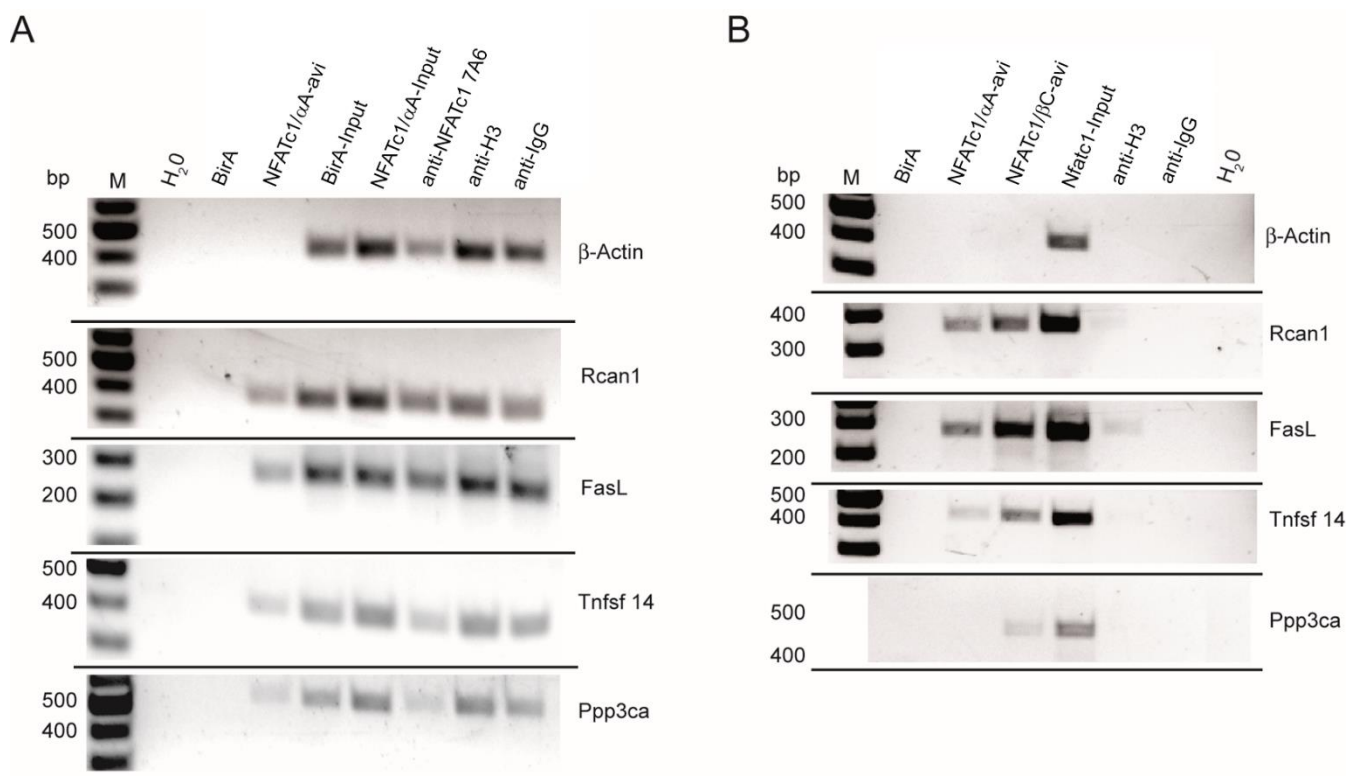
Figure 3.43 | ChIP PCR for the binding of NFATc1/αA-avi and NFATc1/βC-avi to known target genes in WEHI-231 cells
A) PCRs for the detection of template DNAs from WEHI-231 cell overexpressing NFATc1/αA-avi and from control samples, precipitated by streptavidin-agarose beads and eluted with SDS-buffer. B) PCRs for the detection of template DNAs from WEHI-231 cells overexpressing NFATc1/αA-avi and NFATc1/βC-avi, and control samples, precipitated by streptavidin-agarose beads and TEV-cleaved. (Thus, led to more specific results).

In Figure 3.43 A, DNA from WEHI-231 cells overexpressing NFATc1/αA-avi and from control cells, eluted from streptavidin-agarose beads with SDS-elution buffer (2.1.7.9), was used to perform PCRs for known NFATc1 target sites. No binding was detected within the *β*-

actin promoter region, neither with DNA samples from BirA nor with DNA from NFATc1/αA-avi expressing cells. Amplification for a 400 bp long stretch of DNA was achieved with DNA precipitates using NFATc1 (7A6) ab, anti-H3 ab and anti-IgG ab. To a high degree, these products are due to unspecific binding of 7A6 and Ig ab in these assays, using SDS elution and standard the standard ChIP protocol. The input control samples, i.e. DNA from cells overexpressing BirA and NFATc1/αA-avi before ChIP, were also positive for *β-actin* amplification. Primers (2.1.5.2) for published NFATc1 binding sites were used to determine the specific DNA binding of NFATc1/αA-avi in WEHI-231 cells. PCRs showed positive results for binding of NFATc1/αA-avi to the promoter sequences of *Rcan1*, *Fasl*, *Tnfsf14* and *Ppp3ca* genes, whereas no amplification was seen for the DNA precipitated from WEHI-231 BirA cells. However, PCR products were also seen for control samples, NFATc1 7A6 ab, anti-H3 ab and anti-IgG ab and both input-controls. In Figure 3.43 B, PCR products are shown for DNAs precipitated from WEHI-231 cells overexpressing NFATc1/αA-avi, NFATc1/βC-avi and/or BirA. In these assays a modified ChIP protocol was applied, including FGEL (2.1.6) and elution from streptavidin-agarose bound protein/DNA by TEV-cleavage (2.1.7.8). Thus reduced significantly the backround DNA binding and the elution of unspecifically bound DNA from agarose beads. The DNAs from NFATc1/αA-avi, NFATc1/βC-avi and BirA precipitates were negative for *β-actin* binding, and there was also no binding detected for samples treated with NFATc1 7A6 ab or anti-H3 ab. However, NFATc1 input DNA was positive for *β-actin* amplification. NFATc1/αA-avi and NFATc1/βC-avi binding was confirmed for the *Rcan1*, *Fasl* and *Tnfsf14,* promoters which are known NFATc1 targets [70].
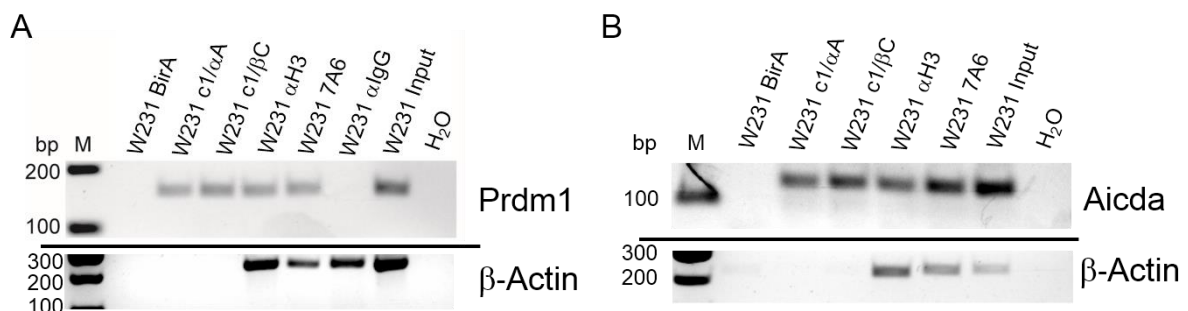
Figure 3.44 | ChIP PCRs for detecting specific NFATc1/αA-avi and NFATc1/βC-avi binding to the *Prdm1* and *Aicda* promoters in WEHI-231 cells
A) PCR products using primers for *Prdm1* (Blimp-1) and *β-actin*, with template DNAs precipitated from WEHI-231 cell overexpressing NFATc1/αA-avi and NFATc1/βC-avi by streptavidin-agarose beads. B) PCR products with primers for *Aicda* (AID) and *β-actin*, with template DNAs precipitated from WEHI-231 cells overexpressing NFATc1/αA-avi and NFATc1/βC-avi by streptavidin-agarose beads.

Ppp3ca binding could only be detected with DNA precipitated from NFATc1/βC-avi overexpressing cells.

In Figure 3.44, PCR assays for the detection of NFATc1 binding to the *Prdm1* and *Aicda* genes are displayed. ChIP was conducted with WEHI-231 cell overexpressing NFATc1/αA-avi, NFATc1/βC-avi or BirA, and DNA samples eluted from streptavidin-beads by TEV-cleavage. Targets within exon 1 of *Prdm1* gene and intron 1 of *Aicda* gene, respectively, were bound by both NFATc1/αA and NFATc1/βC since the DNA precipitates could efficently be amplified by PCR.
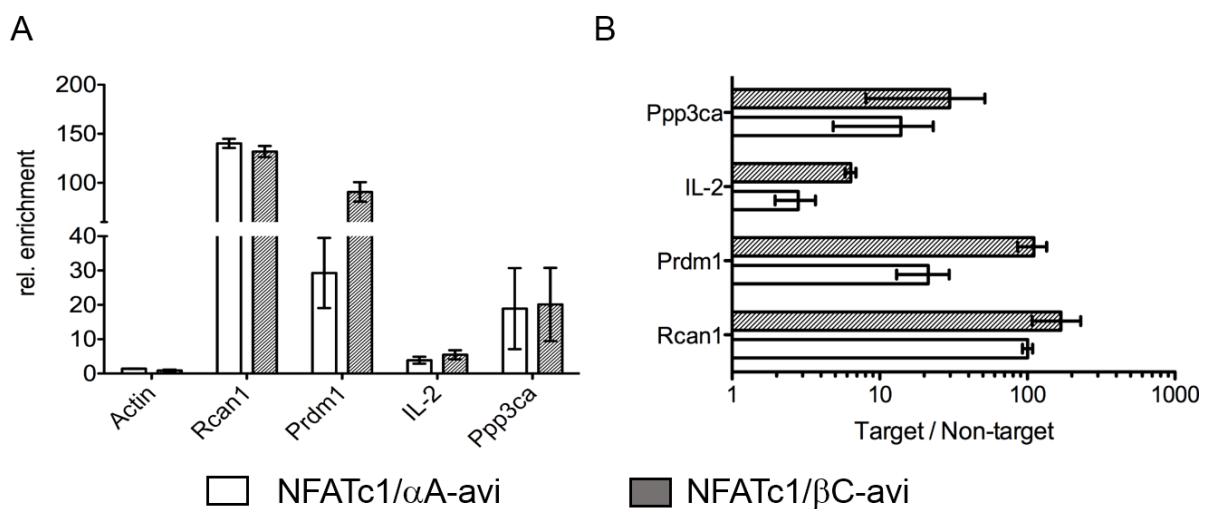
Figure 3.45 | Semi-quantitative Real-Time PCR for detecting NFATc1/αA and NFATc1/βC DNA binding
A) DNA from ChIP experiments, conducted with WEHI-231 cells overexpressing NFATc1/αA-avi, NFATc1/βC-avi and/or BirA. The DNAs were used as templates for semi-quantitative Real-Time PCR to quantify the specific binding of NFATc1 proteins to these genes.

Semi-quantitative Real-Time PCR assays were conducted with DNA from ChIP experiments using chromatin extracts from WEHI-231 cells overexpressing NFATc1/αA-avi, NFATc1/βC-avi or BirA overexpressing cells (Figure 3.45). Primers for known NFATc1 binding sites within the *Rcan*, *Ppp3ca* gene and *Il2* genes were used as positive controls. Primers for *Prdm1*, also shown in Figure 3.44, were used to quantify previously observed binding, and primers for *β-actin* were used as negative controls. High enrichment-rates for NFATc1/αA and NFATc1/βC binding within the regulatory regions of *Rcan1* and *Prdm1* genes were detected. A target-site within the *Ppp3ca* gene was also bound, but rather weakly compared to sites within the *Rcan1* and *Prdm1* promoters. In all WEHI-231 cells, amplification for a binding region within the *Il2* promoter was very weak. Target over noise was calculated for all genes tested. A more than 100 fold-enrichment was determined for *Rcan1* binding by NFATc1/αA and NFATc1/βC.

Prdm1 binding by NFATc1/βC was also well above background with ratios around 100, whereas NFATc1/αA binding was detected with enrichment rates around 30. For both NFATc1/αA and NFATc1/βC, the binding to the *Ppp3ca* gene was low, with enrichment rates around 15. In addition, binding of NFATc1 isoforms to a known binding site within the *Il2* promoter had to be considered as very weak or unspecific, with target over noise ratios below 10. This is probably due to the silencing of *Il2* genes in B-cells.

3.7 ChIP-seq

3.7.1 DNA extraction and ChIP-seq

WEHI-231 stably overexpressing the NFATc1/αA-avi and NFATc1/βC-avi proteins, and/or the prokaryotic ligase BirA (3.2.1 and 3.2.2), were cultured to a density of 4×10^7 cells, stimulated with TPA and ionomycin for 5 h, fixed with formaldehyde and chromatin was isolated as described in 2.2.7.2.
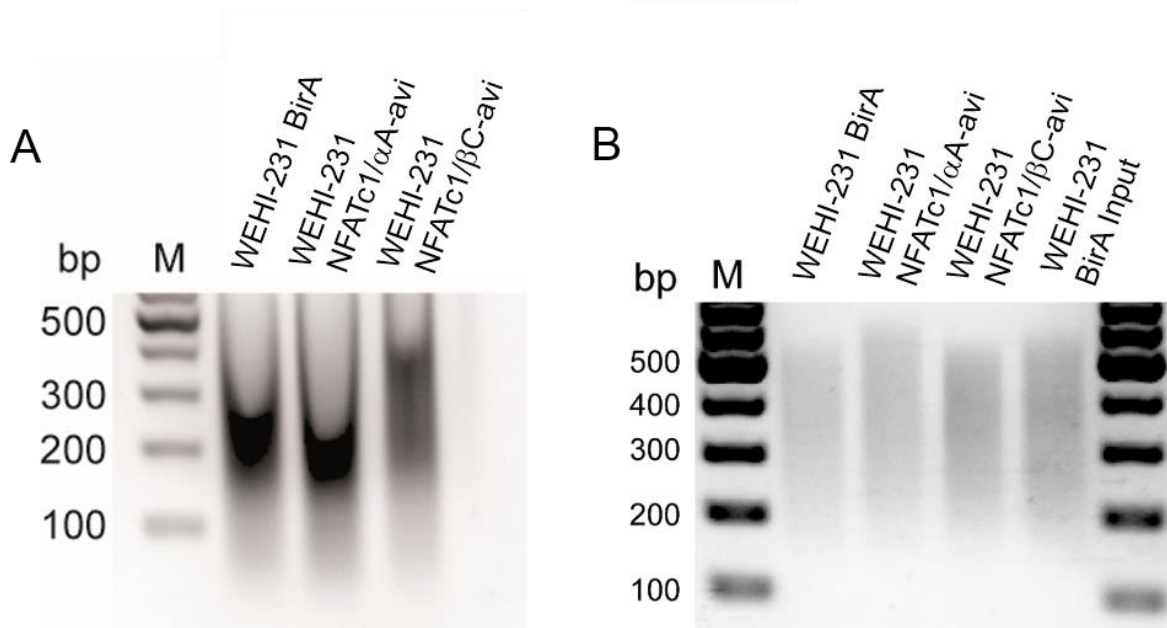
Figure 3.46| Sheared and purified chromatin of WEHI-231 cells expressing NFATc1/αA-avi and NFATc1/βC-avi
A) Fractionations of chromatin from WEHI-231 cells overexpressing BirA alone, or BirA and NFATc1/αA-avi, or BirA and NFATc1/βC-avi on agarose gels. Chromatin was sheared sonication. B) Fractions of sheared chromatin from WEHI-231 cell lines after ChIP performed with streptavidin-agarose beads (Lanes 1-3) and the input control.

In Figure 3.46 A, sheared chromatin DNA extracted from WEHI-231 cells overexpressing NFATc1/αA-avi, NFATc1/βC-avi and/or BirA, was loaded onto a 0.8% agarose gel to determine the degree of fragmentation prior ChIP. The majority of DNA fragments ranged from approximately 150 to 400 bp in size. The DNA was quantified and 30 µg/sample was used to perform ChIP assays with streptavidin bound to agarose-beads. The precipitated DNA was eluted and analyzed on a 0.8 % agarose gel. The DNA was isolated from the gel by standard DNA-agarose purification protocols (2.2.4). In Figure 3.46 B, about 25 % of all DNA material, eluted from DNA-purification columns was loaded and checked for fragment sizes. DNA sizes ranged from 200 to 500 bp. This material was quantified, frozen and sent to TRON for sequencing (2.2.8).

3.7.2 ChIP sequencing (TRON) and data analysis

Peak analysis was done using Bowtie software for short read alignment (version 0.12.8)[185] in reference to the mouse genome (mm9). MACS peaks were established, using MACS software (version 1.01)[186] and analyzed with Peak Analyzer software (version 1.3)[187]. Peak annotation was done using ChIPpeakAnno (version 2.8.0)[188]. Data extraction and mining was done in co-operation with TRON (Martin Löwer, TRON, computational medicine).

Potential DNA-target binding-sites from WEHI-231 NFATc1/αA-avi and NFATc1/βC-avi ChIP-samples were mapped against the mouse genome (mm9). Unspecific background binding, DNA bound, precipitated and sequenced from WEHI-231 BirA overexpressing cells, was subtracted from NFATc1/αA- and NFATc1/βC-reads. Individual reads were grouped as ´tags´ and distributed to present MACS quadrants. MACS peaks were annotated for all three samples and used for further calculations. In total, 1379 potential DNA-binding sites were calculated from all mapped reads for the NFATc1/αA ChIP-samples, and 1132 potential DNA binding-sites were sequenced, mapped and assigned to the NFATc1/βC ChIP-samples.

A

B

ID	ChIP NFATc1/αA		ID	ChIP NFATc1/βC		
Arhgap5	Nsun3	Rock1	Acoxl	Utp20	Btla	Tspyl2
Ccdc132	Osbpl7	Sap30l	Sirpa	Gnl3l	Mocs1	Malat1
Ccdc28a	Pbx3	Taok1	Fam46	Phf8	Dlgap1	Fasn
Eif2c2	Rabgap1l	Tbck	Map3k7	Huwe1	Lpin2	Ephb4
Foxn3	Rel	Tblxv1	Rasgef1a	Syap1	Trim7	Fabp7
Itln1	Refsd	Ttc39b	Ppp1r15a	Dcakd	Crebzf	Pax5
Klf10	Rictor	Uty	Pcid2	Klhdc2	Cyp4f16	Celf2
Lats1	Rn4.5s		Aig1	Ptk2b	Ler5	Rn4.5s

Figure 3.47 | Potential DNA binding sites of NFATc1/αA and NFATc1/βC in WEHI-231 cells
A) NFATc1/αA and NFATc1/βC binding-sites mapped from sequenced reads from ChIP seq experiments with WEHI-231 cells overexpressing NFATc1/αA-avi or NFATc1/βC-avi. Venn-diagram of 477 potential binding-sites for NFATc1/αA (green), 454 potential binding-sites for NFATc1/βC (yellow) and an overlap of 88 sites (grey). B) Potential target gene binding-sites of NFATc1/αA and NFATc1/βC proteins for genes that showed at least a 2-fold transcriptional change in WEHI-231 NFATc1/αA-avi and NFATc1/βC-avi overexpressing cells. Background correction was performed with reads mapped for BirA controls.

All potential binding-sites for NFATc1/αA and NFATc1/βC that displayed a distance greater than 20 kbs from the next transcriptional start or the last exon of the next adjacent gene were neglected, reducing the number of genes linked to specifically bound target sites to 477, for NFATc1/αA samples, and 454 for NFATc1/βC, respectively (Figure 3.48 A). Next, all genes, which were linked to potential NFATc1/αA- (477) and NFATc1/βC-binding-sites (454) were analyzed for change in transcriptional expression, determined by the NGS transcriptome sequencing (3.6), with a 2-fold change threshold at any given time-point. We found 23 genes, potentially bound by NFATc1/αA-avi and 33 genes, potentially bound by NFATc1/βC, which also displayed significant changes in the transcriptional induction of target genes.

III. RESULTS

In Table 3.3, fifty of 477 potential NFATc1/αA binding sites within the mouse genome are listed. Sites were sorted by relative fold enrichment of bound DNA, the number of tags mapped within the depicted genomic area and the distance to the next genetic feature.

Table 3.3| Top 50 binding sites for NFATc1/αA in WEHI-231 cells
Top 50 DNA sites, bound by NFATc1/αA-avi in WEHI-231 cells, sorted by distance to feature, number of tags and relative fold enrichment, normalized against BirA control samples. Ref.seq: Gene ID number listed within the NCBI Reference Sequence database; Tags: Number of reads mapped at a specific site after normalization; x.10.log10: -10*log10 (pvalue) for the peak region; Fold.enr.: fold enrichment for this region against random Poisson distribution with local lambda; Dis.To Feat.: distance to the nearest feature such as transcription start site; Feature: Id of the feature (UCSC kg ID)

GENESYMBOL	REFSEQ.	TAGS	X.10.LOG10	FOLD.ENR.	DIS. TO FEAT.	FEATURE
STARD6	NM_029019	16	76,85	19,21	13946	Inside
OLFR1466	NM_146694	16	108,49	17,59	-7889	Upstream
ADAD1	NM_009350	17	95,24	17,45	4578	Inside
KLK1B16	NM_008454	15	82,74	16,23	11940	Downstream
THSD7A	NM_001164805	21	96,33	16,11	77528	Inside
OLFR172	NM_147001	15	75,17	14,74	-14768	Upstream
CD163L1	NM_172909	19	81,47	14,58	2933	Inside
OLFR1251	NM_001011529	20	81,39	14,11	-8365	Upstream
KLF10	NM_013692	15	66,13	13,36	-7721	Upstream
HPCAL1	NM_016677	15	62,54	13,01	16788	Downstream
OLFR257	NM_207554	16	65,3	12,32	-11399	Upstream
MYC	NM_010849	15	65,6	11,93	-9624	Upstream
GLG1	NM_009149	16	56,53	11,57	31028	Inside
LEPR	NM_010704	16	69,45	11,48	41320	Inside
MIR34A	NR_029751	15	72,61	11,21	-9027	Upstream
GSTO2	NM_030051	15	75,31	11,21	-4207	Upstream
KLRA5	NM_008463	16	71,22	10,87	-10566	Upstream
MSL2		19	63,51	10,74	21534	Inside
WDR63	NM_172864	15	53,24	10,74	6880	Inside
SPTLC2		16	57,94	10,11	5286	Inside
MYO18B	NM_028901	16	60,11	9,93	-8447	Upstream
PTGFR	NM_008966	15	64,5	9,89	25712	Inside
MED7	NM_001104530	15	55,55	9,72	-8496	Upstream
TMEM50B	NM_030018	14	60,34	9,18	10888	Inside
NALCN	NM_177393	17	50,46	8,72	82593	Inside
BDH1	NM_175177	16	61,64	8,58	12842	Inside
OLFR221	NM_001001808	20	60,66	8,44	-3384	Upstream
PISD-PS1		17	66,96	8,39	-11457	Upstream
RNF180	NM_027934	16	58,09	8,33	11181	Inside
TBL1XR1	NM_030732	14	56,54	8,33	6627	Inside
CDH11	NM_009866	22	71,81	8,29	119171	Inside

FERT2	NM_008000	16	59,84	8,27	159084	Inside
FBXW22		18	50,16	8,25	-15358	Upstream
CUX1	NM_198602	15	54,46	8,16	23374	Inside
TUBB2A	NM_009450	22	69,43	8,1	3494	Inside
POR		16	53,91	8,1	1893	Inside
TET2	NM_001040400	14	66,57	8,03	17179	Downstream
VMN2R32	NM_001105063	18	63,43	7,78	-2882	Upstream
KRTAP5-1	NM_015808	16	56,34	7,78	10898	Downstream
VMN2R121		16	67,99	7,76	-2977	Upstream
PET112L		16	58,44	7,76	48525	Inside
SPOCK1	NM_001166464	17	56,66	7,59	249790	Inside
AMPH	NM_175007	21	73,55	7,49	-11072	Upstream
ACAP2	NM_030138	16	59,83	7,44	44688	Inside
GPC5	NM_175500	17	62,7	7,42	505752	Inside
DAPK3	NM_007828	36	61,37	7,29	-874	Upstream
H2AFY2	NR_003523	22	63,14	7,29	-10231	Upstream
ELAVL3	NM_010487	16	51,12	7,29	-9317	Upstream
IGFBP7	NM_008048	18	54,77	7,12	-11550	Upstream
SECISBP2L	NM_177608	18	56,11	7,06	-6527	Upstream

In Table 3.4, fifty of 454 potential NFATc1/βC binding sites within the mouse genome are listed. Binding-sites were sorted by the relative fold enrichment of bound DNA, the number of tags mapped within the depicted genomic area and the distance to the next genomic feature.

Table 3.4| Top 50 binding sites for NFATc1/βC in WEHI-231 cells
Top 50 DNA sites, bound by NFATc1/βC-avi in WEHI-231 cells, sorted by distance to feature, number of tags and relative fold enrichment, normalized against BirA control samples. Ref.seq: Gene ID number listed within the NCBI Reference Sequence database; Tags: Number of reads mapped at a specific site after normalization; x.10.log10: -10*log10 (pvalue) for the peak region; Fold.enr.: fold enrichment for this region against random Poisson distribution with local lambda; Dis.To Feat.: distance to the nearest feature such as transcription start site; Feature: Id of the feature (UCSC kg ID)

GENESYMBOL	REFSEQ.	TAGS	X.10.LOG10	FOLD.ENR.	DIS. TO FEAT.	FEATURE
GRM7	NM_177328	15	98,33	16,2	515082	Inside
CADM2	NM_178721	19	88,12	15,19	286970	Inside
PCDHGA12	NM_033595	15	67,37	15,19	10171	Inside
CENPF	NM_001081363	21	65,75	15,02	-7201	upstream
CCDC148	NM_001001178	17	88,93	14,02	18830	Inside
NFKB1	NM_008689	21	106,08	13,85	11076	Inside
THSD7A	NM_001164805	19	80,04	13,08	77546	Inside
OLFR589	NM_147052	17	75,8	12,71	-7608	upstream
CLCN4-2	NM_011334	23	99,93	12,21	-934	upstream
PEA15A	NM_011063	24	82,3	12,02	13521	downstream
OLFR1453	NM_146700	16	62,13	11,69	-5689	upstream
CNGB3	NM_013927	15	68,26	11,69	84234	Inside
CYP2C66	NM_001011707	16	54,74	11,45	-6351	upstream

CD163L1	NM_172909	16	71,98	11,37	2994	Inside
COPA	NM_009938	15	68,59	11,3	1764	Inside
FAM46C	NM_001142952	17	60,66	10,94	3932	Inside
FAR2	NM_178797	18	59,33	10,71	79033	Inside
FMN2		15	62,06	10,5	95353	downstream
FASN	NM_007988	17	61,86	10,44	-8275	upstream
ATPBD4	NM_025675	16	59,64	10,4	99684	Inside
SMCR7L	NM_178719	24	90,45	10,38	6587	Inside
SGCD		16	62,96	10,38	140682	Inside
PISD-PS1		22	60,09	10,1	-11504	upstream
AHI1	NM_001177776	18	59,68	10,08	10589	Inside
THUMPD1		21	73,84	9,94	-11678	upstream
KLHDC2		26	86,69	9,82	801	Inside
SPOCK1	NM_001166464	22	83,14	9,71	249794	Inside
PEPD		17	61,27	9,63	-1608	upstream
ZFP498		16	51,07	9,44	26030	downstream
KLRB1A	NM_001159902	17	58,4	9,43	-2500	upstream
KCNC3	NM_008422	18	54,57	9,38	29858	downstream
MSL2		19	60,17	9,18	21535	Inside
GPC5	NM_175500	18	71,49	9,18	850528	Inside
CAPZB	NM_009798	15	53,3	9,03	12658	Inside
MAGEB16	NM_001113734	15	72,96	9,03	19492	downstream
OLFR147	NM_146869	17	58,66	8,71	12637	downstream
KCNH8	NM_001031811	18	76,88	8,61	141871	Inside
JPH2	NM_021566	17	53,24	8,34	13034	Inside
PIAS2	NM_001164168	16	71,61	8,32	29989	Inside
CSF2RA	NM_009970	18	63,59	8,27	-4279	upstream
GCAP14	NM_028407	17	59,9	8,25	23910	Inside
BMP6	NM_007556	17	63,78	8,15	-7240	upstream
LUZP4	NM_001114383	30	51,15	8,01	-13077	upstream
CCDC79	NM_180958	17	56,74	7,86	3405	Inside
RAB3GAP2		24	75,75	7,72	-3198	upstream
RAPGEF6	NM_175258	20	67,4	7,72	15695	Inside
R3HDM2	NM_001168292	19	59,57	7,72	15071	Inside
FANCC	NM_001042673	18	53,81	7,72	51663	Inside
AK137190		16	55,64	7,72	20749	downstream
FBXO17	NM_015796	16	61,61	7,61	11645	Inside

IV. DISCUSSION

4.1 *Nfatc1* induction in lymphocytes

In earlier studies, it was shown that *Nfatc1* is constitutively expressed in naïve T- and B-lymphocytes of peripheral lymphoid organs, and unlike many other genes that are only expressed upon activation, the *Nfatc1*-gene locus appears to be in an open and active chromatin configuration [137]. *A. Patra* and colleagues showed that NFATc1, together with STAT5, plays a vital role in early thymocyte development in an IL-7 dependent manner. In peripheral lymphocytes, NFATc1 is activated by cell surface receptors that are coupled to Ca^{2+} mobilization, like PLCγ1 in T-cells and PLCγ2 in B-cells. Activation of PLC-coupled receptors induces SOCE (Store Operated Calcium Entry), which leads to increased intracellular Ca^{2+} concentration. High Ca^{2+} level activate the calcium- and calmodulin-dependent serine-threonine phosphatase CN, which, by de-phosphorylation of multiple serine-threonine residues on NFATc1, initiates NFATc1 activation and translocation to the nucleus [19, 128, 144]. We have shown that a secondary stimulation of T-cells, differentiated into Th1 cells, leads to a 10-fold increase in *Nfatc1* transcript levels. This correlates with the appearance of histone modifications at intron 10 of the *Nfatc1* locus, such as H3K4me3 marks which are an indication for active transcription. This occurs mainly in Th1 and Th2 cells, but not Th17 and Treg cells, in which *Nfatc1* expression is much weaker (Figure 3.2) [137, 138, 144]. Due to prevalent *Nfatc1* P1 promoter employment upon stimulation, *Nfatc1* induction by TCR engagement predominantly leads to NFATc1/αA protein synthesis, as shown by *S. Chuvpilo* and colleagues [142]. These findings were also reported for the stimulation of naïve splenic B-cells from 6 to 8 week old mice with anti-IgM ab *in vitro*. Western-blot analysis of whole B-cell extracts using NFATc1 α-peptide-specific abs revealed a predominant induction of NFATc1/αA expression in primary peripheral B-cells upon anti-IgM stimulation [70, 137].

4.1.1 *Nfatc1* induction in peripheral T-cells

We have reported that naïve, freshly isolated CD4$^+$ T-cells, stimulated with anti-CD3 and anti-CD28 abs, displayed a 5-fold increase in *Nfatc1* P1 transcripts and a weak, but reproducible decrease in P2-directed transcripts upon stimulation for 24 h or 72 h [137]. This induction of P1 stopped, when all T-cells were washed and the anti-CD3 and anti-CD28 abs were removed upon stimulation for 24 h. Furthermore, we reported that secondary induction of primary T-cells with TPA and ionomycin, which initially encountered anti-CD3 and anti-CD28

stimulation for 72 h and a subsequent resting period of 2 days without any stimulation, led to a 10-fold induction of P1 transcripts [137]. As shown in Figure 3.1, incubation of CD4$^+$ T-cells from *Nfatc1/Egfp* tg mice with anti-CD3 and anti-CD28 led to a significant increase of GFP fluorescence from a MFI value of 88 to 184 and 239 upon stimulation for 48 and 96 h, respectively. The addition of synthetic CpG (triggering TLR9) or Pam3CSK4 (triggering TLR2) to those CD4$^+$ T-cells, washed carefully after initial TCR-stimulation for 24 h, led to a reduction in eGFP expression after a further incubation period of 24 h and 72 h, respectively. In line with these results, we have shown that whole-protein extracts from splenic CD4$^+$ T-cells stimulated for 24 h by anti-CD3 and anti-CD28 displayed a strong increase in NFATc1 protein levels, most significantly for NFATc1/αA. Elevated NFATc1 protein expression levels were stable upon anti-CD3 and anti-CD28 stimulation but rapidly dropped as soon as TCR engagement was relieved. Particularly, the high level of NFATc1/αA protein diminished, whereas expression of longer NFATc1 isoforms remained almost stable [137]. This led us to the conclusion that in primary T-lymphocytes *Nfatc1* induction is highly dependent on persistent TCR engagement. This is particularly true for NFATc1/αA expression and cannot be increased by TLR engagement, although this additional stimulus is crucial for T-lymphocyte survival and proliferation under certain physiological circumstances.

4.1.2 *Nfatc1* induction in peripheral B-cells

In a similar fashion, as TCR stimulation was shown to be necessary for *Nfatc1* induction in peripheral T-cells, BCR engagement was shown to increase *Nfatc1* gene expression in peripheral B-cells. Taking advantage of *Nfatc1/Egfp* tg B-cells, we were able to show that the *Nfatc1* gene is highly induced upon anti-IgM stimulation. Increasing amounts of NFATc1/eGFP were detected upon 48 h of BCR engagement, before peripheral B-cells became apoptotic and died, if stimulated by anti-IgM only [137](Figure 3.3). For B-cells from *Nfatc1/Egfp* mice, we were also able to show that TLR4 engagement by LPS and CD40 receptor stimulation by anti-CD40 ab hardly induced any *Nfatc1* transcription on their own, but rather accounted for B-cell survival by inducing NF-κB mediated transcription [70]. *Nfatc1/Egfp* expression almost decreased to levels found in naïve B-cells, if BCR stimulation was discontinued after 24 h and B-cells were subsequently stimulated with LPS or anti-CD 40 ab, respectively [137] (Figure 3.3). To identify specific *Nfatc1* promoter usage and, thereby, particular NFATc1-isform expression, we used primers for the detection of P1- or P2-directed transcripts in PCR- and qReal-Time PCR-assays [70, 137](Figure 3.6). Upon stimulation of naïve splenic B-cells by anti-IgM for 24 h and 48 h, we observed a 3- to 4-fold increase in P1-

directed transcripts, whereas P2-directed RNAs decreased. LPS did not enhance, but rather suppress both P1 and P2 activity. A similar effect was detected for anti-CD40 treatment alone [137]. Adding the NF-κB inducers LPS or anti-CD40 to B-cells, which were pretreated by anti-IgM for 24 h and washed afterward, led to a marked increase in P1-directed transcripts upon further incubation for 48 h and 72 h (Figure 3.6). These effects of anti-IgM-, LPS-, or anti-CD40-mediated stimulation of B-cells on P1- and P2-transcript expression are somewhat contradictorily regarding the flow-cytometry results of *Nfatc1/Egfp* expression, but might contribute to alternative NFATc1-isoform expression.

S. Bhattacharyya and colleagues reported a strong decrease in peritoneal B1a-cells in conditional *Nfatc1* knock-out animals (*Nfatc1*[flx/flx] x *mb1*-cre [70]), and concluded a unique role for NFATc1 during the development of these cells. To further address this point, we compared the *Nfatc1/Egfp* expression in B1a-cells with that in peripheral T- and B2-lymphocytes. While NFATc1/eGFP expression showed similar levels in un-stimulated peripheral T- and B-cells, *Nfatc1/Egfp* induction was found to be 8- to 10-times higher in un-stimulated CD19^{+} B220^{+} CD5high B1a-cells (Figure 3.4). A particular reason for these high tonic levels of *Nfatc1*-induction in B1a-cells remains to be determined, but indicates that NFATc1 not only plays a pivotal role during B1a-cell differentiation, but might also contribute to their unique effector functions.

4.2 Regulation of *Nfatc1* transcription in lymphocytes

Nfatc1 transcription is regulated by the two promoters P1 and P2 located upstream of *Nfatc1* exon 1 and exon 2, and the two poly A sites (pA1 and pA2), downstream of exon 9 and 11, respectively. P1 and P2 correspond to CpG islands that were shown to be hypermethylated in cells from various non-lymphoid tissues but hypomethylated in murine T-lymphocytes. They were also shown to form DNase-I-hypersensitivity sites and to contain numerous transcription-factor binding sites [156](Figures 1.13 and 3.6). The murine *Nfatc1* locus, located on Chr. 18 spanning about 106.87 kbs, contains eleven exons and ten introns, and similar to the human *NFATC1* gene gives rise to six distinct isoforms which differ both in their N- and C-terminal peptides (Figure 1.12, [142]). Expression of NFATc1/αA is directed by the strong promoter P1 and the relatively weak proximal poly A site, pA1. Synthesis of the longer NFATc1/B- and -C-isoforms is directed by either P1 or P2 and by the strong poly A site, pA2. As reported by S. *Chuvpilo* and colleagues, autoregulation of P1 promoter by NFAT proteins leads to an increase of NFATc1/A, but not of NFATc1/B and -C synthesis [142, 156]. Two tandemly arranged

IV. DISCUSSION

NFAT binding sites within P1, designated as NFAT$_{tand}$ situated at position -650 within the distal block of P1, and one unique site at position -90, within the proximal P1 promoter region were described to be unique and crucial for NFAT autoregulation (Figure 1.12;[156]). However, recently the -90 site was identified as a NF-κB site (*E. Serfling*, unpublished data).

4.2.1 Characterization of two potential regulatory elements within the *Nfatc1* locus

By analyzing DNase-I-hypersensitivity studies, we found two elements located within the *Nfatc1* locus, upstream of exon 11, designated E1 and E2, which were shown to be highly susceptible for enzymatic cleavage in human CD34$^+$ progenitor cells. Element E2 was also found to be DNase-I-hypersensitive in human CD3$^+$ T-cells (Figure 3.6). Initially, Dr. S. Klein-Hessling cloned and analyzed luciferase-reporter constructs in El-4 thymoma cells (Figure 3.7). After transduction, El-4 cells were stimulated with TPA and ionomycin and analyzed for luciferase emission. A fusion-construct containing *Nfatc1*-P1 and Element E2 showed very high induction rates, whereas different combinations of P1 and P2 with E1 and E2 showed no luciferase expression, except P2 in combination with *E2*. Additionally, a variant of P1-E2, harboring three mutations which abolish NFAT binding to E2 (P1-E2$_{Nm3}$), showed only very little luciferase expression. This led us to the conclusion that element E2, in combination with either P1 or P2, contributes to *Nfatc1* induction in primary lymphocytes.

In order to assess potential roles for E1 and E2 on *Nfatc1* induction in mice, two BAC transgenes, with site-specific mutations for either element, designated *Nfatc1/*DE1 and *Nfatc1/DE2*, were cloned by Dr. S. Klein-Hessling and tg mouse-lines were generated in cooperation with the Transgenic Facility at the University Mainz (in collaboration with Dr. K. Reifenberg). Peripheral B- and T-cells from several different *Nfatc1/*DE1 and *Nfatc1/*DE2 founder animals were isolated, cultured and stimulated *ex vivo*. FACS analysis with naïve, freshly isolated T-cells from *Nfatc1/Egfp*, *Nfatc1/*DE1 and *Nfatc1/*DE2 mice revealed clear cut differences between their NFATc1 expression levels. Compared to T-cells from *Nfatc1/Egfp* animals, eGFP expression in *Nfatc1/*DE1 T-cells was much higher compared to "regular" *Nfatc1/Egfp* expression. This was also true for T-cells from *Nfatc1/*DE2 B animals, whereas *Nfatc1* induction in T-cells from *Nfatc1/*DE2 A animals was much weaker (Figure 3.9, left panel). When CD4$^+$ T-cells from *Nfatc1/*DE1 and the two *Nfatc1/*DE2 mouse-lines were stimulated for 48 h by plate-bound anti-CD3 and anti-CD28 abs their NFATc1 induction was comparable to the induction seen in *Nfatc1/Egfp* T-cells. However, compared to CD4$^+$ T-cells, from *Nfatc1/Egfp* mice, we observed reduced levels of eGFP emission (MFI) in cells from one

of the two *Nfatc1/*DE2 lines, namely in DE2 A mice. In contrast, a strong eGFP expression was detected in T-cells from *Nfatc1/*DE1 and *Nfatc1/*DE2 B mice (Figure 3.9, right panel). When we investigated B-cells from *Nfatc1/*DE1 and *Nfatc1/*DE2 animals, we also found higher levels of NFATc1/eGFP expression. Freshly isolated primary B-cells from *Nfatc1/*DE2 mice showed *Nfatc1* induction rates similar to that in *Nfatc1/Egfp* mice. Although B-cell stimulation with anti-IgM ab for two days elevated induction of *Nfatc1* significantly in all three transgenic mouse lines, there was no difference in NFATc1/eGFP abundance between B-cells from *Nfatc1/*DE2 A and *Nfatc1/Egfp* mice. So, the effect on *Nfatc1* induction previously seen in CD4$^+$ T-cells, by element E2 was not detected for B-cells.

To further investigate this phenomenon, whole-protein extracts from freshly prepared CD4$^+$ T-cells stimulated for 48 h anti-CD3 and anti-CD28 were isolated and analyzed by immunoblotting using abs directed against GFP and the α-peptide of NFATc1 (Figure 3.10). We observed transcriptional induction of NFATc1/αA upon TCR stimulation for all samples analyzed. Interestingly, NFATc1 expression in T-cells from *Nfatc1/*DE2 *B* mice was also found to be unexpectedly high, similar to the results gathered by flow-cytometry. Furthermore, we detected lower levels of α-GFP expression in T-cells from DE2 B animals upon 48 h of TCR stimulation, compared to control cells.

Although we cannot exclude genotyping artifacts, one explanation for the differences in *Nfatc1* induction described above, would be due to the integration of variable copy-numbers of the *Nfatc1/*DE2 transgene into the recipient mouse genome. Nevertheless, the expression data from *Nfatc1/*DE2 A animals, by definition expressing at least one copy of *Nfatc1/*DE2 BAC DNA, indicate a regulatory role for element E2, as an enhancer element in CD4$^+$ T-cells, especially considering the fact, that NFATc1 expression rates were un-altered in B-cells from *Nfatc1/*DE2 mice compared to *Nfatc1/Egfp* controls. Accordingly, in line with the previous assumption, one would imply a negative role for Element E1 in *Nfatc1* transcription initiation.

4.3 Design and cloning of biotinylatable NFATc1-isoforms

In recent years, several efficient protocols for high throughput proteomic methodologies have been established which allowed the isolation of specific multi-protein complexes. But one particular method for protein complex purification and interaction studies moved into focus, which is based on the very high affinity of streptavidin for isolating biotinylated templates [175, 189]. Biotinylation turned out to be a very specific post-translational modification in *E. coli*,

where a single lysine residue within the biotin carboxyl carrier protein (BCCP) subunit of acetyl-CoA carboxylase is recognized and biotinylated by BirA (the biotin protein ligase from *E. coli*) [189].

In an attempt to identify new interaction partners and, particularly, new NFATc1 binding sites in a genome wide approach, we decided to generate NFATc1-isoforms biotinylatable *in vivo*. They should be used to establish a ChIP protocol for performing ChIP-sequencing with overexpressing cell-lines and primary mouse-cells. Very recently, work has been published by *M. Busslinger* and colleagues [173] and by *D. Rudra* and colleagues [174], applying *in vivo* biotinylation as methodological basis for global approaches to determine transcription factor binding sites and protein-protein interactions, respectively. In a similar fashion, we generated retroviral expression vectors (pEGZ-NFATc1/αA-avi and pEGZ-NFATc1/βC-avi) encoding either NFATc1/αA or NFATc1/βC, which were fused to a small peptide sequence (avidin-tag), encoding a lysin as substrate for BirA biotin ligation. The mRNA sequences for NFATc1/αA (mNfatc1 transcript variant 3) and NFATc1/βC (mNfatc1 transcript variant 5) were obtained from the NCBI Database, and a retroviral expression plasmid, designated pMSCV-bio-iPuro, encoding the prokaryotic biotin ligase BirA, was kindly provided by Prof. M. Busslinger (IMP; Vienna). By PCR amplifications, the NFATc1-isoforms were cloned from B6 RNA and C- and N-terminally tagged with the biotinylatable avidin-tag (Figure 3.13 and Figure 3.16). For unknown reasons, in *in vitro* assays the N-terminally tagged NFATc1-isoforms were never found to be functional. However, it is otherwise a common phenomenon that modification of bait-proteins with specific peptide-tags is functional only at one of both termini. Finally, the cDNAs encoding the C-terminally tagged NFATc1/αA and NFATc1/βC (and NFATc1/βC-aviFL) were sequenced and used for the initial transfections of HEK-293T-cells.

4.4 NFATc1 Ex.9-avidin BAC cloning

One final goal of this work was to create an *in vivo* mouse model to study genome-wide NFATc1 binding events in murine lymphocytes and other cells. Therefore, we decided to generate a NFATc1-avidin BAC transgene (Figure 3.21). This model will be created to identify NFATc1 protein-protein and protein-DNA interactions in any given cell-type. As described in 3.4, we were able to proof this approach with stably expressed NFATc1-avidin proteins in WEHI-231 B-lymphoma cells.

Based on work published by *T. Sparwasser* and colleagues [183] and on the experience in BAC-cloning in our own laboratory (*Hock et al.*[137]), we chose a suitable cloning strategy to introduce a short avidin-peptide sequence into the *Nfatc1* locus within the BAC vector RP23-361H16. In order to introduce the avidin-coding sequence at the 3´-end of *Nfatc1-Exon 9*, we used PCR amplifications to clone two regions of homology at the 3´-end of Ex.9, flanking the avi-tag sequence, into the shuttle vector pLD53-SC2 (Figures 3.18). This vector was introduced into *E. coli* cells, bearing BAC RP23-361H16, by electroporation, and in two rounds of selection-catalyzed RecA homologous-recombination, we introduced the avi-peptide sequence downstream of *Nfatc1-Exon 9* (Figures 3.18). BAC RP23-361H16 Ex.9-avi was analyzed by PCR detection (Figure 3.20), enzymatic digestion and sequencing (data not shown). Sufficient amounts of RP23-361H16 Ex.9-avi DNA were linearized by restriction enzyme digestion, and purified by sepharose-column fractioning (Figure 3.20). In collaboration with the central Animal Facility of the University Mainz (Dr. Eshkind) pronuclear injection of fertilized oocytes are currently performed.

4.5 Functional analysis of biotinylatable NFATc1-isoforms in WEHI-231 B-cells

4.5.1 Transient expression and biotinylation of avidin-tagged NFATc1-isoforms in HEK293T-cells

HEK-293T-cells were double transfected with pEGZ-NFATc1/αA-avi and pMSCV-F-BirA or pEGZ-NFATc1/βC-avi and pMSCV-F-BirA and/or with pMSV-F-BirA individually. Cells were kept in DMEM, supplemented with biotin, and induced with TPA and ionomycin for 5 h. Transfection rates were determined by eGFP expression. To determine *in vitro* biotinylation, transfected HEK293T-cells were intracellularly stained with streptavidin coupled to the fluorophore APC (<u>A</u>llophy<u>c</u>ocyanin) and measured by flow cytometry. Cells expressing either one of the avi-tagged NFATc1-isoforms and no additional BirA were positive for eGFP expression, but negative for APC staining. Cells positive for transgenic NFATc1 expression and expression of BirA were positive for eGFP expression and streptavidin-APC binding in FACS (Figure 3.22), which proofs the successful biotinylation of NFATc1-avi protein in HEK293T-cells.

4.5.2 Expression of NFATc1 avidin-tagged isoforms in WEHI-231 B-lymphoma cells

4.5.2.1 Generation of WEHI-231 cells overexpressing NFATc1/αA-avi and NFATc1/βC-avi

Retroviral particles containing pEGZ-NFATc1/αA-avi, pEGZ-NFATc1/βC-avi or pMSCV-F-BirA, as well as all three expression plasmids, respectively, were produced in HEK293T-cells and used for infections of WEHI-231 B-lymphoma cells (3.4.2). Positively infected WEHI-231 cells were cultured and selected for stable integration of pEGZ-NFATc1 and pMSCV-F-BirA by FACS analysis, followed by antibiotic selection. Cells were fixed and intracellularly stained with streptavidin-coupled APC. After two weeks of antibiotic selection in culture, most of double-infected WEHI-231 cells were positive for either NFATc1/αA-avi and BirA or NFATc1/βC-avi and BirA expression. Compared to WEHI-231 cells infected with BirA alone, most of the double-infected cells (>75% of all cells) were positive for eGFP expression and streptavidin-APC binding (Figures 3.23 and 3.25). We compared the expression levels of intracellular biotinylation in WEHI-231 cells expressing NFATc1/αA to cells expressing the biotin ligase BirA only (Figure 3.24), because it has been reported that histones (H2A, H3 and H4) are naturally modified at their amino-terminal tails by biotin ligases in human lymphocytes [190]. *J. Hymnes* and colleagues have reported a reaction mechanism by which cleavage of biocytin (biotin-ε-lysine) by biotinidase leads to the formation of a biotinyl-thioester intermediate (cysteine-bound biotin) at or near the active site of biotinidase [191], followed by a transfer of the biotinyl moiety from the thioester to the ε-amino group of lysine in histones [190, 192, 193]. Although, we detected significant biotinylation in cells expressing the enzyme BirA only, we could clearly distinguish these cells from NFATc1-avi expressing cells by streptavidin-fluorophore staining. Therefore, we considered the amount of endogenous biotinlyated proteins, detected by flow cytometry, as background which would not affect downstream applications and analysis of modified target proteins.

4.5.2.2 Functional analysis of WEHI-231 cells expressing NFATc1/αA-avi and NFATc1/βC-avi

In order to confirm the function of avidin-tagged NFATc1-isoforms which are expressed and biotinylated in WEHI-231 B-lymphoma cells, we quantified the amounts of *Nfatc1*-P1 and - P2 transcripts, performed protein-immunopreciptation and immune-blotting with streptavidin bound agarose and performed confocal microscopy with these cells.

IV. DISCUSSION

Total RNA was isolated and transcribed into cDNA form WT WEHI-231 or WEHI-231 cells overexpressing NFATc1/αA-avi, NFATc1/βC-avi and/or BirA, stimulated with anti-IgM ab or left untreated. Primers designed to detect transcripts induced by *Nfatc1* P1 or P2 were used to perform PCR analysis. High levels of P1 transcripts were detected in WEHI-231 cells overexpressing NFATc1/αA-avi and, slightly less, in cells overexpressing NFATc1/βC-avi, compared to BirA and wt controls (Figure 3.26). Due to the overexpression of the short NFATc1-isoform αA, high levels of P1 directed transcripts appeared in WEHI-231 NFATc1/αA-avi cells as expected. Elevated levels of P1-directed mRNA in WEHI-231 NFATc1/βC-avi cells, compared to BirA controls and wt-cells, were contributed to an increase in P1 induction. Interestingly, there were no detectable differences in expression levels of P1- and P2-directed transcripts in untreated cells compared to cells that were stimulated with anti-IgM ab for 24 h. Furthermore, P1-directed transcripts were found to be more abundant than P2 transcripts in wt and BirA expressing cells. These findings are in-line with protein expression data, i.e. with western-blot analysis performed with extracts from WEHI-231 cells. They showed high amounts of NFATc1/αA, but only little amounts of NFATc1/B and -C-isoforms that were equally distributed in unstimulated and anti-IgM stimulated cells (Figure 3.27 and data not shown). From these data, we concluded that the NFATc1 expression patterns, found in primary B- and T-lymphocytes, do not apply for transformed and hyperproliferating WEHI-231 B-lymphoma cells.

Whole-protein extracts from WEHI-231 cells were isolated to perform IPs and immunoblotting assays (Figure 3.27). Avidin-tagged and *in vivo* biotinylated NFATc1-isoforms were precipitated with streptavidin-coupled agarose beads and IP eluates, and whole cell lysates were compared by SDS-PAGE and immunoblotting using abs directed against all NFATc1-isoforms (7A6), against the α-peptide of NFATc1 (α-spec) and with streptavidin directly linked to HRP. NFATc1 expression was found to be higher in WEHI-231 cells expressing either NFATc1/αA-avi or NFATc1/βC-avi compared to BirA and WT control cells. With ab against all NFATc1-isoforms (7A6) NFATc1 was detected in both IP-samples from NFATc1/αA-avi and NFATc1/βC-avi overexpressing cells. Using the α-specific anti-NFATc1 ab NFATc1/αA-avi was seen in IP-samples from WEHI-231 NFATc1/αA-avi cells, but not in NFATc1/βC-avi and control cells. Streptavidin-coupled HRP only showed bands for lysates and IPs from avidin-tagged overexpression samples, but there was also some background staining detected in wt and BirA IP samples. This was due to co-precipitations of biotinylated endogenous proteins, or remains of the streptavidin precipitation itself. Noteworthy, elevated levels of NFATc1/αA

protein were detected in cell extracts from WEHI-231 cells overexpressing NFATc1/βC-avi (α-spec ab), similar to increased levels of P1 transcript in these cells, as seen in RT-PCR experiments (Figure 3.26). From these data, the proper expression of NFATc1-avi proteins in WEHI-231 was apparent.

Intracellular ab-staining for NFATc1 and biotinylated avidin, analyzed by fluorescence confocal microscopy, showed the nuclear translocation of NFATc1 proteins in all WEHI-231 cell lines after anti-IgM stimulation for 48 h (Figures 3.28 and 3.29). Streptavidin-Alexa Fluor 488 staining displayed very similar staining patterns in NFATc1/αA-avi and NFATc1/βC-avi overexpressing cells, reflecting the activation of NFATc1. Still, there were very weak, but detectable amounts of Alexa-Fluor 488 in samples from wt and BirA expressing WEHI-231 cells.

In summary, these experiments confirmed the applicability of intracellular biotinylation of avidin-tagged NFATc1 proteins. Expression levels of NFATc1/αA and NFATc1/βC were higher in retrovirally infected cells and showed similarities in mRNA and protein expression. Specific biotinylation of avidin-tagged NFATc1 proteins was detected by flow-cytometry and confocal microscopy, and, efficiently biotinylated NFATc1 proteins were efficiently detected in immunoprecipitation experiments.

4.5.2.3 Retroviral infection of primary B-cell from transgenic Rosa26-BirA mice

Since due to the overexpression of tagged bait-proteins and the prokaryotic ligase BirA, biotinylation of avidin-tagged NFATc1-isoforms in H293T-cells and WEHI-231 B-lymphoma cells was successful, we further assessed the *in vivo* biotinylation of NFATc1/αA expressed from NFATc1-avi constructs in primary B-cells. B-cells were isolated from B6 Rosa26-BirA animals (kindly provided by M. Schäfer, IMP;Vienna) and infected with retroviral particles containing pEGZ-NFATc1/αA-avi. Although, the infection-rates were quite low, we were able to detect positively infected primary B-cells, expressing transgenic eGFP and avidin-tagged NFATc1/αA, labeled with streptavidin APC (Figure 3.30). It is worth mentioning that these primary B-cells, expressing BirA from the Rosa26 locus, showed relatively high-levels of background biotinylation, analyzed by comparing unstained and streptavidin APC-labeled cells.

4.6 Apoptosis and cell-death of WEHI-231 B-lymphoma cells

WEHI-231 wt cells and WEHI-231 cells overexpressing NFATc1/αA-avi or NFATc1/βC-avi were cultured and stimulated by anti-IgM ab for two to four days. To determine their apoptosis and cell-death, they were analyzed by flow cytometry (Figures 3.31 and 3.32). WEHI-231 lymphoma cells have been reported to easily undergo apoptosis after Ig-receptor engagement [93]. Cross-linking of surface IgM with anti-Ig ab reagents caused these cells to arrest in the G_0/G_1 phase of the cell cycle, and led to cell-death about 24 h to 48 h later [85]. PCD may be avoided in these cells by co-culturing them in the presence of bacterial LPS, or by Th2 clones and antigen [86]. In our experiments, FACS analysis showed in logarithmic growth approximately 20-30% of wt WEHI-231 cells were positive for annexin V (Figure 3.31). NFATc1/αA-avi overexpressing cells were generally faster growing and less apoptotic, i.e. 10% to 15% annexin V positive in average, whereas WEHI-231 NFATc1/βC-avi cells were found to behave like wt cells in culture. Anti-IgM stimulation induced apoptosis in all three cell lines, but was found to be significantly less severe in NFATc1/αA-avi expressing cells, compared to wt and NFATc1/βC expressing cells. Supplementation with the NF-κB inducing anti-CD40 ab led to a reduction in annexin V staining in all three lines, but was found to be most effective for cells overexpressing NFATc1/αA. This dampening effect of co-stimulation with anti-CD40 ab was found to be less prominent in WEHI-231 NFATc1/βC-avi cells.

In parallel, wt WEHI-231 cells and cells overexpressing individual NFATc1-isoforms were labeled with PI after anti-IgM or anti-IgM and anti-CD40 treatment (Figure 3.32). We detected high numbers of dead cells after 48 h and 96 h in cultures of wt and NFATc1/βC expressing cells, whereas WEHI-231 NFATc1/αA-avi cells showed very small populations of PI positive cells only. Co-stimulation with anti-CD40 ab showed some effect on survival in wt cells after 48 h, but little to none after 4 days of stimulation. Almost no effect of anti-CD40 treatment was seen for NFATc1/αA and NFATc1/βC overexpressing cells after 48 h, whereas only few NFATc1/βC-avi overexpressing cells were found to survive after stimulation for 96 h. From these data we expected significant differences in gene regulation, induced by the overexpression of NFATc1/αA and NFATc1/βC. Data gathered from whole-transcriptome NGS assays confirmed this assumption. Compared to control cells, they showed the regulation of numerous genes involved in transcriptional regulation in WEHI-231 cells overexpressing NFATc1/αA, and of numerous genes involved in apoptosis and cell-death in WEHI-231 cells overexpressing NFATc1/βC (3.6).

4.7 Transcriptome-sequencing of WEHI-231 cells overexpressing NFATc1/αA and NFATc1/βC

4.7.1 Quantification of NFATc1/α- and NFATc1/β-isoform transcript expression

Total RNA was prepared from WEHI-231 cells overexpressing BirA, WEHI-231 NFATc1/αA-avi or WEHI-231 NFATc1/βC-avi that were stimulated in culture for 6 h, 24 h and 96 h by anti-IgM ab, or they were left untreated. RNA-samples were quantified and sent for RNA-seq assays to TRON in Mainz. There, barcoded RNA-seq libraries were generated and sequenced (1 x 50 bps /reads/sample, 50 cycles) on the Illumina Hiseq2500 apparatus. All sequenced reads were mapped against the mouse genome mm9 and annotated accordingly by TRON.

First, we examined the expression levels of individual NFATc1-isoforms sequenced in all three samples for each time-point. Due to computational correlation, all sequenced *Nfatc1*-reads, spanning exons 3-11, were assigned to all six NFATc1-isoforms. Hence, all reads for *Nfatc1* transcripts in NFATc1/αA-avi and NFATc1/βC-avi overexpressing cells appeared to be equally distributed, respectively (Figure 3.33). As expected, a closer look on individual *Nfatc1* exon distribution revealed high amounts of *Nfatc1*/α-transcripts (*Nfatc1*-exon1 reads) in WEHI-231 cells overexpressing NFATc1/αA-avi, and high amounts of *Nfatc1*/β-transcripts (*Nfatc1*-exon 2 reads) in NFATc1/βC-avi overexpressing cells (Figure 3.34). Expression levels of *Nfatc1*/α- and β-isoforms were ~10-15 times higher in NFATc1 overexpressing cells, compared to BirA expressing control cells. Interestingly, as discussed in 4.5.2.2, elevated levels of *Nfatc1*-exon1 transcripts were found in all samples from NFATc1/βC-avi overexpressing cells, which may be contributed to the ´autoregulation´ of P1 promoter in these cells. Similar amounts of *Nfatc1*/α- and *Nfatc1*/β-transcripts, respectively, were seen for cDNA samples from WEHI-231 cells overexpressing NFATc1/αA-avi and NFATc1/βC-avi in P1 and P2 RT-PCRs and protein expression analysis (3.4.3 and 3.4.4).

4.7.2 Profiles of transcriptional regulation of WEHI-231 B-lymphoma cells overexpressing NFATc1/αA- and NFATc1/βC

Whole transcriptome-sequencing data from WEHI-231 cells overexpressing NFATc1 showed that in total 13.607 genes were expressed. We sorted these genes by a threshold expression rate (2 RPKM) and a gene-induction rate of at least 2-fold (up- or down-regulation), at any of four stimulation time-points (0 h to 96 h). By this means, we detected 3452 genes regulated in WEHI-231 NFATc1/αA-avi and 2573 genes regulated in NFATc1/βC-avi overexpressing cells. When we compared the expression and regulation between NFATc1/αA and NFATc1/βC expressing cells, an intersection of 1267 regulated genes was determined (Figure 3.35 A). In order to find correlations, we classified and clustered all genes by utilizing the Database for Annotation, Visualization and Integrated Discovery (DAVID). Functional annotation and ontology yielded more than 120 individual patterns. Due to their EASE score we selected 8 of these clusters. (EASE score: When members of two independent groups can fall into one of two mutually exclusive categories, Fisher Exact test is used to determine whether the proportions of those falling into each category differs by group [194].) Thereby, 8 % of all genes regulated in cells overexpressing NFATc1/αA-avi and NFATc1/βC-avi were clustered into the group "Apoptosis", 15 % were determined as part of "Programmed Cell Death", 15 % were assigned to "Transcriptional Regulation", 13 % to "Cell Cycle", 8 % to "Regulation of Cell Activation", 6% to "Differentiation, 6 % to "Intracellular Signaling and 4 % to "Hemopoiesis" (Figure 3.35 B). All genes regulated and not captured by one of the above stated clusters were listed in the group "others".

In order to find differences in regulation patterns and to establish distinct gene-ontology profiles, all genes regulated either in WEHI-231 NFATc1/αA-avi or NFATc1/βC-avi cells were clustered individually, and marked differences were found (Figure 3.36). "Regulation of Transcription" (28 %) was found to be the largest group of genes regulated in NFATc1/αA cells, followed by "Intracellular Signaling" (11 %) and "Regulation of Cell Activation" (10 %). 5% of all genes regulated in NFATc1/αA cells were clustered into "Apoptosis" and only 4% were part of "Programmed Cell Death". Genes involved in cell activation processes and hemopoiesis were found to be regulated in roughly similar numbers for both WEHI-231 NFATc1 cell-lines. In contrast to WEHI-231 NFATc1/αA-avi cells, "Apoptosis" (14 %), "Programmed Cell Death" (27 %) and "Cell Cycle" 18 % were found to be the most prominent groups of genes regulated by NFATc1/βC in WEHI-231 cells. These expression profiles

indicate distinct roles of NFATc1/α- and β-isoforms in terms of transcriptional regulation and, particularly, in cell-cycle events, apoptosis and programmed cell death. WEHI-231 annexin V staining data, shown in 3.5, clearly imply an anti-apoptotic role for NFATc1/αA, whereas NFATc1/βC overexpression had certainly no positive, but rather negative effect on cell-survival, compared to wt cells.

NFATc1/αA has been reported to mediate antigen-induced proliferation and protect lymphocytes against rapid AICD, in contrast to NFATc2 and other NFATc proteins [144]. *S. Bhattacharyya* and colleagues have demonstrated that upon anti-IgM stimulation murine splenic *Nfatc1⁻/⁻* B-cells exhibit higher rates of apoptosis than wt B-cells, indicating an anti-apoptotic activity for NFATc1, predominantly for NFATc1/αA which is highly expressed under these conditions [70, 144]. However, it has also been reported, validated by our own data (Figure 3.3), that naïve splenic B-cells express large amounts of NFATc1/αA due to BCR engagement for 48 h *ex vivo*, but BCR stimulation exceeding 48 h leads to AICD, unless these cells are rescued by anti-CD40, LPS or CpG co-stimulation, inducing NF-κB factors [144]. Furthermore, NFATc1/αA was previously shown to act anti-apoptotic when reintroduced into NFATc1-deficient DT40 B-cells (unpublished data), in contrast to other NFATc proteins that act in a pro-apoptotic way [142, 195].

4.7.3 Functional ontology: Genes regulated in NFATc1/αA and NFATc1/βC overexpressing cells

4.7.3.1 Genes regulated by NFATc1/αA and NFATc1/βC involved in apoptosis and programmed cell death

Gene-clustering of all transcripts that were sequenced and mapped from WEHI-231 cells overexpressing NFATc1/αA-avi or NFATc1/βC-avi showed that 8 % of regulated genes were involved in apoptosis and 15 % were part of the regulation of programmed cell death. Some of these genes, selected mainly by expression-rate and level of regulation, are shown in the Figures 3.38 and 3.39. Many Bcl-2 family members were found to be regulated in NFATc1-overexpressing cells. *Bcl-2*, for example, was shown to be up-regulated by NFATc1/αA, but down-regulated in NFATc1/βC overexpressing cells. The proto-oncogene *Myc* was expressed in very high-levels in all WEHI-231 cells, but transcript levels further increased upon long-time anti-IgM stimulation in WEHI-231 cells overexpressing NFATc1/αA and NFATc1/βC. It was reported that B-cell CLL is characterized by the accumulation of clonal B-cells that are resistant to apoptosis as a result of *Bcl2* oncogene overexpression [196]. Furthermore, it was shown that

simultaneous over-expression of *Bcl-2* and the proto-oncogene *Myc* produces aggressive B-cell malignancies, including lymphoma [196]. Deregulation of MYC has been described to produce an "avalanche" effect upon gene expression, thus underlining its central role in cellular processes, such as proliferation, differentiation, and metabolism [197, 198].

PDCD family members, such as *Pdcd1*, *Pdcd4* and *Pdcd10*, were grouped into the list of apoptosis. *Pdcd4* was found to be up-regulated only in NFATc1/αA and down-regulated in NFATc1/βC overexpressing cells. The murine PDCD4 protein was reported to inhibit AP-1 transactivation, which may result in the suppression of tumor promotion [199]. *Pdcd10* was up-regulated in both NFATc1/αA and NFATc1/βC overexpressing cells, respectively, although after 96 h of anti-IgM stimulation it was down-regulated in WEHI-231 NFATc1/βC cells. *Pdcd1*, encoding PD-1 (Programmed Death 1), was only weakly expressed in BirA control cells, but up-regulated in NFATc1/αA and NFATc1/βC overexpressing cells. PD-1 is known to be expressed in T-cells, mediating inhibitory signals that regulate the balance between T cell activation, tolerance, and immunopathology [200]. In primary B-cells, the *Pdcd1* gene was detected as a direct NFATc1-target gene [70].

Foxo1, a member of the Forkhead box protein-family, was found to be completely repressed in NFATc1/βC-overexpressing cells. Recent studies have demonstrated that FOXO1 activity is required for proper B-cell development in mice [201] and *R. Mansson* and associates described a positive feedback circuitry, involving EBF1 and FOXO1, acting to stabilize B-cell fate [202]. Since the long NFATc1 isoforms are selectively expressed in DN2/DN3 thymocytes, as shown by *A. Patra* and colleagues [19], one may speculate that NFATc1 helps to suppress the development of early thymocytes to B-cells.

Traf1, a member of the TNF receptor associated factor (TRAF) protein-family, was generally well expressed in WEHI-231 cells, but was found to be down-regulated in NFATc1/αA-avi overexpressing cells, compared to cells overexpressing NFATc1/βC and BirA. It was published that NF-κB activation serves as a primary mechanism to protect cells against apoptotic stimuli such as TNF, by activation of TRAF1 and TRAF2, and c-IAP1 (Baculoviral IAP repeat-containing protein 1) and c-IAP2 functions to suppress apoptosis at the level of caspase-8 [203]. Furthermore, it was reported that TRAF1 inhibits antigen-induced apoptosis [204].

Expression levels of *Lta* and *Ltb* were also found to be decreased and lower expressed in NFATc1/αA overexpressing cells, compared to cells overexpressing NFATc1/βC. *Lta* and *Ltb*

were described to be expressed by T-cells, but also by fully developed B-cells and to be recognized by macrophages that populate the subcapsular sinus (SCS) of the lymphnode [205].

It is noteworthy that several genes that we found to be regulated in WEHI-231 cells were genes that are rather known to be expressed in T-cells or non-lymphoid cells as in B-cells, e.g. *Pdcd1* or *Lck*, a member of the SRC family kinases, involved in TCR signal transduction [206], which was weakly expressed in WEHI-231 BirA cells, but highly induced in NFATc1/βC-avi overexpressing cells. This is an effect which may solely be contributed to the overexpression of NFATc1-isoforms in these cells, but may also be owed to the severe transformation that defines WEHI-231 B-lymphoma cells.

4.7.3.2 Genes regulated in WEHI-231 cells overexpressing NFATc1/αA and NFATc1/βC involved in the regulation of transcription

Gene-ontology and functional-annotation clustering of all genes regulated at least 2-fold, at one of any given time-points, in WEHI-231 cells overexpressing NFATc1/αA- and βC-isoforms, respectively, assigned 15 % of all genes into the cluster of "Regulation of Transcription". Among a selection of these genes, shown in Figure 3.39, were the members of the NF-κB family, such as *Rela*, *Relb*, *Rel* (*c-Rel*) and *Nfκb2*. *Rela*, *Relb* and *Nfκb2* were all up-regulated, whereas *c-Rel* transcription was severely repressed in NFATc1/αA overexpressing cells upon 96 h of anti-IgM stimulation. The canonical NF-κB-pathway, triggered by TNFα, IL-1, LPS, and antigen receptors, activates IKKβ which leads to degradation of IκBα, IκBβ, and IκBε. This pathway activates NF-κB heterodimers consisting of p50 (NFκB1) associated with Rel-A (p65) or c-Rel. The non-canonical pathway, utilized by LTβ, BAFF and CD40, activates IKKα. This leads to phosphorylation and proteolytic processing of the C-terminal domain of p100 and in the release of p52 (NFκB2)-Rel-B heterodimers to activate gene expression [207].

Prdm1, the gene encoding Blimp-1, was found to be significantly repressed in WEHI-231 NFATc1/αA-avi cells. At the same time, it was up-regulated in NFATc1/βC overexpressing cells. Blimp-1 is a zinc finger transcriptional repressor that was originally identified as a silencer of β-interferon gene expression and a "master regulator" of plasma cell differentiation. It was shown to control patterns of gene expression in T-lymphocytes and macrophages. In B-cells, Blimp-1/*Prdm1* directly represses transcription at the *Myc* promoter and, thereby, blocks cell cycle progression and silences expression of key transcription factors, such as PAX5 and CIIta (Class II, Major Histocompatibility Complex, Transactivator) to dramatically shift the gene expression program towards terminal plasma-cell differentiation [208]. On the other hand,

the *Aicda* gene encoding AID (Activation Induced Cytidine Deaminase), was found to be activated by NFATc1/αA but suppressed by NFATc1/βC. Since AID expression controls SHM and CSR in GC cells one may speculate that NFATc1/αA and βC exert opposite effects on GC and plasma-cell differentiation. While NFATc1/αA supports GC and PC formation, NFATc1/βC seems to inhibit GC but support PC formation.

The c-AMP dependent transcription factor *Atf4* was highly expressed in all WEHI-231 cells and its transcriptional induction was found to be enhanced in NFATc1/αA overexpressing cells. *Atf3* transcription was generally lower, but severely induced upon 96 h of anti-IgM stimulation in WEHI-231 NFATc1/αA-avi cells. *Atf3* has been described as an adaptive response gene that is induced by a wide variety of signals including those initiated by cytokines, genotoxic agents or physiological stresses. High *Atf3* expression was correlated to human breast- and prostate cancer and observed in Hodgkin compared to non-Hodgkin lymphomas and non-malignant tissue [209]. AP-1/Atf family members, such as *Batf*, *Junb*, *Jund* and *Fos,* were found to be affected in WEHI-231 NFATc1 overexpressing cells. *Batf* was highly expressed and induced in WEHI-231 NFATc1/αA cells. The nuclear basic-leucine-zipper protein BATF has been shown to be activated upon TCR stimulation and to stimulate IL-17 gene transcription [210].

Runx2 transcription levels were elevated in WEHI-231 NFATc1/βC cells but reduced in NFATc1/αA overexpressing cells. *Runx1* transcription was increased in both overexpressing cell lines upon anti-IgM stimulation, compared to control cells. RUNX1 was reported to serve as tumor suppressor in TLX1 (T-cell leukemia homeobox1)- and TLX3-mediated T-ALL and several other leukemia[211].

4.7.3.3 Genes regulated in WEHI-231 cells overexpressing NFATc1/αA and NFATc1/βC involved in cell cycle processes

Important cell-cycle regulators, such as *Ccnd2* and *Ccng1,* were highly expressed in WEHI-231 cells. *Ccnd2* encoding cyclin D2 was up-regulated by NFATc1/αA-avi overexpression, but remained unaltered in NFATc1/βC overexpressing cells. *Ccng1* transcription was strictly repressed in WEHI-231 NFATc1/βC cells, compared to NFATc1/αA and control cells. An absence of cyclin D2 induction was reported in B-cells stimulated with partial mitogens that act to promote G_1-phase, but not S-phase entry, whereas CD40 or BCR agonists induced sustained expression of cyclin D2. Notably, cyclin D2-deficient splenic B-cells exhibited defective proliferation in response to anti-Ig, but not to CD40- or LPS-induced proliferation [212, 213]. Several reports indicate that cyclin G1 serves as a negative regulator of the *p53* activation

pathway. Furthermore cyclin G1 expression was suggested to be associated with growth promotion rather than growth arrest [214, 215]. Many members of the cell division gene family, such as *Cdc6*, *Cdc20*, *Cdc27* and *Cdc73*, were highly expressed and up-regulated, particularly at later stages of anti-IgM stimulation in NFATc1/βC overexpressing cells. *Cdc6* is critical for pre-replication complex assembly [216], whereas *Cdc20* and *Cdc27* are part of the anaphase-promoting complex/cyclosome (APC/C), an evolutionarily conserved E3 ubiquitin ligase, crucial for cyclin degradation and mitotic progression [217].

Transcription of *Cdkn1a* (*p21*), *Cdkn2a* (*p16*) and *Cdkn2b* (p15) genes was highly induced in WEHI-231 cells. *Cdkn1a* and *Cdkn2a* were found to be oppositely regulated in WEHI-231 NFATc1/αA and NFATc1/βC overexpressing cells. P21, implicated in cell death, DNA repair, cellular senescence [218], and aging was up-regulated in NFATc1/αA overexpressing cells, but strongly repressed in cells overexpressing NFATc1/βC-avi. P16, a cyclin-dependent kinase inhibitor that stabilizes cell cycle arrest by activating retinoblastoma (RB) checkpoint function [219], was found to be highly abundant in all WEHI-231 cells, but severely induced by NFATc1/βC overexpression.

Regulation and counter-regulation of cyclin D2 and cyclin G1, but also the observed oppositional induction of other genes, e.g. *p16* and *p21*, in WEHI-231 NFATc1/αA and NFATc1/βC overexpressing cells, respectively, might explain earlier findings regarding the induction of apoptosis and cell death (4.6). These data also support earlier work referring to NFATc1/αA as anti-apoptotic factor and NFATc1/βC as a pro-apoptotic factor in lymphocytes [144].

4.7.3.4 Stimulation-independent gene-induction and repression by NFATc1/αA and NFATc1/βC in WEHI-231 B-cells

Of all 3452 genes that were either induced or repressed by NFATc1/αA in WEHI-231 cells, 94 genes were found to be induced or repressed at all four time-points (Table 3.1). Among these genes, 32 genes were constantly induced, e.g. *Irf7* (Interferon regulatory factor 7), *Iltn1* (Interlectin 1) and *Cd70*, a CD27 ligand, which has been shown to be only transiently expressed by cells of the immune system upon activation. The CD27 - CD70 axis was reported to play an important role in priming of T-cells in a variety of immunization and infection models [220]. On the other hand, 62 genes were constantly down-regulated in WEHI-231 NFATc1/αA overexpressing cells, e.g. *Cd36*, *Cd44* and *Foxp1*. Expression of *Foxp1* mRNA has been reported to be up-regulated during non-malignant B-cell activation and is highly expressed in

the activated B-cell–like DLBCL [221]. In Table 3.2, 154 genes from 2573 genes regulated in WEHI-231 NFATc1/βC overexpressing cells are shown which were either induced (70) or repressed (86) independently of anti-IgM stimulation.

Creb3l4 was found to be strictly down-regulated in NFATc1/αA overexpressing cells but severely up-regulated in WEHI-231 cells overexpressing the long isoform NFATc1/βC. In a similar fashion, PTK2B *(Pyk2/Ptk2b)*, a protein phosphorylated downstream of adhesion receptors and the TCR, shown to control actin reorganization in numerous cell types [222], was also repressed in NFATc1/αA-avi overexpressing cells, but strongly induced in WEHI-231 NFATc1/βC-avi cells (s.Figure 3.42B). Similar regulation patterns were found for several other genes, e.g. *Prdm1*, *Alcam* (CD166), *Xcr1* (Chemokine (C-motif) receptor 1), *Il15ra* (Interleukin 15 receptor, alpha) and more. This illustrates again a distinct modulatory role of NFATc1-isoforms in lymphocytes. The highly inducible NFATc1/αA appears as a counter regulator for constitutively expressed NFATc1/βC, thereby balancing regulatory receptor/ligand proteins.

Interestingly, *Cd30* was found to be induced in WEHI-231 NFATc1/βC overexpressing cells, whereas its ligand, *Cd30l*, was completely repressed. CD30L was reported to induce numerous biological effects on human CD30-positive cell lines such as activation, proliferation, differentiation, and cell death [223]. Furthermore, CD30-deficient mice showed impaired negative selection in the thymus [224]. Signals mediated by CD30 were reported to regulate gene expression through activation of NF-κB [225]. This remarkable regulation pattern implies a unique role for NFATc1/βC as a regulator of CD30/CD30L signaling.

4.8 ChIP analysis of NFATc1/αA-avi and NFATc1/βC-avi proteins

4.8.1 NFATc1/αA-avi, NFATc1/βC-avi and BirA streptavidin ChIP

ChIP experiments with whole-cell extracts from WEHI-231 cells overexpressing NFATc1/αA-avi, NFATc1/βC avi and/or BirA were performed after six h of TPA and ionomycin stimulation. NFATc1 target genes [70] in primary B-cells reported previously were analyzed for NFATc1/αA and NFATc1/βC binding in WEHI-231 cells (Figure 3.44). Target gene binding was confirmed by PCR, with both avidin-tagged NFATc1-isoforms. In order to establish an efficient and reproducible ChIP method, two very diverging protocols were combined and optimized. The "classical" ChIP approach is based on peptide-specific antibody-binding and the moderate affinity capacity of sepharose coupled to immunoglobulin-binding proteins like

bacterial protein-A or -G. With this approach, the quality of results are determined by antibody specificity and bait-protein abundance. Another weak point of this conventional protocol is protein/DNA elution from bead-bound antibody, which is usually done by SDS-based protein degradation at elevated temperature. As we initially applied this protocol (shown in Figure 3.44 A), we were never able to get specific ChIP results with the commercially available anti-NFATc1 ab (monoclonal murine, clone 7A6), which was seen to produce very high background binding. In antibody independent protocols, on the other hand, affinity tags have been used to study protein interactions and protein bound complexes. Three criteria were reported to be crucial for this method. The tags must have a high binding affinity, they should be preferably small and not strongly charged to minimize possible interference with transcription factor function, and tags should be fairly insensitive to formaldehyde fixation [226]. The avidin-tag, based on the high-affinity interaction of biotin to avidin, has been shown to be highly efficient and applicable [174, 175].

By ChIP, performed with WEHI-231 cells overexpressing NFATc1/αA-avi and NFATc1/βC avi, and BirA as negative control, we were able to confirm the binding of NFATc1/αA to the regulatory regions of NFATc1 target genes *Rcan1*, *Fasl*, *Tnfsf14* and *Ppp3ca* genes (Figure 3.44). The specificity and efficiency were found to be significantly higher for tag-based precipitation compared to the antibody protocol. Therefore, we further improved this protocol by lysate clearing and replacement of SDS-based elution by TEV-cleavage (Figure 3.44 B).

4.8.2 *Prdm1* and *Aicda* binding by NFATc1/αA and -β/C in WEHI-231 cells

The *Prdm1* gene transcription was found to be severely altered in WEHI-231 cells overexpressing NFATc1/αA or NFATc1/βC, compared to BirA controls. The induction of the *Prdm1* gene was almost completely repressed in NFATc1/αA overexpressing cells, but strongly induced upon prolonged anti-IgM stimulation in WEHI-231 cells overexpressing NFATc1/βC (Figure 3.42). These findings matched results from primary B-cells (Figure 3.42 B), as *Prdm1* gene expression was shown to be enhanced upon LPS stimulation in wt-cells, whereas it was repressed in B-cells from mice expressing constitutively NFATc1/αA from the Rosa26 locus (*Nfatc1^flx/flx* x CD23cre x Rosa26caNFATc1/αA). Furthermore, it was shown that the overexpression of NFATc1/αA in *Nfatc1*-deficient chicken DT40 cells (*Nfatc1^-/-/αA* DT-40) suppressed *Prdm1* induction (unpublished Data, Dr. Kondo, E.).

K. Nishikawa and colleagues published recently that Blimp1 is induced by RANKL through NFATc1 and functions as a global repressor of NFATc1 during osteoclastogenesis. In osteoclasts they described NFATc1 recruitment to a highly conserved binding-site within the first exon of *Prdm1* [227]. Primers designed to amplify this binding region were designed and used for DNA precipitation samples from stimulated WEHI-231 BirA, NFATc1/αA-avi and NFATc1/βC-avi overexpressing cells (Figure 3.44A). Binding of NFATc1/αA-avi as well as - βC-avi to *Prdm1*-sitze were detected by PCR, respectively. Semi-quantitative Real-Time PCR showed relative enrichment rates of 30-35 x for NFATc1/αA-avi and 90-100 x for NFATc1/βC-avi binding to *Prdm1* (Figure 3.45).

In contrast to the *Prdm1* gene, the RNA-seq data showed that *Aicda* (Activation-Induced Cytidine Deaminase) expression was strongly enhanced by NFATc1/αA, but suppressed by NFATc1/βC (3.6). By analyzing the genomic conservation between mouse and man, we identified a potential NFATc1 binding site (an atttcc motif) within the regulatory region of *Aicda*. In PCR assaysa using ChIP samples from WEHI-231 NFATc1/αA-avi, NFATc1/βC-avi and BirA cells we were able to detect the binding of NFATc1/αA-avi and NFATc1/βC-avi to this site. Recently it was reported that NFATc1-deficiency in mice leads to a defect in IgG3 class switch in B-cells, after T-cell independent type II antigen (NP-Ficoll) stimulation [70]. Supported by these findings, we assume that NFATc1 is an important regulator of *Aicda* expression in GC B-cells. Further studies have to confirm NFATc1 binding to *Aicda* in primary B-cells and the role of NFATc1 in class switch and somatic hypermutation that are controlled by AID.

4.8.3 ChIP sequencing

Chromatin was extracted from WEHI-231 cells overexpressing NFATc1/αA-avi, NFATc1/βC-avi and/or BirA and used for streptavidin-based ChIP-assays (Figure 3.46 A). To increase assay specificity it is crucial to fragment chromatin-DNA into small pieces (200-500 bps) before ChIP is performed. Furthermore, size selection is mandatory for subsequent NG-sequencing, since template libraries are amplified with adaptor-modified template DNA ranging from 200 to 400 nts. DNA captured and eluted from NFATc1/αA-avi, NFATc1/βC-avi and BirA ChIP-samples was purified by agarose gel electrophoresis, quantified and sent for library preparation and sequencing to TRON, our collaboration partner at the University Mainz (Figure 3.46 B).

IV. DISCUSSION

DNA-samples were analyzed with an (Agilent Technologies 2100) Bioanalyzer and showed good results for integrity, quantity and overall quality. Initial bioinformatics were done by Dr. M. Löwer (TRON) as described in 3.7.2.

For all reads, sequenced and mapped against the mouse genome (mm9), gained from NFATc1/αA-avi and NFATc1/βC-avi ChIP experiments, we received 2511 potential NFATc1 binding-sites, after BirA background subtraction: 1379 potential binding-sites for NFATc1/aA-avi and 1132 sites for NFATc1/βC-avi in WEHI-231 B-lymphoma cells. In order to exclude false-positive binding-sites we only considered sites as positive that were within 20 kbs from the next transcriptional start or the last exon of the next adjacent gene. 477 potential DNA-binding sites for NFATc1/αA and 454 sites for NFATc1/βC were found to fullfill this criterion (Figure 3.47 A). When we compared all genes that were assigned to these NFATc1 binding-sites to our mRNA sequencing data, we only detected 23 genes for NFATc1/αA-avi and 33 genes for NFATc1/βC, respectively, which were affected in their transcription by the NFATc1 proteins (Figure 3.47B).

The amount of potential target sites, gained by NFATc1/αA-avi and NFATc1/βC-avi ChIP-seq experiments was comparatively low. When we analyzed target-site fold-enrichment and the amount of individually assigned tags (reads/site), we could not find particularly strong NFATc1 binding-sites for any one isoform. Unfortunately, we could also not find any NFATc1 binding within the regulatory regions of genes which we, and others, already determined as NFATc1 target genes, e.g. the *Rcan1*, *Fasl*, *Prdm1* (Figures 3.42 and 3.45) or *Nfatc1* [142] genes. Tables 3.3 and 3.4 show the top 50 genes of 477 binding-sites and 454 binding-sites for NFATc1/αA and NFATc1/βC binding, respectively, sorted by relative fold-enrichment and number of tags.

From these data, we concluded that in this first assay we were unable to overcome the high background binding in our ChIP approach. This might be due to sample elution by SDS-buffer which was used here. In other attempts, the ChIP-samples were eluted by TEV-cleavage, which produced much higher specificity. However, with this technique we were unable to precipitate suitable amounts of DNA per sample to generate NGS libraries. As stated earlier and displayed in work by *J. Strouboulis* and colleagues [226], there are many variables that must be taken into consideration and need to be optimized to gain excellent results in ChIP-seq approaches. Nevertheless, we are convinced to have a valuable new tool to study NFATc1 protein binding to DNA and, as already shown by PCR amplification we will be able to gain solid and reproducible results in the next series of ChIPseq assays.

V. SUMMARY

The transcription factor NFATc1 has been shown to regulate the activation and differentiation of T-cells and B-cells, of DCs and megakaryocytes. Dysregulation of NFAT signaling was shown to be associated with the generation of autoimmune diseases, malignant transformation and the development of cancer [71].

The primary goal of this work was to gain insights on *Nfatc1* induction and regulation in lymphocytes and to find new direct NFATc1 target genes. Three new BAC -transgenic reporter mouse strains (*tgNfatc1/Egfp*, *tgNfatc1/DE1* and *tgNfatc1/DE2*) were applied to analyze *Nfatc1* induction and regulation in primary murine B- and T-cells. As a result, we were able to show the persistent requirement of immunoreceptor-signaling for constant *Nfatc1* induction, particularly, for NFATc1/αA expression. Furthermore, we showed that NF-κB inducing agents, such as LPS, CpG or CD40 receptor engagement, in combination with primary receptor-signals, positively contributed to *Nfact1* induction in B-cells [137].

We sought to establish a new system which could help to identify direct NFATc1 target genes by means of ChIP and NGS in genom-wide approaches. We were able to successfully generate a new BAC-transgene encoding a biotinylatable short isoform of NFATc1, which is currently injected into mice oocyte at the TFM in Mainz. In addition, *in vivo* biotinylatable NFATc1– isoforms were cloned and stably expressed in the murine B-cell lymphoma line WEHI-231. The successful use of these cells stably overexpressing either the short NFATc1/αA or the long NFATc1/βC isoform along with the bacterial BirA biotin ligase was confirmed by intracellular stainings, FACS analysis, confocal microscopy and protein IP. By NGS, we detected 2185 genes which are specifically controlled by NFATc1/αA, and 1306 genes which are exclusively controlled by NFATc1/βC. This shows that the *Nfatc1* locus encodes "two genes" which exhibit alternate, in part opposite functions. Studies on the induction of apoptosis and cell-death revealed opposed roles for the highly inducible short isoform NFATc1/αA and the constantly expressed long isoform NFATc1/βC. These findings were confirmed by whole transcriptome-sequencing performed with cells overexpressing NFATc1/αA and NFATc1/βC. Several thousand genes were found to be significantly altered in their expression profile, preferentially genes involved in apoptosis and PCD for NFATc1/βC or genes involved in transcriptional

regulation and cell-cycle processes for NFATc1/αA. In addition we were able to perform ChIP-seq for NFATc1/αA and NFATc1/βC in an ab-independent approach. We found potential new target-sites, but further studies will have to address this ambitious goal in the future. In individual ChIP assays, we showed direct binding of NFATc1/αA and NFATc1/βC to the *Prdm1* and *Aicda* promoter regions which are individually controlled by the NFATc1 isoforms.

ZUSAMMENFASSUNG

Der Transkriptionsfaktor NFATc1 wurde als Regulator der Aktivierung und Differenzierung für T-Zellen, B-Zellen, Dendritische-Zellen und Megakaryozyten beschrieben. Autoimmunerkrankungen und die Entstehung von Krebs wurden mit Fehlregulationen der NFAT-Signalwege in Verbindung gebracht [71].

Ziel dieser Arbeit war der Gewinn neuer Erkenntnisse über die Induktion und Regulation von NFATc1 in Lymphozyten. Darüber hinaus sollten Gene, welche direkt durch NFATc1 gebunden und reguliert werden, identifiziert werden. Um die Induktion und Regulation von NFATc1 in primären T- und B-Zellen untersuchen zu können, wurden drei BAC transgene Reporter Maus Linien (*tgNfatc1/Egfp*, *tgNfatc1/DE1* and *tgNfatc1/DE2*) verwendet. Dadurch war es uns möglich zu zeigen, dass es einer ununterbrochenen Antigen-Rezeptor Stimulation bedarf, um NFATc1, im Besonderen die Transkription der kurzen Isoform NFATc1/αA, dauerhaft zu induzieren. Zusätzlich konnten wir zeigen, dass Induktoren wie LPS, CpG oder auch die Stimulation des CD40-Rezeptors, die die Expression des Transkriptionsfaktors NF-κB zur Folge haben, einen positiven Einfluss auf die *Nfatc1*-Induktion haben [137].

Unser Interesse lag darin, ein System zu etablieren, dass es uns ermöglichen sollte, neue NFATc1-Zielgene durch ChIP assays und Genom-weite Sequenzierungen zu ermitteln. Es ist uns gelungen, ein neues BAC-Transgen, welches für eine *in vivo* biotinylierbare Variante des NFATc1/αA Proteins kodiert, zu erzeugen. Dieses Konstrukt wird zum gegenwärtigen Zeitpunkt - in Zusammenarbeit mit der Universität Mainz (TFM) - in die Vorkerne von Maus-Eizellen injiziert. Ferner wurden biotinylierbare NFATc1-Isoformen kloniert und mit Hilfe retroviraler Plasmide stabil in WEHI-231 B-Lymphom-Zellen integriert. Durch intrazellulare Färbungen, FACS-Analysen, Konfokalmikroskopie und Immunpräzipitationen konnten wir eine erfolgreiche *in vivo* Biotinylierung in NFATc1/αA- und NFATc1/βC-exprimierenden WEHI-231 Zellen nachweisen. Mittels Next-Generation-Sequencing, in Kollaboration mit TRON, Univ. Mainz, konnten wir 2185 Gene, die spezifisch durch NFATc1/αA kontrolliert

wurden, und 1306 Gene, die ausschließlich durch die Überexpression von NFATc1/βC reguliert wurden, identifizieren. Diese Ergebnisse zeigen, dass im *Nfatc1* Locus „zwei Gene" mit alternativer, zum Teil gegensätzlicher Funktion, kodiert sind. Untersuchungen zu Apoptose und Zelltod haben entgegengesetzte Eigenschaften der stark induzierbaren, kurzen Isoform NFATc1/αA und der stetig exprimierten langen Isoform NFATc1/βC aufgezeigt. Daten von Sequenzierungen des gesamten Transkriptoms, die mit NFATc1/αA und -βC überexprimierenden WEHI-231 Zellen durchgeführt wurden (TRON, Mainz), bestätigten diese Befunde. Es zeigte sich, dass es wesentliche Veränderungen der Expressionsprofile Tausender von Genen gab. In WEHI-231-Zellen, die NFATc1/βC überexprimierten, waren viele dieser Gene an Apoptose und Zelltod beteiligt. Demgegenüber waren in NFATc1/αA-Zellen vor allem Gene betroffen, die an transkriptionaler Regulation und dem Zellzyklus beteiligt waren. Überdies war es uns möglich, ChIPseq Assays für NFATc1/αA und NFATc1/βC in einem Antikörper-unabhängigen Ansatz durchzuführen. Dadurch konnten wir neue NFATc1-Bindungstellen identifizieren. Es bedarf jedoch noch weiterer Untersuchungen, um diese Ergebnisse der Genom-weiten ChIPseq Assays zu bestätigen. Durch weitere ChIP Experimente konnten wir eine direkte Bindung von NFATc1/αA und NFATc1/βC an die regulatorischen Regionen der *Prdm1-* und *Aicda-Gene* nachweisen. Die Transkription beider Gene wurde durch die Überexpression von NFATc1/αA und -βC deutlich reguliert und spielt offenbar bei der Bildung von Plasma-B-Zellen, die für die Antikörper-Produktion verantwortlich sind, eine wesentliche Rolle.

VI. ABBREVIATIONS

AA	Amino Acid
ab	Antibody
ADAM	A Disintegrin And Metalloproteinase
AICD	Activation Induced Cell Death
Aicda	Activation-Induced Cytidine Deaminase
AID	Activation-Induced Cytidine Deaminase
AIRE	Autoimmune Regulator
ALKP	Alkaline Phosphatase
AP-1	Activator Protein 1
APC	Allophycocyanin
AP-C	Antigen Presenting Cell
APS	Ammonium Persulfate
α-spec	NFATc1 antibody specific for the α-peptide
avi	Avidin
BAC	Bacterial Artificial Chromosom
BCCP	Biotin Carboxyl Carrier Protein
Bcl2	B-cell lymphoma 2
BCR	B-Cell Receptor
bHLH	basic Helix-Loop-Helix
BLIMP-1	B-Lymphocyte-Induced Maturation Protein-1
BLNK	B-cell Linker
BMM	Bone Marrow-derived Macrophage
BTK	Bruton´s Tyrosine Kinase
CAM	Calmodulin
CARD	Caspase Activation and Recruitment Domains
CBF-1	C-promoter Binding Factor 1
CCR	CC-chemokine receptor
cDNA	complemantary DNA
ChIP	Chromatin Immunoprecipitation
CLL	Chronic Lymphocyte Leukemia
CLP	Common Lymphoid Progenitor
CMV	Cytomegalovirus
CN	Calcineurin
CsA	Cyclosporine A
CSR	Class Switch Recombination
cTEC	Cortical Thymic Epithelial Cell
CTL	Cytotoxic T-Cell
CtsK	Cathepsin K
CXC	Transmembrane receptors with two N-terminal cysteines separated by one random amino acid
DAG	Diacylglycerol
DAPI	4,6-Diamidino-2-Phenylindole, Dilactate

VI. ABBREVIATIONS

DC	Dendritic Cell
DC-STAMP	Dendritic Cell-Specific Transmembrane Protein
DED	Death Effector Domain
DMEM	Dulbecco´s Modified Eagle Medium
DN	Double Negative
DP	Double Positive
ds	double-stranded
DYRK	Dual-specificity tyrosine-Y-phosphorylation Regulated Kinase
E	Embryonic day
E1	Enhancer 1
E2	Enhancer 2
EAE	Experimental Autoimmune Encephalomyelitis
eGFP/Egfp	Enhanced Green-Fluorescent Protein
env	Envelope gene
ER	Endoplasmatic Rendoplasmatic reticulum eticulum
Erk	Extracellular signal regulated kinase
ES	Embryonic Stemcell
FACS	Fluorescence-Activated Cell Sorting
FADD	FAS-adaptor protein
FASL	TNF Superfamily, Member 6
FCS	Fetal Calf Serum
FK-506	Forskolin
FKBP12	FK506 binding protein
FOS	FBJ Murine Osteosarcoma Viral Oncogene Homolog
FRET	Fluorescence Resonance Energy Transfer
FSC	Forward Scatter
gag	Nucleocapsid Core Protein gene
γc	Common γ-chain
GC	Germinal Center
gDNA	genome DNA
GM-CSF	Granulocyte macrophage colony-stimulating factor
GSK3	Glycogen synthase kinase 3
h	hour
H3K4me3	Tri-methylated Histon H3 at Lysin 4
HCS	Human Holocarboxylase Synthetase
HEK	Human Emryonic Kidney Cells
HES	Hairy-Enhancer of Split
HRP	Horse Radish Peroxidase
ICAD	Inhibitor of Caspase-Activated DNAse
ICOS	Inducible co-stimulator
IFN-γ	Interferon-γ
Ig	immunoglobulin
IL	Interleukin
IP	Immunoprecipitation
IP3	1,4,5-inositol trisphosphate

VI. ABBREVIATIONS

ITAM	Immunoreceptor Tyrosine-based Activation Motif
ITIM	Immunoreceptor Tyrosine-based Inhibitory Motifs
iTreg	induced regulatory T-cell
JAK	Janus Kinase
JNK	c-Jun N-terminal Kinase
JUN	Jun Proto-Oncogene
LB	Lysogeny Broth
LFA-1	Lymphocyte Function-Associated antigen 1
loxp	Cre recognition sequence
LPS	Lipopolysaccharide
LYN	Lck/Yes related novel tyrosine kinase
MCL	Mantle Cell Lymphoma
MCS	Multiple Cloning Site
MCSF	Macrophage Colony Stimulating Factor
MEK1	Mitogen Activated Kinase-Kinase 1
MFI	Mean Fluorescent Intensity
MHC	Major-Histocompatibility-Complex
mIG	membrane immunoglobulin
MLV	Murine Leukemia Virus
MO	Macrophage
mTEC	Medullary Thymic Epithelial Cells
MZ	Marginal Zone
NCBI	National Center for Biotechnology Information
NFAT	Nuclear Factor of Activated T-cell
NFkB	Nuclear Factor kappa B
NGS	Next-Generation Sequencing
NHL	Non-Hodgkin´s Lymphoma
NIK	NF-kB Inducing Kinase
NK	Natural Killer Cell
NLS	Nuclear Localization Sequence
nts	nucleotides
NZB	New Zealand Black
OFT	Outflow Tract
pA	Polyadenylation site
PAMP	Pathogen-Associated Molecular Pattern
PAX5	Paired Box5
PC	Plasma cell
PCD	Programmed Cell Death
PCR	Polymerase Chain Reaction
pEGZ	Plasmid eGFP and Zeocin
PI3K	Phosphoinositide 3-kinase
PI	Propidium Iodide
PKA	Protein Kinase A
PKC	Protein Kinase C
pol	Referring to a viral Protease, Integrase and Reverse Transcriptase

PSGL1	Platelet-Selectin Clycoprotein Ligand 1
RAG	Recombination Activation Gene
RANKL	Receptor Activator of NF-kB Ligand
RecA	Recombinase A
RSD	Rel-Similarity Domain
RSD	Rel-similarity domain
RT	Room Temperature
RTK	Receptor Tyrosine Kinase
S1P1	Sphingosine-1-Phosphate Receptor
SCS	Subcapsular Sinus
SHM	Somatic Hypermutation
SOC	Super Optimal broth with Catabolite repression
SOCE	Store Operated Calcium Entry
SP	Single Positive
ss	single stranded
SSC	Sideward Scatter
TAD	Transactivation Domain
TCR	T-Cell Receptor
TE	Tris-EDTA
TEMED	Tetramethylethylenediamine
TEV	Tobacco Etch Virus
tg	transgenic
Th	T-helper (cell)
TLR	Toll-like Receptor
TNF	Tumor Necrosis Factor
TRAF	TNF Receptor Associated Factor
Treg	natural regulatory T-cell
VEGF	Vascular Endothelial Growth Factor
wt	wild-type

VII. REFERENCES

1. Beck G, Habicht GS: **Immunity and the invertebrates**. *Scientific American* 1996, **275**(5):60-63, 66.
2. Abbas A, Lichtman AH, Pillai S: **Cellular and molecular immunology**. *Elsevier Saunders* 2012, **7th edition**.
3. Pancer Z, Cooper MD: **The evolution of adaptive immunity**. *Annual review of immunology* 2006, **24**:497-518.
4. Flajnik MF, Du Pasquier L: **Evolution of innate and adaptive immunity: can we draw a line?** *Trends in immunology* 2004, **25**(12):640-644.
5. Goodnow CC, Sprent J, Fazekas de St Groth B, Vinuesa CG: **Cellular and genetic mechanisms of self tolerance and autoimmunity**. *Nature* 2005, **435**(7042):590-597.
6. Rioux JD, Abbas AK: **Paths to understanding the genetic basis of autoimmune disease**. *Nature* 2005, **435**(7042):584-589.
7. Walker LS, Abbas AK: **The enemy within: keeping self-reactive T cells at bay in the periphery**. *Nature reviews Immunology* 2002, **2**(1):11-19.
8. Takahama Y: **Journey through the thymus: stromal guides for T-cell development and selection**. *Nature reviews Immunology* 2006, **6**(2):127-135.
9. Sainte-Marie G, Leblond CP: **Cytologic Features and Cellular Migration in the Cortex and Medulla of Thymus in the Young Adult Rat**. *Blood* 1964, **23**:275-299.
10. Cantor H, Weissman I: **Development and function of subpopulations of thymocytes and T lymphocytes**. *Progress in allergy* 1976, **20**:1-64.
11. Gray DH, Ueno T, Chidgey AP, Malin M, Goldberg GL, Takahama Y, Boyd RL: **Controlling the thymic microenvironment**. *Current opinion in immunology* 2005, **17**(2):137-143.
12. Artavanis-Tsakonas S, Rand MD, Lake RJ: **Notch signaling: cell fate control and signal integration in development**. *Science* 1999, **284**(5415):770-776.
13. Dontu G, Jackson KW, McNicholas E, Kawamura MJ, Abdallah WM, Wicha MS: **Role of Notch signaling in cell-fate determination of human mammary stem/progenitor cells**. *Breast cancer research : BCR* 2004, **6**(6):R605-615.
14. Iso T, Kedes L, Hamamori Y: **HES and HERP families: multiple effectors of the Notch signaling pathway**. *Journal of cellular physiology* 2003, **194**(3):237-255.
15. Osborne B, Miele L: **Notch and the immune system**. *Immunity* 1999, **11**(6):653-663.
16. Oswald F, Liptay S, Adler G, Schmid RM: **NF-kappaB2 is a putative target gene of activated Notch-1 via RBP-Jkappa**. *Molecular and cellular biology* 1998, **18**(4):2077-2088.
17. Radtke F, Wilson A, Stark G, Bauer M, van Meerwijk J, MacDonald HR, Aguet M: **Deficient T cell fate specification in mice with an induced inactivation of Notch1**. *Immunity* 1999, **10**(5):547-558.
18. Jiang Q, Li WQ, Aiello FB, Mazzucchelli R, Asefa B, Khaled AR, Durum SK: **Cell biology of IL-7, a key lymphotrophin**. *Cytokine & growth factor reviews* 2005, **16**(4-5):513-533.
19. Patra AK, Avots A, Zahedi RP, Schuler T, Sickmann A, Bommhardt U, Serfling E: **An alternative NFAT-activation pathway mediated by IL-7 is critical for early thymocyte development**. *Nature immunology* 2012, **14**(2):127-135.
20. Foxwell BM, Beadling C, Guschin D, Kerr I, Cantrell D: **Interleukin-7 can induce the activation of Jak 1, Jak 3 and STAT 5 proteins in murine T cells**. *European journal of immunology* 1995, **25**(11):3041-3046.
21. Lin JX, Leonard WJ: **The role of Stat5a and Stat5b in signaling by IL-2 family cytokines**. *Oncogene* 2000, **19**(21):2566-2576.
22. Macian F: **Noncanonical NFATc1 activation in DN thymocytes**. *Nature immunology* 2013, **14**(2):116-117.

VII. REFERENCES

23. von Freeden-Jeffry U, Vieira P, Lucian LA, McNeil T, Burdach SE, Murray R: **Lymphopenia in interleukin (IL)-7 gene-deleted mice identifies IL-7 as a nonredundant cytokine**. *The Journal of experimental medicine* 1995, **181**(4):1519-1526.

24. Peschon JJ, Morrissey PJ, Grabstein KH, Ramsdell FJ, Maraskovsky E, Gliniak BC, Park LS, Ziegler SF, Williams DE, Ware CB *et al*: **Early lymphocyte expansion is severely impaired in interleukin 7 receptor-deficient mice**. *The Journal of experimental medicine* 1994, **180**(5):1955-1960.

25. Akashi K, Kondo M, von Freeden-Jeffry U, Murray R, Weissman IL: **Bcl-2 rescues T lymphopoiesis in interleukin-7 receptor-deficient mice**. *Cell* 1997, **89**(7):1033-1041.

26. Kondo M, Akashi K, Domen J, Sugamura K, Weissman IL: **Bcl-2 rescues T lymphopoiesis, but not B or NK cell development, in common gamma chain-deficient mice**. *Immunity* 1997, **7**(1):155-162.

27. Maraskovsky E, O'Reilly LA, Teepe M, Corcoran LM, Peschon JJ, Strasser A: **Bcl-2 can rescue T lymphocyte development in interleukin-7 receptor-deficient mice but not in mutant rag-1-/- mice**. *Cell* 1997, **89**(7):1011-1019.

28. Fooksman DR, Vardhana S, Vasiliver-Shamis G, Liese J, Blair DA, Waite J, Sacristan C, Victora GD, Zanin-Zhorov A, Dustin ML: **Functional anatomy of T cell activation and synapse formation**. *Annual review of immunology* 2010, **28**:79-105.

29. Mempel TR, Henrickson SE, Von Andrian UH: **T-cell priming by dendritic cells in lymph nodes occurs in three distinct phases**. *Nature* 2004, **427**(6970):154-159.

30. Scholer A, Hugues S, Boissonnas A, Fetler L, Amigorena S: **Intercellular adhesion molecule-1-dependent stable interactions between T cells and dendritic cells determine CD8+ T cell memory**. *Immunity* 2008, **28**(2):258-270.

31. Monks CR, Freiberg BA, Kupfer H, Sciaky N, Kupfer A: **Three-dimensional segregation of supramolecular activation clusters in T cells**. *Nature* 1998, **395**(6697):82-86.

32. Varma R, Campi G, Yokosuka T, Saito T, Dustin ML: **T cell receptor-proximal signals are sustained in peripheral microclusters and terminated in the central supramolecular activation cluster**. *Immunity* 2006, **25**(1):117-127.

33. Kuhns MS, Girvin AT, Klein LO, Chen R, Jensen KD, Newell EW, Huppa JB, Lillemeier BF, Huse M, Chien YH *et al*: **Evidence for a functional sidedness to the alphabetaTCR**. *Proceedings of the National Academy of Sciences of the United States of America* 2010, **107**(11):5094-5099.

34. Mustelin T, Tasken K: **Positive and negative regulation of T-cell activation through kinases and phosphatases**. *The Biochemical journal* 2003, **371**(Pt 1):15-27.

35. Timmerman LA, Clipstone NA, Ho SN, Northrop JP, Crabtree GR: **Rapid shuttling of NF-AT in discrimination of Ca2+ signals and immunosuppression**. *Nature* 1996, **383**(6603):837-840.

36. Rao A, Luo C, Hogan PG: **Transcription factors of the NFAT family: regulation and function**. *Annual review of immunology* 1997, **15**:707-747.

37. Sieber M, Baumgrass R: **Novel inhibitors of the calcineurin/NFATc hub - alternatives to CsA and FK506?** *Cell communication and signaling : CCS* 2009, **7**:25.

38. LeBien TW, Tedder TF: **B lymphocytes: how they develop and function**. *Blood* 2008, **112**(5):1570-1580.

39. Cooper MD, Peterson RD, Good RA: **Delineation of the Thymic and Bursal Lymphoid Systems in the Chicken**. *Nature* 1965, **205**:143-146.

40. Cooper MD, Raymond DA, Peterson RD, South MA, Good RA: **The functions of the thymus system and the bursa system in the chicken**. *The Journal of experimental medicine* 1966, **123**(1):75-102.

41. Coombs RR, Feinstein A, Wilson AB: **Immunoglobulin determinants on the surface of human lymphocytes**. *Lancet* 1969, **2**(7631):1157-1160.

42. Froland S, Natvig JB, Berdal P: **Surface-bound immunoglobulin as a marker of B lymphocytes in man**. *Nature: New biology* 1971, **234**(51):251-252.

43. Brack C, Hirama M, Lenhard-Schuller R, Tonegawa S: **A complete immunoglobulin gene is created by somatic recombination**. *Cell* 1978, **15**(1):1-14.

VII. REFERENCES

44.   Bradl H, Wittmann J, Milius D, Vettermann C, Jack HM: **Interaction of murine precursor B cell receptor with stroma cells is controlled by the unique tail of lambda 5 and stroma cell-associated heparan sulfate**. *J Immunol* 2003, **171**(5):2338-2348.

45.   Lam KP, Kuhn R, Rajewsky K: **In vivo ablation of surface immunoglobulin on mature B cells by inducible gene targeting results in rapid cell death**. *Cell* 1997, **90**(6):1073-1083.

46.   Muramatsu M, Kinoshita K, Fagarasan S, Yamada S, Shinkai Y, Honjo T: **Class switch recombination and hypermutation require activation-induced cytidine deaminase (AID), a potential RNA editing enzyme**. *Cell* 2000, **102**(5):553-563.

47.   Nutt SL, Kee BL: **The transcriptional regulation of B cell lineage commitment**. *Immunity* 2007, **26**(6):715-725.

48.   Nutt SL, Heavey B, Rolink AG, Busslinger M: **Commitment to the B-lymphoid lineage depends on the transcription factor Pax5**. *Nature* 1999, **401**(6753):556-562.

49.   IMGT®. In., vol. 2013: Marie-Paule Lefranc, Montpellier, France; 2013.

50.   Cobaleda C, Jochum W, Busslinger M: **Conversion of mature B cells into T cells by dedifferentiation to uncommitted progenitors**. *Nature* 2007, **449**(7161):473-477.

51.   Hardy RR, Hayakawa K: **B cell development pathways**. *Annual review of immunology* 2001, **19**:595-621.

52.   Dorshkind K, Montecino-Rodriguez E: **Fetal B-cell lymphopoiesis and the emergence of B-1-cell potential**. *Nature reviews Immunology* 2007, **7**(3):213-219.

53.   Radbruch A, Muehlinghaus G, Luger EO, Inamine A, Smith KG, Dorner T, Hiepe F: **Competence and competition: the challenge of becoming a long-lived plasma cell**. *Nature reviews Immunology* 2006, **6**(10):741-750.

54.   McHeyzer-Williams LJ, McHeyzer-Williams MG: **Antigen-specific memory B cell development**. *Annual review of immunology* 2005, **23**:487-513.

55.   Shapiro-Shelef M, Calame K: **Regulation of plasma-cell development**. *Nature reviews Immunology* 2005, **5**(3):230-242.

56.   DiLillo DJ, Hamaguchi Y, Ueda Y, Yang K, Uchida J, Haas KM, Kelsoe G, Tedder TF: **Maintenance of long-lived plasma cells and serological memory despite mature and memory B cell depletion during CD20 immunotherapy in mice**. *J Immunol* 2008, **180**(1):361-371.

57.   Reth M, Wienands J: **Initiation and processing of signals from the B cell antigen receptor**. *Annual review of immunology* 1997, **15**:453-479.

58.   Harwood NE, Batista FD: **Early events in B cell activation**. *Annual review of immunology* 2010, **28**:185-210.

59.   Reth M: **Antigen receptor tail clue**. *Nature* 1989, **338**(6214):383-384.

60.   Dal Porto JM, Gauld SB, Merrell KT, Mills D, Pugh-Bernard AE, Cambier J: **B cell antigen receptor signaling 101**. *Molecular immunology* 2004, **41**(6-7):599-613.

61.   Lanzavecchia A: **Antigen-specific interaction between T and B cells**. *Nature* 1985, **314**(6011):537-539.

62.   Schamel WW, Reth M: **Monomeric and oligomeric complexes of the B cell antigen receptor**. *Immunity* 2000, **13**(1):5-14.

63.   Tolar P, Sohn HW, Pierce SK: **The initiation of antigen-induced B cell antigen receptor signaling viewed in living cells by fluorescence resonance energy transfer**. *Nature immunology* 2005, **6**(11):1168-1176.

64.   **B cell Signaltransduction** [http://www.uci.edu/]

65.   Schreiner GF, Braun J, Unanue ER: **Spontaneous redistribution of surface immunoglobulin in the motile B lymphocyte**. *The Journal of experimental medicine* 1976, **144**(6):1683-1688.

66.   Stackpole CW, Jacobson JB, Lardis MP: **Two distinct types of capping of surface receptors on mouse lymphoid cells**. *Nature* 1974, **248**(445):232-234.

67.   Reth M: **Oligomeric antigen receptors: a new view on signaling for the selection of lymphocytes**. *Trends in immunology* 2001, **22**(7):356-360.

68.   Depoil D, Fleire S, Treanor BL, Weber M, Harwood NE, Marchbank KL, Tybulewicz VL, Batista FD: **CD19 is essential for B cell activation by promoting B cell receptor-antigen microcluster formation in response to membrane-bound ligand**. *Nature immunology* 2008, **9**(1):63-72.

69.   Weber M, Treanor B, Depoil D, Shinohara H, Harwood NE, Hikida M, Kurosaki T, Batista FD: **Phospholipase C-gamma2 and Vav cooperate within signaling microclusters to propagate B cell spreading in response to membrane-bound antigen**. *The Journal of experimental medicine* 2008, **205**(4):853-868.

70.   Bhattacharyya S, Deb J, Patra AK, Thuy Pham DA, Chen W, Vaeth M, Berberich-Siebelt F, Klein-Hessling S, Lamperti ED, Reifenberg K *et al*: **NFATc1 affects mouse splenic B cell function by controlling the calcineurin--NFAT signaling network**. *The Journal of experimental medicine* 2011, **208**(4):823-839.

71.   Muller MR, Rao A: **NFAT, immunity and cancer: a transcription factor comes of age**. *Nature reviews Immunology* 2010, **10**(9):645-656.

72.   Ron Y, De Baetselier P, Gordon J, Feldman M, Segal S: **Defective induction of antigen-reactive proliferating T cells in B cell-deprived mice**. *European journal of immunology* 1981, **11**(12):964-968.

73.   Ron Y, Sprent J: **T cell priming in vivo: a major role for B cells in presenting antigen to T cells in lymph nodes**. *J Immunol* 1987, **138**(9):2848-2856.

74.   Rosenberg SA: **National-Cancer-Institute Sponsored Study of Classifications of Non-Hodgkins Lymphomas - Summary and Description of a Working Formulation for Clinical Usage**. *Cancer* 1982, **49**(10):2112-2135.

75.   Jaffe ES, Raffeld M, Medeiros LJ, Stetler-Stevenson M: **An overview of the classification of non-Hodgkin's lymphomas: an integration of morphological and phenotypical concepts**. *Cancer research* 1992, **52**(19 Suppl):5447s-5452s.

76.   Jaffe ES: **The role of immunophenotypic markers in the classification of non-Hodgkin's lymphomas**. *Seminars in oncology* 1990, **17**(1):11-19.

77.   Spillmann FJ, Beck-Engeser G, Wabl M: **Differentiation and Ig-allele switch in cell line WEHI-231**. *J Immunol* 2007, **179**(10):6395-6402.

78.   Harris NL: **Mantle cell lymphoma**. *Journal of clinical oncology : official journal of the American Society of Clinical Oncology* 1994, **12**(4):876-877.

79.   Raible MD, Hsi ED, Alkan S: **Bcl-6 protein expression by follicle center lymphomas. A marker for differentiating follicle center lymphomas from other low-grade lymphoproliferative disorders**. *American journal of clinical pathology* 1999, **112**(1):101-107.

80.   Lardelli P, Bookman MA, Sundeen J, Longo DL, Jaffe ES: **Lymphocytic lymphoma of intermediate differentiation. Morphologic and immunophenotypic spectrum and clinical correlations**. *The American journal of surgical pathology* 1990, **14**(8):752-763.

81.   Benhamou LE, Cazenave PA, Sarthou P: **Anti-immunoglobulins induce death by apoptosis in WEHI-231 B lymphoma cells**. *European journal of immunology* 1990, **20**(6):1405-1407.

82.   Gottschalk AR, McShan CL, Merino R, Nunez G, Quintans J: **Physiological cell death in B lymphocytes: I. Differential susceptibility of WEHI-231 sublines to anti-Ig induced physiological cell death and lack of correlation with bcl-2 expression**. *International immunology* 1994, **6**(1):121-130.

83.   Gottschalk AR, Quintans J: **Apoptosis in B lymphocytes: the WEHI-231 perspective**. *Immunology and cell biology* 1995, **73**(1):8-16.

84.   Haggerty HG, Wechsler RJ, Lentz VM, Monroe JG: **Endogenous expression of delta on the surface of WEHI-231. Characterization of its expression and signaling properties**. *J Immunol* 1993, **151**(9):4681-4693.

85.   Jakway JP, Usinger WR, Gold MR, Mishell RI, DeFranco AL: **Growth regulation of the B lymphoma cell line WEHI-231 by anti-immunoglobulin, lipopolysaccharide, and other bacterial products**. *J Immunol* 1986, **137**(7):2225-2231.

86.   Tsubata T, Wu J, Honjo T: **B-cell apoptosis induced by antigen receptor crosslinking is blocked by a T-cell signal through CD40**. *Nature* 1993, **364**(6438):645-648.

VII. References

87.   Staruch MJ, Sigal NH, Dumont FJ: **Differential effects of the immunosuppressive macrolides FK-506 and rapamycin on activation-induced T-cell apoptosis**. *International journal of immunopharmacology* 1991, **13**(6):677-685.

88.   Bierer BE, Mattila PS, Standaert RF, Herzenberg LA, Burakoff SJ, Crabtree G, Schreiber SL: **Two distinct signal transmission pathways in T lymphocytes are inhibited by complexes formed between an immunophilin and either FK506 or rapamycin**. *Proceedings of the National Academy of Sciences of the United States of America* 1990, **87**(23):9231-9235.

89.   Sigal NH, Dumont FJ: **Cyclosporin A, FK-506, and rapamycin: pharmacologic probes of lymphocyte signal transduction**. *Annual review of immunology* 1992, **10**:519-560.

90.   Tocci MJ, Matkovich DA, Collier KA, Kwok P, Dumont F, Lin S, Degudicibus S, Siekierka JJ, Chin J, Hutchinson NI: **The immunosuppressant FK506 selectively inhibits expression of early T cell activation genes**. *J Immunol* 1989, **143**(2):718-726.

91.   Zipfel PF, Irving SG, Kelly K, Siebenlist U: **Complexity of the primary genetic response to mitogenic activation of human T cells**. *Molecular and cellular biology* 1989, **9**(3):1041-1048.

92.   Brabletz T, Pietrowski I, Serfling E: **The immunosuppressives FK 506 and cyclosporin A inhibit the generation of protein factors binding to the two purine boxes of the interleukin 2 enhancer**. *Nucleic acids research* 1991, **19**(1):61-67.

93.   Gottschalk AR, Boise LH, Thompson CB, Quintans J: **Identification of immunosuppressant-induced apoptosis in a murine B-cell line and its prevention by bcl-x but not bcl-2**. *Proceedings of the National Academy of Sciences of the United States of America* 1994, **91**(15):7350-7354.

94.   Vaux DL: **Toward an understanding of the molecular mechanisms of physiological cell death**. *Proceedings of the National Academy of Sciences of the United States of America* 1993, **90**(3):786-789.

95.   Golstein P, Ojcius DM, Young JD: **Cell death mechanisms and the immune system**. *Immunological reviews* 1991, **121**:29-65.

96.   Korsmeyer SJ: **Bcl-2 initiates a new category of oncogenes: regulators of cell death**. *Blood* 1992, **80**(4):879-886.

97.   Vaux DL, Cory S, Adams JM: **Bcl-2 gene promotes haemopoietic cell survival and cooperates with c-myc to immortalize pre-B cells**. *Nature* 1988, **335**(6189):440-442.

98.   Bissonnette RP, Echeverri F, Mahboubi A, Green DR: **Apoptotic cell death induced by c-myc is inhibited by bcl-2**. *Nature* 1992, **359**(6395):552-554.

99.   Strasser A, Harris AW, Vaux DL, Webb E, Bath ML, Adams JM, Cory S: **Abnormalities of the immune system induced by dysregulated bcl-2 expression in transgenic mice**. *Current topics in microbiology and immunology* 1990, **166**:175-181.

100.   Budd RC: **Activation-induced cell death**. *Current opinion in immunology* 2001, **13**(3):356-362.

101.   Krammer PH: **CD95(APO-1/Fas)-mediated apoptosis: live and let die**. *Advances in immunology* 1999, **71**:163-210.

102.   Irmler M, Thome M, Hahne M, Schneider P, Hofmann K, Steiner V, Bodmer JL, Schroter M, Burns K, Mattmann C *et al*: **Inhibition of death receptor signals by cellular FLIP**. *Nature* 1997, **388**(6638):190-195.

103.   Gupta S, Su H, Bi R, Agrawal S, Gollapudi S: **Life and death of lymphocytes: a role in immunesenescence**. *Immunity & ageing : I & A* 2005, **2**:12.

104.   Koonin EV, Aravind L, Hofmann K, Tschopp J, Dixit VM: **Apoptosis. Searching for FLASH domains**. *Nature* 1999, **401**(6754):662; discussion 662-663.

105.   Kothakota S, Azuma T, Reinhard C, Klippel A, Tang J, Chu K, McGarry TJ, Kirschner MW, Koths K, Kwiatkowski DJ *et al*: **Caspase-3-generated fragment of gelsolin: effector of morphological change in apoptosis**. *Science* 1997, **278**(5336):294-298.

106.   Liu X, Zou H, Slaughter C, Wang X: **DFF, a heterodimeric protein that functions downstream of caspase-3 to trigger DNA fragmentation during apoptosis**. *Cell* 1997, **89**(2):175-184.

107.   Enari M, Sakahira H, Yokoyama H, Okawa K, Iwamatsu A, Nagata S: **A caspase-activated DNase that degrades DNA during apoptosis, and its inhibitor ICAD**. *Nature* 1998, **391**(6662):43-50.

VII. REFERENCES

108. Li H, Zhu H, Xu CJ, Yuan J: **Cleavage of BID by caspase 8 mediates the mitochondrial damage in the Fas pathway of apoptosis**. *Cell* 1998, **94**(4):491-501.
109. Pestano GA, Zhou Y, Trimble LA, Daley J, Weber GF, Cantor H: **Inactivation of misselected CD8 T cells by CD8 gene methylation and cell death**. *Science* 1999, **284**(5417):1187-1191.
110. Mixter PF, Russell JQ, Morrissette GJ, Charland C, Aleman-Hoey D, Budd RC: **A model for the origin of TCR-alphabeta+ CD4-CD8- B220+ cells based on high affinity TCR signals**. *J Immunol* 1999, **162**(10):5747-5756.
111. Bonfoco E, Stuart PM, Brunner T, Lin T, Griffith TS, Gao Y, Nakajima H, Henkart PA, Ferguson TA, Green DR: **Inducible nonlymphoid expression of Fas ligand is responsible for superantigen-induced peripheral deletion of T cells**. *Immunity* 1998, **9**(5):711-720.
112. Chambers CA, Sullivan TJ, Allison JP: **Lymphoproliferation in CTLA-4-deficient mice is mediated by costimulation-dependent activation of CD4+ T cells**. *Immunity* 1997, **7**(6):885-895.
113. Punt JA, Osborne BA, Takahama Y, Sharrow SO, Singer A: **Negative selection of CD4+CD8+ thymocytes by T cell receptor-induced apoptosis requires a costimulatory signal that can be provided by CD28**. *The Journal of experimental medicine* 1994, **179**(2):709-713.
114. Donjerkovic D, Scott DW: **Activation-induced cell death in B lymphocytes**. *Cell research* 2000, **10**(3):179-192.
115. Scott DW, Lamers M, Kohler G, Sidman CL, Maddox B, Carsetti R: **Role of c-myc and CD45 in spontaneous and anti-receptor-induced apoptosis in adult murine B cells**. *International immunology* 1996, **8**(9):1375-1385.
116. Parry SL, Hasbold J, Holman M, Klaus GG: **Hypercross-linking surface IgM or IgD receptors on mature B cells induces apoptosis that is reversed by costimulation with IL-4 and anti-CD40**. *J Immunol* 1994, **152**(6):2821-2829.
117. McCormack JE, Kappler J, Marrack P: **Stimulation with specific antigen can block superantigen-mediated deletion of T cells in vivo**. *Proceedings of the National Academy of Sciences of the United States of America* 1994, **91**(6):2086-2090.
118. Tisch R, Roifman CM, Hozumi N: **Functional differences between immunoglobulins M and D expressed on the surface of an immature B-cell line**. *Proceedings of the National Academy of Sciences of the United States of America* 1988, **85**(18):6914-6918.
119. Fischer G, Kent SC, Joseph L, Green DR, Scott DW: **Lymphoma models for B cell activation and tolerance. X. Anti-mu-mediated growth arrest and apoptosis of murine B cell lymphomas is prevented by the stabilization of myc**. *The Journal of experimental medicine* 1994, **179**(1):221-228.
120. Kaptein JS, Lin CK, Wang CL, Nguyen TT, Kalunta CI, Park E, Chen FS, Lad PM: **Anti-IgM-mediated regulation of c-myc and its possible relationship to apoptosis**. *The Journal of biological chemistry* 1996, **271**(31):18875-18884.
121. Wu M, Yang W, Bellas RE, Schauer SL, FitzGerald MJ, Lee H, Sonenshein GE: **c-myc promotes survival of WEHI 231 B lymphoma cells from apoptosis**. *Current topics in microbiology and immunology* 1997, **224**:91-101.
122. Sonenshein GE: **Down-modulation of c-myc expression induces apoptosis of B lymphocyte models of tolerance via clonal deletion**. *J Immunol* 1997, **158**(5):1994-1997.
123. Lee H, Arsura M, Wu M, Duyao M, Buckler AJ, Sonenshein GE: **Role of Rel-related factors in control of c-myc gene transcription in receptor-mediated apoptosis of the murine B cell WEHI 231 line**. *The Journal of experimental medicine* 1995, **181**(3):1169-1177.
124. Potter M, Marcu KB: **The c-myc story: where we've been, where we seem to be going**. *Current topics in microbiology and immunology* 1997, **224**:1-17.
125. Schauer SL, Wang Z, Sonenshein GE, Rothstein TL: **Maintenance of nuclear factor-kappa B/Rel and c-myc expression during CD40 ligand rescue of WEHI 231 early B cells from receptor-mediated apoptosis through modulation of I kappa B proteins**. *J Immunol* 1996, **157**(1):81-86.

VII. References

126. Wang Z, Karras JG, Howard RG, Rothstein TL: **Induction of bcl-x by CD40 engagement rescues sIg-induced apoptosis in murine B cells**. *J Immunol* 1995, **155**(8):3722-3725.

127. Aramburu J, Yaffe MB, Lopez-Rodriguez C, Cantley LC, Hogan PG, Rao A: **Affinity-driven peptide selection of an NFAT inhibitor more selective than cyclosporin A**. *Science* 1999, **285**(5436):2129-2133.

128. Li H, Rao A, Hogan PG: **Interaction of calcineurin with substrates and targeting proteins**. *Trends in cell biology* 2011, **21**(2):91-103.

129. Serfling E, Avots A, Neumann M: **The architecture of the interleukin-2 promoter: a reflection of T lymphocyte activation**. *Biochimica et biophysica acta* 1995, **1263**(3):181-200.

130. Chuvpilo S, Schomberg C, Gerwig R, Heinfling A, Reeves R, Grummt F, Serfling E: **Multiple closely-linked NFAT/octamer and HMG I(Y) binding sites are part of the interleukin-4 promoter**. *Nucleic acids research* 1993, **21**(24):5694-5704.

131. Zhang SL, Yu Y, Roos J, Kozak JA, Deerinck TJ, Ellisman MH, Stauderman KA, Cahalan MD: **STIM1 is a Ca2+ sensor that activates CRAC channels and migrates from the Ca2+ store to the plasma membrane**. *Nature* 2005, **437**(7060):902-905.

132. Hogan PG, Chen L, Nardone J, Rao A: **Transcriptional regulation by calcium, calcineurin, and NFAT**. *Genes & development* 2003, **17**(18):2205-2232.

133. Griffith JP, Kim JL, Kim EE, Sintchak MD, Thomson JA, Fitzgibbon MJ, Fleming MA, Caron PR, Hsiao K, Navia MA: **X-ray structure of calcineurin inhibited by the immunophilin-immunosuppressant FKBP12-FK506 complex**. *Cell* 1995, **82**(3):507-522.

134. Kissinger CR, Parge HE, Knighton DR, Lewis CT, Pelletier LA, Tempczyk A, Kalish VJ, Tucker KD, Showalter RE, Moomaw EW *et al*: **Crystal structures of human calcineurin and the human FKBP12-FK506-calcineurin complex**. *Nature* 1995, **378**(6557):641-644.

135. Shaw KT, Ho AM, Raghavan A, Kim J, Jain J, Park J, Sharma S, Rao A, Hogan PG: **Immunosuppressive drugs prevent a rapid dephosphorylation of transcription factor NFAT1 in stimulated immune cells**. *Proceedings of the National Academy of Sciences of the United States of America* 1995, **92**(24):11205-11209.

136. Isakov N, Altman A: **Protein kinase C(theta) in T cell activation**. *Annual review of immunology* 2002, **20**:761-794.

137. Hock M, Vaeth M, Rudolf R, Patra AK, Pham DA, Muhammad K, Pusch T, Bopp T, Schmitt E, Rost R *et al*: **NFATc1 induction in peripheral T and B lymphocytes**. *J Immunol* 2013, **190**(5):2345-2353.

138. Santos-Rosa H, Schneider R, Bannister AJ, Sherriff J, Bernstein BE, Emre NC, Schreiber SL, Mellor J, Kouzarides T: **Active genes are tri-methylated at K4 of histone H3**. *Nature* 2002, **419**(6905):407-411.

139. Arron JR, Winslow MM, Polleri A, Chang CP, Wu H, Gao X, Neilson JR, Chen L, Heit JJ, Kim SK *et al*: **NFAT dysregulation by increased dosage of DSCR1 and DYRK1A on chromosome 21**. *Nature* 2006, **441**(7093):595-600.

140. Gwack Y, Sharma S, Nardone J, Tanasa B, Iuga A, Srikanth S, Okamura H, Bolton D, Feske S, Hogan PG *et al*: **A genome-wide Drosophila RNAi screen identifies DYRK-family kinases as regulators of NFAT**. *Nature* 2006, **441**(7093):646-650.

141. Okamura H, Garcia-Rodriguez C, Martinson H, Qin J, Virshup DM, Rao A: **A conserved docking motif for CK1 binding controls the nuclear localization of NFAT1**. *Molecular and cellular biology* 2004, **24**(10):4184-4195.

142. Chuvpilo S, Jankevics E, Tyrsin D, Akimzhanov A, Moroz D, Jha MK, Schulze-Luehrmann J, Santner-Nanan B, Feoktistova E, Konig T *et al*: **Autoregulation of NFATc1/A expression facilitates effector T cells to escape from rapid apoptosis**. *Immunity* 2002, **16**(6):881-895.

143. Crabtree GR: **Generic signals and specific outcomes: signaling through Ca2+, calcineurin, and NF-AT**. *Cell* 1999, **96**(5):611-614.

144. Serfling E, Avots A, Klein-Hessling S, Rudolf R, Vaeth M, Berberich-Siebelt F: **NFATc1/alphaA: The other Face of NFAT Factors in Lymphocytes**. *Cell communication and signaling : CCS* 2012, **10**(1):16.

VII. REFERENCES

145. de la Pompa JL, Timmerman LA, Takimoto H, Yoshida H, Elia AJ, Samper E, Potter J, Wakeham A, Marengere L, Langille BL *et al*: **Role of the NF-ATc transcription factor in morphogenesis of cardiac valves and septum**. *Nature* 1998, **392**(6672):182-186.

146. Ranger AM, Grusby MJ, Hodge MR, Gravallese EM, de la Brousse FC, Hoey T, Mickanin C, Baldwin HS, Glimcher LH: **The transcription factor NF-ATc is essential for cardiac valve formation**. *Nature* 1998, **392**(6672):186-190.

147. Xanthoudakis S, Viola JP, Shaw KT, Luo C, Wallace JD, Bozza PT, Luk DC, Curran T, Rao A: **An enhanced immune response in mice lacking the transcription factor NFAT1**. *Science* 1996, **272**(5263):892-895.

148. Hodge MR, Ranger AM, Charles de la Brousse F, Hoey T, Grusby MJ, Glimcher LH: **Hyperproliferation and dysregulation of IL-4 expression in NF-ATp-deficient mice**. *Immunity* 1996, **4**(4):397-405.

149. Schuh K, Twardzik T, Kneitz B, Heyer J, Schimpl A, Serfling E: **The interleukin 2 receptor alpha chain/CD25 promoter is a target for nuclear factor of activated T cells**. *The Journal of experimental medicine* 1998, **188**(7):1369-1373.

150. Ranger AM, Oukka M, Rengarajan J, Glimcher LH: **Inhibitory function of two NFAT family members in lymphoid homeostasis and Th2 development**. *Immunity* 1998, **9**(5):627-635.

151. Rengarajan J, Tang B, Glimcher LH: **NFATc2 and NFATc3 regulate T(H)2 differentiation and modulate TCR-responsiveness of naive T(H)cells**. *Nature immunology* 2002, **3**(1):48-54.

152. Rengarajan J, Mittelstadt PR, Mages HW, Gerth AJ, Kroczek RA, Ashwell JD, Glimcher LH: **Sequential involvement of NFAT and Egr transcription factors in FasL regulation**. *Immunity* 2000, **12**(3):293-300.

153. Oukka M, Ho IC, de la Brousse FC, Hoey T, Grusby MJ, Glimcher LH: **The transcription factor NFAT4 is involved in the generation and survival of T cells**. *Immunity* 1998, **9**(3):295-304.

154. Yoshida H, Nishina H, Takimoto H, Marengere LE, Wakeham AC, Bouchard D, Kong YY, Ohteki T, Shahinian A, Bachmann M *et al*: **The transcription factor NF-ATc1 regulates lymphocyte proliferation and Th2 cytokine production**. *Immunity* 1998, **8**(1):115-124.

155. Ranger AM, Hodge MR, Gravallese EM, Oukka M, Davidson L, Alt FW, de la Brousse FC, Hoey T, Grusby M, Glimcher LH: **Delayed lymphoid repopulation with defects in IL-4-driven responses produced by inactivation of NF-ATc**. *Immunity* 1998, **8**(1):125-134.

156. Serfling E, Chuvpilo S, Liu J, Hofer T, Palmetshofer A: **NFATc1 autoregulation: a crucial step for cell-fate determination**. *Trends in immunology* 2006, **27**(10):461-469.

157. Nurieva RI, Chuvpilo S, Wieder ED, Elkon KB, Locksley R, Serfling E, Dong C: **A costimulation-initiated signaling pathway regulates NFATc1 transcription in T lymphocytes**. *J Immunol* 2007, **179**(2):1096-1103.

158. Negishi-Koga T, Takayanagi H: **Ca2+-NFATc1 signaling is an essential axis of osteoclast differentiation**. *Immunological reviews* 2009, **231**(1):241-256.

159. Suda T, Takahashi N, Udagawa N, Jimi E, Gillespie MT, Martin TJ: **Modulation of osteoclast differentiation and function by the new members of the tumor necrosis factor receptor and ligand families**. *Endocrine reviews* 1999, **20**(3):345-357.

160. Anderson DM, Maraskovsky E, Billingsley WL, Dougall WC, Tometsko ME, Roux ER, Teepe MC, DuBose RF, Cosman D, Galibert L: **A homologue of the TNF receptor and its ligand enhance T-cell growth and dendritic-cell function**. *Nature* 1997, **390**(6656):175-179.

161. Kong YY, Feige U, Sarosi I, Bolon B, Tafuri A, Morony S, Capparelli C, Li J, Elliott R, McCabe S *et al*: **Activated T cells regulate bone loss and joint destruction in adjuvant arthritis through osteoprotegerin ligand**. *Nature* 1999, **402**(6759):304-309.

162. Dougall WC, Glaccum M, Charrier K, Rohrbach K, Brasel K, De Smedt T, Daro E, Smith J, Tometsko ME, Maliszewski CR *et al*: **RANK is essential for osteoclast and lymph node development**. *Genes & development* 1999, **13**(18):2412-2424.

163. Takayanagi H, Kim S, Koga T, Nishina H, Isshiki M, Yoshida H, Saiura A, Isobe M, Yokochi T, Inoue J *et al*: **Induction and activation of the transcription factor NFATc1 (NFAT2) integrate**

VII. REFERENCES

RANKL signaling in terminal differentiation of osteoclasts. *Developmental cell* 2002, **3**(6):889-901.

164. Asagiri M, Sato K, Usami T, Ochi S, Nishina H, Yoshida H, Morita I, Wagner EF, Mak TW, Serfling E *et al*: **Autoamplification of NFATc1 expression determines its essential role in bone homeostasis**. *The Journal of experimental medicine* 2005, **202**(9):1261-1269.

165. Kim K, Kim JH, Lee J, Jin HM, Lee SH, Fisher DE, Kook H, Kim KK, Choi Y, Kim N: **Nuclear factor of activated T cells c1 induces osteoclast-associated receptor gene expression during tumor necrosis factor-related activation-induced cytokine-mediated osteoclastogenesis**. *The Journal of biological chemistry* 2005, **280**(42):35209-35216.

166. Kukita T, Wada N, Kukita A, Kakimoto T, Sandra F, Toh K, Nagata K, Iijima T, Horiuchi M, Matsusaki H *et al*: **RANKL-induced DC-STAMP is essential for osteoclastogenesis**. *The Journal of experimental medicine* 2004, **200**(7):941-946.

167. Fishman MC, Chien KR: **Fashioning the vertebrate heart: earliest embryonic decisions**. *Development* 1997, **124**(11):2099-2117.

168. Chakraborty S, Combs MD, Yutzey KE: **Transcriptional regulation of heart valve progenitor cells**. *Pediatric cardiology* 2010, **31**(3):414-421.

169. Combs MD, Yutzey KE: **VEGF and RANKL regulation of NFATc1 in heart valve development**. *Circulation research* 2009, **105**(6):565-574.

170. Lange AW, Yutzey KE: **NFATc1 expression in the developing heart valves is responsive to the RANKL pathway and is required for endocardial expression of cathepsin K**. *Developmental biology* 2006, **292**(2):407-417.

171. Lange AW, Molkentin JD, Yutzey KE: **DSCR1 gene expression is dependent on NFATc1 during cardiac valve formation and colocalizes with anomalous organ development in trisomy 16 mice**. *Developmental biology* 2004, **266**(2):346-360.

172. Chan C, Heid R, Zheng S, Guo J, Zhou B, Furuuchi T, Danishefsky SJ: **Total synthesis of cribrostatin IV: fine-tuning the character of an amide bond by remote control**. *Journal of the American Chemical Society* 2005, **127**(13):4596-4598.

173. McManus S, Ebert A, Salvagiotto G, Medvedovic J, Sun Q, Tamir I, Jaritz M, Tagoh H, Busslinger M: **The transcription factor Pax5 regulates its target genes by recruiting chromatin-modifying proteins in committed B cells**. *The EMBO journal* 2011, **30**(12):2388-2404.

174. Rudra D, deRoos P, Chaudhry A, Niec RE, Arvey A, Samstein RM, Leslie C, Shaffer SA, Goodlett DR, Rudensky AY: **Transcription factor Foxp3 and its protein partners form a complex regulatory network**. *Nature immunology* 2012, **13**(10):1010-1019.

175. de Boer E, Rodriguez P, Bonte E, Krijgsveld J, Katsantoni E, Heck A, Grosveld F, Strouboulis J: **Efficient biotinylation and single-step purification of tagged transcription factors in mammalian cells and transgenic mice**. *Proceedings of the National Academy of Sciences of the United States of America* 2003, **100**(13):7480-7485.

176. Graham FL, Smiley J, Russell WC, Nairn R: **Characteristics of a human cell line transformed by DNA from human adenovirus type 5**. *The Journal of general virology* 1977, **36**(1):59-74.

177. Boyd AW, Schrader JW: **The regulation of growth and differentiation of a murine B cell lymphoma. II. The inhibition of WEHI 231 by anti-immunoglobulin antibodies**. *J Immunol* 1981, **126**(6):2466-2469.

178. Gong S, Kus L, Heintz N: **Rapid bacterial artificial chromosome modification for large-scale mouse transgenesis**. *Nature protocols* 2010, **5**(10):1678-1696.

179. Mardis ER: **Next-generation DNA sequencing methods**. *Annual review of genomics and human genetics* 2008, **9**:387-402.

180. **An Introduction to Next-Generation Sequencing Technology** [http://www.illumina.com/Documents/products/Illumina_Sequencing_Introduction.pdf]

181. Koboldt DC, Larson DE, Chen K, Ding L, Wilson RK: **Massively parallel sequencing approaches for characterization of structural variation**. *Methods in molecular biology* 2012, **838**:369-384.

VII. REFERENCES

182. Bernstein BE, Stamatoyannopoulos JA, Costello JF, Ren B, Milosavljevic A, Meissner A, Kellis M, Marra MA, Beaudet AL, Ecker JR *et al*: **The NIH Roadmap Epigenomics Mapping Consortium**. *Nature biotechnology* 2010, **28**(10):1045-1048.

183. Sparwasser T, Gong S, Li JY, Eberl G: **General method for the modification of different BAC types and the rapid generation of BAC transgenic mice**. *Genesis* 2004, **38**(1):39-50.

184. Huang da W, Sherman BT, Tan Q, Collins JR, Alvord WG, Roayaei J, Stephens R, Baseler MW, Lane HC, Lempicki RA: **The DAVID Gene Functional Classification Tool: a novel biological module-centric algorithm to functionally analyze large gene lists**. *Genome biology* 2007, **8**(9):R183.

185. Langmead B, Trapnell C, Pop M, Salzberg SL: **Ultrafast and memory-efficient alignment of short DNA sequences to the human genome**. *Genome biology* 2009, **10**(3):R25.

186. Zhang Y, Liu T, Meyer CA, Eeckhoute J, Johnson DS, Bernstein BE, Nusbaum C, Myers RM, Brown M, Li W *et al*: **Model-based analysis of ChIP-Seq (MACS)**. *Genome biology* 2008, **9**(9):R137.

187. Salmon-Divon M, Dvinge H, Tammoja K, Bertone P: **PeakAnalyzer: genome-wide annotation of chromatin binding and modification loci**. *BMC bioinformatics* 2010, **11**:415.

188. Zhu LJ, Gazin C, Lawson ND, Pages H, Lin SM, Lapointe DS, Green MR: **ChIPpeakAnno: a Bioconductor package to annotate ChIP-seq and ChIP-chip data**. *BMC bioinformatics* 2010, **11**:237.

189. Chapman-Smith A, Cronan JE, Jr.: **In vivo enzymatic protein biotinylation**. *Biomolecular engineering* 1999, **16**(1-4):119-125.

190. Kothapalli N, Camporeale G, Kueh A, Chew YC, Oommen AM, Griffin JB, Zempleni J: **Biological functions of biotinylated histones**. *The Journal of nutritional biochemistry* 2005, **16**(7):446-448.

191. Ausio J, van Holde KE: **Histone hyperacetylation: its effects on nucleosome conformation and stability**. *Biochemistry* 1986, **25**(6):1421-1428.

192. Hymes J, Fleischhauer K, Wolf B: **Biotinylation of histones by human serum biotinidase: assessment of biotinyl-transferase activity in sera from normal individuals and children with biotinidase deficiency**. *Biochemical and molecular medicine* 1995, **56**(1):76-83.

193. Hymes J, Wolf B: **Biotinidase and its roles in biotin metabolism**. *Clinica chimica acta; international journal of clinical chemistry* 1996, **255**(1):1-11.

194. (LIB) LoIaB: **The Database for Annotation, Visualization and Integrated Discovery DAVID Bioinformatics Resources 6.7** In.: National Institute of Allergy and Infectious Diseases (NIAID), NIH; 2013.

195. Serfling E, Berberich-Siebelt F, Avots A: **NFAT in lymphocytes: a factor for all events?** *Science's STKE : signal transduction knowledge environment* 2007, **2007**(398):pe42.

196. Otake Y, Soundararajan S, Sengupta TK, Kio EA, Smith JC, Pineda-Roman M, Stuart RK, Spicer EK, Fernandes DJ: **Overexpression of nucleolin in chronic lymphocytic leukemia cells induces stabilization of bcl2 mRNA**. *Blood* 2007, **109**(7):3069-3075.

197. Horn H, Ziepert M, Becher C, Barth TF, Bernd HW, Feller AC, Klapper W, Hummel M, Stein H, Hansmann ML *et al*: **MYC status in concert with BCL2 and BCL6 expression predicts outcome in diffuse large B-cell lymphoma**. *Blood* 2013, **121**(12):2253-2263.

198. Dave SS, Fu K, Wright GW, Lam LT, Kluin P, Boerma EJ, Greiner TC, Weisenburger DD, Rosenwald A, Ott G *et al*: **Molecular diagnosis of Burkitt's lymphoma**. *The New England journal of medicine* 2006, **354**(23):2431-2442.

199. Zhang H, Ozaki I, Mizuta T, Hamajima H, Yasutake T, Eguchi Y, Ideguchi H, Yamamoto K, Matsuhashi S: **Involvement of programmed cell death 4 in transforming growth factor-beta1-induced apoptosis in human hepatocellular carcinoma**. *Oncogene* 2006, **25**(45):6101-6112.

200. Keir ME, Butte MJ, Freeman GJ, Sharpe AH: **PD-1 and its ligands in tolerance and immunity**. *Annual review of immunology* 2008, **26**:677-704.

VII. REFERENCES

201. Dengler HS, Baracho GV, Omori SA, Bruckner S, Arden KC, Castrillon DH, DePinho RA, Rickert RC: **Distinct functions for the transcription factor Foxo1 at various stages of B cell differentiation**. *Nature immunology* 2008, **9**(12):1388-1398.
202. Mansson R, Welinder E, Ahsberg J, Lin YC, Benner C, Glass CK, Lucas JS, Sigvardsson M, Murre C: **Positive intergenic feedback circuitry, involving EBF1 and FOXO1, orchestrates B-cell fate**. *Proceedings of the National Academy of Sciences of the United States of America* 2012, **109**(51):21028-21033.
203. Wang CY, Mayo MW, Korneluk RG, Goeddel DV, Baldwin AS, Jr.: **NF-kappaB antiapoptosis: induction of TRAF1 and TRAF2 and c-IAP1 and c-IAP2 to suppress caspase-8 activation**. *Science* 1998, **281**(5383):1680-1683.
204. Speiser DE, Lee SY, Wong B, Arron J, Santana A, Kong YY, Ohashi PS, Choi Y: **A regulatory role for TRAF1 in antigen-induced apoptosis of T cells**. *The Journal of experimental medicine* 1997, **185**(10):1777-1783.
205. Upadhyay V, Fu YX: **Lymphotoxin signalling in immune homeostasis and the control of microorganisms**. *Nature reviews Immunology* 2013, **13**(4):270-279.
206. Palacios EH, Weiss A: **Function of the Src-family kinases, Lck and Fyn, in T-cell development and activation**. *Oncogene* 2004, **23**(48):7990-8000.
207. Sen R: **Control of B lymphocyte apoptosis by the transcription factor NF-kappaB**. *Immunity* 2006, **25**(6):871-883.
208. Bikoff EK, Morgan MA, Robertson EJ: **An expanding job description for Blimp-1/PRDM1**. *Current opinion in genetics & development* 2009, **19**(4):379-385.
209. Thompson MR, Xu D, Williams BR: **ATF3 transcription factor and its emerging roles in immunity and cancer**. *Journal of molecular medicine* 2009, **87**(11):1053-1060.
210. Hwang ES: **Transcriptional regulation of T helper 17 cell differentiation**. *Yonsei medical journal* 2010, **51**(4):484-491.
211. Chuang LS, Ito K, Ito Y: **RUNX family: Regulation and diversification of roles through interacting proteins**. *International journal of cancer Journal international du cancer* 2013, **132**(6):1260-1271.
212. Chiles TC: **Regulation and function of cyclin D2 in B lymphocyte subsets**. *J Immunol* 2004, **173**(5):2901-2907.
213. Solvason N, Wu WW, Parry D, Mahony D, Lam EW, Glassford J, Klaus GG, Sicinski P, Weinberg R, Liu YJ *et al*: **Cyclin D2 is essential for BCR-mediated proliferation and CD5 B cell development**. *International immunology* 2000, **12**(5):631-638.
214. Ohtsuka T, Jensen MR, Kim HG, Kim KT, Lee SW: **The negative role of cyclin G in ATM-dependent p53 activation**. *Oncogene* 2004, **23**(31):5405-5408.
215. Ohtsuka T, Ryu H, Minamishima YA, Ryo A, Lee SW: **Modulation of p53 and p73 levels by cyclin G: implication of a negative feedback regulation**. *Oncogene* 2003, **22**(11):1678-1687.
216. Liu J, Smith CL, DeRyckere D, DeAngelis K, Martin GS, Berger JM: **Structure and function of Cdc6/Cdc18: implications for origin recognition and checkpoint control**. *Molecular cell* 2000, **6**(3):637-648.
217. McLean JR, Chaix D, Ohi MD, Gould KL: **State of the APC/C: organization, function, and structure**. *Critical reviews in biochemistry and molecular biology* 2011, **46**(2):118-136.
218. Jung YS, Qian Y, Chen X: **Examination of the expanding pathways for the regulation of p21 expression and activity**. *Cellular signalling* 2010, **22**(7):1003-1012.
219. Sperka T, Wang J, Rudolph KL: **DNA damage checkpoints in stem cells, ageing and cancer**. *Nature reviews Molecular cell biology* 2012, **13**(9):579-590.
220. Nolte MA, van Olffen RW, van Gisbergen KP, van Lier RA: **Timing and tuning of CD27-CD70 interactions: the impact of signal strength in setting the balance between adaptive responses and immunopathology**. *Immunological reviews* 2009, **229**(1):216-231.
221. Shaffer AL, Rosenwald A, Staudt LM: **Lymphoid malignancies: the dark side of B-cell differentiation**. *Nature reviews Immunology* 2002, **2**(12):920-932.

VII. References

222. Ostergaard HL, Lysechko TL: **Focal adhesion kinase-related protein tyrosine kinase Pyk2 in T-cell activation and function**. *Immunologic research* 2005, **31**(3):267-282.

223. Gruss HJ, Boiani N, Williams DE, Armitage RJ, Smith CA, Goodwin RG: **Pleiotropic effects of the CD30 ligand on CD30-expressing cells and lymphoma cell lines**. *Blood* 1994, **83**(8):2045-2056.

224. Amakawa R, Hakem A, Kundig TM, Matsuyama T, Simard JJ, Timms E, Wakeham A, Mittruecker HW, Griesser H, Takimoto H *et al*: **Impaired negative selection of T cells in Hodgkin's disease antigen CD30-deficient mice**. *Cell* 1996, **84**(4):551-562.

225. Biswas P, Smith CA, Goletti D, Hardy EC, Jackson RW, Fauci AS: **Cross-linking of CD30 induces HIV expression in chronically infected T cells**. *Immunity* 1995, **2**(6):587-596.

226. Kolodziej KE, Pourfarzad F, de Boer E, Krpic S, Grosveld F, Strouboulis J: **Optimal use of tandem biotin and V5 tags in ChIP assays**. *BMC molecular biology* 2009, **10**:6.

227. Nishikawa K, Nakashima T, Hayashi M, Fukunaga T, Kato S, Kodama T, Takahashi S, Calame K, Takayanagi H: **Blimp1-mediated repression of negative regulators is required for osteoclast differentiation**. *Proceedings of the National Academy of Sciences of the United States of America* 2010, **107**(7):3117-3122.

VIII. PUBLICATIONS

1. Dlaske H, Karauzum H, Monzon-Casanova E, Rudolf R, Starick L, Muller I, Wildner G, Diedrichs-Mohring M, Koch N, Miyoshi-Akiyama T *et al*: **Superantigen-presentation by rat major histocompatibility complex class II molecules RT1.Bl and RT1.Dl**. *Immunology* 2009, **128**(1 Suppl):e572-581.

2. Serfling E, Avots A, Klein-Hessling S, Rudolf R, Vaeth M, Berberich-Siebelt F: **NFATc1/alphaA: The other Face of NFAT Factors in Lymphocytes**. *Cell communication and signaling : CCS* 2012, **10**(1):16.

3. Hock M, Vaeth M, Rudolf R, Patra AK, Pham DA, Muhammad K, Pusch T, Bopp T, Schmitt E, Rost R *et al*: **NFATc1 induction in peripheral T and B lymphocytes**. *J Immunol* 2013, **190**(5):2345-2353.

In preparation:

Rudolf R, Khalid M, Thuy-Pham DA, Klein-Hessling S, Ellenrieder V, Boisguerin V, Sahin U, Kondo E, Serfling E: **NFATc1 suppresses Blimp-1 and plasmablast formation; manuscript in preparation.** In*.*: Institute of pathology, Würzburg; 2013.

Others:

Poster prize 2011: 15th annual meeting of the Signal Transduction Society, Weimar.

IX. VITAE

Education

2009 – 2013	Doctoral research study / Thesis: "Transcriptional Regulation of and by NFATc1 in Lymphocytes", Julius-Maximilians-Universität Wuerzburg, Institute of Pathology, Department of Molecular Pathology
2008 – 2009	Diploma Thesis: „Vergleichende Analyse der MHC Klasse II Moleküle RT1-Dβ2 und H2-Eβ2", Julius-Maximilians-Universität Wuerzburg, Institute of Virology and Immunobiology
2005 – 2008	Major studies (Biology), Major Subject: Biochemistry, Minor Subjects: Genetics, Mikrobiology, Julius-Maximilians-Universität Wuerzburg
2003 – 2005	Intermidiate diploma; Minor Studies (Biology), University of Bayreuth
1992 – 2001	Final secondary school examinations (Abitur); Secondary school, Geschwister-Scholl-Gymnasium Stuttgart, Riedenberg
1988 – 1992	Elementary School, Stuttgart, Uhlbach.

Languages

German:	Native language
English:	Fluent
French:	Elementary

Personal Details

Surname:	Rudolf
First name:	Ronald
Sex:	Male
Date of birth:	25.10.1981
Place of birth:	Stuttgart, Germany
Nationality:	Austrian
Marital status:	Single

X. ACKNOWLEDEGMENTS